

### 6.5.6 SUMMARY

The above-described discussion on thermodynamics, kinetics, and catalysis of the APR process gives the following conclusions about the APR process [1–6,16]:

1. The basis for the APR process is that while alkanes reforming is only favorable at high temperatures, the reforming of oxygenated carbon (with a C/O ratio of 1:1) and the water–gas shift reaction are possible at low temperatures. This allows APR to be carried out in the liquid phase.
2. The activation energy required to break up the C–C bond in oxygenated compounds is lower than that required in alkanes. Thus, H<sub>2</sub> and CO<sub>2</sub> from oxygenated compounds can be obtained in a single reactor. This can be accomplished in liquid phase only for high boiling compounds such as glucose and sorbitol, whereas for low boiling compounds such as glycerol, ethylene glycol, and methanol, the reactions can occur in both the gas and liquid phases.
3. The choice of a catalyst can affect the products. Pt, Pd, and Ni–Sn alloys show high selectivity for hydrogen, whereas Ni catalysts tend to make more alkanes. Ru and Rh catalysts also make alkanes with very little hydrogen. More acidic support favors alkanes production, whereas more basic/neutral support such as alumina favors hydrogen production. The acidic aqueous solution similarly promotes alkanes production due to acid-catalyzed dehydrogenation reactions (followed by the hydrogenation on the metal). The basic aqueous solution favors hydrogen production. The promoters such as Re add acidity to the catalyst, thereby reducing hydrogen formation.
4. The type of feed and its concentration affect the product distribution. Sorbitol gives higher selectivity for hydrogen than glucose. Within polyols, hydrogen selectivity decreases with an increase in carbon number of the feed and an increase in feed concentration due to an increase in side reactions. APR of platform chemical glycerol has been very widely studied. APR can also be applied to the secondary feedstock as long as they are properly pretreated by hydrolysis (either acid or enzymatic) and/or hydrogenation depending on the nature of the feedstock.
5. Davda et al. [2,16,41,58,59] outlined a number of different pathways that can occur in the APR reactor depending on the nature of catalyst, its acidity and acidity level of aqueous solution, the temperature, and the pressure to obtain the desired product distributions. Generally, higher carbon number in the feed and more acidity on the catalyst or aqueous solution favor C–O scission and more alkanes production. The reverse conditions promote C–C bond cleavages to form hydrogen and CO<sub>2</sub>. The latter compounds can, however, undergo undesirable methanation and FT reactions to produce more alkanes. Some metals such as Ru and Rh favor C–O scission and form more alkanes. Pt and Pd, however, favor C–C scission. More bifunctional catalysis can occur by the combination of metal, support, and solutions. In general, high hydrogen selectivity requires high

C–C scission, low rates of C–H scission, and low rates of methanation and F–T reactions. Low CO level can be obtained by operating the reactor with low partial pressures of hydrogen and carbon dioxide. In the recent years, the use of microchannel reactors has been found to have positive effects on the APR process [9,31].

## 6.6 PRODUCTION OF SYNGAS AND MONOFUNCTIONAL GROUPS AND THEIR UPGRADING

### 6.6.1 SYNGAS

Besides hydrogen and alkanes, reforming has also been used to produce syngas from glycerol feedstock [34–36,44,47,51–57,65]. This once again requires the selective breakage of C–C bonds. This can be achieved with Pt catalyst in the temperature range of 498–548 K but at lower pressure. Under these conditions, Pt surface is covered by CO molecules, which hinder gas-phase reaction. Pt/Ru or Pt/Re was identified as alloys that bind CO less strongly on the surface, thus mitigating the reaction inhibition in the presence of products. These catalysts will produce syngas by the reaction [34–36,44,47,51–57,65]:



The syngas produced at these low temperatures can be easily used for the subsequent conversion of syngas to liquid fuels by the FT synthesis. The increase in Re to carbon-supported Pt catalysts also promotes the water–gas shift reaction, which increases the  $\text{H}_2/\text{CO}$  ratio and decreases the  $\text{CO}/\text{CO}_2$  ratio in syngas [34–36,44,47,51–57,65].

### 6.6.2 MONOFUNCTIONAL GROUPS

The literature results [4,32,48,58,59,65,68–86] also showed that for Pt/Re/C catalyst, an increase in pressure shifted the reaction away for reforming reaction to more in the direction of alkanes production. This shift also produced partially deoxygenated intermediates [70–78] such as alcohols and ketones. This suggests that it is possible to couple biomass reforming with hydrodeoxygenation to improve the energy density without an external source of hydrogen [4,32,48,58,59,65,68–86]. Thus, Pt–Re/C catalyst operating at low temperature, high pressure, and high oxygenate feed concentration will favor C–O bond breakage and partially deoxygenate polyols to produce monofunctional intermediates that are predominantly 2-ketones, secondary alcohols, heterocycles, and carboxylic acids [4,32,48,58,59,65,67–86]. These monofunctional groups provide a platform for a variety of upgrading strategies that allow the productions of fuel additives and fuels such as jet fuel, diesel, and gasoline.

Thus, C–C coupling (i.e., condensation reactions) can be employed along with oxygen removal to obtain larger hydrocarbons starting from biomass-derived  $\text{C}_5$  and  $\text{C}_6$  sugar compounds. Ketones are coupled via aldol condensation using basic catalysts such as  $\text{MgAlO}_x$ ,  $\text{MgAl}$ ,  $\text{Pd–MgO/ZrO}_2$ ,  $\text{MgZrO}_2$ ,  $\text{La/ZrO}_2$ ,  $\text{Y/ZrO}_2$ , and  $\text{Mg/TiO}_2$

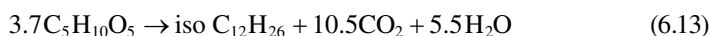
[4,32,48,58,59,65,68–86]. Furthermore, the introduction of bifunctional metal basic catalysts allows for the coupling of secondary alcohols in the presence of hydrogen. More condensation reactions are also driven for ketones in the presence of hydrogen [32]. C–C coupling can also be enhanced by ketonization of carboxylic acid [4]. The complete hydrogenations of monofunctional groups can also produce alcohols. The alcohols can then be converted to gasoline using methanol-to-gasoline (MTG) technology of Mobil Oil Co. that uses H-ZSM-5 catalyst [4,32,48,58,59,65,68–86]. Alcohols can also be dehydrated to produce olefins.

Kunkes et al. [10,30,83] designed a process of converting monofunctional group to pentanol and hexanol and converting these alcohols to  $C_6^+$  gasoline by H-ZSM-5 catalyst at 673 K. In a two-step process, alcohols can also be dehydrated by acidic niobia catalyst to form olefins that can be coupled over H-ZSM-5 to form branched olefins centered around  $C_{12}$  [1–6,16]. Less branched and more complex diesel fuel can also be created by using a mixed system of catalysts  $CuMg_{10}Al_7O_x$ ,  $Pd/CeZrO_x$ , and  $CeZrO_x$  to achieve ketonization and aldol condensation of biomass-derived monofunctional groups as shown in Figure 6.5 [4]. All of these strategies closely follow the details outlined in an excellent review by Alonso et al. [4] and they were the starting points for the development of a complete Virent's BioForming process described in Section 6.7 [60–63,66,67,87–89].

## 6.7 VIRENT'S BIOFORMING PROCESS

While the original work of Dumesic et al. [1–6,16] focused on the generation of hydrogen, syngas, alkanes, and monofunctional groups from the biomass-derived carbohydrates such as alcohols, glycerols, ketones, aldehydes, furans, and other polyols [1–6,16], more recently Virent Inc. (Madison, WI) developed a more complete BioForming process that integrates APR with proven catalytic upgrading technologies to generate hydrocarbons for direct use as a biofuel or as blending components for conventional liquid fuels such as gasoline, diesel, and jet fuels [60–63,66,67,87–89]. This process has been recently described by Blommel and Cortright [15]. Here, we briefly summarize their description of the process [15,60–63,66,67,87–89].

The overall objective of the Virent's bioforming process is to develop a continuous process of converting a wide variety of feedstock into various synthetic liquid fuels, fuel additives, and some useful chemicals. Blommel and Cortright [15] point out that for this process, based on the stoichiometry of the overall conversions of xylose and sucrose to  $C_6^+$  hydrocarbons, carbon dioxide, and water by the following set of reactions,



it is theoretically possible for the resulting hydrocarbons to capture 64% of the carbon from the carbohydrates and over 94% of the lower heating value of sugar. Since APR technology is the centerpiece of this process, the discussion and the studies reported

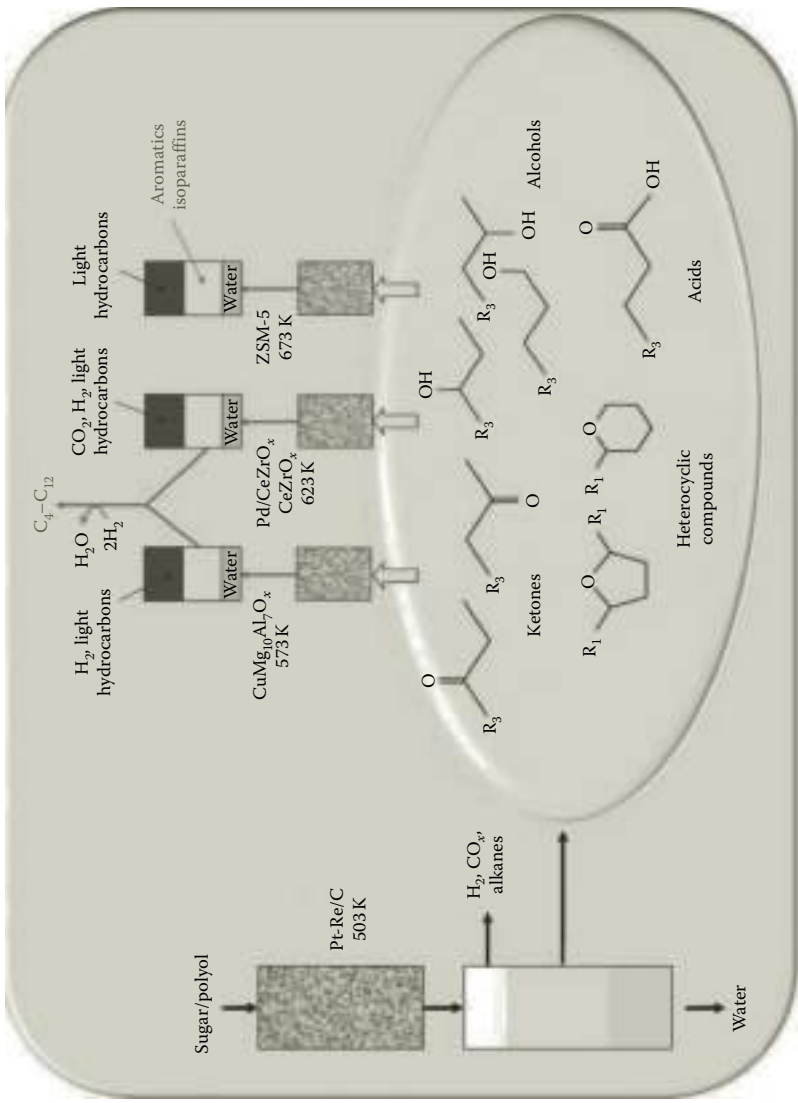


**FIGURE 6.5 (See color insert.)** Schematic pathways to convert sugar and polyols to biofuel through production of monofunctional intermediates. (Reprinted from *Green Chemistry*, 12, Alonso, D.M., Bond, J.Q., and Dumesic, J.A., Catalytic conversion of biomass to biofuels, 1493–1513, Copyright 2010, with permission from Elsevier.)

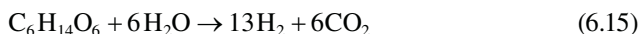
in Section 6.6 indicated that monofunctional groups generated by APR technology can be upgraded to mono-oxygenated hydrocarbons using conventional condensation and hydrotreating techniques. The discussion also indicated such upgrading of monofunctional groups to a variety of end products will require different catalytic strategies.

The development of bioforming process for the secondary feedstock outlined in Table 6.1 requires fractionation and pretreatment of these feedstock to separate hemicellulose, cellulose, and lignin. This fractionation can be carried out using various acidic and enzymatic hydrolyses, which result in the production of five- and six-carbon ring sugars such as xylose and glucose and other oxygenated compounds [15,60–63,66,67,87–89]. The separated lignin can be used for the process heating. The separated polysaccharides, C<sub>5</sub> and C<sub>6</sub> sugars, furans, phenolics, and acids are further upgraded by hydrogenation and hydrogenolysis to sugar alcohols such as sucrose and corn sugar, as well as water-soluble oxygenated compounds such as diols, glycerol, and sugar alcohols [15,60–63,66,67,87–89]. The required hydrogen for these processes can be generated *in situ*, recycled with excess hydrogen from the overall process, or provided by hydrogen from an external source [15].

The centerpiece of Virent's BioForming process is still APR technology, originally developed by Virent Inc. and Dumesic et al. [1–6,16], which utilizes heterogeneous catalysts at moderate temperatures (450–575 K) and pressures (10–90 bar) in a number of series and parallel reactions to reduce the oxygen content of the carbohydrate feedstock. As pointed out by Blommel and Cortright [15], a key feature of this method is the use of *in situ*-generated hydrogen for the defunctionalization of the highly reactive carbohydrates to a less reactive mono-oxygenated species.

While, as discussed earlier, the APR process can generate hydrogen, syngas, alkanes, and condensable monofunctional groups, for the purpose of BioForming process, the most important products are hydrogen and condensable monofunctional intermediates. Just like lignin, the lower alkanes can be used for the process heating purposes. Both hydrogen and condensable products can be formed using Pt–Re catalysts on ZrO<sub>2</sub>. The literature shows the range of oxygenates generated from a sucrose solution through a consecutive deoxygenation and APR processing [1–6,15,16,60–63,66,67,87–89]. These results were generated by first hydrogenating aqueous solution of sucrose by Ru/C catalyst into sorbitol/mannitol mixture. This mixture was then subjected to an APR process using Pt/Re catalyst supported on ZrO<sub>2</sub>[15]. The process generated 0.76 mol of hydrogen per mole of sugar monomer and 35% of feed carbon to CO<sub>2</sub> [1–6,15,16,60–63,66,67,87–89]. Besides C<sub>1</sub>–C<sub>6</sub> alkanes, the process generated alcohols, ketones, acids, and cyclized components suitable for condensation to longer chain hydrocarbons [1–6,15,16,60–63,66,67,87–89].

The total amount of hydrogen generated by the APR process is governed by the reaction [15]:



The generated hydrogen is either recovered or used within the overall process. If the sorbitol is converted to xylitol, one will obtain a H<sub>2</sub>/CO<sub>2</sub> ratio of 2/1 instead of

13/6 as indicated by the above reaction [15,60–63,66,67,87–89]. Very little CO will be produced due to very favorable conditions for forward water–gas shift reaction.

While the original APR process identified various strategies for upgrading monofunctional groups to different types of liquid fuels (Figure 6.5), bioforming process further developed these strategies to build a continuous process (Figure 6.6). The process tested various system operating conditions to produce different intermediate compounds appropriate for use in the downstream condensation reactions that generate different types of fuels or chemicals. The research showed that monofunctional groups can be converted to aromatics and isoalkanes via direct catalytic condensation over acid catalysts, such as solid acids and zeolites [32,48,58,59,64,65,67–86,90–98]. Zeolite ZSM-5 carries out a series of reactions that include the following [15,78,60–64,66,67,87–98]: (1) dehydration of oxygenates to alkenes, (2) oligomerization of the alkenes, (3) cracking, (4) cyclization and dehydrogenation of larger alkenes to form aromatics, (5) alkane isomerization, and (6) hydrogen transfer to form alkanes [95,96]. All of these reactions are important to produce liquid fuels of varying properties such as gasoline, diesel, and jet fuel. The heavier components are generally separated by distillation and blended into jet fuel [15].

Based on further research and development of BioForming process, Blommel and Cortright at Virent [15,60–63,66,67,87–89] proposed a unified continuous process for the conversion of sucrose and xylose into gasoline-range hydrocarbons using proprietary APR catalyst and ZSM-5 (Figure 6.6). The new integrated process, which uses four different types of catalyst beds with no intermediate separation, is schematically described in Figure 6.7 [15]. In this process, each catalyst bed carries out different set of reactions and hydrogen is added with sucrose/xylose mixture in the first reactor. The first reactor (with two stages) operates with aqueous mixtures. The APR process is carried out at 523 K that generates hydrogen, light alkanes, and monofunctional groups. The product from the first reactor is heated to 648 K and passed over two different catalyst beds, both containing different types of acid catalysts. The final carbon number distribution coming out of the second reactor includes  $C_6^+$ , which is necessary for the liquid fuel productions. About 60% of hydrogen used in the first reactor is recovered by the APR process [15].

Blommel and Cortright [15,60–63,66,67,87–89] pointed out that this transformation requires numerous types of condensation reactions such as (1) aldol condensation to form beta-hydroxy ketone and aldehydes; (2) dehydration of these products to form enone; (3) hydrogenation of conjugated enone to ketone, aldehyde, or alcohol; and finally (4) dehydration/hydrogenation or hydrogenolysis to form alkanes. This multifunctional process allows the formation of longer chain and branched hydrocarbons needed to produce gasoline, diesel, and jet fuels with subsequent distillation [15,60–64,66,67,78,87–89,98]. Many oxygenates such as alcohols, carbonyls, and acids can form C–C bonds through aldol and decarboxylative condensation reactions [15,64,78,98]. Further analysis and details on various types of condensation reactions and the role of different catalysts are given by Blommel and Cortright [15] along with some other published reports [60–63,66,67,87–89]. Currently, Virent Inc. is building a pilot plant to demonstrate the viability of the BioForming process at a larger scale with the aim of making a commercial process.

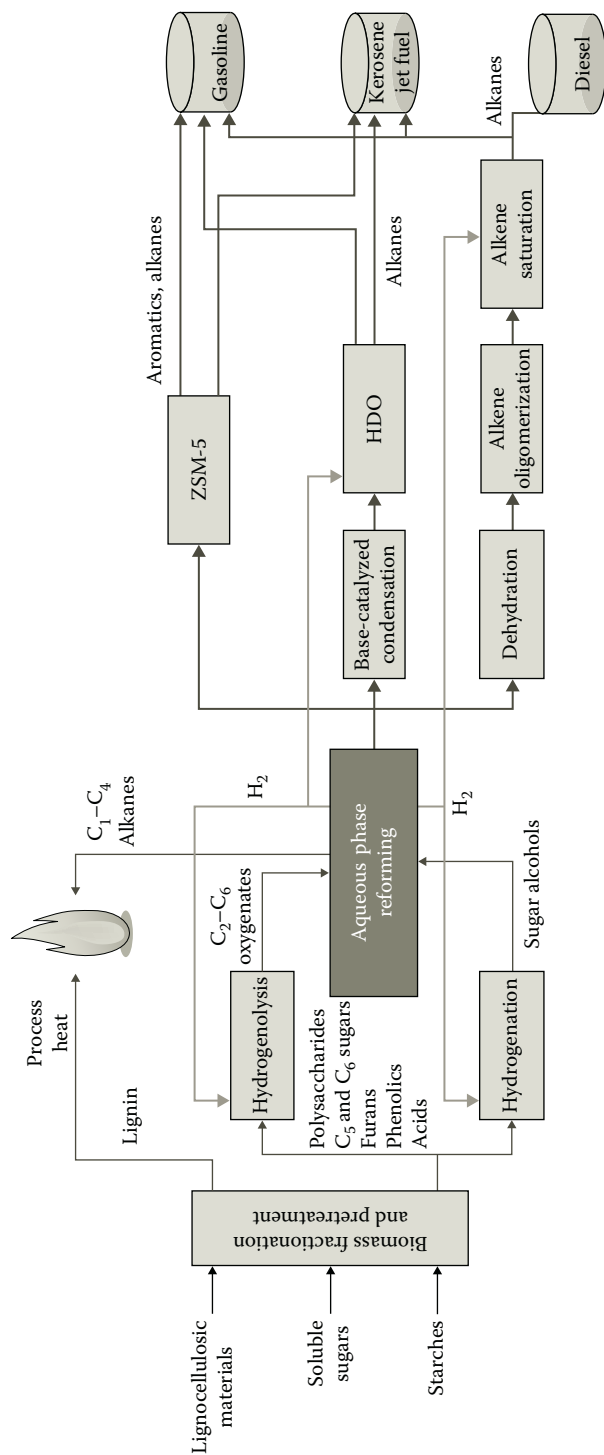


**FIGURE 6.6** (See color insert.) Virent's BioForming® process to produce liquid transportation fuels from biomass feedstock. APR enables the process to partially defunctionalize carbohydrate feedstock for further catalytic upgrading. (Reprinted from White Paper for European Platform on Biofuels, Blommel, P.G. and Cortright, R.D., Production of conventional liquid fuels from sugars, Copyright 2012, with permission from Elsevier.)

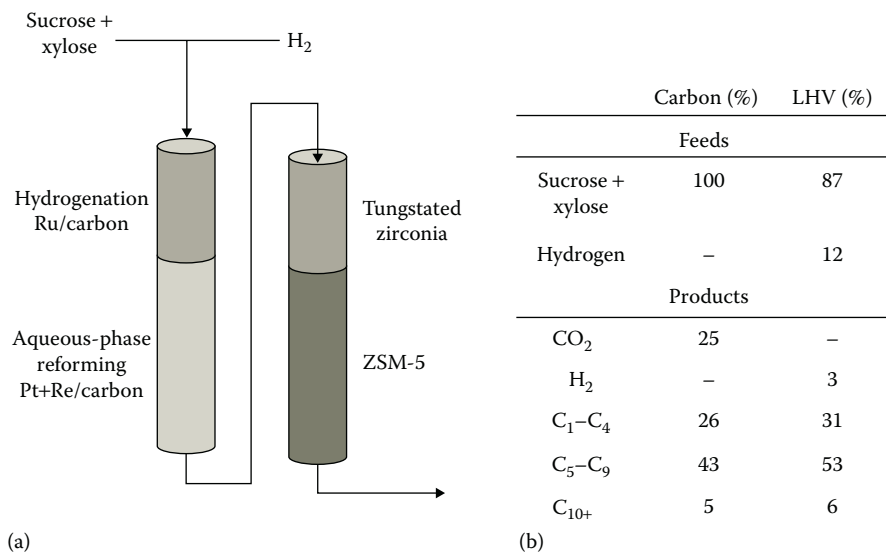


**FIGURE 6.7** (See color insert.) Detailed two-stage reactor setup for BioForming process: Panel (a) illustrates the catalytic steps used to convert glucose and xylose to gasoline-range hydrocarbons; panel (b) summarizes the molar carbon and heating value yields of the resulting products. (Reprinted from White Paper for European Platform on Biofuels, Blommel, P.G. and Cortright, R.D., Production of conventional liquid fuels from sugars, Copyright 2012, with permission from Elsevier.)

## REFERENCES

- Huber, G.W., Cortright, R.D., and Dumesic J.A., “Renewable alkanes by aqueous phase reforming of biomass derived oxygenates,” *Angewandte Chemie International Edition*, 43, 1549–1551 (2004).
- Davda, R. and Dumesic, J., “Catalytic reforming of oxygenated hydrocarbons for hydrogen with low levels of carbon monoxide,” *Angewandte Chemie International Edition*, 42, 4068 (2003).
- Tao, J., Shishi, C., and Fahai, C., “Advances in H<sub>2</sub> production from the aqueous-phase reforming of biomass-derived polyols: A review,” *Chemical Industry and Engineering Progress*, 31 (5), 1010–1017 (2012).
- Alonso, D.M., Bond, J.Q., and Dumesic, J.A., “Catalytic conversion of biomass to bio-fuels,” *Green Chemistry*, 12, 1493–1513 (2010).
- Cortright, R., Davda, R., and Dumesic, J., “Hydrogen from catalytic reforming of bio-mass derived hydrocarbons in liquid water,” *Nature*, 418, 964–967 (2002).
- Huber, G. and Dumesic, J., “An overview of aqueous phase catalytic processes for pro-duction of hydrogen and alkanes in a biorefinery,” *Catalysis Today*, 111 (1–2), 119–132 (2006).
- King, D., “Hydrogen production via aqueous phase reforming,” Paper presented by Pacific Northwest National Laboratory at Niche Catalysis Conference, Washington, DC, September 21 (2011).
- Cortright, R.D., “Hydrogen generation from sugars via aqueous-phase reforming,” *Proceedings of the 16th World Hydrogen Energy Conference*, June 13–16, Lyon, France (2006).

9. D'Angelo, M., Ordonsky, V., van der Schaaf, J., Schouten, J., and Nijhuis, T., "Aqueous phase reforming in a microchannel reactor: The effect of mass transfer on hydrogen selectivity," *Catalysis Science & Technology*, 3, 2834–2842 (2013).
10. Kunkes, E.L., Simonetti, D.A., West, R.M., Serrano-Ruiz, J.C., Gartner, C.A., and Dumesic, J.A., *Science*, 322, 417–421 (2008).
11. Dunn, S., "Hydrogen futures: Toward a sustainable energy system," *International Journal of Hydrogen Energy*, 27, 235–264 (2002).
12. Huber, G., Iborra, S., and Corma, A., "Synthesis of transportation fuels from biomass: Chemistry, catalysts, and engineering," *Chemical Reviews*, 106, 4044–4098 (2006).
13. Soares, R., Simonetti, D., and Dumesic, J., *Angewandte Chemie International Edition*, 45, 3982–3985 (2006).
14. King, D., "Biomass-derived liquids distributed (aqueous phase) reforming," 2012 DOE Hydrogen and Fuel Cells Program Review, Pacific Northwest National Laboratory, May 17, Richland, WA (2012).
15. Blommel, P.G. and Cortright, R.D., "Production of conventional liquid fuels from sugars," a White Paper for European Platform on Biofuels, UK (2012).
16. Davda, R., Shabaker, J., Huber, G., Cortright, R., and Dumesic, J., "A review of catalytic issues and process conditions for renewable hydrogen and alkanes by aqueous-phase reforming of oxygenated hydrocarbons over supported metal catalysts," *Applied Catalysis B: Environmental*, 56, 171–186 (2005).
17. Huber, G., Shabaker, J., and Dumesic, J., "Raney Ni-Sn catalyst for H<sub>2</sub> production from biomass-derived hydrocarbons," *Science*, 300, 2075–2077 (2003).
18. Vos, B., Poels, E., and Blik, A., *Journal of Catalysis*, 198, 77 (2001).
19. Zhu, X., Huo, P., Zhang, Y., Cheng, D., and Liu, C., *Applied Catalysis B: Environmental*, 81, 132 (2008).
20. Zhang, J., Xu, H., Jin, X., Ge, Q., and Li, W., *Applied Catalysis A: General*, 290, 87 (2005).
21. Alberton, A., Souza, M., and Schmal, M., *Catalysis Today*, 123, 257 (2007).
22. Bartholomew, C.H. and Pannell, R.B., *Journal of Catalysis*, 65, 390 (1980).
23. Mustard, D. and Bartholomew, C., *Journal of Catalysis*, 67, 186 (1981).
24. Lehnert, K. and Claus, P., *Catalysis Communications*, 9, 2543 (2008).
25. Wang, Z., Pan, Y., Dong, T., Zhu, X., Kan, T., Yuan, L., Torimoto, Y., Sadakata, M., and Li, Q., *Applied Catalysis A: General*, 320, 24 (2007).
26. Minowa, T., Fang, Z., Ogi, T., and Varhegyi, G., *Journal of Chemical Engineering of Japan*, 31, 131 (1998).
27. Trimm, D., "Coke formation and minimisation during steam reforming reactions," *Catalysis Today*, 37, 233–238 (1997).
28. Shabaker, J., Huber, G., and Dumesic, J., "Aqueous-phase reforming of oxygenated hydrocarbons over Sn-modified Ni catalysts," *Journal of Catalysis*, 222, 180–191 (2004).
29. Park, H.J., Kim, H.-D., Kim, T.-W., Jeong, K.-E., Chae, H.-J., Jeong, S.-Y., Chung, Y.-M., Park, Y.-K., and Kim, C.-U. "Production of biohydrogen by aqueous phase reforming of polyols over platinum catalysts supported on three-dimensionally bimodal mesoporous carbon," *ChemSusChem*, 5, 629–633 (2012).
30. Kunkes, E., Simonetti, D., Dumesic, J., Pyrz, W., Murillo, L., Chen, J., and Buttrey, D., *Journal of Catalysis*, 260, 164–177 (2008).
31. D'Angelo, M.F.N., Ordonsky, V., Paunovic, V., van der Schaaf, J., Schouten, J.C., and Nijhuis, T.A., "Hydrogen production through aqueous-phase reforming of ethylene glycol in a washcoated microchannel," *ChemSusChem*, 6, 1708–1716 (2013).
32. Huber, G., Chheda, J., Barrett, C., and Dumesic, J., "Chemistry: Production of liquid alkanes by aqueous phase processing of biomass-derived carbohydrates," *Science*, 308 (5727), 1446–1450 (2005).

33. Serrano-Ruiz, J. and Dumesic, J., "Catalytic production of liquid hydrocarbon transportation fuels," in Gucci, L. and Erdohelyi, A. (eds.), *Catalysis for Alternative Energy Generation*. Springer, New York, pp. 29–56 (2012).
34. Wen, G., Xu, Y., Ma, H., Xu, Z., and Tian, Z., "Production of hydrogen by aqueous phase reforming of glycerol," *International Journal of Hydrogen Energy*, 33, 6657–6666 (2008).
35. Boonyanuwat, A., Jentys, A., and Lercher, J.A., "Hydrogen production by aqueous phase reforming of glycerine on noble supported catalysts," DGMK-Tagungsbericht, October 4–6, Dresden, Germany (2006).
36. Luo, N., Fu, X., Cao, F., Xiao, T., and Edwards, P., "Glycerol aqueous phase reforming for hydrogen generation over Pt catalyst—Effect of catalyst composition and reaction conditions," *Fuel*, 87, 3483–3489 (2008).
37. Valenzuela, M., Jones, C., and Agrawal, P., "Batch aqueous phase reforming of woody biomass," *Energy & Fuels*, 20, 1744–1752 (2006).
38. Chu, X., Liu, J., Sun, B., Dai, R., Pei, Y., Qiao, M., and Fan, K., "Aqueous phase reforming of ethylene glycol on Co/ZnO catalysts prepared by the coprecipitation method," *Journal of Molecular Catalysis A: Chemical*, 335, 129–135 (2011).
39. Wen, G., Xu, Y., Xu, Z., and Tian, Z., "Characterization and catalytic properties of the Ni/Al<sub>2</sub>O<sub>3</sub> catalysts for aqueous phase reforming of glucose," *Catalysis Letters*, 129, 250–257 (2009).
40. Ni, M., Leung, D.Y.C., Leung, M.K.H., and Sumathy, K., *Fuel Processing Technology*, 87, 461 (2006).
41. Davda, R. and Dumesic, J., "Renewable hydrogen by aqueous phase reforming of glucose," *Chemical Communications*, 36 (2004).
42. Tanksale, A., Wong, Y., Beltramini, J.N., and Lu, G.Q., "Hydrogen generation from liquid phase catalytic reforming of sugar solutions using metal-supported catalysts," *International Journal of Hydrogen Energy*, 32, 717 (2007).
43. Xu, Y.P., Tian, Z.J., Wen, G.D., Xu, Z.S., Qu, W., and Lin, L.W., *Chemistry Letters*, 35, 216 (2006).
44. Manfro, R., Pires, T., Ribeiro, N., and Souza, M., "Aqueous phase reforming of glycerol using Ni-Cu catalysts prepared from hydrotalcite like precursors," *Catalysis Science & Technology*, 3, 1278–1287 (2013).
45. Tungal, R. and Shende, R., "Subcritical aqueous phase reforming of wastepaper for biocrude and H<sub>2</sub> generation," *Energy & Fuels*, 27 (6), 3194–3203 (2013).
46. Manfro, R., de Costa, A., Ribeiro, N., and Souza, M., "Hydrogen production by aqueous phase reforming of glycerol over nickel catalysts supported on CeO<sub>2</sub>," *Fuel Processing Technology*, 92, 330–335 (2013).
47. Vaidya, P. and Rodrigues, A., "Glycerol reforming for hydrogen production: A review," *Chemical Engineering & Technology*, 32, 1463–1469 (2009).
48. Shabaker, J., Davda, R., Huber, G., Cortright, R., and Dumesic, J., "Aqueous phase reforming of methanol and ethylene glycol over alumina-supported platinum catalysts," *Journal of Catalysis*, 215, 344–352 (2003).
49. Shabaker, J., Huber, G., Cortright, R., and Dumesic, J., "Aqueous-phase reforming of ethylene glycol over supported platinum catalysts," *Catalysis Letters*, 88, 1–8 (2003).
50. Cruz, I., Ribeiro, N., Aranda, D., and Souza, M., "Hydrogen production by aqueous-phase reforming of ethanol over nickel catalysts prepared from hydrotalcite precursors," *Catalysis Communications*, 9, 2606–2611 (2008).
51. Behr, A., Eilting, J., Irawadi, K., Leschinski, J., and Lindner, F., "Improved utilization of renewable resources: New important derivatives of glycerol," *Green Chemistry*, 10, 13–30 (2008).
52. Iriondo, A., Barrio, V., Cambra, J., Arias, P., Güemez, M., Navarro, R., Sanchez-Sanchez, M., and Fierro, J., "Hydrogen production from glycerol over nickel catalysts supported on Al<sub>2</sub>O<sub>3</sub> modified by Mg, Zr, Ce or La," *Topics in Catalysis*, 49, 46–58 (2008).

53. Buffoni, I., Pompeo, F., Santori, G., and Nichio, N., "Nickel catalysts applied in steam reforming of glycerol for hydrogen production," *Catalysis Communications*, 10, 1656–1660 (2009).
54. Zhang, B., Tang, X., Li, Y., Xu, Y., and Shen, W., "Hydrogen production from steam reforming of ethanol and glycerol over ceria-supported metal catalysts," *International Journal of Hydrogen Energy*, 32, 2367–2373 (2007).
55. Wawrzetz, A., Peng, B., Hrabar, A., Jentys, A., Lemonidou, A., and Lercher, J., "Towards understanding the bifunctional hydrodeoxygenation and aqueous phase reforming of glycerol," *Journal of Catalysis*, 269, 411–420 (2010).
56. Chheda, J. and Dumesic, J., "An overview of dehydration, aldol condensation, and hydrogenation processes for production of liquid alkanes from biomass-derived carbohydrates," *Catalysis Today*, 123 (1–4), 59–70 (2007).
57. Cho, S.H. and Moon, D.J., "Aqueous phase reforming of glycerol over Ni-based catalysts for hydrogen production," *Journal of Nanoscience and Nanotechnology*, 11 (8), 7311–7314 (2011).
58. Davda, R., Shabaker, J., Huber, G., Cortright, R., and Dumesic, J., *Applied Catalysis B: Environmental*, 56, 171–186 (2005).
59. Davda, R.R., Shabaker, J.W., Huber, G.W., Cortright, R.D., and Dumesic, J.A., *Applied Catalysis B: Environmental*, 43, 13–26 (2003).
60. Cortright, R.D. and Blommel, P.G., "Synthesis of liquid fuels and chemicals from oxygenated hydrocarbons," Publication No. US2008/0216391 (September 11, 2008).
61. Cortright, R.D. and Blommel, P.G., "Synthesis of liquid fuels and chemicals from oxygenated hydrocarbons," Publication No. WO2008/109877 (September 12, 2008).
62. Cortright, R.D. and Blommel, P.G., "Synthesis of liquid fuels and chemicals from oxygenated hydrocarbons," US Application No. 12/044908 (December 4, 2008).
63. Cortright, R.D. and Blommel, P.G., "Synthesis of liquid fuels and chemicals from oxygenated hydrocarbons," US Application No. 12/044876 (December 4, 2008).
64. Ipatieff, V., Corson, B., and Egloff, G., "Polymerization: A new source of gasoline," *Industrial & Engineering Chemistry Research*, 27 (9), 1077–1081 (1935).
65. Tuza, P., Manfro, R., Ribeiro, N., and Souza, M., "Production of renewable hydrogen by aqueous-phase reforming of glycerol over Ni–Cu catalysts derived from hydrotalcite precursors," *Renewable Energy*, 50, 408–414 (2013).
66. Cortright, R.D., "Bioforming process—Production of conventional liquid fuels from sugar," ACS/EPA Green Chemistry Conference, June 23, College Park, MD (2009).
67. Held, A., "Catalytic conversion of renewable plant sugars to fungible liquid hydrocarbon fuels using Bioforming process," TAPPI, IBCC Session 3, Conversion Pathways, October 15, Memphis, TN (2009).
68. Alonso, D., Gallo, J., Mellmer, M., Wettstein, S., and Dumesic, J., "Direct conversion of cellulose to levulinic acid and gamma-valerolactone using solid acid catalysts," *Catalysis Science Technology*, 3, 927–931 (2013).
69. Cortright, R., Davda, R., and Dumesic, J., *Nature*, 418, 964–967 (2002).
70. West, R., Kunkes, E., Simonetti, D., and Dumesic, J., *Catalyst Today*, 147, 115–125 (2009).
71. Sasaki, M.K., Goto, K., Tajima, K., Adschiri, T., and Arai, K., *Green Chemistry*, 4, 285–287 (2002).
72. Climent, M., Corma, A., Iborra, S., Epping, K., and Velty, A., *Journal of Catalysis*, 225, 316–326 (2004).
73. Barrett, C., Chheda, J., Huber, G., and Dumesic, J., *Applied Catalysis B: Environmental*, 66, 111–118 (2006).
74. Di Cosimo, J., Torres, G., and Apesteguia, C., *Journal of Catalysis*, 208, 114–123 (2002).
75. Nikolopoulos, A., Jang, B., and Spivey, J., *Applied Catalysis A: General*, 296, 128–136 (2005).

76. Renz, M., *European Journal of Organic Chemistry*, 6, 979–988 (2005).
77. Corma, A., Renz, M., and Schaverien, C., *ChemSusChem*, 1, 739–741 (2008).
78. Dooley, K., Bhat, A., Plaisance, C., and Roy, A., “Ketones from acid condensation using supported CeO<sub>2</sub> catalysts: Effect of additives,” *Applied Catalysis A: General*, 320, 122–133 (2007).
79. Serrano-Ruiz, J. and Dumesic, J., *Green Chemistry*, 11, 1101–1104 (2009).
80. Gayubo, A., Aguayo, A., Atutxa, A., Aguado, R., and Bilbao, J., *Industrial & Engineering Chemistry Research*, 43, 2610–2618 (2004).
81. West, R., Braden, D., and Dumesic, J., *Journal of Catalysis*, 262, 134–143 (2009).
82. Blommel, P., Keenan, G., Rozmiarek, R., and Cortright, R., *International Sugar Journal*, 110, 672 (2008).
83. Kunkes, E., Gurbuz, E., and Dumesic, J., *Journal of Catalysis*, 266, 236–249 (2009).
84. Gurbuz, E., Kunkes, E., and Dumesic, J., *Green Chemistry*, 12, 223–227 (2010).
85. Gurbuz, E., Kunkes, E., and Dumesic, J., *Applied Catalysis B: Environmental*, 94, 134–141 (2010).
86. Huber, G., Cortright, R., and Dumesic, J., *Angewandte Chemie International Edition*, 43, 1549–1551 (2004).
87. Blommel, P., “Catalytic conversion of carbohydrates to hydrocarbons,” DOE Biomass R&D TAC Meeting, May 19, Washington, DC (2011).
88. Held, A., “Production of renewable aromatic chemicals using Virent’s catalytic bioforming process,” Frontiers in Biorefining, October 19–22, St. Simons Island, GA (2010).
89. “Hydrogen generation from waste antifreeze via the BioForming process,” VIRENT Co., 11th Electrochemical Power Sources, July 16, Baltimore, MD (2009).
90. Chang, C., “Mechanism of hydrocarbon formation from methanol,” *Studies in Surface Science and Catalysis*, 36, 127–143 (1988).
91. Chang, C., “Methanol to gasoline and olefins,” *Chemical Industries*, 57, 133–173 (1994).
92. Chang, C., Lang, W., and Silvestri, A., “Conversion of carbonyl compounds to aromatics,” US Patent No. 3,907,915 (1975).
93. Chang, C. and Silvestri, A., “MTG: Origin, evolution, operation,” *CHEMTECH*, 17 (10), 624–631 (1987).
94. De Klerk, A., Nel, R., and Schwarzer, R., “Oxygenate conversion over solid phosphoric acid,” *Industrial & Engineering Chemistry Research*, 46 (8), 2377–2382 (1998).
95. Goguen, P., Xu, T., Barich, D.H., Skloss, T.W., Song, W., Wang, Z., Nicholas, J.B., and Haw, J.F., “Pulse-quench catalytic reactor studies reveal a carbon pool mechanism in methanol to gasoline chemistry on zeolite HZSM-5,” *Journal of the American Chemical Society*, 120 (11), 2650–2651 (1998).
96. Chheda, J., Huber, G., and Dumesic, J., “Liquid phase catalytic processing of biomass derived oxygenated hydrocarbons to fuels and chemicals,” *Angewandte Chemie International Edition*, 46 (38), 7164–7183 (2007).
97. Holmgren, J. and Arena, B., “Solid base as catalysis in aldol condensation,” US Patent No. 5,254,743 (1993).
98. King, F., Kelly, G., and Stitt, E., “Improved base catalysts for industrial condensation reactions,” *Studies in Surface Science and Catalysis*, 145, 443–446 (2003).

---

# 7 Biofine Hydrolysis Process and Derivative Product Upgrading Technologies

## 7.1 INTRODUCTION

Cellulose is the most abundant raw material on the Earth exceeding at any given time known fossil fuel reserves. Its annual production is estimated to be around 100 billion tons [1–8] (Fitzpatrick, 2011, pers. comm.). Unlike fossil fuels, cellulose is renewable: Using modern forestry techniques to grow short-rotation hybrid tree species such as willow or poplar, sustainable wood yields up to 10 dry tons per acre per year have been predicted [2–5]. Furthermore, in the United States, about 250 million tons of municipal solid waste (MSW) per year is discarded, 50% of which is cellulosic in nature. Globally, this number will shortly exceed one billion tons per year. Thus, the biomass could be a primary source of energy, chemicals, and materials for the United States and the rest of the world. It is estimated that using the current one-third of forest and marginally arable land for the production of short-rotation hybrid species or grassy energy crops such as switchgrass, it would be possible to supply all transportation needs and a large fraction of petrochemical needs from woody biomass sources [5–7] (Fitzpatrick, 2011, pers. comm.). Replacing fossil fuels by these sources will also have enormous environmental benefits because the use of biomass is carbon dioxide neutral and will be favorable to the issue of global warming. Also, the cellulosic fraction of MSW is most difficult to recycle, and making its use for energy and products will also help the environment (Fitzpatrick, 2011, pers. comm.).

In this chapter, we outline a novel aqueous-phase “Biofine process,” which is an acid hydrolysis process to convert cellulose to levulinic acid (LA), a platform chemical with dozens of known potential use for both fuels and chemicals. Formic acid is a coproduct of the LA. Furfural is also produced if the feedstock contains hemicellulose pentosan polymer. The basic features of the Biofine process are as follows [8–11]:

1. Biofine is a simple thermochemical process allowing the conversion of cellulose and hemicellulose from a wide variety of sources.
2. Biofine is an acid hydrolysis process, which can be used for the feedstock containing up to 50% water without significantly affecting the overall

system economics. This also alleviates the need for water removal from the feedstock, which can be costly and cumbersome.

3. The process does not require lengthy pretreatment, enzymatic hydrolysis, or fermentation. The reaction occurs in minutes rather than days resulting in lower capital costs, smaller physical footprint, and larger production rate.
4. No specially designed bugs or microorganisms are required, thus lowering the costs and eliminating the risks from contamination and biological stability. The entire process is purely a chemical process.
5. One of the greatest strengths of the process is its ability to process a variety of feedstock. Any input furnished with sufficient cellulose or other carbohydrates is a suitable feedstock including low-value forest residues, whole tree chips, agricultural residues, food wastes, recycled paper, and sorted MSW.
6. Gasification processes that convert biomass into gas and then catalyze the gas into liquid fuels via Fischer–Tropsch synthesis can be hindered by the high natural variability in biomass. The Biofine process, however, can handle most cellulosic-based biomass without significant changes in the process.
7. One of the drawbacks of the fermentation technology is that a very effective enzyme and microbes for conversion of five-carbon sugars such as xylose and pentose has not yet been found. The Biofine process works well for both six-carbon (glucose) and five-carbon (xylose) sugars.
8. The cellulose fraction is broken down to form two coproducts: LA and formic acid.
9. The hemicellulose fraction is broken down into furfural, which can be delivered as a product with many other applications or can be chemically converted to LA.
10. Lignins, along with some degraded cellulose and hemicellulose and any inert components of the feed, come out of the process as a carbon-rich char mixture that can be burned to produce steam and power for the process or can be further converted to products such as carbon black, activated carbon, or carbon fiber.

In sum, the Biofine process is operated as a two-stage continuous process that allows the complete breakdown of cellulosic and starchy feedstock to LA, formic acid, furfural, and ligneous char in sufficiently high yield to be economically attractive. The typical operating conditions of the Biofine process are as follows: the temperature in the range of 190°C–220°C, the acid concentration in the range of 1–5 wt%, and the residence time in the order of 15 min overall [8–11] (Fitzpatrick, 2011, pers. comm.). The primary products are potent “platforms” for other valuable products including fuels and chemicals. The major features of the Biofine process are schematically illustrated in Figure 7.1 [12].

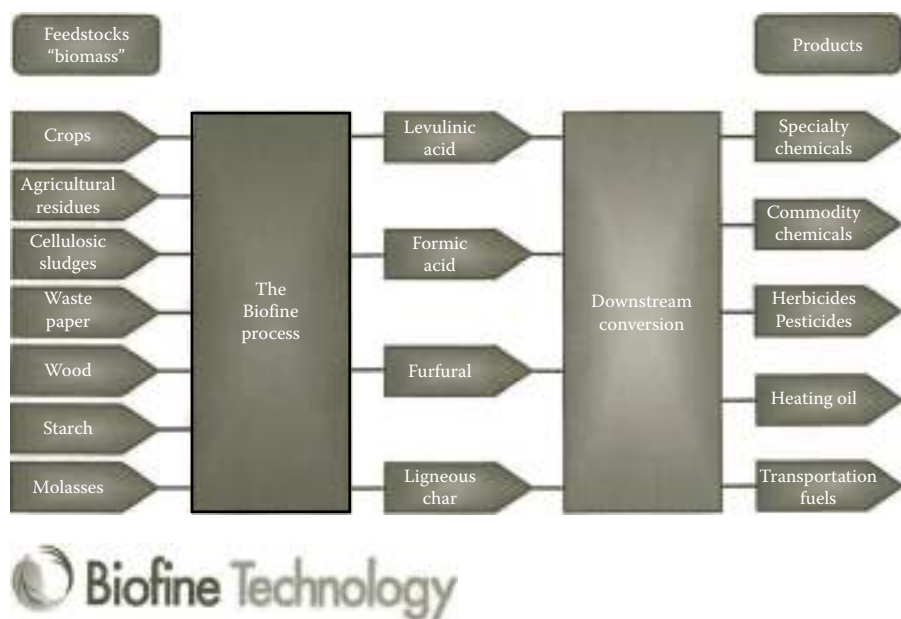


**FIGURE 7.1** (See color insert.) A schematic of the overall Biofine process that includes product upgrading. (From Fitzpatrick, S. and Nace, P., “Biofine Technology, LLC: Renewable chemicals and biofuels,” Paper presented for Sustainable Bioplastics Council of Maine, 2012. With permission.)

## 7.2 THE HYDROLYSIS PROCESS

The Biofine process uses one of the most advanced and commercially viable lignocellulosic-fractionating technologies that are currently available. The process involves the acid hydrolysis of polysaccharides to their monomeric constituents, and these are then used to produce valuable platform chemicals such as furfural, LA, and gamma-valerolactone (GVL). The major polysaccharides of importance in biomass are the glutans and hemicelluloses. Glucans (which are carbohydrate homopolysaccharides consisting of repeated D-glucopyranose units) largely contain starch and cellulose [8–11] (Fitzpatrick, 2011, pers. comm.).

The hydrolysis of starch using alpha-amylase and glucoamylase enzymes can be carried out with relative ease and high efficiency. This is because, as shown in Figure 7.2, alpha(1 → 4) linkages in the amylose component of starch and alpha(1 → 6) amylopectin branches in the starch are easy to break as there is no internal hydrogen bonding preventing the breakage [8]. This has allowed the production of ethanol from grains (94% from corn) to the level of 1.48 billion gallons in the United States in 2011. The hydrolysis and fermentation of cellulose, however, is about 100 times more difficult than that of starch due to the presence of hydrogen bonding as shown in Figure 7.2. Cellulose is much more abundant than starch and requires less energy to produce than starch crops [1–8] (Fitzpatrick, 2011, pers. comm.).

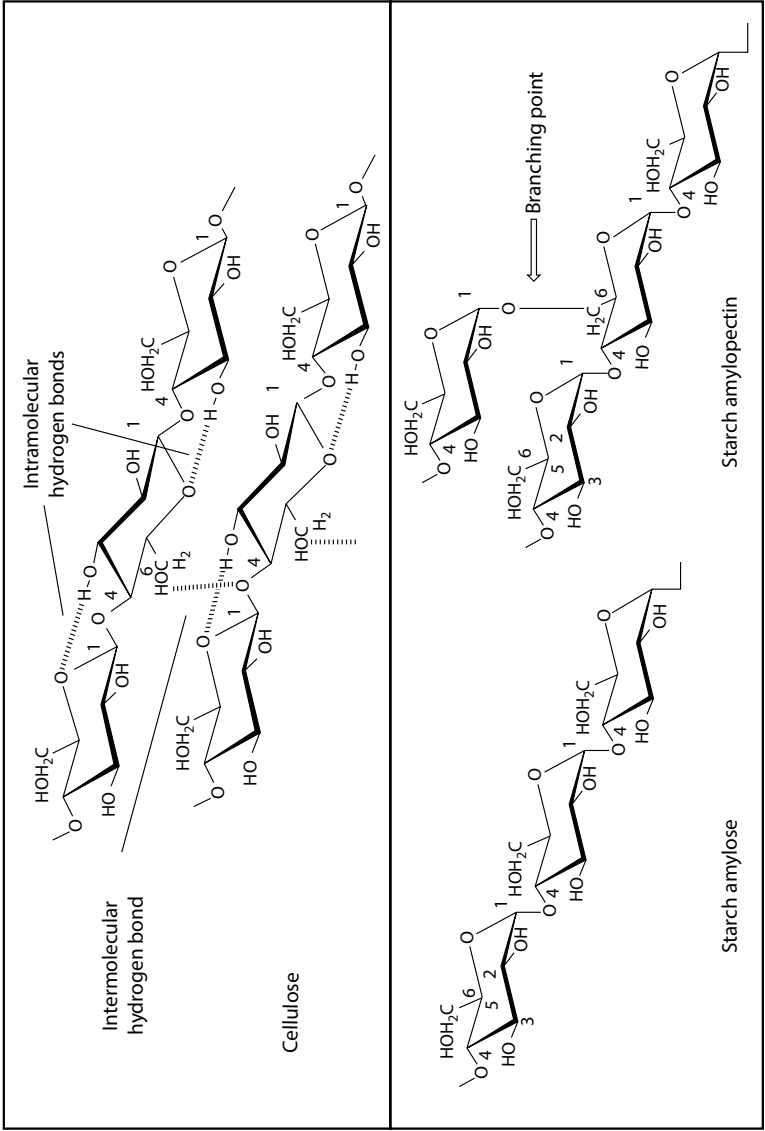


**FIGURE 7.2** Physical structure of cellulose and starch amylose and amylopectin. (From Hayes, D., Ross, J., Hayes, M., and Fitzpatrick, S., “The Biofine process: Production of levulinic acid, furfural and formic acid from lignocellulosic feedstocks,” in *Biorefinery (8b) Industrial Processes and Products: Status Quo and Future Directions*. Wiley, New York, 2008. With permission; Fitzpatrick, S. and Nace, P., “Biofine Technology, LLC: Renewable chemicals and biofuels,” Paper Presented for Sustainable Bioplastics Council of Maine, 2012. With permission.)

The hydrolysis of cellulose can be carried out through attack by the electrophilic hydrogen atoms in the water on the glucosidic oxygen (Figure 7.2). This is, however, a very slow reaction. The reaction can be accelerated using high temperatures and pressures, and acid (dilute or concentrated) as a catalyst, or by highly selective enzymes such as cellulases. The reaction path for acid-catalyzed hydrolysis is identified by Sjöström [13] and Hayes et al. [8], and it generally involves the protonation of the glycosidic oxygen. In this process,  $H^+$  ions equilibrate between the O atoms in the system such that there is an equilibrium concentration of protonated glucoside. The equilibrium shifts more toward the protonated form of glucoside as the temperature increases. The protonated conjugate acid then slowly breaks down to the carbonium ion, and after a rapid addition of water, free sugar is liberated [8]. Because sugar competes with water, a small amount of disaccharides is also produced by the reverse reaction. In general, the reaction requires a longer time, but this can be reduced with the use of larger concentrations of acids. The temperature, pressure, time, and acid concentration can be economically optimized. The ash content of feedstock is important because it lowers the acidity of the mixture, thus requiring higher amount of acid making the process less economical [13,14].

The reaction paths of the two-stage hydrolysis process are schematically described in Figure 7.3 [8,12]. As shown in the figure, the hydrolysis process follows a fast set

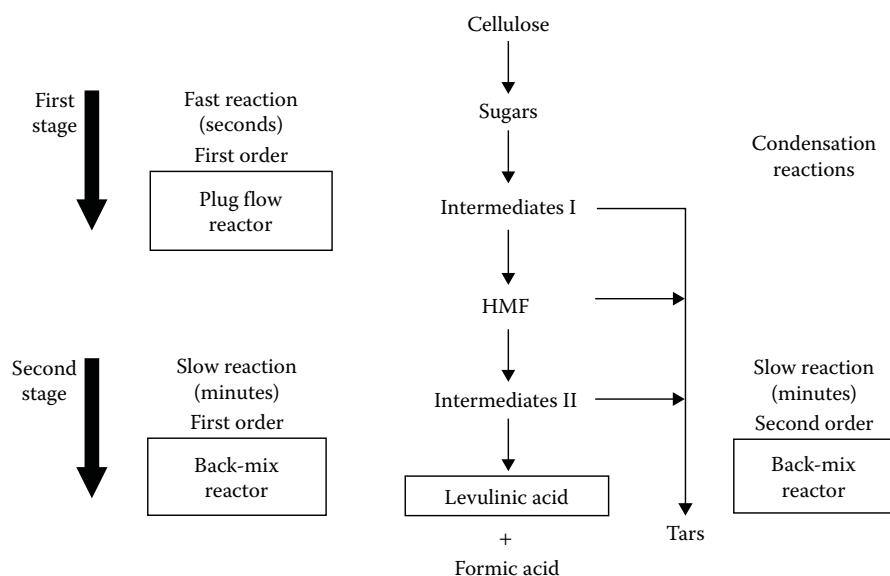


**FIGURE 7.3** Chemical conversion of cellulose to LA (major product), formic acid (by-product), and tars (minor condensation products) in the two-stage Biofine hydrolysis process. (From Fitzpatrick, S. and Nace, P., “Biofine Technology, LLC: Renewable chemicals and biofuels,” Paper presented for Sustainable Bioplastics Council of Maine, 2012. With permission; Hayes, D., Ross, J., Hayes, M., and Fitzpatrick, S., “The Biofine process: Production of levulinic acid, furfural and formic acid from lignocellulosic feedstocks,” in *Biorefinery (8b) Industrial Processes and Products: Status Quo and Future Directions*. Wiley, New York, 2008. With permission.)

of reactions followed by a slow set of reactions. Both steps generate a large number of intermediates. These intermediates produce tars via the second-order condensation reactions along with the main products (hydroxymethylfurfural [HMF] in the first stage and LA and formic acid in the second stage). Short reactor residence time is important for the first rapid kinetic step and good mixing is important for the kinetically controlled second reaction.

The detailed flow diagram for the entire process is illustrated in Figure 7.4 [12]. The process can use a variety of biomass such as wood and crops; cellulosic wastes such as waste paper, cellulosic sludges, and agriculture residues; and carbohydrates such as starch and molasses. The solid feedstock is shredded to reduce its particle size to 0.5–1.0 cm. This ensures an efficient hydrolysis and an optimum yield of the desired products. This shredded feedstock is mixed with fresh and recycled dilute sulfuric acid (1.5–3.0 wt%) solution. The acid concentration can be adjusted depending on the requirement based on the nature of the feedstock and rest of the process conditions. Sulfuric acid acts as a catalyst for the hydrolysis process. The hydrolysis process differs from other similar processes in that free monomeric sugars are not the products. Instead, six- and five-carbon monosaccharides undergo multiple acid-catalyzed reactions to give the platform chemicals furfural, LA, and formic acid along with ligneous char.

As shown in Figure 7.4, the hydrolysis process is carried out in two distinct acid-catalyzed stages that are operated to give optimum yields with a minimum degradation of products and tar formation. The first fast reaction produces HMF and is carried out in a plug flow reactor, whereas the second slow reaction of HMF hydration to form LA is carried out in a back-mixed reactor. The first stage is carried out at 210°C–220°C and pressure of 25 bar, and the reaction lasts only for 12 s. The reaction is the first-order acid hydrolysis of carbohydrate polysaccharides to their soluble intermediates. The second reactor is operated at 190°C–200°C and pressure of 14 bar, and the reaction takes about 20 min [8]. As mentioned earlier, along with the desired products, the intermediates in both reactors and HMF produce tars by the second-order condensation reactions. After the second stage, furfural and other volatile products are removed, and levulinic and formic acids are separated from water by the dehydration unit. The separated acid solution is recycled back to the feed unit. LA (4-oxopentanoic acid) is recovered by boiling under reduced pressure and further purified in a product refining stage. Ligneous char is bone-dried and recovered separately both from product separation and product refining stage. The maximum theoretical yield of LA from a hexose is 71.6 wt% and the remainder is formic acid [15].

HMF is an intermediate product formed in the first stage of the process. A series of consecutive reactions that occur to produce HMF have been established by numerous studies that aimed at the identification of intermediate products and analyses of pathways for their further transformation [9]. These reactions involve dehydrations of six-carbon compounds such as D-glucose, D-mannose, and D-fructose to form enediol, which undergoes a series of further dehydration reactions to form 3,4-dideoxyglucosulosene. This substance is readily converted to dienediol that eventually forms HMF [16,17].

The five-carbon sugar, namely, xylose and pentose, is produced by substituting CH<sub>2</sub>OH group of the hexoses by hydrogen. The hydrolysis of xylose and pentose

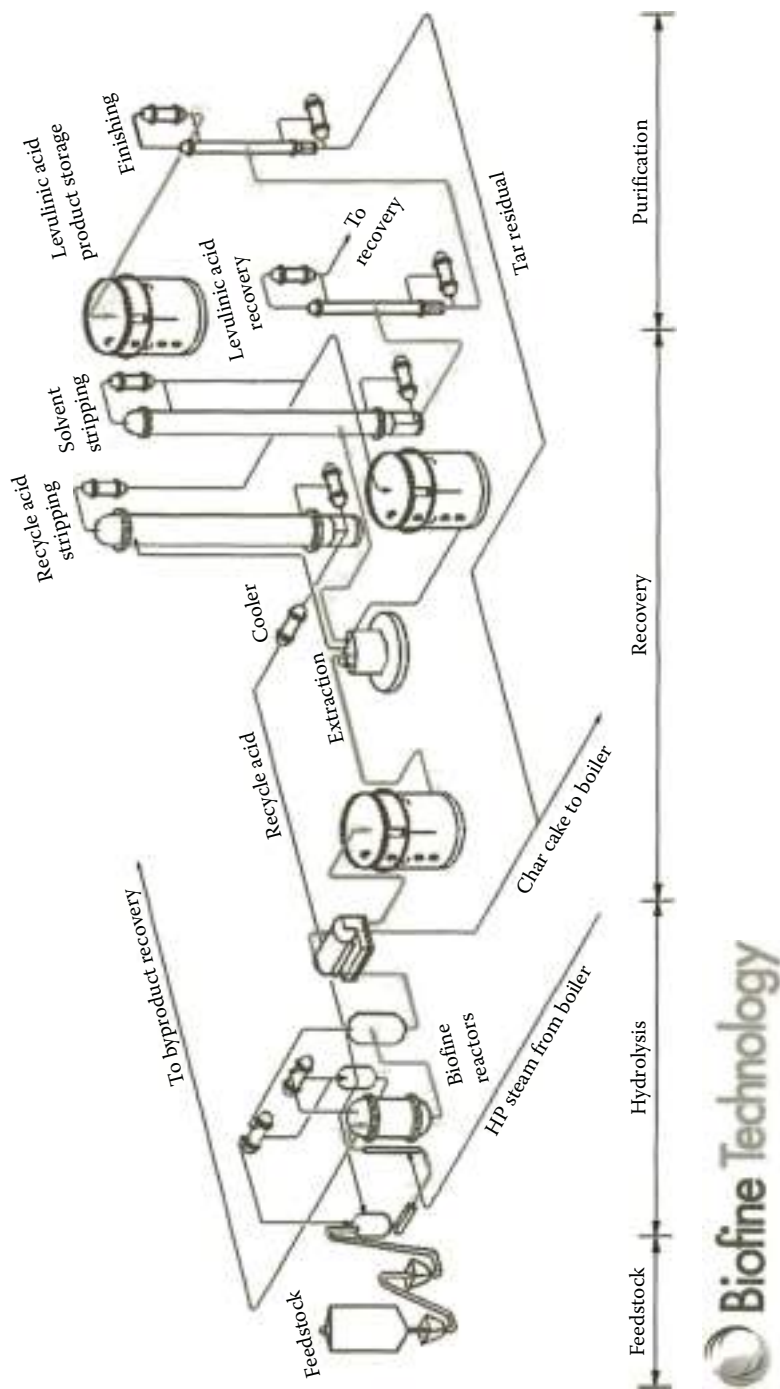


**FIGURE 7.4** (See color insert.) A complete process flow diagram of the Biofine process. (From Fitzpatrick, S. and Nace, P., “Biofine Technology, LLC: Renewable chemicals and biofuels,” Paper presented for Sustainable Bioplastics Council of Maine, 2012. With permission.)

will result in the final product HMF. Hydration of HMF by addition of a water molecule to the  $C_2-C_3$  olefinic bond of the furan ring leads to an unstable tricarbonyl intermediate [18], which decomposes to the LA [13] and formic acid [8]. While the intermediates proposed and some of the reaction steps identified by Sjostrom [13], Klass [18], and Hayes et al. [8] are not completely proven, they were proposed by Horvat et al. [19,20] based on the  $^{13}C$  nuclear magnetic resonance (NMR) spectra of the reaction mixture formed in the hydration of HMF. The reaction paths discussed earlier indicate that both five- and six-carbon sugars can be converted to LA by the appropriate hydrolysis process chemistry. This makes the process more attractive than sugar fermentation process in which the conversion of five-carbon sugar by enzymatic fermentation is problematic [8,21].

The actual hydrolysis process involves many degradation reactions producing many intermediates. Some authors have estimated more than 100 such intermediates [19,20]. These intermediates tend to cross-react and ultimately coalesce (partly by a series of condensation reactions) to form an acid-resistant tar, which incorporates many insoluble residues such as humins. The overall objective of the Biofine process is to minimize the degradation and subsequent condensation reactions that produce tar and increase the yield of LA. An improved reactor system and the use of polymerization inhibitors can provide LA yields of up to 70%–80% of the theoretical yield. This means that a typical product distribution will have about 50% LA, 20% formic acid, and about 30% tar for six-carbon sugars. The mass yield of furfural from five-carbon sugars is about 50% of the original mass, the remainder being incorporated in the Biofine char. These data are supported by the pilot-scale experiments from the Biofine process at Glens Falls, New York [8]. The pilot plant that is in operation since 1996 has used numerous feedstock including paper sludges from the paper mill.

Biofine char contains ash and acid-insoluble ligneous materials. The properties of char can be changed and optimized using high-temperature and high-pressure cracking. Feedstock that contains high amount of extractive such as barks (that may contain up to 25% fats, waxes, and terpenes) or a large amount of water-soluble carbohydrates will have those components largely end up in Biofine char [8,22]. While these components reduce the overall yield per unit biomass processed, they improve the heating value of char when the char is combusted [8,22].

The hydrothermal conversion of biomass to LA in the presence of homogeneous acid catalysts was also examined by Galletti et al. [23]. They examined different types of cheap raw materials such as poplar sawdust, paper mill sludge, tobacco chops, wheat straw, and olive tree pruning. The yield of LA was improved by optimization of the operating parameters such as the type and amount of acid catalysts, temperature, reactor residence time, biomass concentration, and electrolyte addition. The catalytic performances were also improved by the use of microwave radiation for heating the system. The microwave heating required less time for heating and was more energy efficient. The hydrothermal conversion of inulin and wheat straw was also examined in the presence of niobium phosphate catalyst.

The experimental data reported by Galletti et al. [23] showed that for both hydrochloric and sulfuric acid solutions in water, the favorable yields of LA were obtained. For wheat straw with hydrochloric acid at 200°C and residence time of 1 h, the yields for LA based on the cellulose content varied from 49% to 55% and the theoretical

yields varied from 69% to 77%. For tobacco chops, lower yields were obtained for sulfuric acid solution (about 13%–14% based on the cellulose content and 17%–21% based on the theoretical yield) than for hydrochloric acid solution (about 21% to as high as 59% based on the cellulose content and 29%–82% based on the theoretical yield). The optimization of the main operating parameters mentioned earlier allowed an increase of yield up to 83% of the theoretical yield. The use of microwave improved the catalyst performance with significant energy and time saving. The hydrothermal conversion of soluble inulin and wheat straw/water slurry to LA in the presence of a heterogeneous niobium phosphate catalyst also gave favorable results.

### 7.3 UPGRADING OF INTERMEDIATE PRODUCTS FROM THE BIOFINE PROCESS

Three most important products resulting from the hydrolysis of cellulosic materials are furfural (or HMF), LA, and GVL. The process also produces two coproducts: formic acid and ligneous char. Both of them have significant market values. Furfural is produced from the hydrolysis of five-carbon sugars and LA is produced from the hydrolysis of six-carbon sugars as well as from HMF. The GVL is produced from LA and it is a very good feedstock for various kinds of fuels. LA produced from the Biofine process has two highly reactive functional groups (as shown in Figure 7.6) that allow a great number of synthetic transformation. LA is readily soluble in water, alcohols, esters, ketones, and ethers. It can react as both a carboxylic acid and a ketone [24–27]. Due to the special relationship of the carboxylic and ketone groups, many of the reactions proceed with cyclization to form heterocyclic molecules such as methyltetrahydrofuran (MTHF). A vast number of derivatives are possible from the LA as a platform chemical [24–27]. As shown by Hayes et al. [8] and others [23–28], the intermediate products from the Biofine process, namely, LA, formic acid, furfural, and char containing lignin, can be upgraded to numerous products that can be used in five separate markets [8,23–28]:

#### 1. *Energy and Fuel Industries*

The products can be upgraded and used for heating and turbine fuels, gasifier fuels, and electric power. In this respect, Biofine char has a significant heating value. The products can also be upgraded to make MTHF, methyl and ethyl levulinate (fuel additives), jet fuel, fuel esters, and hydrocarbons useful for fuel industries.

#### 2. *Specialty Chemical, Pharmaceutical, and Polymer Industries*

LA, angelica lactone, delta-aminolevulinic acid (DALA), ketals, and others are used for specialty chemical and pharmaceutical products. The products can also be upgraded to monomers and polymers such as epoxies, polycarbonates, diphenolic acid (DPA), GVL, tetrahydrofuran (THF), succinic acid, and furans.

#### 3. *Agricultural Industry*

The coproducts such as formic acid and the upgraded products such as DALA and DPA have agricultural usages. Biochar can be used as a soil conditioner.

#### 4. *Transportation Industry*

A number of products such as CMA (calcium magnesium acetate), carbon, sodium, succinic acid, DALA, and levulinate can also be used in the transportation industries.

#### 5. *Chemical Industry*

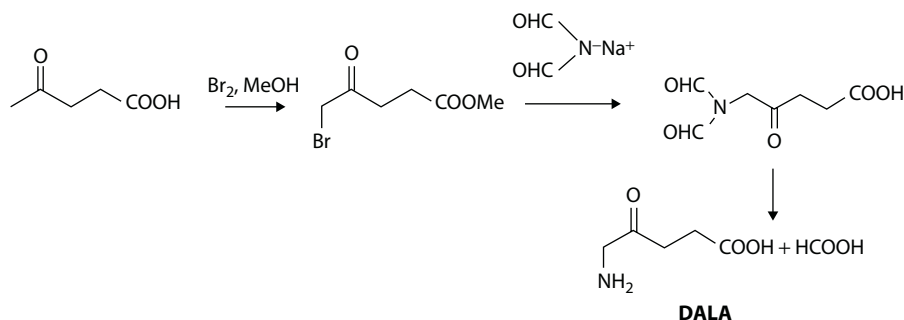
Both coproducts and upgraded products have significant values as general chemical solvents. These include coproducts such as formic acid and furfural, as well as upgraded and byproducts such as *N*-methylpyrrolidinone (NMP), pyridine, gamma-butyrolactone (GBL), pentanediol, THF, succinic acid, and ethyl formate.

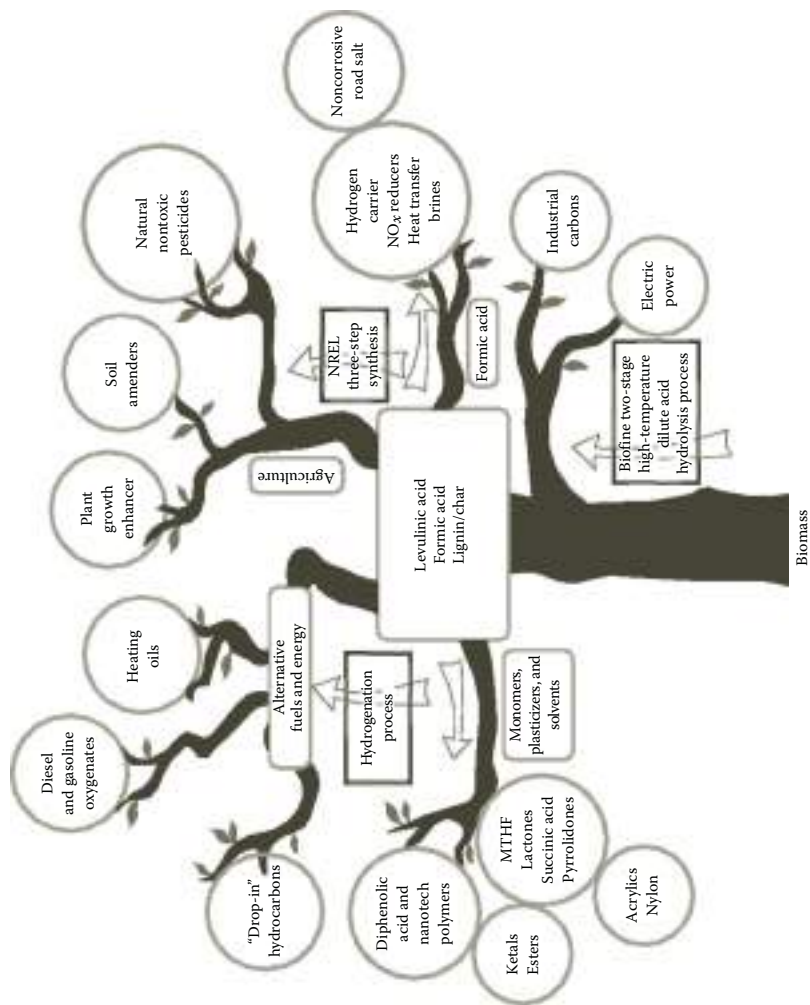
Various end products formed from the conversion of LA, formic acid, and ligneous char are graphically illustrated in Figure 7.5 [12]. In Sections 7.3.1 through 7.3.5, we briefly examine some of the upgrading strategies for the products (LA, formic acid, furfural, GVL, and char) of the Biofine hydrolysis process. These strategies closely follow the excellent article by Hayes et al. [8] and others [12,23–42].

### 7.3.1 TRANSFORMATION OF LEVULINIC ACID

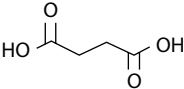
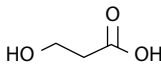
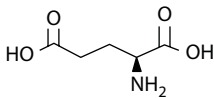
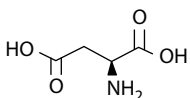
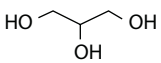
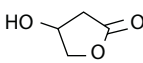
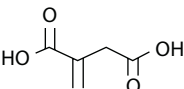
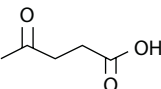
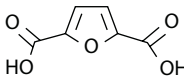
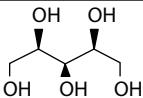
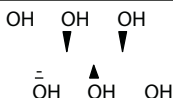
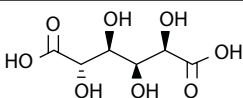
As shown in Figure 7.6 [12], the Department of Energy has identified LA as one of the 12 important platform chemicals produced from biomass. LA can be transformed into a number of important industrial chemicals, fuel additives, or platform chemicals for fuels. For example, the reaction of LA with two molecules of phenol produces DPA [27], a material that can be substituted for bisphenol A (BPA) in polycarbonates, epoxy resins, polyarylates, and other polymers. The use of DPA can also reduce the cost of lubricants, adhesives, and paints [10]. The succinic acid obtained from the oxidation of LA is very useful for food additives, soldering fluxes, and pharmaceutical products. Succinic acid can also be used to produce THF, 1,4-butanediol, and GBL. Both THF and GBL are also very important intermediate chemicals [8]. THF, a cyclic ether, is useful for the production of polytetramethylene ether glycol, a component of polyurethane stretch fibers, and it is also used as a reaction solvent for the poly(vinyl chloride) (PVC) cements, pharmaceuticals, and coatings. GBL is used for the production of pyrrolidone solvents, pesticides, herbicides, and plant growth regulators [8].

Another important product from LA is DALA, which is an active ingredient in a broad spectrum of herbicides. It is also used as an insecticide and for cancer treatment [44]. The most efficient way of making DALA from LA is [8,10]





**FIGURE 7.5** (See color insert.) Biorefinery products “family tree.” (From Fitzpatrick, S. and Nace, P., “Biofine Technology, LLC: Renewable chemicals and biofuels,” Paper presented for Sustainable Bioplastics Council of Maine, 2012. With permission.)

 Succinic acid	 3-Hydroxypropionic acid	 Glutamic acid
 Aspartic acid	 Glycerol	 4-Hydroxybutyrolactone
 Itaconic acid	 Levulinic acid	 2,5-Furandicarboxylic acid
 Xylitol	 Sorbitol	 Glucaric acid



**FIGURE 7.6** (See color insert.) “Select 12” platform chemicals from biomass as identified by the Department of Energy. (From Fitzpatrick, S. and Nace, P., “Biofine Technology, LLC: Renewable chemicals and biofuels,” Paper presented for Sustainable Bioplastics Council of Maine, 2012. With permission.)

The National Renewable Energy Laboratory (NREL) mechanism produces two moles of formic acid per mole of DALA. Significant research for the production of cheap DALA is being pursued because it has a large potential in agricultural and horticultural industries.

While LA is an important platform chemical for many products of industrial values, its greatest potential is in the production of fuel additives. MTHF obtained from LA can be added up to 30% by volume with petroleum with no adverse effects on performance and requires no engine modifications. Esters of LA produced by methanol or ethanol have a significant potential as blend components in diesel formulation. LA esters (ethyl and methyl levulinate) are similar to fatty acid methyl esters (FAMES), and addition of ethyl or methyl levulinate to FAME alleviates cold flow properties and gum formation of FAME [45]. Ethyl levulinate made from LA and fuel-grade ethanol is one of the most important oxygenate additives to diesel fuel, and its addition in diesel (by 20%) gives a significantly cleaner burning diesel fuel [46]. The ethyl levulinate and diesel blend also gives lower sulfur emission and higher lubricity compared to regular diesel. The levulinate esters can also replace kerosene as a home-heating oil and can be used as a fuel for the direct firing of

gas turbines for electrical generation [47]. The production of LA esters from LA produced by the Biofine process has an added advantage that this method does not produce glycerol as coproduct that needs to be disposed.

LA can be converted to GVL by dehydration to angelica lactone and subsequent reduction or by reduction to 4-hydroxy-pentanoic acid and subsequent dehydration. These reductions are carried out at relatively low temperatures (373–543 K) and high pressures (50–150 bar), and both homogeneous and heterogeneous catalysts can be employed [48]. The highest yield of GVL (97%) was obtained at 423 K and 34.5 bar using Ru/C catalyst and dioxane as solvent [49]. The external hydrogen is often replaced by formic acid that acts as a hydrogen donor solvent. More recently, GVL has also been produced by integrating hydrolysis/dehydration/hydrogenation of carbohydrates in a single vessel [48,50]. LA can also be catalytically hydrogenated to GVL, which upon further hydrogenation yields 1,4-pentanediol and finally MTHF [10,32]. The reaction is carried out at an elevated temperature of 240°C and a pressure of 100 atm. This method uses trifluoroacetic acid as a hydrolysis medium due to the poisoning of Ru/C catalyst by sulfuric acid. Fructose and sucrose gave better yields of GVL than glucose and cellulose when formic acid as a hydrogen donor solvent and external hydrogen are used [8].

MTHF insertion in a blend (gasoline and ethanol) has led to the creation of P-series fuels. These types of fuels can be either used alone or mixed with any proportions with gasoline [8]. These types of fuels reduce ozone-forming potential and reduce emission of non-methane hydrocarbons and total hydrocarbons. MTHF is also an excellent solvent (better than THF) and can also be produced from furfuryl alcohol [8]. Dimethyl THF can also be produced from HMF.

### 7.3.2 GAMMA-VALEROLECTONE

GVL is a versatile platform chemical, which can be used as a fuel additive, a solvent, or a reactant for diverse upgrading strategies for the production of fuels and chemicals [51]. GVL's low-energy density, blending limits, and high solubility in water limit its use as a direct fuel. GVL needs to be separated from water, or an aqueous solution of GVL should be processed to produce hydrophobic liquid alkanes with an appropriate molecular weight to be used as liquid fuels.

Dumesic et al. [29–42] have outlined some of the alternatives for converting GVL to liquid hydrocarbons. Serrano-Ruiz et al. [52] have shown that the aqueous solution of GVL (50 wt%) can be upgraded to C<sub>9</sub> hydrocarbons by ring opening to produce pentenoic acids and subsequent hydrogenation to produce pentanoic acids [53]; both of these reactions can be catalyzed by water-soluble Pb/Nb<sub>2</sub>O<sub>5</sub> catalysts. The yield of pentanoic acid is controlled by the metal content in the catalyst and the partial pressure of hydrogen. The best yields of pentanoic acid (92%) were obtained with 0.1% Pd at 598 K and 35 bar (50% H<sub>2</sub> and 50% He) [32,54].

The pentanoic acid can be upgraded to 5-nonanone by ketonization over CeZrO<sub>x</sub> at 698 K and pressures from 1 to 20 bar [55]. The hydrogenation/dehydration of 5-nonanone over Pt/Nb<sub>2</sub>O<sub>5</sub> at 528–568 K and 60 bar produces nonane [56]. In the overall process, lower ketones are converted to C<sub>6</sub>–C<sub>7</sub> alkanes that can be removed in the gas phase, and nonane remains in the liquid phase to be used as a blender in diesel fuels [29–42].

Another alternative is to hydrogenate ketones to produce alcohols that can be dehydrated to produce nonene which can be coupled by acid-catalyzed oligomerization [32,57]. Smaller ketones can be converted to alkenes, which also undergo oligomerization to produce the final mixture of  $C_6$ – $C_{27}$  alkenes that can be hydrogenated over Pt/Nb<sub>2</sub>O<sub>5</sub> to produce liquid alkenes to be used as jet fuels or diesel blenders [29–42].

Bond et al. [58] reported that GVL can undergo ring opening to produce pentenoic acid and isomers which subsequently undergo decarboxylation to produce equimolar mixture of butenes and carbon dioxide. Both reactions occur on solid acid catalyst SiO<sub>2</sub>/Al<sub>2</sub>O<sub>3</sub>. The butene monomers products can be coupled by oligomerization over an acid catalyst to form  $C_8^+$  alkenes that can be converted to jet fuels upon hydrogenation. More details of this reaction chemistry are described by Alonso et al. [32].

### 7.3.3 FURFURYL AND HYDROXYMETHYL FURFURYL

Furfuryl is produced from the hemicellulose pentose fractions of biomass. Xylose is the predominant pentose and hemicellulosic arabinose is found to a lesser extent in most of the feedstock. Furfuryl can be sold as a solvent or converted to furfuryl alcohol, which in turn can be converted to THF and LA as shown by Hayes et al. [8]. Furfuryl alcohol is a monomer of furan resins that are mainly used as foundry binders. It is produced by hydrogenation of furfuryl. THF is produced by decarbonylation of furfuryl to furan followed by catalytic hydrogenation [40]. Furfuryl alcohol, when boiled in ethyl methyl ketone in the presence of HCl, gives rise to 90%–93% yield of LA [17].

HMF and furfuryl are also precursors of liquid hydrocarbon fuels and are an option for the production of linear alkanes in the molecular weight range appropriate for diesel and jet fuels. Since furans can be produced from both cellulose and hemicellulose, they utilize the larger fraction of available lignocellulosic feedstock. Furfuryl and HMF can be produced with good selectivity (90%) from xylose and fructose in biphasic reactors; the yields for glucose are lower. The addition of dimethyl sulfoxide (DMSO) improves the selectivity of HMF from fructose. In the presence of water, HMF is readily hydrated to LA and formic acid. Furfuryl can be extracted from water using solvents such as THF, butanol, and methyl isobutyl ketone (MIBK), and by adding salts to the aqueous phase [8,32].

Dumesic et al. [29–42] have shown different strategies to upgrade HMF to liquid fuels. HMF can be converted to DMF over Cu–Ru/C catalyst by hydrogenolysis. DMF can be used as a blender in transportation fuels. Higher hydrocarbons are produced by aldol condensation with ketones. Single condensation of HMF produces  $C_9$  intermediates that can react with HMF again to produce  $C_{15}$  intermediates [32]. The condensation products are hydrogenated and dehydrated over a bifunctional catalyst with metal and acid sites to produce linear  $C_9$  or  $C_{15}$  alkanes that can be easily separated from water [32]. Aldol condensation can be coupled with hydrogenation steps using a bifunctional catalyst such as Pd/MgO–ZrO<sub>2</sub> leading to high yields of condensation products at 326–353 K [59]. The selective hydrogenation of HMF and furfuryl can also be converted to  $C_{12}$  and  $C_{10}$  alkanes through a series of reaction steps involving self-condensation and hydrogenation/dehydration, respectively [32].

### 7.3.4 FORMIC ACID

As shown earlier, the conversion of cellulose to LA produces formic acid as a byproduct. Formic acid produced in this manner can be either directly sold as a commodity or further purified by distillation. As pointed out by Hayes et al. [8], formic acid is a very versatile product and can be used in a number of different ways as indicated below:

1. It can be used as road salt in the form of calcium magnesium formate. It can also be used as a silage additive and a decalcifier as well as an acidulating agent in textile dyeing and finishing and leather tanning [60].
2. Formic acid is a hydrogen donor solvent. It can also be used in catalyst preparation and regeneration of catalyst metals that are poisoned by sulfur.
3. It can be used in the manufacture of organic esters, drugs, dyes, insecticides, and refrigerants. Esters of formic acid can be fuel components and platform chemicals.

Thus, formic acid is a very valuable byproduct of Biofine process.

### 7.3.5 BIOFINE CHAR

Since Biofine char largely contains lignin, the amount of residual char in the Biofine process depends on the acid-insoluble lignin content, along with the ash content, any insoluble protein present, and the amount of degradation and reversion products formed from cellulose and hemicellulose fractions during LA production [8]. As mentioned earlier, extractives and any water-soluble carbohydrates can also be a part of Biofine char. Since boiling of volatiles and LA cracks char, it is difficult to predict the final composition of char [8]. The Biofine char, however, has a significant heating value. This heating value can significantly exceed the heating value of the original biomass with its water content. If the feedstock lignin content is about 25% of biomass, and if the process is larger than 270 tons of feedstock per day, it has been estimated [8] that the energy provided by the residual char is greater than that needed to completely fuel the steam and electric power needs of the biorefinery.

Biofine char is a good soil conditioner. The chars from straw and paper show significant carbonyl/carboxyl and acidic functionalities [8]. The char can also be used to produce syngas via steam gasification/reforming process. This syngas can be converted to various fuels and chemicals via Fischer–Tropsch synthesis.

## 7.4 COMPARISON OF BIOFINE PROCESS WITH OTHER TECHNOLOGIES

### 7.4.1 DIBANET PROJECT

The Development of Integrated Biomass Approaches Network (DIBANET) is a collaborative research project between the European Union and Latin America to produce sustainable diesel miscible biofuels (DMBs) from the residues and wastes

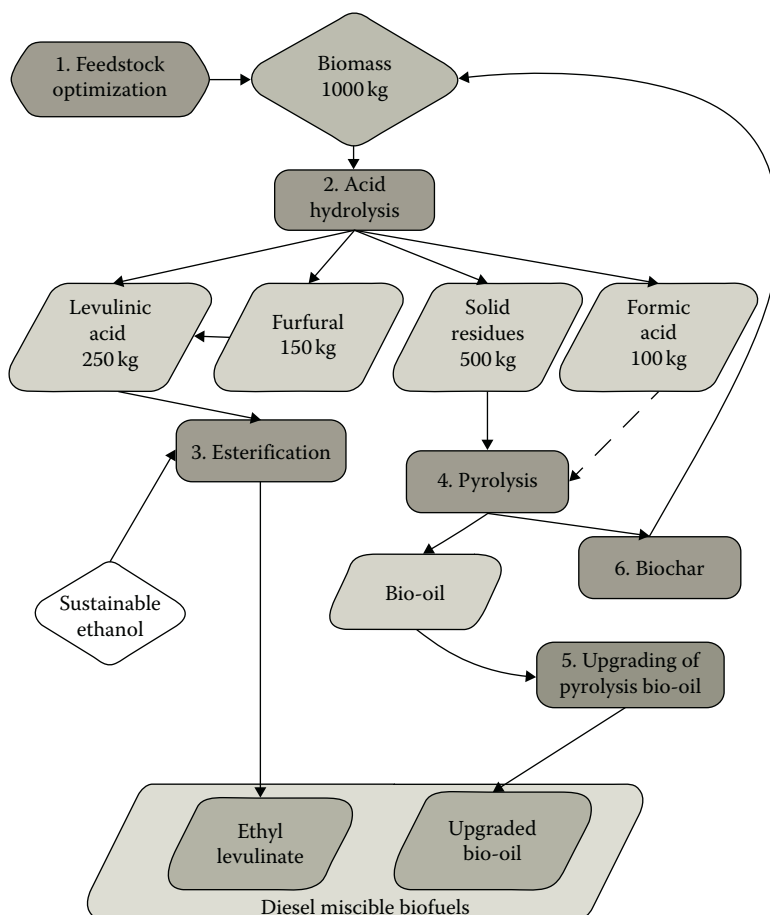


**FIGURE 7.7** (See color insert.) Process chain to produce maximum yields of DMB from organic waste and residue. (From Hayes, D., DiBANET project, 2013. With permission.)

from these places [61–66]. This project is coordinated by Carbolea at the University of Limerick in Ireland. The basic process is graphically illustrated in Figure 7.7. While the process is similar to the Biofine process for the hydrolysis step to produce LA, the subsequent part of the process focuses on the production of ethyl levulinate and bio-oil (via pyrolysis) that will be upgraded to a DMB, which is in compliance with EN 590 requirements. Ethyl levulinate is produced from LA and ethanol via the esterification process. The overall process shown in Figure 7.7 has the following objectives:

1. Optimize the sourcing, selection, and preparation of the feedstock followed by hydrolysis and subsequent degradation of biomass. This step is very similar to that in the Biofine process, and it produces LA, furfural, formic acid, and residue.
2. Produce ethyl levulinate by esterification in the presence of ethanol.

3. Convert solid residue to bio-oil and biochar by pyrolysis. This process can be enhanced by the use of formic acid produced earlier as a coproduct.
4. Upgrade bio-oil with the use of a catalyst to produce upgraded bio-oil that is miscible with diesel.
5. Utilize the biochar as a soil conditioner or to provide fuel for the process.

This project is thus an application of the overall concept of the Biofine process with specifically tailored upgrading of the hydrolysis products. The process is well described by Hayes et al. [61–66] and at <http://www.carbolea.ul.ie/project.php?=dibanet>.

#### **7.4.2 BIOFINE PROCESS VERSUS FERMENTATION PROCESS**

As indicated earlier, Biofine process is a chemical process and does not rely on microorganism or enzymes [68,69]. The biochemical process generally produces only alcohols and can use only a limited range of feedstock, whereas the Biofine process can use a variety of feedstock (containing both five- and six-carbon sugars and starch) and deliver a host of products by a suitable transformation of platform chemicals LA and HMF.

The fermentation process takes about seven days to generate ethanol from cellulose, whereas the Biofine process takes two days for hydrolysis and about 30 min for the production of LA. The fermentation process often gives poor yields due to the inhibition effect of products on enzymes and microbes, whereas no such inhibition occurs in the Biofine process. The fermentation process is also very difficult and economically unattractive for five-carbon sugars such as xylose, whereas these sugars can give up to 50% yield to an important intermediate HMF or furfural in the Biofine process. The contaminants in feedstock such as those in MSW and sewage can significantly inhibit fermentation, whereas the experiments in New York plant has shown that these feedstock can be easily processed by the Biofine process [8]. Finally, the lignin content in biomass can affect the effectiveness of enzymatic process due to steric hindrance caused by lignin–polysaccharide linkages, whereas the same lignin content has no effect on the Biofine process. The lignin content in the enzymatic process limits the access of fibrolytic enzymes to specific carbohydrate moieties and requires steam explosion pretreatment, which adds cost to the overall fermentation process [67]. Fundamentally, all these differences are inherent partly due to the difference in the basic nature of a biochemical (i.e., fermentation) and a chemical (i.e., Biofine process) process.

#### **7.4.3 BIOFINE PROCESS VERSUS BIOFORMING PROCESS**

Another competing technology is the most recently developed “Bioforming process” described in Chapter 6. The basic difference between these two technologies is the reaction path chosen to obtain fuels, fuel additives, and chemicals. As discussed earlier, the Bioforming process can generate both gaseous (hydrogen and syngas) and liquid fuels and chemicals, and in that sense, it offers more product upgrading possibilities. However, the intermediate platform chemicals produced by the Biofine process,



**FIGURE 7.8** Commercial plant in Caserta, Italy. Recovery vessels (top left); outside of building (bottom left); mixing tank (top middle); second reactor (bottom middle); aerial view (right). (From “Fitzpatrick, S., Renewable chemicals and biofuels for sustainable bioplastics council of Maine,” Paper presented by Biofine Technology, LLC, 2012. With permission; Hayes, D., Ross, J., Hayes, M., and Fitzpatrick, S., “The Biofine process: Production of levulinic acid, furfural and formic acid from lignocellulosic feedstocks,” in *Biorefinery (8b) Industrial Processes and Products: Status Quo and Future Directions*. Wiley, New York, 2008. With permission.)

namely, LA and HMF, are extremely versatile in producing a host of end products mentioned earlier. When both the Bioforming and Biofine processes are fully commercialized, they together will offer a wide range of possibilities to generate synthetic fuels and chemicals. Water plays the most important role in both of these processes.

## 7.5 LARGE-SCALE BIOFINE PROCESS

The Biofine technology is commercially viable. A commercial plant processing 50 dry tons of feedstock per day has been operating in Caserta, Italy [8]. The primary feedstock of this plant is paper sludge, agricultural residue, and waste paper with the major products LA and ethyl levulinate (for use as fuel). The process char is gasified to produce a fuel gas for the process boilers. The images of the various parts of the plant are illustrated in Figure 7.8 and this plant has been successfully operating for several years. A number of larger-scale (250 and 1000 tons per day) plants are under considerations in Ireland, the United Kingdom, and the United States.

## REFERENCES

1. Bozell, J.J., *Chemicals and Materials from Renewable Resources*. American Chemical Society, Washington, DC (2001).
2. *Renewable Energy Resources: Opportunities and Constraints 1990–2020*. World Energy Council, London (1993).  
Referred in Bull, S. and Billman, L., “Renewable energy: Ready to meet its promise,” NREL report (December 7, 1998). [www.nrel.gov/docs/legosti/old/25890.pdf](http://www.nrel.gov/docs/legosti/old/25890.pdf)

3. Sterzinger, G., "Making biomass energy a contender," *Technology Review*, 98, 34 (1995).
4. Spedding, C., *Biofuels and the Future*. British Association for Bio Fuels and Oils, Gloucester, MA (2002).
5. Borjesson, P., *Biomass & Bioenergy*, 16, 291, (1999).
6. Paul, S., *Plant/Crop-Based Renewable Resources 2020*, DOE/GO-10098-385. US Department of Energy, Washington, DC (1998).
7. Jarnefeld, J. et al., *Biomass*, 16, 33–49 (1998).
8. Hayes, D., Ross, J., Hayes, M., and Fitzpatrick, S., "The Biofine process: Production of levulinic acid, furfural and formic acid from lignocellulosic feedstocks," in Kamm, B., Gruber, P., and Kamm, M. (eds.), *Biorefinery (8b) Industrial Processes and Products: Status Quo and Future Directions*. Wiley, New York, pp. 139–164 (2008).
9. "Biofine's voyage from the lab to the plant," *Proceedings of the 7th National Bioenergy Conference*, SE Regional Biomass Energy Program, Vol. 2, 1083 (1996).
10. Bozella, J., Moensa, L., Elliott, D.C., Wang, Y., Neuenschwander, G., Fitzpatrick, S.W., Bilskid, R.J., and Jarnefeld, J.L., "Production of levulinic acid and use as a platform chemical for derived products," *Resources, Conservation and Recycling*, 28, 227–239 (2000).
11. Fitzpatrick, S. and Framingham, M.A., "Levulinic acid in organic synthesis," *Russian Chemical Reviews*, 68 (1), 73–84 (1999).
12. Fitzpatrick, S. and Nace, P., "Biofine Technology, LLC: Renewable chemicals and biofuels," Paper presented for Sustainable Bioplastics Council of Maine, April 11, Bangor, ME (2012).
13. Sjostrom, E., *Wood Chemistry: Fundamentals and Applications*. Academic Press, London (1981).
14. Zerbe, J.I. and Baker, A.J., "Investigation of fundamentals of two-stage, dilute sulphuric acid hydrolysis of wood," in Klass, D.L. (ed.), *Energy from Biomass and Wastes X*. Institute of Gas Technology, Chicago, IL, 927–947 (1987).
15. Leonard, R.H., "Levulinic acid as a basic chemical raw materials," *Industrial & Engineering Chemistry*, 48 (8), 1331–1334 (1956).
16. Kooherkov, N.A., Bochkov, A.F., Dimitriev, B.A., Usov, A.I., Chizbov, O.S., and Shibaev, Y.N., *Khimiya Uglevodov (The Chemistry of Carbohydrates)*. Khimiya, Moscow (1967).
17. Timokhin, B.V., Baransky, V.A., and Eliseeva, G.D., "Levulinic acid in organic synthesis," *Russian Chemical Reviews*, 68 (1), 73–84 (1999).
18. Klass, D.L., *Biomass as a Nonfossil Fuel Source*. American Chemical Society, Washington, DC (1981).
19. Horvat, J., Klaic, B., Metelko, B., and Sunjic, V., "Mechanism of levulinic acid formation," *Tetrahedron*, 26, 2111–2114 (1985).
20. Horvat, J., Klaic, B., Metelko, B., and Sunjic, V., "Mechanism of levulinic acid formation in acid-catalyzed hydrolysis of 2-hydroxymethylfuran and 5-hydroxymethylfuran-2-carbaldehyde," *Croatica Chemica Acta*, 59, 429–438 (1986).
21. Lee, S. and Shah, Y.T., *Biofuels and Bioenergy: Processes and Technologies*. CRC Press, New York (2012).
22. USDA, *Bark and Its Possible Uses*. USDA, Madison, WI (1971).
23. Galletti, A., Antonetti, C., de Luise, V., Licursi, D., and Di Nasso, N., "Levulinic acid production from waste biomass," *BioResources*, 7 (2), 1824–1835 (2012).
24. Oono, T., Saito, S., Shinohara, S., and Takakuwa, K., "Fluxes for electric circuit board soldering and electric circuit boards," Japanese Patent No. 0824378 (1996).
25. Shimizu, A., Nishio, S., Wada, Y., and Metoki, I., "Photographic processing method for processing silver halide photographic light-sensitive material," European Patent No. 704756 (1996).
26. Adams, P.E., Lange, R.M., Yodice, R., Baker, M.R., and Dietz, J.G., "Intermediates useful for preparing dispersant-viscosity improvers for lubricating oils," European Patent No. 882745 (1998).

27. Isoda, Y. and Azuma, M., "Preparation of bis(hydroxyaryl)pentanoic acids," Japanese Patent No. 08053390 to Honshu Chemical Industries (1996).
28. Sheldo-Coulson, G., *Production of Levulinic Acid in Urban Biorefineries*. Department of Technology and Policy, MIT, Cambridge, MA (2011).
29. Huber, G.W., Cortright, R.D., and Dumesic, J.A., "Renewable alkanes by aqueous phase reforming of biomass derived oxygenates," *Angewandte Chemie International Edition*, 43, 1549–1551 (2004).
30. Davda, R. and Dumesic, J., "Catalytic reforming of oxygenated hydrocarbons for hydrogen with low levels of carbon monoxide," *Angewandte Chemie International Edition*, 42, 4068 (2003).
31. Cortright, R.D., Davda, R., and Dumesic, J., "Hydrogen from catalytic reforming of biomass derived hydrocarbons in liquid water," *Nature*, 418, 964–967 (2002).
32. Alonso, D.M., Bond, J.Q., and Dumesic, J.A., "Catalytic conversion of biomass to bio-fuels," *Green Chemistry*, 12, 1493–1513 (2010).
33. Huber, G. and Dumesic, J., "An overview of aqueous phase catalytic processes for production of hydrogen and alkanes in a biorefinery," *Catalysis Today*, 111 (1/2), 119–132 (2006).
34. King, D., "Hydrogen production via aqueous phase reforming," Paper presented by Pacific Northwest National Laboratory at NiChE Catalysis Conference, September 21, Washington, DC (2011).
35. Cortright, R.D., "Hydrogen generation from sugars via aqueous phase reforming," *Proceedings of the 16th World Hydrogen Energy Conference*, June 13–16, Lyon, France (2006).
36. Huber, G.W., Shabaker, J.W., and Dumesic, J.A., *Science*, 300, 2075 (2003).
37. Kunkes, E.L., Simonetti, D.A., West, R.M., Serrano-Ruiz, J.C., Gartner, C.A., and Dumesic, J.A., *Science*, 322, 417 (2008).
38. Dunn, S., "Hydrogen futures: Toward a sustainable energy system," *International Journal of Hydrogen Energy*, 27, 235–264 (2002).
39. Huber, G., Iborra, S., and Corma, A., "Synthesis of transportation fuels from biomass: Chemistry, catalysts, and engineering," *Chemical Reviews*, 106, 4044–4098 (2006).
40. Soares, R., Simonetti, D., and Dumesic, J., *Angewandte Chemie International Edition*, 45, 3982–3985 (2006).
41. King, D., "Biomass derived liquids distributed (aqueous phase) reforming," 2012 DOE Hydrogen and Fuel Cells Program Review, Pacific Northwest National Laboratory, Richland, WA (May 17, 2012).
42. Blommel, P.G. and Cortright, R.D., "Production of conventional liquid fuels from sugars," White Paper for European Platform on Biofuels (2012).
43. Rebeiz, C.A., Gut, L.J., Lee, K., Juvik, J.A., Rebeiz, C.C., and Bouton, C.E., "Photodynamics of porphyrin insecticides," *Critical Reviews Plant Science*, 14, 329–366 (1995).
44. Bedwell, J., McRoberts, A.J., Phillips, D., and Brown, S.G., "Fluorescence distribution and photodynamic effect of ALA-induced PP IX in the DMF rat colonic tumor model," *British Journal of Cancer*, 65, 818–824 (1992).
45. Huang, C. and Wilson, D., "Improving the cold flow properties of biodiesel," Paper presented at 91st American Oil Chemists' Society Annual Meeting, April 26, San Diego, CA (2000).
46. Texaco/NYSERDA/Biofine, *Ethyl Levulinate D-975 Diesel Additive Test Program*. Biofine, Glenham, NY (2000).
47. Erner, W.E., "Synthetic liquid fuel and fuel mixtures for oil burning devices," US Patent No. 4364743 (1982).
48. Heeres, H., Handana, R., Chunai, D., Rasrendra, B., Girisuta, B., and Heeres, H., *Green Chemistry*, 11, 1247–1255 (2009).
49. Manzer, L., *Applied Catalysis A: General*, 272, 249–256 (2004).

50. Deng, L., Li, J., Lai, D., Fu, Y., and Guo, Q., *Angewandte Chemie International Edition*, 48, 6529–6532 (2009).
51. Horvath, I., Mehdi, H., Fabos, V., Boda, L., and Mika, L., *Green Chemistry*, 10, 238–242 (2008).
52. Serrano-Ruiz, J., Wang, D., and Dumesic, J., *Green Chemistry*, 12, 574–577 (2010).
53. Ayoub, P. and Lange, J. “Process for converting levulinic acid into pentanoic acid,” World Patent No. WO/2008/142127 (2008).
54. Renz, M., “Ketonization of carboxylic acids by decarboxylation mechanism and scope,” *European Journal of Organic Chemistry*, 6, 979–988 (2005).
55. Serrano-Ruiz, J. and Dumesic, J., *Green Chemistry*, 11, 1101–1104 (2009).
56. Werst, R.M., Liu, Z., Peter, M., and Dumesic, J., *ChemSusChem*, 1, 417–424 (2008).
57. Alonso, D., Bond, J., Serrano-Ruiz, J., and Dumesic, J., *Green Chemistry*, 12, 992–999 (2010).
58. Bond, J., Alonso, D., Wang, D., West, R., and Dumesic, J., *Science*, 327, 1110–1114 (2010).
59. Barrett, C., Chheda, J., Huber, G., and Dumesic, J., *Applied Catalysis B: Environmental*, 66, 111–118 (2006).
60. Bizzari, S. and Ishikawa, Y., *CEH Report: Formic Acid*. SRI, Menlo Park, CA (2001).
61. Girisuta, B., Kalogiannis, K.G., Dussan, K., Leahy, J.J., Hayes, M.H.B., and Stefanidis, S., “An integrated process for the production of platform chemicals and diesel miscible fuels by acid-catalyzed hydrolysis and downstream upgrading of the acid hydrolysis residues with thermal and catalytic pyrolysis,” *Bioresource Technology*, 126, 92–100 (2012).
62. Melligan, F., Dussan, K., Aucaise, R., Novotny, E.H., Leahy, J.J., Hayes, M.H.B., and Kwapinski, W., “Characterisation of the products from pyrolysis of residues after acid hydrolysis of *Miscanthus*,” *Bioresource Technology*, 108, 258–263 (2012).
63. Melligan, F., Aucaise, R., Novotny, E.H., Leahy, J.J., and Hayes, M.H.B., “Pressurised pyrolysis of *Miscanthus* using a fixed bed reactor,” *Bioresource Technology*, 102 (3), 3466–3470 (2011).
64. Hayes, D.J.M., “DIBANET, an integrated approach for making the best use of biomass,” *1st Iberoamerican Congress on Biorefineries*, October 24–26, Los Cabos, Mexico (2012).
65. Hayes, D.J.M., “Review of biomass feedstocks and guidelines of best practice,” DIBANET WP2 Report, 150p (2012).
66. Hayes, D.J., “Protection of NIR calibration equations and their application for biomass analysis,” DIBANET WP2 Report, 71p (2012).
67. Donaldson, L.A., Wong, K.K.Y., and Mackie, K.L., “Ultrastructure of steam-exploded wood,” *Wood Science and Technology*, 22, 103–114 (1988).
68. Fitzpatrick, S.W., “Lignocellulose degradation to furfural and levulinic acid,” US Patent No. 4897497 (1990).
69. Fitzpatrick, S.W., “Production of levulinic acid from carbohydrate-containing materials,” US Patent No. 5608105 (1997).



Taylor & Francis

Taylor & Francis Group

<http://taylorandfrancis.com>

---

# 8 Anaerobic Digestion of Aqueous Waste for Methane and Hydrogen

## 8.1 INTRODUCTION

The global energy usage is growing rapidly due to increasing demands from countries like China, India, Russia, Brazil, Mexico and other developing nations. The report from International Energy Agency (IEA [1]) predicts that global energy demand during this century will increase by two fold. Currently 86% of world's energy demand is supplied by fossil energy such as coal, oil, and natural gas. However, over next several decades the supply of oil may go down and the major suppliers of oil and gas are in the politically unstable regions of Middle East. Furthermore, fossil energy is also causing more environmental problems due to emissions of greenhouse gases (GHGs) such as carbon dioxide and lower volatile hydrocarbons. According to the Intergovernmental Panel on Climate Change (IPCC) [2], GHG emissions must be reduced to less than half of global GHG emissions level of 1990.

An alternate to fossil energy, renewable energy from biomass has a significant potential. Biogas from wastes, residues, energy crops, and many other organic materials is a versatile renewable energy source. Methane-rich biogas can be used for heat and power applications, as fuel for vehicles, and for the production of a variety of chemicals and materials. Fehrenbach et al. [3] showed that biogas generated by anaerobic digestions of numerous different types of biomass and effluent wastes is the most energy-efficient and environment-friendly source of bioenergy. Like natural gas, methane in biogas can be used in a variety of ways. Biogas will drastically reduce the emission of GHG compared to fossil fuels by utilizing locally available sources of wastes and other forms of biomass. The digestate from the biogas facilities is an improved fertilizer in terms of its availability to crops than conventional mineral fertilizers.

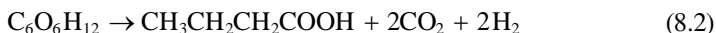
In Europe, biogas is the fastest growing bioenergy and it reached six million tons of oil equivalent (Mtoe) in 2007 with a yearly increase of >20% [4]. Germany is the biggest producer of biogas with about 4000 agricultural biogas production plants by the end of 2008. Within the agriculture sector of the European Union, 1500 million tons of biomass could be digested anaerobically each year, half of which will come from energy crops [5,6]. Besides the agriculture sector, biogas coming from landfills is also becoming more important source of power generation. Biogas is generated not only from various wastewater effluent streams with solids concentration <10 wt%, but also from various streams with high solids concentration (25–35 wt%) such as municipal solid waste (MSW) and animal wastes. The amount of MSW generated

in the United States is close to 250 million tons per year, and globally, this number will soon reach one billion tons per year. Biogas is an effective way to convert this waste into useful and environmentally acceptable form of energy for growing waste industry. Since every country in the world has waste problem, biogas industry is universally applied [5].

The literature on biogas deals with both biomethanation and biohydrogenation. As will be discussed later, the hydrolysis of organic waste followed by anaerobic digestion can produce hydrogen or methane depending on the nature of operating conditions, the nature of microorganisms present, and the nature of feedstock. It should also be noted that methane can be converted to hydrogen by reforming reactions.

## 8.2 BASIC PRINCIPLES OF ANAEROBIC DIGESTION

Anaerobic digestion (in the absence of oxygen) with anaerobic bacteria or methane fermentation is used worldwide for disposal of domestic, municipal, agricultural, and industrial biomass wastes. This reaction generally produces methane and carbon dioxide, and it also occurs in the ecosystem as well as in the digestive tract. As shown by the following reactions, hydrogen along with acetic and butyric acids can be produced by dark fermentation processes using anaerobic and facultative anaerobic chemoheterotrophs [5–8]:

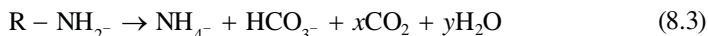


Different types of waste materials can be used for hydrogen fermentation. Hydrogen production highly depends on the pH, retention time, and gas partial pressure along with the nature of microbes [5,9]. Generally, hydrogen production increases with the retention time. Hydrogen production is important for its use in fuel cell or microbial electrolytic cell. Wang [10] described the use of low-cost cathode catalysts for high-yield biohydrogen production in microbial electrolytic cell [10–32]. Cheng and Logan [27,32] and Logan et al. [28,29] evaluated both catalysts and membranes for high-yield biohydrogen production via electrohydrogenesis in microbial electrolytic cells.

Fan et al. [33] examined the possible pathways of fermentative hydrogen evolution and other byproducts during biohydrogen fermentation of wheat straw waste by cow dung compost. They found the hydrogen content in the biogas to be 52% with very little methane. Their experimental results showed that the pretreatment of the substrate plays a key role in the conversion of wheat straw waste into biohydrogen by the compost generating hydrogen.

Ding et al. [34] evaluated the effect of protein on biohydrogen production from carbohydrates, particularly starch. They used two model compounds: rice as starch-rich and soybean as protein-rich food waste. They found that the maximum hydrogen production potential was 0.99 mol of  $\text{H}_2$ /mol of initial starch as glucose and the maximum hydrogen production rate occurred at a starch/protein ratio of 1.7. The protein content in the food waste increased the hydrogen production in two ways. First, it provided the buffering capacity to neutralize the volatile fatty acids as concurrent products.

Second, it provided the readily available organic nitrogen such as soluble proteins and amino acids to microorganisms. Thus, the existence of protein in the substrate of biohydrogen production is important. To get the maximum hydrogen production from carbohydrates, the protein content in feedstock should be optimized. Organic nitrogen in proteins is transformed into inorganic ammonia nitrogen in anaerobic degradation. Ammonia and amino groups released from proteins neutralize the potential pH decrease imposed by volatile fatty acids. Thus, proteins can maintain a suitable pH by the production of bicarbonate, which is given by the following reaction:



The pH stabilization by these two counteracting effects requires the protein-to-starch ratio to be at least 2 to have a pH decrease within 0.5 limit. Lay [35] showed that the pH window for optimal hydrogen production from carbohydrates may be so narrow that a half-unit decrease in pH can cause a 50% decrease in hydrogen production from optimum.

Biogas produced from landfills generally contains methane (about 55%) and carbon dioxide with traces of hydrogen, ethane, and other impurities. The description of the sequence of biochemical reactions that occur to convert complex molecules to methane given here closely follows the excellent review by Weiland [5].

In general, methane fermentation can be divided into four phases: hydrolysis, acidogenesis, acetogenesis/dehydrogenation, and methanation. As shown by Weiland [5], the degradation of complex polymers such as polysaccharides, proteins, and lipids results in the formation of monomers and oligomers such as sugars, amino acids, and long-chain fatty acids (LCFAs). The individual degradation steps are carried out by different consortia of microorganisms, which place different requirements on the environment [36–40]. Initial conversion of polymers and monomers to acetate, hydrogen, and different amount of fatty acids is carried out by hydrolyzing and fermenting microorganisms [5]. *Hydrolytic microorganisms* such as *Bacteroides*, *Clostridia*, and *Bifidobacteria* (all of them are strict anaerobes) excrete hydrolytic enzymes such as cellulase, cellobiase, xylanase, amylase, lipase, and protease, which participate in the hydrolysis and fermentation of organic materials [5]. The higher volatile fatty acids are converted into acetate and hydrogen by obligate hydrogen-producing acetogenic bacteria. The maintenance of an extremely low partial pressure of hydrogen is very important for the acetogenic and hydrogen-producing bacteria. The current state of knowledge indicates that hydrogen may be a limiting substrate for methanogens [30], because an addition of hydrogen-producing bacteria to the natural biogas-producing consortium increases the biogas production [5].

The studies have shown that only two groups of methanogenic bacteria produce methane from acetate, hydrogen, and carbon dioxide [5]. These bacteria are strictly anaerobes and require a lower redox potential for growth than most other anaerobic bacteria. Only few species are able to degrade acetate into  $CH_4$  and  $CO_2$ , for example, *Methanosarcina barkeri*, *Methanococcus mazei*, and *Methanotherix soehngen*, whereas all methanogenic bacteria are able to convert hydrogen to methane [5]. The first and second groups of microbes and the third and fourth groups of microbes are linked closely with each other [38], allowing the overall process to be divided into two stages.

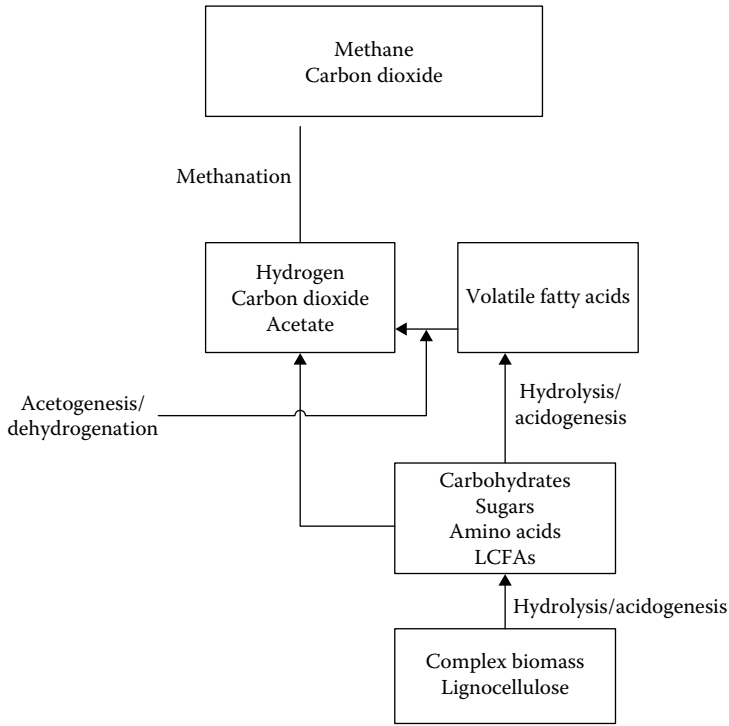


**FIGURE 8.1** The stages of methane fermentation process. (Modified from Weiland, P., *Applied Microbiology Technology*, 85, 849–860, 2010.)

The above description of the four steps of waste-to-methane conversion (methane fermentation) is graphically illustrated in Figure 8.1. This process involves two stages: in the first stage, waste is converted to acetate, hydrogen, and carbon dioxide, and in the second stage, acetate and hydrogen are converted to methane. A balanced anaerobic digestion process demands that in both stages, the rates of degradation must be equal in size. If the first degradation step runs too fast, the acid concentration rises and the pH drops below 7.0 that inhibits methanogenic bacteria for conversion to methane. If the second phase runs too fast, methane production is limited by the rate of the hydrolytic stage to produce hydrogen and acetates.

Thus, the rate-limiting step depends on the compounds of the substrate that is used for the biogas production. Undissolved compounds such as cellulose, proteins, and fats take several days to crack, whereas soluble carbohydrates crack in few hours. The overall process design must take into account the substrate properties for achieving complete degradation without process failure. Each step of the overall process described in Figure 8.1 requires an independent assessment. For example, hydrolysis of complex insoluble substrate depends on the parameters such as particle size, productions of enzymes, pH, and temperature. The conversion of acetate and hydrogen to methane depends on the effectiveness of the methanogenic bacteria [5].

In the following discussion, we examine the effects of microbes, operating conditions (Section 8.3), nature of feedstock (Section 8.4), methods of harvesting, storage

and pretreatment (Section 8.6), co-digestion (Section 8.5), and digester technology (Section 8.7) on the biogas production. Some details of biogas purification (Section 8.9) and the usage of produced biogas and digestate (Section 8.10) are also briefly examined.

### 8.3 MICROBES AND THE EFFECTS OF OPERATING CONDITIONS

While the success of anaerobic treatment depends on the effectiveness of various microbes, very little is known about how they work and the interactions between them, and this lack of knowledge sometimes results in malfunction and failure of biogas digestive process. Furthermore, only few percent of bacteria and archaea have been isolated. However, with new molecular techniques, more information about the community structure in the anaerobic processes can be obtained [41–44]. The quantification of methanogens can be carried out by fluorescence *in situ* hybridization technique. Klocke et al. [43] detected 68 taxonomic groups by 16SrDNA analysis of samples from agricultural biogas plants and showed that hydrogenotrophic methanogens dominate most of the agricultural biogas plants [5]. The effectiveness of microbes in anaerobic digestion process depends on the temperature, ammonia inhibition, pH, and presence of nutrients. The effects of these operating variables on the digestive process are briefly described in Sections 8.3.1 through 8.3.3.

#### 8.3.1 EFFECTS OF TEMPERATURE AND AMMONIA INHIBITION

The digestive process can be operated at lower temperature, that is, mesophilic conditions (temperature range of 35°C–42°C), or at high temperature, that is, thermophilic conditions (temperature range of 45°C–60°C). Generally, temperature fluctuation decreases the biogas productivity. In general, under thermophilic conditions, the growth rate of methanogenic bacteria is higher, and the process is more efficient and faster [42,45]. However, these bacteria are more temperature sensitive and have difficult time adjusting to temperature variations. The faster rate allows the operations to run at lower hydraulic retention time (HRT) than in mesophilic operations. Mesophilic bacteria, however, can tolerate temperature fluctuation of  $\pm 3^\circ$  variations without a significant variation in methane production.

Since ammonia toxicity increases with temperature, thermophilic operations are more susceptible to ammonia inhibition (particularly for the ammonia concentration above 80 mg/l). An increase in ammonia concentration is, however, accompanied by an increase in volatile fatty acid concentration [5]. This can lower the pH and thus counterbalance the effect of ammonia. Many strategies to reduce the ammonia inhibition effects have been examined [46,47]; the most stable digestive process was observed when biomass was diluted with reactor effluent.

#### 8.3.2 pH EFFECT

The pH of the reacting solution has also significant effects on the effectiveness of bacteria and methane production. The anaerobic digestion process best operates between pH of 6.5 and 8.5 with an optimum value between 7 and 8 [5]. The process is severely affected when pH drops below 6 or increases above 8.5 [5]. While ammonia accumulation increases the pH, and VFA (volatile fatty acid) accumulation

decreases the pH, the latter is not always valid due to buffer capacity of some substrate. For example, animal manure has surplus alkalinity that counteracts the increase in VFA concentration [5]. While acetic acid is always present in larger amount than volatile fatty acids, only propionic and butyric acids are more inhibitory to methanogens [48,49]. The inhibition effect of VFA is higher in the reacting systems with lower pH values [5].

### 8.3.3 NUTRIENTS EFFECT

Besides temperature and pH, the availability of several macro- and micronutrients is also very important for the growth and survival of specific groups of microorganisms. Very low amount of macronutrients such as carbon, nitrogen, phosphorus, and sulfur is needed (C:N:P:S = 600:15:5:1) because only a small amount of biomass is developed [5]. Micronutrients such as iron, nickel, cobalt, selenium, molybdenum, and tungsten are important for the growth rate of microorganisms, and they must be added, particularly if the energy crops are the only substrate for biogas production [5]. Nickel is important for all methanogenic bacteria because it is necessary for the cell component cofactor F430, which is involved in the methane formation [5]. For optimum growth, the cell requires cobalt to build up the Co-containing corrinoid factor III [5]. The growth of only few methanogens depends on the trace elements such as selenium, molybdenum and tungsten. The required concentration is only 0.05–0.06 mg/l [5]. The iron is, however, necessary in higher concentration of 1–10 mg/l [50]. These micronutrients are very important for the stable process and high loading for energy crops [51]. While the addition of manure reduces the need for micronutrients addition, even with 50% manure in the reaction medium, the addition of micronutrients can increase the biogas production rate [5].

## 8.4 FEEDSTOCK EFFECTS

All substrates containing carbohydrates, proteins, fats, cellulose, and hemicellulose as major components can produce biogas by anaerobic digestion. The composition of biogas and methane yield depends on carbohydrates, proteins, and fat content of biomass feedstock (Table 8.1) along with other operating parameters. As pointed out by

**TABLE 8.1**  
**Maximal Gas Yields and Theoretical Methane Contents**

Substrate	Biogas (Nm <sup>3</sup> /t TS)	CH <sub>4</sub> /CO <sub>2</sub>
Carbohydrates (not including inulins and single hexoses)	790–800	1/1
Raw proteins	700	~70/30
Raw fat	1200–1250	~67/33
Lignin	0	Both 0

Source: Weiland, P., *Applied Microbiology Technology*, 85, 849–860, 2010; Baserga, U., Landwirtschaftliche Co-vergarungs-Biogasanlagen, FAT-Berichte No. 512, Tanikon, 1998. With permission.

TS, total solids.

Weiland [5], while the data shown in Table 8.1 need to be corrected for solubilization of CO<sub>2</sub> in digestate, they clearly indicate that the biogas production follows the order: raw fat > carbohydrates > protein. Lignin cannot be digested by the anaerobic process.

Protein generates more methane in biogas. Thus, the properties of the feedstock play a very important role in the rate and composition of the biogas production. For example, wood undergoes very slow anaerobic decomposition and therefore not suitable for anaerobic decomposition. However, as shown in Table 8.2, several plants, plant materials, and energy crops produce significant biogas by the anaerobic digestion process [52–54].

The data shown in Table 8.2 are the arithmetic averages of the ranges for each plant identified by Braun et al. [52], Braun [53], and Braun and Wellinger [54],

---

**TABLE 8.2**  
**Average Methane Yields from Various Energy Crops, Plants,**  
**and Plant Materials**

Materials	Average Methane Yield (m <sup>3</sup> /kg Volatile Solid)
Barley	0.56
Triticale	0.49
Leaves	0.48
Alfalfa	0.46
Wheat (grain)	0.45
Peas	0.43
Grass	0.42
Hemp	0.42
Clover	0.38
Potatoes	0.37
Sorghum	0.37
Rapeseed cake	0.36
Maize (whole crop)	0.36
Sugar beet	0.34
Kale	0.31
Straw	0.31
Sunflower	0.30
Oats (grain)	0.30
Sudan grass	0.28
Flax	0.23
Miscanthus	0.22

*Source:* Braun, R., Weiland, P., and Wellinger, A., “Biogas from energy crop digestion,” IEA Bioenergy Task 37-Energy from Biogas and Landfill gas, 2011. With permission; Braun, R., “Potential of co-digestion,” 2002, <http://www.novaenergie.ch/iea-bioenergy-task37/Dokumente/final.PDF>; Braun, R. and Wellinger, A., “Potential for co-digestion,” IEA Bioenergy Report-Task 37, Energy from Biogas and Landfill gas, 2002. With permission.

*Note:* These data are calculated from the arithmetic averages of the ranges.

---

and they show nearly twofold variation in biogas production even within different types of plants and plant materials. Energy crops are extensively used as pure or co-substrate for anaerobic digestion. In general, easily degradable biomass results in biogas production. The biogas generated from landfills generally contains about 50%–55% methane and the remaining composition consists of largely CO<sub>2</sub> and traces of water, hydrogen, and other impurities. Thus, the nature of feedstock makes a significant difference in the level and composition of biogas production.

A vast amount of literature on the effect of feedstock on biogas production is available. A brief summary of this literature is outlined in Table 8.3. Biogas production from some of these feedstock is further discussed below in Sections 8.4.1 through 8.4.12.

#### **8.4.1 COIR PITH**

Coir pith is a lignocellulosic agro residue that is produced as a byproduct in coir industry in large quantities. Kunchikannan et al. [56] examined the production of methane from this waste material by anaerobic digestion. The study indicated that the yield of methane is 38.1% per kilogram of dry pith weight in 44 days; the yield can be improved by about 1.5 times by the reduction of particle size. The increase in acidity during the digestion process decreases the methane yield, whereas an increase in alkalinity does not significantly change the methane yield.

#### **8.4.2 WHEY**

The wastes from various food industries are capable of generating methane due to their high organic content. Whey is normally used as a component of dairy products or as an additive for food product. Beszedes et al. [60] examined biogas generation from membrane-separated fractions, that is, permeate and concentrate of whey. The study examined the effects of pH, thermal, and microwave pretreatment, and their combinations on the biogas yield. The pretreatment had a significant effect on the biogas yield. The hydrolysis of large molecules enhanced the biodegradability of whey, thereby increasing the productions of biogas and methane. The long-time classical heat treatment and the microwave radiation in an acidic medium significantly increased the methane production. The concentrate of whey was more adaptable to anaerobic digestion than the permeate or the whole whey.

#### **8.4.3 DISTILLERY SPENT WASH**

Distillery spent wash is a major pollutant in water. In recent years, methane is generated from anaerobic digestion of distillery spent wash by fixed-film systems and two-phase anaerobic systems. Pathe et al. [58] showed that a treatment option that involved two-stage aerobic oxidation processes (activated sludge and extended aeration) followed by a physical chemical treatment using lime, polyaluminum chloride, polyelectrolyte, and carbon adsorption as the tertiary treatment can be the most efficient method for methane generation from the distillery spent wash. The treated effluent can be used for green belt development and in the agriculture industry.

**TABLE 8.3****Some Typical Literature Studies on Anaerobic Digestion of Waste Materials**

<b>Types of Waste</b>	<b>Authors</b>
Swine waste	Chen et al. [55]
Coir path	Kunchikannan et al. [56]
Wastewater and organic kitchen waste	Weichgrebe et al. [57]
Distillery spent wash	Pathe et al. [58]
Biodiesel byproducts	Kolesarova et al. [59]
Whey (a component of dairy product or an additive for food product)	Beszedes et al. [60]
Palm oil effluent	Yusoff et al. [61]
Tofu wastewater	Zheng et al. [62]
Starch of food waste	Ding et al. [34]
MSW	Abderrezaq [63]
Solid organic waste and energy crops	Angelidaki et al. [64]
Food residuals	Shin et al. [65]; Haug et al. [66]
Dairy effluent	Desai et al. [67]
Organic solid waste	Zhang [68]; Mata-Alvarez et al. [69]
Household organic waste	Narra et al. [70]
Distillery spent waste	Nandy et al. [71]
LCFAs	Alves et al. [72]
Horse and cow dung	Yusuf et al. [73]
Agricultural and industrial wastes	Kujawski and Steinmetz [74]
MSW/FOG (fats, oils, and greases) wastes	Martin-Gonzalez et al. [75]
Nonedible oil cake and cow dung	Singh and Mandal [76]
Food wastes	Zhu et al. [77]; Chen et al. [46]
Maize grains and maize silage	Hutnan et al. [78]
Co-digestion of olive mill wastewater and swine manure	Azaizeh and Jadoun [79]
Cow dung and water hyacinth	Yusuf and Ify [80]
Cattle manure and slaughterhouse waste	Bagge et al. [81]
Co-digesting swine manure with three crop residues	Wu et al. [82]
Biomass (IFBB) and whole crop digestion (WCD)	Buhle et al. [83]
Organic solid poultry slaughterhouse waste	Salminen and Rintala [84]
MSW/agricultural waste/dairy cow manure	Macias-Corral et al. [85]
Animal manure	Holm-Nielsen et al. [86]
Maize hybrids	Oslaj et al. [87]
Byproducts of sugar production/cow manure	Fang et al. [88]
Biomass	Gunaseelan [89]
Fruit waste	Kaparaku and Rintala [90]; Lopez et al. [91]

IFBB, integrated generation of solid fuel and biogas from biomass.

Nandy et al. [71] treated high-strength distillery spent wash in the fixed-film, fixed-bed, two-stage anaerobic reactors using cheaper and abundantly available pebbles as media. The experiments were carried out in the laboratory as well as in the pilot-scale operation. The results showed that the overall chemical oxygen demand (COD) removal was about 80% with a specific biogas yield of  $0.3 \text{ m}^3 \text{ CH}_4/\text{kg COD}$ . For a two-stage system, while the packed bed reactor can be easily fed with the spent wash, the detention period for each reactor has to be increased to obtain the COD removal close to 80%. In both reactors, the biogas yield decreased for HRT beyond 2.43 days. Feeding to the reactors can only be stopped for a maximum of three days, and the reactors become sour and need to be reenergized for a pH level  $<6.0$ . Most efficient operation was obtained at a temperature of  $35^\circ\text{C}$ – $40^\circ\text{C}$  and a pH of 7.0. Greater depth of reactor gave poorer performance and no clogging of the reactor was observed for 18 months.

#### 8.4.4 SWINE WASTE

Chen et al. [55] examined various engineering options of conversion of swine waste to biomethanol. They applied target costing method in the development of marketable and environment-friendly product such as biomethanol from swine waste. Biomethanol is produced from methane, which is generated by anaerobic digestion of swine waste.

#### 8.4.5 BYPRODUCTS OF BIODIESEL PRODUCTION

The process of biodiesel production is predominantly carried out by catalyzed transesterification. Besides the desired methyl esters, the process produces several byproducts such as crude glycerol, oil-pressed cakes, and washing water. Crude glycerol or g-phase is a heavier, separate liquid phase, composed mainly of glycerol. Numerous types of oil cakes such as canola, rapeseed, coconut, cottonseed, groundnut oil, mustard oil, olive oil, palm kernel, sesame oil, soybean, and sunflower are also created in this process. Although their composition widely varies depending on the parameters and substrates used for biodiesel production, all these byproducts provide valuable feedstock for biogas production. The study by Kolesarova et al. [59] leads to the following conclusions:

1. Crude glycerol from biodiesel production is a valuable substrate for anaerobic degradation and the production of biogas using g-phase as a single substrate.
2. G-phase also has a great potential as a co-substrate by anaerobic treatment of different types of organic wastes such as organic fraction of MSW, mixture of olive mill wastewater, slaughterhouse wastewater, corn maize, maize silage, and swine manure.
3. Olive cakes and olive meals along with rapeseed and sunflower oil cakes can be used for anaerobic digestion to produce biogas and methane. High stability of the anaerobic digestion of sunflower oil cake under mesophilic conditions was obtained. With the increased amount of oil gained from

rapeseed meal by the extraction process, the possible biogas production from rapeseed cake decreased. Pretreatment (thermal and chemical) of sunflower and rapeseed residues did not enhance the methane yield.

4. Washing water from biodiesel production is a good candidate for anaerobic degradation due to its high content of biodegradable organic substances.
5. Specific inhibition effects resulting from the substrate composition should be considered during anaerobic treatment of biodiesel byproducts. In the case of anaerobic digestion of crude glycerol, high salinity of the substrates may negatively affect the methanogenic microorganisms. The concentration of ammonium should also be monitored. Since nitrogen is an essential nutrient for microorganisms, its low concentration in the crude glycerol and washing water has to be compensated by the ammonium supplement. However, nitrogen-rich substances have high concentration in rapeseed cake, which may cause ammonium accumulation in the reactor, thereby inhibiting the digestion process.

The use of byproducts of the biodiesel process as a potential source of energy producer makes the process of biodiesel more economically attractive.

#### **8.4.6 PALM OIL MILL EFFLUENT**

Yusoff et al. [61] examined the effects of HRT and volatile fatty acids produced during fermentation on biohydrogen production from palm oil mill effluent. Both HRT and volatile fatty acid concentration played a vital role in the biohydrogen concentration, rate, and yield. The results were obtained for HRT of two, three, and five days, and two days gave the optimum operation with a maximum biohydrogen yield, rate, and concentration of 30%. The VFA as soluble metabolites reduced the amount of biohydrogen production by 8%–10%. The study concluded that HRT and VFA affect the biohydrogen production and should be considered in biohydrogen fermentation.

#### **8.4.7 LCFAs IN WASTEWATER**

As shown in Table 8.1 [5,92], the potential for biogas and methane production from lipids is much higher than that from proteins and carbohydrates. LCFAs commonly found in wastewaters include lauric acid, myristic acid, palmitic acid, palmitoleic acid, stearic acid, oleic acid, and linoleic acid among others [72]. An extensive number of studies for the treatment of wastewater containing lipids and LCFAs in different types of anaerobic reactors have been reported. These studies are evaluated by Alves et al. [72].

The high-rate anaerobic technology (HR-AnWT) for the wastewater treatment requires the expansion of suitable substrates, in particular better treatment of the wastewater with high-lipid content. Waste lipids are good candidates for substrates needed to improve biogas and methane production, compared to proteins and carbohydrates. Alves et al. [72] presented a review of how LCFA degradation is accomplished by syntrophic communities of anaerobic bacteria and methanogenic archaea. For optimal performance, these syntrophic communities need to be clustered in compact aggregate, which is often difficult to achieve with wastewater that contains fats and lipids.

Alves et al. [72] proposed a new reactor concept that provides the primary biomass retention through floatation and the secondary biomass retention through settling.

The types of bacteria involved in methanogenic conversion of LCFA are known and the biochemical mechanism of LCFA degradation by beta-oxidation is well understood. The initial steps in the anaerobic conversion of unsaturated LCFA are, however, unclear. Besides the obligate hydrogen-producing acetogens (OHPAs) that degrade the unsaturated LCFA, bacteria exist which have the ability to hydrogenate unsaturated LCFA to saturated LCFA. This conversion can be coupled to growth and these bacteria may compete with hydrogenotrophic methanogens for hydrogen.

LCFAs require the syntrophic cooperation of OHPA and methanogens. These syntrophic communities perform optimally when they are organized in microcolonies; the interspecies hydrogen transfer is enhanced with a short intermicrobial distance. It is yet not clear how microcolonies are developed in a fatty matrix and what is the effect of hydrogen transfer. Since hydrogen is poorly soluble in water, hydrogen transfer is increased when the matrix is LCFA. More work in this area is needed.

#### **8.4.8 FOOD AND KITCHEN ORGANIC WASTE**

Significant efforts have been made to generate biogas (biomethane) from different types of organic wastes [64,65,68,70,71]. Anaerobic digestion is a preferred method for energy resource recovery from organic residuals because this method (1) generates biomethane, (2) reduces the volume of the waste, and (3) stabilizes the waste. Shin et al. [65] showed how this method has been successfully applied to food waste from restaurants, markets, institutions, and households. They described a multi-step sequential batch two-phase anaerobic composting (MUSTAC) process that was stable, reliable, and effective in treating food residuals. The process can remove 82.4% of volatile solids and convert 84.4% of biomethane potential into methane in 10 days. The output from the posttreatment can be used as a soil amendment. The MUSTAC process was simple to operate and had high performance. Haug et al. [66] described the use of Los Angeles Wastewater Hyperion Treatment plant to anaerobically digest the food residual from the Los Angeles airport and the surroundings serving airline industry and passengers. The plant was cost effective and handled waste in an environmentally acceptable way.

Weichgrebe et al. [57] examined the energy and CO<sub>2</sub> reduction potentials of anaerobic treatment of wastewater and organic kitchen wastes. They considered three different scenarios: (1) the classical waste treatment and the composting of the organic waste fraction, (2) the anaerobic treatment of wastewater combined with deammonification and the digestion of the organic waste fraction, and (3) a mutual anaerobic treatment of wastewater and waste as co-digestion with deammonification. Scenario 2 was found to be the best. With the today's state of the art concerning the wastewater and waste treatment, both energy surplus and simultaneous CO<sub>2</sub> emission reduction was accomplished for scenario 2 at 20°C without the use of the dissolved methane into the reactor's effluent. If in the future an economical process for the usage of dissolved methane is developed, GHG emission can be further lowered. A further positive effect of scenario 2 is that the dissolved nutrients can be reused. Since a small part of these nutrients is needed for the anaerobic

metabolism (<20%), a majority of mineral fertilizer can be substituted by using the effluent for irrigation. Furthermore, energy and GHGs would be additionally saved and the wastewater treatment costs will be reduced.

#### 8.4.9 WASTEWATER TREATMENT

Cowan [93] points out that one way to reduce the emission of  $\text{CO}_2$  and increase the energy production from bioprocess technologies for wastewater treatment is to use an integrated algae pond system (IAPS) to address the range of wastewater treatment problems. The growth of algae requires the use of  $\text{CO}_2$  that minimizes the emission to the environment. Furthermore, the IAPS system produces a quality effluent suitable for irrigation, negates the food versus fuel debate, and reduces the demand for fossil fuel-derived energy and fertilizers.

Ryan et al. [94] addressed the issue of wastewater treatment from ethanol-producing biorefineries. They suggested that in order to treat the effluent from these refineries efficiently and economically which meets the local requirements and minimizes the net water consumption, a process integration that (1) improves the existing secondary (i.e., biological) treatment to maximize COD reduction, (2) incorporates a tertiary “polishing” stage to remove color, and (3) uses the reverse osmosis membrane technology to recover process water would be desirable. They also showed that the energy required for the secondary and tertiary treatment stages can be obtained from biogas-derived power from the anaerobic digester. Thus, this type of an integrated approach of postbiological treatment of ethanol stillage can address the issues of efficient refinery operation with minimum net water consumption.

#### 8.4.10 DAIRY EFFLUENT

Energy generation potential from dairy effluent was recently evaluated by Desai et al. [67]. India is the largest milk producer in the world (100 MMT). In an organized sector, which produces only 30% of the total milk generated in the country, the 140 dairy processing plants generate a very significant amount of effluent that is rich in organic waste. Desai et al. [67] described an anaerobic digestion system for one dairy processing 100,000 l/day milk to generate biogas (biomethane) that can provide energy for the aerators of the existing aerobic treatment system (mostly activated sludge system). The study presented the details of the anaerobic filter system. The 40 million liters of milk handled by the organized sector of milk industry in India has potential of generating 11 MW power from methane produced by the anaerobic digestion filter system.

#### 8.4.11 TOFU WASTEWATER

Zheng et al. [62] examined the hydrogen production from organic wastewater from tofu production by photo bacteria. While this is a very useful process,  $\text{NH}_4^+$ , which is normally the integrant in organic wastewater, is the inhibitor for hydrogen production with photo bacteria. They showed that the concentration of  $\text{NH}_4^+$  at  $\geq 2$  mmol/l significantly affected the hydrogen production of wild-type *sphaeroides* because  $\text{NH}_4^+$  concentration

inhibited the nitrogenase activity. They generated the mutant named AR-3 that can produce hydrogen in the medium containing even 4 mmol/l  $\text{NH}_4^+$  due to the release of the inhibition of  $\text{NH}_4^+$  to the nitrogenase activity. Under suitable conditions, they also showed that the hydrogen generation rate of AR-3 from tofu wastewater could reach 14.2 ml/l/h. It was increased by >100% compared to that of wild-type R sphaeroides.

#### 8.4.12 FRUIT WASTE

Methane can be produced from waste orange peel. The thermophilic anaerobic digestion of industrial orange waste pulp and peel with a subsequent aerobic post-treatment of the digestate has been successfully demonstrated by Kaparaju and Rintala [90]. In this study, in anaerobic batch cultures, the methane production rate of 0.49 m<sup>3</sup>/kg volatile solids, and in a semicontinuous process, the methane production rate as high as 0.6 m<sup>3</sup>/kg VS was generated. This did require the pH adjustment from 3.2 to 8.0 by  $\text{CaCO}_3$  addition. An aerobic follow-up treatment with activated sludge produced  $\text{CO}_2$  and water and converted ammonia into nitrate. The removal of nitrogen required an additional denitrification step. The process can be adapted to other fruit and vegetable wastes such as mango, pineapple, tomato, jackfruit, banana, and whole orange. The methane production rate from these fruits can be improved by using selected strains of *Sporotrichum*, *Aspergillus*, *Fusarium*, and *Penicillium* [5,90,91]. These fungal pretreatments enhanced the availability of nutrient in the medium, decreased the concentrations of antimicrobial components, and enabled the higher loading rate utilization.

Besides other fruits and vegetable wastes, the wastewater from pressing of these byproducts is also good substrate for methane production [91]. This wastewater is generated by pressing the rind of orange peel and it contains a large amount of organic matter and alkalinity because in the pressing process,  $\text{Ca}(\text{OH})_2$  is used as binder. Before the anaerobic treatment, the waste is pretreated by aluminum phosphate flocculent to remove solids that can hinder the anaerobic treatment and to reduce the pH from 11.21 to 5.5. In the batch process, this treatment removed 84% of soluble COD and generated 295 ml of methane per gram of COD removal. The presence of antimicrobial components reduced the methane production when COD loadings were high [5,91].

### 8.5 CO-DIGESTION

Co-digestion is the simultaneous digestion of a homogeneous mixture of multiple substrates. The most common situation is when a major amount of basic substances is mixed and digested together with minor amounts of a single or a variety of additional substrates. As pointed out by Braun et al. [52], Braun [53], and Braun and Wellinger [54], co-digestion can improve the overall nutrient balance and digestion, and create an additional biogas and fertilizer. It can also equalize the particulates, floating and settling materials, and acidity in settlers by a suitable dilution by manure and sewage sludge to the agricultural waste. The co-digestion can, however, create an increased COD in the digester effluent, may require more pretreatment of the waste, and increase the mixing requirement in the digester. It may also cause an

increased hygienic requirement and restriction on the available land use. Finally, its economics is very much dependent on the crop cost and yield.

Recent research results by Wu et al. [82] and numerous others [53,54,73,78,79,80, 83–85,88,95–108] demonstrate that using co-substrates in the anaerobic digestive systems improves the biogas yields through positive synergisms established in the digestion medium and the supply of missing nutrients by the co-substances. This subject is under an extensive investigation in the anaerobic digestion industry.

Historically, anaerobic digestion was carried out for animal manure and sewage sludge from aerobic wastewater treatment. In the recent years, agricultural biogas plants use pig, cow, and chicken manure with co-substrates, which increase the organic content of the total substrate. The co-wastes can be organic wastes from the agriculture-related industries, food waste, collected municipal biowaste from households, energy crops, tops and leaves of sugar beets, and so on. Fats provide the largest biogas yield but require high retention time. Carbohydrates and proteins have faster conversion rates but lower yields. If pathogens or other organisms are present, pasteurization at 70°C and sterilization at 130°C of feed materials are needed prior to fermentation. The carbon/nitrogen (C/N) ratio should be between 15 and 30 to avoid the process failure by ammonia accumulation. The fermentation residue should be used as an fertilizer.

## **8.6 EFFECTS OF HARVESTING, STORAGE, AND PRETREATMENT**

### **8.6.1 EFFECT OF HARVESTING**

The specific methane yield obtained from this material depends on its age [5,109,110,111]. Harvesting time and its frequency are important for biogas yield. Crops can be grown as preceding crop, main crop, or succeeding crop, each leading to a different biogas yield [5]. Weiland [5] pointed out that maize crops harvested after 97 days of milk ripeness produced 37% more methane yield than those at full ripeness.

### **8.6.2 STORAGE**

Easy storage is an important factor in the selection of energy crops. The storage of energy crops by ensiling converts soluble carbohydrates into lactic acid, acetate, propionate, and butyrate, which inhibit the growth of detrimental microorganisms by a strong drop in pH between 3 and 4 [112]. The starter cultures, enzymes, and easily degradable carbohydrates can control and accelerate the acid formation. The optimum ensiling conditions are obtained by cutting particle length between 10–20 mm, and maintaining the total solid contents between 25% and 35%. Often, the storage by ensiling can be considered as a pretreatment process [5,113].

The structural polysaccharides of plant material are partly degraded during storage. They lose about 8%–20% of energy due to aerobic degradation, which is largely caused by oxygen, pH, and growth of yeasts that are responsible for heat upon exposure to oxygen. During storage, a plastic wrap should cover the plant material to minimize degradation.

### 8.6.3 PRETREATMENT

Muller et al. [5,114] showed that thermal, chemical, mechanical, or enzymatic processes as pretreatment can alter the degradation rate. Particle size reduction accelerates the biogas production rate but not the methane yield [5,115]. This is often achieved by the use of a crushing device or an ultrasonic treatment of the feed stream [5]. Also, thermal pressure hydrolysis at 230°C and 20–30 atm splits polymers into short-chain compounds, which can give better biogas yields with reduced retention time in the digesters [116,117].

The addition of an enzyme to the feed can have a mixed effect. While it can increase the biogas yield up to about 20% [5] by the acceleration of decomposition of polysaccharides, if added in excess, the protease of anaerobic microorganisms can degrade the enzyme, thus limiting its effectiveness [5,118]. In general, the enzyme reduces the viscosity of the substrate mixture and increases the degradation rates by avoiding the formation of floating layers [5]. For wheat grass, the addition of an enzyme improved the biogas production, but at the end of the digestion period, no significant improvement of methane yield or degradation rate was observed [119].

## 8.7 TYPES OF FERMENTATION AND ASSOCIATED DIGESTER CONFIGURATIONS

The nature of digester configuration depend on the method of fermentation. Four types of fermentation and associated digester configurations have been most widely used: wet fermentation, dry fermentation, batch fermentation, and two-stage fermentation. Solid concentration plays an important role in the choice of the fermentation. Wet fermentation is used for low solids concentration (<10%), dry fermentation is used for an intermediate concentration (between 15 and 35 wt%), and batch fermentation is used for solids concentration as high as 70 wt%. More details on the different types of digester are briefly described in Sections 8.7.1 through 8.7.4.

### 8.7.1 WET FERMENTATION

In the wet fermentation process, the solids concentration is <10% and generally carried out in a vertical, continuous stirred slurry fermenter [5]. Low slurry concentration allows the stirring at lower power cost. The digested material is spread on the fields for the fertilization. For energy crops, the feed must be mixed with recycled process water or liquid manure to make the slurry pumpable. In the agriculture sector, wet fermentation is the preferred mode of operation.

Often the fermenter is covered with gas-tight, single- or double-membrane roof to store the gas before utilization. To achieve the uniform temperature and good contact between microbes and feedstock, good mixing of the slurry is very important. While mixing can be provided by different types of stirrer (mechanical, hydraulic, or pneumatic), mechanical stirrers are often used. In order to obtain maximum mixing in the reactor, the number, size, direction, and depth of the stirrer paddles depend on the nature of feedstocks, solids concentration, and height

of the slurry. The stirring can be slow if it is continuous or it can be high if it is intermittent.

Most wet fermenters are operated at temperature between 38°C and 42°C (mesophilic condition). Since higher temperature gives faster degradation rate requiring lower HRT and reactor volume, some fermenters do operate under thermophilic conditions. Ultimate methane yield is, however, not influenced by higher temperature. Under mesophilic conditions, both ammonia toxicity and growth rate of microorganisms are reduced which can lead to the washout problem of microbial population [5,120]. In general, mesophilic processes are more energy efficient than thermophilic processes. The energy crops require very high retention time (weeks to months) and are generally fed at lower solids concentration (2–4 wt%) in wet fermenter [5,121].

### 8.7.2 DRY FERMENTATION

Dry solids fermentation is carried out with solids concentration between 15% and 35% [5]. Dry fermentation is operated either batchwise or in a continuous mode. For dry fermentation of slurry containing >25% solids, a horizontal mechanically mixed fermenter or a vertical plug flow reactor can be used [5]. These have been used for the anaerobic treatment of municipal organic solids [5,122,123]. In the vertical fermenter, the substrate flows from top to bottom by gravity only. The substrate fed at the top is mixed with the digestate coming from the bottom. This recycling and mixing of digestate with fresh feedstock prevents the accumulation of VFA and allows the high organic loading rate in the fermenter. The typical vertical fermenter volume in dry fermentation varies from 1000 to 4000 m<sup>3</sup> [5,122,123].

### 8.7.3 BATCH FERMENTATION

For energy crops, dry fermentation in batch processes is preferred. For these processes, sometimes no mixing is required and solid inoculum up to 70% is necessary [5,124]. The batch process is operated with gas-tight lids, and operated for several weeks of digestion period.

### 8.7.4 TWO-STAGE FERMENTATION

Horizontal digesters are generally a part of a two-stage system in which high solids concentration flows in a horizontal plug flow mode with a low rotating horizontal paddle mixer. The reactor volume of such a reactor is limited to 700 m<sup>3</sup>. For energy crops and processing of high solids concentration slurry, a two-stage digester system includes a high-loaded main fermenter followed by a low-loaded secondary fermenter.

The two-stage process generally gives higher biogas production and a lower methane potential of the final digestate [5,121,125]. In the two-stage process, hydrolysis and methanation take place in both reactors, although it is possible to use the first bed only for hydrolysis and treat the leachate coming out of the first bed in a second fixed-bed methanation reactor [5,126,127]. For achieving better metabolization of solid organic compounds, a two-stage reactor system with a separate hydrolysis

stage can be advantageous because the ideal pH required for hydrolysis (5.5–6.5) is different from that required for methanation (6.8–7.2) [5,126,128]. This technology is mainly applied to MSW, industrial solid wastes and solid manure and seldom to energy crops. The control of operation and process parameters for the two-stage fermentation system is generally difficult. Furthermore, if the hydrolysis stage does not work properly, methane and hydrogen can escape in the environment [5,129].

### 8.7.5 NOVEL DIGESTER TECHNOLOGY

The University of California at Davis developed a new anaerobic digester technology called anaerobic-phased solids (APS) digester for biogasification of organic waste solids that are normally difficult to process using conventional anaerobic digesters. A variety of feedstock including crop residues, animal manures, feed processing residuals, paper sludge, and MSW can be processed by APS digesters. The digester has been used to generate power for the University of California. The first commercial APS digester was built in Boynton Beach, Florida, to process 80 tons/day horse stable wastes. The possible benefits of this plant are renewable energy generation, odor control, pathogen and insect control, truck traffic reduction, and production of high-quality soil amendment.

The APS digester combines the favorable features of both batch and continuous operations in one system. Solids to be digested are handled in batches while biogas production is continuous. This allows the solids to be loaded and unloaded without disrupting an anaerobic environment for bacteria. The typical APS digester system consists of four hydrolysis reactors and one biogasification reactor. Liquid is recirculated intermittently between each hydrolysis reactor and the biogasification reactor. The solids are housed in the hydrolysis reactor, whereas the bacteria (methanogens) are housed in the biogasification reactor. The solids are broken down and liquefied in soluble compounds, which are mainly organic acids, and transferred to the biogasification reactor to generate biogas. The four hydrolysis reactors are operated in different time schedules so that biogasification reactor is constantly fed with the dissolved organic acid. High bacteria concentration in the biogasification reactor is maintained to get the optimum performance. More details on the APS digester are given by Zhang [68].

## 8.8 SIMULATION, MODELING, SCALE-UP, AND CONTROL OF FERMENTATION PROCESS

Angelidaki et al. [39,40] and Gavala et al. [130] gave a systematic assessment of complex kinetic models for organic waste digestion. They described the degradation by a simple first-order reaction that can be applied knowing the yield of substrate and the specific reaction rate [5]. Their kinetic models also depended on the nature of feedstock and the temperature range of the digestion process. The kinetic of biogas production from energy crops and manure was reported extensively by Mahnert [131]. Several kinetic models were developed for low-temperature (35°C–42°C) mesophilic conditions as well as high-temperature (45°C–60°C) thermophilic conditions by Andara and Esteban [132], Linke [133], and Biswas et al. [134].

As the interest in using the anaerobic digestion technique to generate biogas and biomethane increases due to economical and environmental reasons, it is important to determine the ultimate methane potential for a given solid substance. In fact, this parameter determines to some extent both design and economic analysis of a biogas plant. The ultimate methane potential thus identifies the “thermodynamic limit” for a given substance. Furthermore, to compare the potentials of various substrates, the definition of common units to be used in anaerobic assays is becoming increasingly important. Angelidaki et al. [39,40,64] presented some guidelines for biomethane assays of the anaerobic digestion prepared by the specialists group of the International Water Association. The guidelines include the considerations of biodegradability, bioactivity, inhibition, and matrices for biostability.

Narra et al. [70] evaluated a model for anaerobic digestion of household organic waste in high solids concentration (25 wt%) in an urban city in India and showed with pilot-scale experiments that the biogas production of 209 l/kg of the total solids is possible in a 30-day incubation period. High solids concentration reduces the water requirement and slurry handling problems. Composting takes 35 days and yields a quality product that can be used either as manure or a part of chemical fertilizer. A batch pilot plant was developed. Abderrezaq [63] evaluated the use of anaerobic digester for the MSW generated in Jordan. They showed that the digester technology can generate the energy from waste without generating GHG.

It is difficult to find a suitable and simple control parameter to control the complex fermentation process. Furthermore, only few parameters can be measured on-line. In agricultural biogas plants, the methane production is the only continuously measured parameter. However, complex and variable process dynamics make the interpretation of data difficult [5,135]. Only VFA can serve as an efficient indicator of process imbalances. Weiland [5,135] proposed that an indicator for process failure is the propionic acid/acetic acid ratio of  $>1$ .

Ahring et al. [136] suggested that if the propionic acid concentration is  $>1000$  mg/l, the concentration of both butyrate and isobutyrate could be a reliable tool for indication of process failure. Nielsen et al. [137] suggested that propionate is the key parameter for process control and optimization. VFA analysis by manual sampling and the subsequent analysis by gas chromatography or high-pressure liquid chromatography is a slow process. On-line measurement is a difficult process [138]. A fast control of the process stability is possible by determining the ratio of total VFA to total inorganic carbonate. If this ratio is  $>0.3$ , the process is stable.

## 8.9 PURIFICATION OF BIOGAS

Biogas mainly contains methane and carbon dioxide with some impurities of hydrogen sulfide (with sulfur concentration from 100 to 3000 ppm) and ammonia, and it is generally saturated with water vapor. Before it can be used for heat and electricity generation, sulfur concentration should be reduced to the level below 250 ppm [5]. This will prevent the excessive corrosion and expensive deterioration of lubrication oil.

H<sub>2</sub>S removal is carried out by biological desulfurization either within digester or outside digester. For this type of desulfurization, *Sulfobacter oxydans* bacteria and

2%–5% air must be present in the digester, which converts  $H_2S$  to elemental sulfur and sulfurous acid [5]. These bacteria are often present in the digester or added in the headspace of the digester. An efficient desulfurization requires a high contact area for microorganisms' fixation, which can be accomplished by an installation of specific wood or fabric support at the top of the fermenter.

For biological desulfurization outside the fermenter, trickling filter installations filled with plastic support materials on which the microorganisms can grow are used [139]. Raw biogas and air are injected at the bottom of the column, and the aqueous solution of nutrients is circulated to wash out the acidic products and supply the nutrients to microorganisms. The process is carried out at 35°C (mesophilic condition), and the support material is washed with air/water mixture at regular intervals to prevent sulfur deposits on the filters.

Desulfurization can also be done by adding commercial ferrous solution to the digester. In this expensive method, the production of hydrogen sulfide is prevented because ferrous binds sulfur to produce compounds which are insoluble in the liquid phase.

## 8.10 UTILIZATION OF BIOGAS AND DIGESTATE

The purified biogas can be used to generate electricity with about 43% efficiency [5]. It can be used in microgas turbine or fuel cell. While it is used in microgas turbine with a lower (25%–31%) efficiency, it gives good loading efficiency and long maintenance intervals for the turbines [5]. Furthermore, the exhaust heat from microgas turbine can be used to generate the process heat. The use of clean biogas in various fuel cells, which are operated at temperatures between 80°C and 800°C, gives higher efficiency. The investment costs for such applications are, however, higher. In the recent years, significant efforts are being made to upgrade the biogas and inject it into the grid or utilize it as a vehicle fuel [5].

The injection of biogas into natural gas grid requires further removal of all contaminants and carbon dioxide such that the final product must contain at least 95% methane. Both bacteria and molds must also be removed to make the use of biogas environmentally acceptable. The carbon dioxide is absorbed with the use of polyethylene glycol or mono- or diethanolamines. Carbon dioxide can also be removed using cryogenic separation, pressure swing adsorption, or membrane separation technology [5].

The process of anaerobic digestion reduces 80% of odor of the feedstock. The digestate generated from anaerobic digestion process possess valuable properties as fertilizers. Both nitrogen (in the form of ammonia) and carbon are useful as fertilizers. The nitrogen content in the digestate depends on the feedstock; it can be increased by a factor of 3 when only energy crops as substrate are used [5,52]. The faster permeation of digestate with improved flow properties can reduce loss of ammonia in air, thereby making “digestate fertilizer” more effective. While the “digestate fertilizer” inactivates weed seeds, bacteria, viruses, fungi, and parasites, their decay rates depend on the temperature, pH, treatment time, and VFA concentration. The best and faster results are obtained at higher temperature (>50°C) [5]. For certain wastes, while a separate pasteurization after digestion (at 70°C) is effective, digestate is prone to recontamination [5].

## REFERENCES

1. IEA, *World Energy Outlook*. International Energy Agency, Paris, France (2006).
2. Davidson, O., Mertz, B., and coauthors, IPCC Special report on emission scenarios, Intergovernmental Panel on Climate Change (IPCC) working group III (2000).
3. Fehrenbach, H., Giegrich, J., Reinhardt, G., Sayer, U., Gretz, M., Lanze, K., and Schmitz, J., "Kriterien einer nachhaltigen Bioenergienutzung im globalen Maßstab," *UBA-Forschungsbericht*, 206, 41–112 (2008).
4. EurObserver Report, The state of renewable energies in Europe, 47–51 (2008) <http://www.euroobserver.org>.
5. Weiland, P., "Biogas production: Current state and perspectives," *Applied Microbiology Technology*, 85, 849–860 (2010).
6. Amon, T., Hackl, E., Jeremic, D., Amon, B., and Boxberger, J., "Biogas production from animal wastes, energy plants and organic wastes," in van Velsen, A. and Verstraete, W. (eds.), *Proceedings of the 9th World Congress on Anaerobic Digestion*, Antwerp, Belgium, September 2–6, 381–386 (2001).
7. Gujer, W. and Zehnder, A.J.B., "Conversion processes in anaerobic digestion," *Water Science and Technology*, 15, 127–167 (1983).
8. Fachverband Biogas, "Biogas dezentral erzeugen, regional profitieren, international gewinnen," *Proceedings of the 18th Jahrestagung des Fachverbandes Biogas*, February 3–5, Hannover, Germany (2009).
9. Rader, G. and Logan, B., "Multi-electrode continuous flow microbial electrolysis cell for biogas production from acetate," *International Journal of Hydrogen Energy*, 35, 8848–8854 (2010).
10. Wang, A., Liu, W., Cheng, S., Xing, D., Zhou, J., and Logan, B.E., "Source of methane and methods to control its formation in single chamber microbial electrolysis cells," *International Journal of Hydrogen Energy*, 34, 3653–3658 (2009).
11. Liu, H., Grot, S., and Logan, B.E., "Electrochemically assisted microbial production of hydrogen from acetate," *Environmental Science & Technology*, 39, 4317–4320 (2005).
12. Selembo, P.A., Merrill, M.D., and Logan, B.E., "The use of stainless steel and nickel alloys as low-cost cathodes in microbial electrolysis cells," *Journal of Power Sources*, 190, 271–278 (2009).
13. Call, D.F., Merrill, M.D., and Logan, B.E., "High surface area stainless steel brushes as cathodes in microbial electrolysis cells (MECS)," *Environmental Science & Technology*, 43, 2179–2183 (2009).
14. Clauwaert, P. and Verstraete, W., "Methanogenesis in membraneless microbial electrolysis cells," *Applied Microbiology and Biotechnology*, 82, 829–836 (2009).
15. Parameswaran, P., Zhang, H., Torres, C.I., Rittmann, B.E., and Krajmalnik-Brown, R., "Microbial community structure in a biofilm anode fed with a fermentable substrate: The significance of hydrogen scavengers," *Biotechnology and Bioengineering*, 105 (1), 69–78 (2010).
16. Lee, H.-S. and Rittman, B.E., "Significance of biological hydrogen oxidation in a continuous single-chamber microbial electrolysis cell," *Environmental Science & Technology*, 44, 948–954 (2010).
17. Ye, Y., Wang, L., Chen, Y., Zhu, S., and Shen, S., "High yield hydrogen production in a single-chamber membrane-less microbial electrolysis cell," *Water Science and Technology*, 61 (3), 721–727 (2010).
18. Call, D.F. and Logan, B.E., "Hydrogen production in a single chamber microbial electrolysis cell lacking a membrane," *Environmental Science & Technology*, 42, 3401–3406 (2008).
19. Chae, K.-J., Choi, M.-J., Kim, K.-Y., Ajayi, F.F., Chang, I.-S., and Kim, I.S., "Selective inhibition of methanogens for the improvement of biohydrogen production in microbial electrolysis cells," *International Journal of Hydrogen Energy*, 35 (24), 13379–13386 (2010).

20. Lalaurette, E., Thammannagowda, S., Mohagheghi, A., Maness, P.-C., and Logan, B.E., "Hydrogen production from cellulose in a two-stage process combining fermentation and electrohydrogenesis," *International Journal of Hydrogen Energy*, 34 (15), 6201–6210 (2009).
21. Selembo, P.A., Perez, J.M., Lloyd, W.A., and Logan, B.E., "High hydrogen production from glycerol or glucose by electrohydrogenesis using microbial electrolysis cells," *International Journal of Hydrogen Energy*, 34, 5373–5381 (2009).
22. Hu, H., Fan, Y., and Liu, H., "Hydrogen production using single-chamber membrane-free microbial electrolysis cells," *Water Research*, 42, 4172–4178 (2008).
23. Zhang, Y., "The use and optimization of stainless steel mesh cathodes in microbial electrolysis cells," Masters thesis, Pennsylvania State University, University Park, PA (2010).
24. Liu, H., Cheng, S., Huang, L., and Logan, B.E., "Scale-up of membrane-free single-chamber microbial fuel cells," *Journal of Power Sources*, 179, 274–279 (2008).
25. Shimoyama, T., Komukai, S., Yamazawa, A., Ueno, Y., Logan, B.E., and Watanabe, K., "Electricity generation from model organic wastewater in a cassette-electrode microbial fuel cell," *Applied Microbiology and Biotechnology*, 80, 325–330 (2008).
26. Tartakovsky, B., Manuel, M.-F., Wang, H., and Guiot, S.R., "High rate membrane-less microbial electrolysis cell for continuous hydrogen production," *International Journal of Hydrogen Energy*, 34 (2), 672–677 (2009).
27. Cheng, S. and Logan, B.E., "Ammonia treatment of carbon cloth anodes to enhance power generation of microbial fuel cells," *Electrochemistry Communications*, 9 (3), 492–496 (2007).
28. Logan, B., Cheng, S., Watson, V., and Estadt, G., "Graphite fiber brush anodes for increased power production in air-cathode microbial fuel cells," *Environmental Science & Technology*, 41, 3341–3346 (2007).
29. Logan, B.E., Call, D., Cheng, S., Hamelers, H.V.M., Sleutels, T.H.J.A., Jeremiasse, A.W., and Rozendal, R.A., "Microbial electrolysis cells for high yield hydrogen gas production from organic matter," *Environmental Science & Technology*, 42 (23), 8630–8640 (2008).
30. Bagi, Z., Acs, N., Balint, B., Horvath, L., Dobo, K., Perei, K., Rakhely, G., and Kovacs, K., "Biotechnological intensification of biogas production," *Applied Microbiology and Biotechnology*, 76, 473–482 (2007).
31. Xu, K., Liu, H., and Chen, J., "Effect of classic methanogenic inhibitors on the quantity and diversity of archaeal community and the reductive homoacetogenic activity during the process of anaerobic sludge digestion," *Bioresource Technology*, 101 (8), 2600–2607 (2010).
32. Cheng, S. and Logan, B.E., "Evaluation of catalysts and membranes for high yield biohydrogen production via electrohydrogenesis in microbial electrolysis cells (MECS)," *Water Science and Technology*, 58, 4, 853–857 (2008).
33. Fan, Y., Zhang, Y., Zhang, S., Hou, H., and Ren, B., "Efficient conversion of wheat straw wastes into biohydrogen gas by cow dung compost," *Bioresource Technology*, 97 (3), 500–505 (2006).
34. Ding, H.B., Liu, X.Y., Stabnikova, O., and Wang, J.-Y., "Effect of protein on biohydrogen production from starch of food waste," *Water Science and Technology*, 57, 7, 1031–1036 (2008).
35. Lay, J., "Modelling and optimization of anaerobic digested sludge converting starch to hydrogen," *Biotechnology Bioengineering*, 68 (3), 269–278 (2000).
36. Ange Abdoun, E. and Weiland, P., *Bermimer Agrartechnische Berichte*, 68, 69–78 (2009).
37. Ahrens, T. and Weiland, P., "Biomethane for future mobility," *Landbauforschung Volkenrode*, 57, 71–79 (2007).

38. Schink, B., "Energetics of syntrophic cooperation in methanogenic degradation," *Microbiology Molecular Biology Review*, 61, 262–280 (1997).
39. Angelidaki, I., Ellegard, L., and Ahring, B., "A comprehensive model of anaerobic bio-conversion of complex substrates to biogas," *Biotechnology Bioengineering*, 63, 363–372 (1999).
40. Angelidaki, I., Ellegaard, L., and Ahring, B.K., "A mathematical model for dynamic simulation of anaerobic digestion of complex substrates: Focusing on ammonia inhibition," *Biotechnology Bioengineering*, 42, 159–166 (1993).
41. Elferink, S., van Lis, R., Heilig, H., Akkermans, A., and Stams, A., "Detection and quantification of microorganisms in anaerobic bioreactors," *Biodegradation*, 9, 169–177 (1998).
42. Karakashev, D., Bastone, D., and Angelidaki, I., "Influence of environmental conditions on methanogenic compositions in anaerobic biogas reactors," *Applied and Environmental Microbiology*, 71, 331–338 (2005).
43. Klocke, M., Nettman, E., Bergmann, I., Mundt, K., Soudiu K., Mumme, I., and Linke, B., "Characterization of the methanogenic archaea within two-phase biogas reactor systems operated with plant biomass," *Systematic and Applied Microbiology*, 31, 190–205 (2008).
44. Yu, Y., Lee, C., Kim, J., and Hwangs, S., "group specific primer and probe sets to detect methanogenic communities using quantitative real time polymerase chain reaction," *Biotechnology Bioengineering*, 89, 670–679 (2005).
45. Leven, L., Eriksson, A., and Schnurer, A., "Effect of process temperature on bacterial and archaeal communities in two methanogenic bioreactors treating organic household waste," *FEMS Microbiology Ecology*, 59, 683–693 (2007).
46. Chen, Y., Cheng, J., and Creamer, K., "Inhibition of anaerobic digestion process: A review," *Bioresource Technology*, 99 (10), 4044–4064 (2008).
47. Nielsen, H. and Angelidaki, I., "Strategies for optimizing recovery of biogas process following ammonia inhibition," *Bioresource Technology*, 99, 7995–8001 (2008).
48. Wang, Q., Kuninobu, M., Ogawa, H., and Kato, Y., "Degradation of volatile fatty in highly efficient anaerobic digestion," *Biomass & Bioenergy*, 16, 407–416 (1999).
49. Mosche, M. and Jordening, H., "Comparison of different models of substrate and product inhibition in ammonia digestion," *Water Research*, 33, 2545–2554 (1999).
50. Bischoff, M., "Erkenntnisse beim Einsatz von Zusatz- und Hilfsstoffen sowie von Spurenelementen in Biogasanlagen," *VDI-Ber.*, 2057, 111–123 (2009).
51. Friedmann, H. and Kobe, J., "Optimierung der Biogasproduktion aus nachwachsenden Rohstoffen durch den Einsatz von Mikronährstoffen—ein Erfahrungsbericht," in Tagungsband 17, Jahrestagung des Fachverbandes Biogas, Nuremberg, Germany, 125–130 (2008).
52. Braun, R., Weiland, P., and Wellinger, A., "Biogas from energy crop digestion," IEA Bioenergy Task 37 Energy from Biogas and Landfill Gas IEA, Paris, France (2011).
53. Braun, R., "Potential of co-digestion," (2002), <http://www.novaenergie.ch/iea-bioenergy-task37/Dokumente/final.PDF>.
54. Braun, R. and Wellinger, A., "Potential for co-digestion," IEA Bioenergy Task 37 Energy from Biogas and Landfill Gas (2002).
55. Chen, Y.S., Zuckerman, G.J., and Zering, K., "Applying target costing in the development of marketable and environmentally friendly products from swine waste," *The Engineering Economics*, 53, 156–170 (2008).
56. Kunchikannan, L.K.N.V., Mande, S.P., Kishore, V.V.N., and Jain, K.L., "Cair pith: A potential agro residue for anaerobic digestion," *Energy Sources, Part A*, 29, 293–301 (2007).
57. Weichgrebe, D., Urban, I., and Friedrich, K., "Energy and CO<sub>2</sub> reduction potentials by anaerobic treatment of wastewater and organic kitchen wastes in consideration of different climate conditions," *Water Science and Technology*, 58, 2, 379–384 (2008).

58. Pathe, P.P., Rao, N.N., Kharwade, M.R., Lakhe, S.B., and Kaul, S.N., "Performance evaluation of a full scale effluent treatment plan for distillery spent wash," *Journal of Environmental Studies*, 59 (4), 415–437 (2002).
59. Kolesarova, N., Hutnan, M., Bodik, I., and Spalkova, V., "Utilization of biodiesel by-products for biogas production," *Journal of Biomedicine and Biotechnology*, 126798, 1–15 (2011).
60. Beszedes, S., Laszlo, Z., Szabo, G., and Hodur, C., "The possibilities of bioenergy production from whey," *Journal of Agricultural Sciences Technology*, 4 (1), 62–68 (2010).
61. Yusoff, M., Rahman, N., Abd-Aziz, S., Ling, C.M., Hassan, M., and Shirai, Y., "The effect of hydraulic retention time and volatile fatty acids on biohydrogen production from palm oil mill effluent under non-sterile condition," *Australian Journal of Basic and Applied Sciences*, 4 (4), 577–587 (2010).
62. Zheng, G.H., Kang, Z.H., Qian, Y.F., Wang, L., Zhou, Q., and Zhu, H.G., "Biohydrogen production from tofu wastewater with glutamine auxotrophic mutant of *Rhodobacter sphaeroides*," in Tohji, K., Tsuchiya, N., and Jeyadevan, B. (eds.), *Proceedings of the 5th International Workshop on Water Dynamics*, Sendai, Japan, American Institute of Physics, 143–148 (2008).
63. Abderrezag, I.A., "Employment of anaerobic digestion process of municipal solid waste for energy," *Energy Sources, Part A*, 29, 657–668 (2007).
64. Angelidaki, I., Alves, M., Bolzonella, D., Borzacconi, L., Campos, L., Guwy, A., Kalyuzhnyi, S., Jenicek, P., and van Lier, J.B., "Defining the biomethane potential (BMP) of solid organic wastes and energy crops: A proposed protocol for batch assays," *Water Science and Technology*, 59, 5, 927–934 (2009).
65. Shin, H.K., Han, S., Song, Y., and Hwan, E., "Biogasification of food residuals," *Biocycle*, 82–86 (2000).
66. Haug, R.T., Hernandez, G., Sarullo, T., and Gerringer, F., "Using wastewater digesters to recycle food residuals into energy," *Biocycle*, 74–77 (2000).
67. Desai, H., Nagori, G., and Vahora, S., "Energy generation potential of dairy effluent—A case study of Vidya dairy," *Proceedings of the International Conference on Energy and Environment*, March 19–21, Chandigarh, India (2009).
68. Zhang, R., "Biogasification of organic solid wastes," *Biocycle*, 43, 56–59 (2002).
69. Mata-Alvarez, J., Mace, S., and Llabres, P., "Anaerobic digestion of organic solid wastes. An overview of research achievements and perspectives," *Bioresource Technology*, 74, 3–16 (2000).
70. Narra, M., Nagori, G.P., and Pushalkar, S., "Biomethanation of household organic waste at high solid content a package for waste disposal and energy generation," *Proceedings of the International Conference on Energy and Environment*, March 19–21, Chandigarh, India (2009).
71. Nandy, T., Kaul, S.N., Pathe, P.P., Deshpande, C.V., and Daryapurkar, R.A., "Pilot plant studies on fixed bed reactor system for biomethanation of distillery spent wash," *International Journal of Environmental Studies*, 41, 87–107 (1992).
72. Alves, M., Pereira, M., Sousa, D., Cavaleiro, A.J., Picavet, M., Smidt, H., and Stams, A., "Waste lipids to energy: How to optimize methane production from long-chain fatty acids (LCFA)," *Microbial Biotechnology*, 2 (5), 538–550 (2009).
73. Yusuf, M., Debora, A., and Ogheneruona, D., "Ambient temperature kinetic assessment of biogas production from co-digestion of horse and cow-dung," *Research in Agricultural Engineering*, 57 (3), 97–104 (2011).
74. Kujawski, O. and Steinmetz, H., "Development of instrumentation systems as a base for control of digestion process stability in full-scale agricultural and industrial biogas plants," *Water Science and Technology*, 60 (8), 2055–2063 (2009).

75. Martin-Gonzalez, L., Castro, R., Pereira, M., Alves, M., Font, X., and Vicent, T., "Thermophilic co-digestion of organic fraction of MSW with FOG wastes from a sewage treatment plant: Reactor performance and microbial community monitoring," *Bioresource Technology*, 102 (7), 4734–4741 (2011).
76. Singh, R. and Mandal, S., "The utilization of non-edible cake along with cow dung for methane enriched biogas production using mixed inoculums," *Energy Resources, Part A, Recovery, Utilization and Environmental Effects*, 33 (5), 449–458 (2011).
77. Zhu, H., Parker, W., Basnar, R., Proracki, A., Falletta, P., Beland, M., and Seto, P., "Buffer requirements for enhanced hydrogen production in acidogenic digestion of food wastes," *Bioresource Technology*, 100 (21), 5097–5102 (2009).
78. Hutnan, M., Spalkova, V., Bodik, I., Kolesarova, N., and Lazor, M., "Biogas production from maize grains and maize silage," *Polish Journal of Environmental Studies*, 19 (2), 323–329 (2010).
79. Azaizeh, H. and Jadoun, J., "Co-digestion of olive mill wastewater and swine manure using up-flow anaerobic sludge blanket reactor for biogas production," *Journal Water Resource and Protection*, 2, 314–321 (2010).
80. Yusuf, M. and Ify, N., "The effect of waste paper on the kinetics of biogas yield from the co-digestion of cow dung and water hyacinth," *Biomass & Bioenergy*, 35 (3), 1345–1351 (2011).
81. Bagge, E., Peterson, M., and Johansson, K.E., "Diversity of spore forming bacteria in cattle manure, slaughterhouse waste and samples from biogas plants," *Journal of Applied Microbiology*, 109 (5), 1549–1565 (2010).
82. Wu, X., Yao, W., Zhu, J., and Miller, C., "Biogas and CH<sub>4</sub> productivity by co-digesting swine manure with three crop residues as an external carbon source," *Bioresource Technology*, 101 (11), 4042–4047 (2010).
83. Buhle, L., Stulpagel, R., and Wachendorf, M., "Comparative life cycle assessment of the integrated generation of solid fuel and biogas from biomass (IFBB) and whole crop digestion (WCD) in Germany," *Biomass & Bioenergy*, 35 (1), 363–373 (2011).
84. Salminen, E. and Rintala, J., "Anaerobic digestion of organic solid poultry slaughterhouse waste: A review," *Bioresource Technology*, 83 (1), 13–26 (2002).
85. Macias-Corral, M., Samani, Z., Hanson, A., Smith, G., Funk, P., Yu, H., and Longworth, J., "Anaerobic digestion of municipal solid waste and agricultural waste and the effect of co-digestion with dairy cow manure," *Bioresource Technology*, 99 (17), 8288–8293 (2008).
86. Holm-Nielsen, J., Seadi, T., and Oleskowicz-Popiel, P., "The future of anaerobic digestion and biogas utilization," *Bioresource Technology*, 100 (922), 5478–5484 (2009).
87. Oslaj, M., Mursec, B., and Vindis, P., "Biogas production from maize hybrids," *Biomass & Bioenergy*, 34 (11), 1538–1545 (2010).
88. Fang, C., Boe, K., and Angelidaki, I., "Anaerobic co-digestion of by products from sugar production with cow manure," *Water Research*, 45 (11), 3473–3480 (2011).
89. Gunaseelan, V.N., "Anaerobic digestion of biomass for methane production: A review," *Biomass & Bioenergy*, 13, 83–114 (1997).
90. Kaparaju, P. and Rintala, J., "Anaerobic co-digestion of potato tuber and its industrial by-products with pig manure," *Resources, Conservation and Recycling*, 43, 175–188 (2005).
91. Lopez, J., Li, Q., and Thompson, I., "Biorefinery of waste orange peel," *Critical Reviews in Biotechnology*, 30 (1), 63–69 (2010).
92. Baserga, U., Landwirtschaftliche Co-vergarungs-Biogasanlagen, FAT-Berichte No. 512, Tanikon, Switzerland (1998).
93. Cowan, A.K., "Bio-refineries: Bioprocess technologies for waste water treatment, energy and product valorization," in Tarasenko, O. (ed.), *Proceedings of the 4th Bionanotox Conference*, Little Rock, AK, American Institute of Physics, College Park, MD, November 4–5, 80–86 (2010).

94. Ryan, D., Gadd, A., Kavanagh, J., and Barton, G., "Integrated biorefinery wastewater design," *Chemical Engineering Research and Design*, 87, 1261–1268 (2009).
95. Agdag, O.N. and Sponza, D.T., "Co-digestion of mixed industrial sludge with municipal solid wastes in anaerobic simulated landfilling bioreactors," *Journal of Hazardous Materials Volume*, 140, 75–85 (2007).
96. Alvarez, R. and Liden, G., "Semi-continuous co-digestion of solid slaughterhouse waste, manure, and fruit and vegetable waste," *Renewable Energy*, 33 (4), 726–734 (2007).
97. Davidsson, A., Lovstedt, C., la Cour Jansen, J., Gruvberger, C., and Aspegren, H., "Co-digestion of grease trap sludge and sewage sludge," *Waste Management*, 28 (6), 986–992 (2008).
98. Fernandez, A., Sanchez, A., and Font, X., "Anaerobic co-digestion of a simulated organic fraction of municipal solid wastes and fats of animal and vegetable origin," *Biochemical Engineering*, 26, 22–28 (2005).
99. Fezzani, B. and Cheikh, R., "Thermophilic anaerobic co-digestion of olive mill wastewater with olive mill solid wastes in a tubular digester," *Chemical Engineering Journal*, 132 (1–3), 195–203 (2007).
100. Gelegenis, J., Georgakakis, D., Angelidaki, I., and Mavris, V., "Optimization of biogas production by co-digesting whey with diluted poultry manure," *Renewable Energy*, 32, 2147–2160 (2007).
101. Gomez, G., Cuertos, M., Cara, J., Moran, A., and Garcia, A., "Anaerobic co-digestion of primary sludge and the fruit and vegetable fraction of the municipal solid wastes: Conditions for mixing and evaluation of the organic loading rate," *Renewable Energy*, 31, 2017–2024 (2006).
102. Lehtomäki, A., Huttunen, S., and Rintala, J., "Laboratory investigations on co-digestion of energy crops and crop residues with cow manure for methane production: Effect of crop to manure ratio," *Resources, Conservation and Recycling*, 51, 591–609 (2007).
103. Murto, M., Björnsson, L., and Mattiasson, B., "Impact of food industrial waste on anaerobic co-digestion of sewage sludge and pig manure," *Journal of Environmental Management*, 70, 101–117 (2004).
104. Neves, L., Oliveira, R., and Alves, M., "Anaerobic co-digestion of coffee waste and sewage sludge," *Waste Management*, 26, 176–181 (2006).
105. Romano, R.T. and Zhang, R., "Co-digestion of onion juice and wastewater sludge using an anaerobic mixed biofilm reactor," *Bioresource Technology*, 99 (3), 631–637 (2007).
106. Zupancic, G.D., Uranjek-Zevart, N., and Ros, M., "Full-scale anaerobic co-digestion of organic waste and municipal sludge," *Biomass & Bioenergy*, 32 (2), 162–167 (2008).
107. Alvarez, J., Otero, L., and Lema, J., "A methodology for optimizing feed composition for anaerobic co-digestion of agro-industrial wastes," *Bioresource Technology*, 101, 1153–1158 (2010).
108. McDonald, N., "Experiences with anaerobic digestion of energy crops and high solids manures," OWS Report, AgSTAR, Mankato, MN (May 2011).
109. Dohler, H., Eckel, H., and Frisch, J., *Energiepflanzen*, KTBL, Darmstadt (2006).
110. KTBL/FNR Faustzahlen Biogas, Kuratorium für Technik und Bauwesen in der Landwirtschaft, Darmstadt, Germany, 49–51 (2007).
111. Karpenstein-Machan, *Energiepflanzenbau für Biogasanlagenbetreiber*. DLG-Verlag, Frankfurt, Germany (2005).
112. Weinberg, Z., Muck, R., and Weimer, P., "The survival of silage inoculant lactic acid bacteria in rumen fluid," *Journal of Applied Microbiology*, 93, 1066–1071 (2003).
113. Banemann, D. and Nelles, M., Von der Emte bis in den Fermenter, VDI-Ber 2057, 29–46 (2009).
114. Muller, J., Tiehm, A., Eder, B., Günthert, F., Hruschka, H., Kopp, J., Kunz, P., Otte-Witte, R., Schmelz, K., and Seiler, K., "Thermische, Chemische, und biochemische Desintegrationsverfahren," *Korresp Abwasser*, 50, 796–804 (2003).

115. Mahandete, A., Bjornsson, L., Kivaishi, A., Rubindamayugi, M.S.T., and Matthiasson, B., "Effect of particle size on biogas yield from sisal fiber waste," *Renewable Energy*, 31, 2385–2392 (2006).
116. Prechtel, S., Anzer, T., Schneider, R., and Faulstich, M., "Biogas production from substrate with high amount of organic nitrogen," *Proceedings of the 10th World Congress—Anaerobic Digestion 2004*, Montreal, QC, August 29–September 2 (2004).
117. Mladenovska, Z., Hartmann, H., Kvist, T., Sales-Cruz, M., Gani, R., and Ahring, B., "Thermal pretreatment of the solid fraction of manure: Impact of the biogas reactor performance and microbial community," *Water Science and Technology*, 53, 59–67 (2006).
118. Romano, R., Zhang, R., Teter, S., and McGarry, J., "The effect of enzyme addition on anaerobic digestion of Jose Tall Wheat Grass," *Bioresource Technology*, 100, 4564–4571 (2009).
119. Morgavi, D., Beauchemin, K., and Nsereko, L., "Resistance of feed enzymes to proteolytic inactivation by rumen microorganisms and gastrointestinal proteases," *Journal of Animal Science*, 79, 1621–1630 (2001).
120. Angelidaki, I., Ellegaard, L., and Ahring, B., "Application of the anaerobic digestion process," in Ahring, B. (ed.), *Biomethanation II, Advances in Biochemical Engineering/Biotechnology*, Springer, Berlin, Germany, 82, 2–33 (2003).
121. Gemmeke, B., Rieger, C., and Weiland, P., Biogas-Messprogramm II, 61 Biogaaanlagen im Vergleich, FNR, Gulzow (2009).
122. Schon, M., *Verfahren zur Vergarung organischer Ruckstande in der Abfallwirtschaft*, Erich Schmidt Verlag, Berlin, Germany (1994).
123. de Baere L. and Mattheeuws, B., "State of the art 2008-anaerobic digestion of solid waste," *Waste Management World*, 9, 1–8 (2008).
124. Kusch, S., Oechsner, H., and Jungbluth, T., "Vergarung landwirtschaft-licher substrtae in diskontinuierlichen Feststofffermentern," *Agratechnische Forschung* 11, 81–91 (2007); Biogashandbuch Bayern-Materialband. Bayerisches Landesamt fur Umwelt, Augsburg, Germany (2005).
125. Lethomaki, A., "Biogas production from energy crops and crop residues," *Jyvask Studies in Biological and Environmental Science*, 163, 1–91 (2006).
126. Parawira, W., Read, J., Mattiasson, B., and Bjornsson, L., "Energy production from agricultural residues: High methane yields in a pilot scale two-stage anaerobic digestion," *Biomass & Bioenergy*, 32, 44–50 (2008).
127. Busch, G., Grossmann, J., Sieber, M., and Burkhardt, M., "A new and sound technology for biogas from solid waste and biomass," *Water, Air, & Soil Pollution: Focus*, 9, 89–97 (2009).
128. Vieitez, E. and Gosh, S., "Biogasification of solid wastes by two phase anaerobic fermentation," *Biomass & Bioenergy*, 16, 299–309 (1999).
129. Oechsner, H. and Lemmer, A., "Was Kann die Hydrolyse bei der Biogasvergarung leisten?" VDI-Ber 2057, 37–46 (2009).
130. Gavala, H., Angelidaki, I., and Ahring, B., "Kinetics and modeling of anaerobic digestion process," in Scheper, T. and Ahring, B.K. (eds.), *Biomethanation I*. Springer, Berlin, Germany, pp. 57–93 (2003).
131. Mahnert, P., "Kinetic der Biogas produktion aus nachwachsenden Rohstoffen und Gulle," Dissertation, Humboldt-Universitat, Berlin, Germany, 202 (2007).
132. Andara, A.R. and Esteban J.M.B., "Kinetic study of the anaerobic digestion of the solid fraction of piggery slurries," *Biomass & Bioenergy*, 17, 435–443 (1999).
133. Linke, B., "Kinetic study of thermophilic anaerobic digestion of solid wastes from potato processing," *Biomass & Bioenergy*, 30, 892–896 (2006).
134. Biswas, L., Chowdhury, R., and Battacharya, P., "Mathematical modeling for the prediction of biogas generation characteristics of an anaerobic digester based on food/vegetable residues," *Biomass & Bioenergy*, 31, 80–86 (2007).

135. Weiland, P., "Wichtige Messdaten für den Prozessablauf und Stand der Technik in der Praxis," *Gulzower Fachgespräche*, 27, 17–31 (2008).
136. Ahring, B., Sandberg, M., and Angelidaki, I., "Volatile fatty acids as indicators of process imbalance in anaerobic digesters," *Applied Microbiology and Biotechnology*, 34, 559–565 (1995).
137. Nielsen, H., Uellendahl, H., and Ahring, B., "Regulation and optimization of biogas process: Propionate as a key factor," *Biomass & Bioenergy*, 31, 820–830 (2007).
138. Boe, K., Bastone, D., and Angelidaki, I., "Online headspace chromatographic method for measuring VFA in biogas reactor," *Water Science and Technology*, 52, 473–478 (2005).
139. Schneider, R., Quicker, P., Anzer, T., Prechtel, S., and Faulstich, M., "Grundlegende Untersuchungen zur effektiven, kostengünstigen Entfernung von Schwefelwasserstoff aus Biogas," in *Biogasanlagen Anforderungen zur Luftreinhaltung*, Bayerisches Landesamt für Umweltschutz, Augsburg, Germany (2002).
140. Klocke, M., Netterman, E., and Bergmann, I., "Monitoring der methanbildenden Mikroflora in Praxis-Biogasanlagen im ländlichen Raum: Analyse des Ist-zustandes und Entwicklung eines quantitativen Nachweissystems," *Bornimer Agrartechnische Berichte*, 67, (2009).

---

# 9 Hydrolysis and Fermentation Technologies for Alcohols

## 9.1 INTRODUCTION

Water plays an essential role in the hydrolysis and fermentation of lignocellulosic materials to produce alcohols. While most of the efforts have been made to generate ethanol, in the recent years, some research has been pursued to generate higher alcohols such as butanol via fermentation technologies [1]. In this chapter, we mainly focus on ethanol with a brief update on the recent advances in the generation of butanol via hydrolysis and fermentation technologies.

Ethanol is the second largest solvent (next to water) in the world [2]. While ethanol has been generated from sugars via fermentation technology for more than 2000 years in all parts of the world, its expanded use as a fuel or fuel additive has substantially increased its production by the use of innovative technologies. Ethanol is a very versatile material with the following usages [2]:

1. It is a raw material for the manufacture of plastics, lacquers, polishes, plasticizers, perfumes, and cosmetics.
2. Ethyl acetate and ethyl acrylate (i.e., ethyl esters produced by the reaction of ethanol with carboxylic acid) are raw materials for acrylate polymers.
3. Vinegar can be produced by *Acetobacter* bacteria in ethanol solutions.
4. It is a raw material for polylactic acid and polylactide (PLA). Polylactic acid is a biodegradable polymer and can also be used with other polymers as a composite.
5. It is a source for hydrogen via processes of reforming or supercritical water gasification.
6. It can be a substitute for methanol for transesterification of triglycerides to make biodiesel.
7. It is a very good substitute for reformulated gasoline and additive as well as a source of renewable fuel.

Ethanol can be used as E10 (10% ethanol in gasoline), E22 (gasohol used in Brazil), E85 (85% ethanol used in flexible fuel automobiles in Brazil as well in the United

States), or E100 (100% ethanol) [2]. It has a high research octane number, makes the engine more efficient, has reasonable vapor pressure, and helps reduce emissions of  $\text{NO}_x$ , volatile organic compound (VOC), CO, and  $\text{CO}_2$ . It fits well the new Clean Air Act Amendments (CAAA) of 1990, which requires (1) 2% of oxygen by weight in gasoline, (2) maximum benzene content of 2%, and (3) maximum of 25% by volume aromatic hydrocarbons. While ethanol can be used up to 20% in gasoline for conventional cars, it is also very useful for flexible cars and two-cycle engines. Up to 25% ethanol can also be added in acetylene-based dual-fuel systems. Cellulose ethanol will be an important contributor to 32 billion of renewable fuel mandate by the US government by 2022 [2].

During the past several decades, the hydrolysis and fermentation technologies to convert sugar or starch materials have been commercialized very extensively in the United States and Brazil among other countries. While Brazil has chosen sugarcane as starting raw materials, in the United States corn (starch such as wheat, barley, and rice) has been the major feedstock for the ethanol production. Corn refining in the United States has a relatively long history going back in time of the Civil War with the development of cornstarch hydrolysis process. The first cornstarch plant was built in Jersey City, NJ. By 1857, the cornstarch industry accounted for a significant portion of the US starch industry (along with starch from wheat and potatoes). The industrial production of dextrose (sugar) from cornstarch started in 1866. This led to the production of corn sugar, corn sweeteners, corn syrup, and so on [2–7]. After the World War II, ethanol was produced by the fermentation of corn sugar, but major quantities of ethanol from corn were produced only after 1970. While starch and glucose are important parts of corn refineries, about 13.2 billion gallons of ethanol was produced from corn in the United States in 2010. The United States is the world's leading producer of corn, totaling about 331 million tons of corn (worth \$66.7 billion) in 2010. As shown in Figure 9.1, about 34.9% of this production was used to make ethanol [2–7].

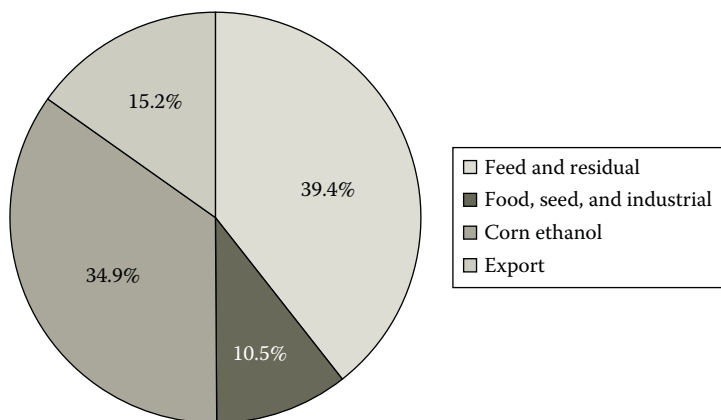


**FIGURE 9.1** Breakdown by categories of 2010 end uses of corn in the United States. (Adapted from Lee, S. and Shah, Y., *Biofuels and Bioenergy—Processes and Technologies*, CRC Press, Boca Raton, FL, 2012; US Grains Council, 2011.)

Today, there are two types of ethanol depending on the source of feedstock: grain ethanol [8–10] and cellulosic ethanol [11,12]. Grain ethanol is made from starch or sugar feedstock such as corn, wheat, barley, rice, and sugarcane, while cellulosic ethanol is produced from lignocellulosic materials. The process for cellulosic ethanol is much more complex than that for grain ethanol due to the complexity of the feedstock in the former case. Here, we describe the processes for both types of ethanol in detail.

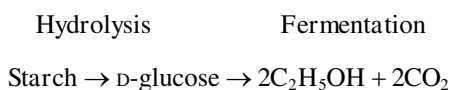
## 9.2 GRAIN (CORN) ETHANOL

Grain ethanol suffers from the fact that the feedstock has food value, and the use of corn, wheat, and so on for the purpose of fuel may become challenging in times of drought or when the corn is in short supply. The need for food is always higher than that for fuel, and these competitive usages for corn may make the price of corn too high for an economical ethanol process. The advantages of grain ethanol are that the starting feedstock is starch (or sugar) and it only requires hydrolysis and fermentation steps and not the pretreatment step as it is required in cellulosic ethanol.

Ethanol production facilities for corn (grain) ethanol are classified into two broad categories: wet milling [2,13–15] and dry milling operations [2,16,17]. As the terms indicate, in dry milling operation, the entire corn kernel is pulverized into flour called “corn meal,” and it is then mixed with water and processed for hydrolysis and fermentation. Dry mills are usually smaller in size and are built primarily to manufacture ethanol only. The remaining stillage from ethanol purification undergoes a different process treatment to produce highly nutritious animal feedstock (often called dried distillers grains [DDGs]). In 2008, a total of 86% of corn ethanol was produced by this method in about 150 dry milling plants [17].

Wet milling processes are called “corn refineries,” which along with ethanol also produce high-value coproducts such as high-fructose corn syrup, dextrose, cornstarch, DDG, and Splenda. They are larger and have more capital and operating costs. While the wet milling process is more versatile and produces many co- and byproducts, it is less efficient than the dry milling process. Thermal energy and electricity are the main types of energy used in both dry and wet milling processes. Dry milling uses natural gas in several parts of the process such as generating steam for mash cooking, distillation, and evaporation. In many new ethanol plants, the use of combined heat and power (CHP) has been very popular due to its increased production efficiencies and expanded fuel capabilities. A CHP system improves the efficiency by 10%–30% more than 50% efficiency obtained in conventional operations [2].

The process of hydrolysis and fermentation of starch involves the following steps:



The theoretical yield of ethanol from sugar (D-glucose) is 51% by weight basis.

### 9.2.1 STARCH HYDROLYSIS

Starch is regarded as a long-chain polymer of glucose (i.e., many glucose molecular units are bonded in a polymeric chain similar to a condensation polymerization product) [18]. This starch is first broken down to simple sugar units by the hydrolysis process. In this process, starch feedstock is ground and mixed with water containing about 15%–20% starch. The mash is then cooked at or above its boiling point and subsequently treated with two enzyme preparations. The first enzyme hydrolyzes the starch into short-chain molecules and the second enzyme hydrolyzes the short-chain molecules into glucose. The first enzyme is amylase, which liberates “maltodextrin” by the liquefaction process. These maltodextrins are very sweet and contain a group of low-molecular-weight carbohydrates called dextrins and oligosaccharides (a polymer of small number of simple sugars, monosaccharides). The dextrins and oligosaccharides are further hydrolyzed in the second step by an enzyme called pullulanase and glucoamylase in a process known as saccharification. Complete saccharification converts all the dextrins to glucose, maltose, and isomaltose. The mash is then cooled and subjected to yeast fermentation.

### 9.2.2 YEAST FERMENTATION

Yeasts convert sugar into ethanol via a biochemical process called fermentation. The yeasts of primary interest to industrial fermentation of ethanol include *Saccharomyces cerevisiae*, *Saccharomyces uvarum*, *Schizosaccharomyces pombe*, and *Kluyveromyces* sp. Under anaerobic conditions, the yeasts metabolize glucose to ethanol primarily via the Embden–Meyerhof pathway. This pathway for glucose metabolism is the series of enzymatic reactions in the anaerobic conversion of glucose to lactic acid or ethanol, resulting in the energy in the form of adenosine triphosphate (ATP) [19]. Generally, the yield is about 90%–95% of the stoichiometric relationship mentioned earlier. About 1716 kg of fermentable sugar is required for the production of 1000 l of ethanol. When the fermentation is completed, the remaining solution is called distilled mash or stillage that contains a large amount of non-fermentable portions of fibers or proteins.

### 9.2.3 ETHANOL PURIFICATION AND PRODUCT SEPARATION

Ethanol is separated from the mash by distillation. Unfortunately, conventional distillation process works only up to 95.63% ethanol because water and ethanol form an azeotrope that will not allow any further concentration of ethanol. The minimum boiling point temperature of 78.2°C is attainable at the azeotropic concentration and not at the pure ethanol concentration. The additional concentration of ethanol is carried out by dehydration by one of the two methods. In the first method, a third component (such as benzene) is used to change the boiling characteristics of the solution. The third component breaks azeotrope and allows conventional distillation to be carried out in a tertiary system to achieve the desired separation. The second method uses the molecular sieves that absorb water selectively and therefore concentrate ethanol further. There are different forms of molecular sieves that are based

on the dimensions of effective pore opening, which include 3A, 4A, 5A, and 13X. Commercial molecular sieves are typically available in powder, bead, granular, and extrudate forms.

### 9.2.4 BYPRODUCTS AND COPRODUCTS

The nonfermentable solids in distilled mash (stillage) contain variable amounts of proteins and fibers depending on the feedstock. The recovery of protein and other nutrients in stillage for use as an animal feedstock is essential for making the overall ethanol production process profitable. Corn and barley yield solid byproducts called DDGs. The protein content of DDG typically ranges from 25% to 30% by mass and makes an excellent feedstock for the animals. Byproducts and coproducts are very important for corn refineries (wet milling process).

### 9.2.5 ENVIRONMENTAL IMPLICATIONS

The liquid effluent generated from ethanol process may contain some harmful chemicals and other pollutants that must be discarded properly. About 9 l of liquid effluent is generated for every liter of ethanol produced. The biological oxygen demand (BOD) of effluent can be high and the effluent can be acidic. Both of these factors require additional treatments before discarding the effluents to fields or water streams.

## 9.3 CORN TO ETHANOL PROCESS TECHNOLOGIES

As mentioned earlier, the conversion of corn to ethanol can be carried out as either (1) wet milling corn ethanol (or corn refinery) technology or (2) dry milling corn ethanol technology. We briefly describe both of these technologies in Sections 9.3.1 and 9.3.2.

### 9.3.1 WET MILLING TECHNOLOGY FOR CONVERSION OF CORN TO ETHANOL

The corn wet milling process to produce ethanol separates corn into its four basic components: starch, germ, fiber, and protein. There are eight basic steps involved to accomplish this corn refining and alcohol fermentation process [10].

Step 1: This step inspects the incoming corn visually and removes cob, dust, chaff, and any other foreign unwanted materials before the next processing step of steeping. The inspected and screened corn is then conveyed to storage silos holding up to 350,000 bushels.

Step 2: This step carries out the steeping process in which about 2,000–13,000 bushels of corn is soaked in water at 50°C–52°C for 20–48 h in a stainless steel tank. A series of tanks are used. During this process, the kernel of corn (Figure 9.2) absorbs water from 15% to 45% by weight and swells by more than double its original size. The addition of 0.1% sulfur dioxide to water suppresses the excessive bacterial growth in the warm water environment.

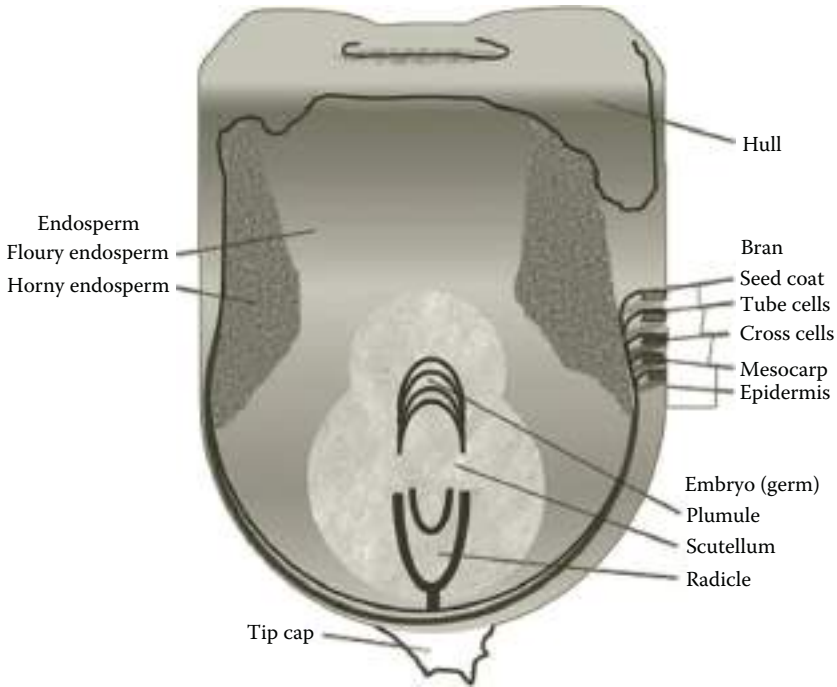


**FIGURE 9.2** Corn kernel. (Adapted from Lee, S. and Shah, Y., *Biofuels and Bioenergy—Processes and Technologies*, CRC Press, Boca Raton, FL, 2012.)

As the corn swells, the mild acidity of the steeping water loosens the gluten bond within the corn eventually releasing the starch [10]. Thus, this step initiates polymeric bond cleavage of starch and protein into simpler molecules.

**Step 3:** The third step is the germ separation. The coarse grinding of corn in the slurry separates germ (Figure 9.2) from corn. This germ separation is accomplished by cyclone separator that removes the low-density corn germ from the slurry. The germs are repeatedly washed to remove any left-over starch, and then with the use of mechanical and solvent processes, oil from the germ is extracted. The oil is then refined and filtered into finished corn oil. The germ residue is saved as another important component of animal feed. Both corn oil and germ residues are important byproducts of the process.

**Step 4:** In this step, the remaining slurry containing fiber, starch, and protein is finely ground and screened to separate the fiber from starch and protein. A thorough grinding in impact or attrition-impact mill releases the starch and gluten from the fiber in the kernel. Fiber is separated from starch and gluten using concave screens. Fiber is collected and slurried again to reclaim any residual starch and protein, and then sent to the feed house as a major ingredient for animal feed. The starch–gluten suspension (called mill starch) is sent to starch separators [20].

Step 5: In this step, starch is separated from gluten by hydrocyclones. Separated gluten that contains proteins and is called corn gluten meal (CGM) is used for animal feed. CGM can also be used as an organic herbicide. The last 1%–2% protein remained in the starch is further removed by repeated washings and the high-quality starch is now called unmodified cornstarch. While most of cornstarch is converted to corn syrups and dextrose, the cornstarch is also used for a variety of industrial and domestic uses [20].

Step 6: This is a starch-to-sugar conversion step. The starch–water suspension is liquefied in the presence of acid or enzymes. Enzymes help convert the starch to dextrose that is soluble in water as an aqueous solution. If needed, the solution is also treated with another enzyme. The process of acid and enzymatic reactions is controlled according to the desired mixtures of sugars such as dextrose and maltose (a disaccharide) for syrup. The reaction time is used to control the concentration of dextrose and maltose in the final product. Once the conversion is completed, the syrup is passed through filters, centrifuges, or ion exchange columns, and the excess water is evaporated. Syrup can be sold directly as is, crystallized into pure dextrose, or processed further to produce high-fructose corn syrup. Across the corn wet milling industry, about 80% of starch slurry goes to corn syrup, sugar, and fermentation.

Step 7: In this step, corn syrup is converted to several products through a fermentation process. Dextrose (called corn sugar or grape sugar) also known as D-glucose is easily fermentable. The process of fermentation can be carried out either in a continuous way in a series of fermenters to give higher throughput or in a batch fermenter for about 48 h to get a better quality product.

Step 8: The resulting broth from step 7 is distilled to recover ethanol or concentrated through membrane separation to produce other byproducts. Carbon dioxide generated from fermenter is recaptured to produce dry ice for sale, and nutrients still remaining in the broth after fermentation are used as components of animal feed ingredients. These byproducts contribute significantly to the overall economics of the corn refineries. A schematic of corn refinery or wet milling corn-to-ethanol process is described in Figure 9.3.

### 9.3.2 DRY MILLING CORN-TO-ETHANOL PROCESS

This process also contains eight steps, which are as follows:

Step 1: In this step, corn is received and stored in silos designed to hold grain supply for 7–12 days of plant operation.

Step 2: The grain is inspected and screened to remove corn cobs, stalks, finer materials, stones, and other foreign objects by a blower and screen. The cleaned material is coarse grinded using hammer mill. The grinded material is combined with hot water to form slurry.

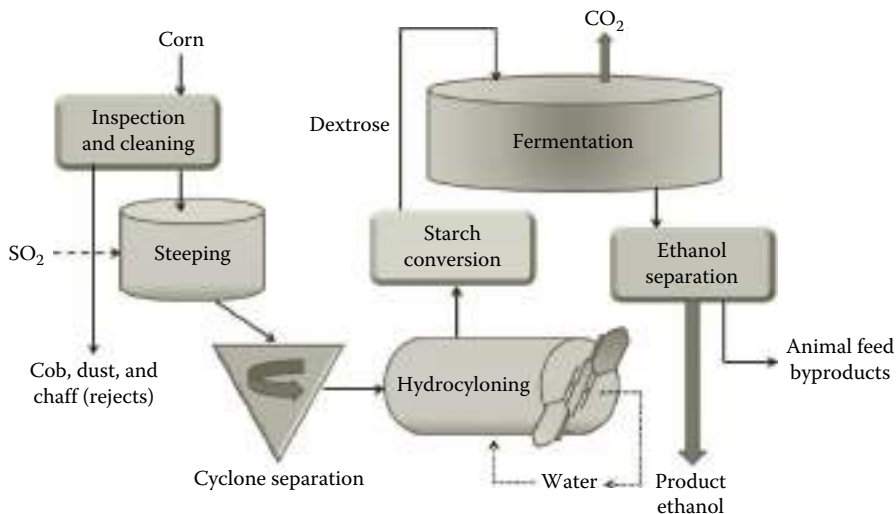


**FIGURE 9.3** A schematic of a typical wet milling corn-to-ethanol process. (Adapted from Lee, S. and Shah, Y., *Biofuels and Bioenergy—Processes and Technologies*, CRC Press, Boca Raton, FL, 2012.)

Step 3: This step has three parts and involves the cooking process, which is also called hot slurry primary and secondary liquefaction. In this process, the starch in the flour is physically prepared and chemically modified for fermentation. In the first part, coarsely ground grain is soaked in hot process water, the pH is adjusted to about 5.8, and alpha-amylase enzyme is added. The agitated slurry is heated to 82°C–88°C for 30–60 min. In the second part of primary liquefaction, the slurry is pumped through a pressurized jet cooker at 105°C and held there for about 5 min. The mixture is then cooled by an atmospheric or vacuum flash condenser. Within jet cooker, the steam rapidly heats the slurry and evenly hydrolyzes. The fluid dynamic relationship between the jet cooker's steam injector and the condensing tube produces a pressure drop to help maximize shear action to improve starch conversion [14]. In the third part of secondary liquefaction, the mixture is held for 1–2 h at 82°C–88°C to give alpha-amylase enzyme sufficient time to break down starch into short-chain low-molecular-weight dextrans. This chemical conversion is called gelatinization. As the conversion of starch proceeds, the viscosity of slurry decreases. Dextrans are a mixture of polymers of D-glucose units. After pH and temperature adjustment, a second enzyme glucoamylase is added as the mixture is pumped into the fermentation tanks. Glucoamylase is an amylase enzyme that cleaves the last alpha-1,4-glycosidic linkages at the nonreducing end of amylase and amylopectin to yield glucose. The cleavages of the bonds near the ends of long-chain starches release maltose as well as glucose. Maltose, or malt sugar, is a disaccharide that is formed from the two units of glucose joined with alpha(1 → 4) bond.

- Step 4: The fourth step is called simultaneous saccharification fermentation. Once the mixture of milled kernel and water, now known as mash, is inserted in the fermentation tank, the glucoamylase enzyme breaks down the dextrins and oligosaccharides to form simple sugars that are monosaccharides. Yeast is added to convert sugar into ethanol and carbon dioxide. The mash is allowed to ferment for 50–60 h, resulting in a mixture that contains about 15% ethanol as well as solids from the grain and added yeast [16,20].
- Step 5: The fermented mash is pumped into the distillation system to separate ethanol from water at a concentration of up to 95% ethanol by volume (a level of azeotropic mixture). The residue from this process called stillage contains nonfermentable solids and water, and is pumped out of the bottom of the distillation columns into the centrifuges.
- Step 6: The near-azeotropic binary mixture of 95% ethanol and 5% water is dehydrated by a molecular sieve that physically separates the remaining water from the ethanol based on the size difference between the two molecules [16]. The process produces nearly 100% ethanol.
- Step 7: The produced ethanol is stored up to 7–12 days. The ethanol is appropriately used as a fuel blend with gasoline.
- Step 8: Ethanol production process creates two coproducts: carbon dioxide and distillers grains. These coproducts are captured and sold as dry ice and animal feed, respectively, to improve the overall economics of the process.

## 9.4 CELLULOSIC ETHANOL

While starch and sugar produce grain ethanol, the feedstock obtained from this method is also used as food [2,21–54]. In the recent years, more efforts are made to convert all lignocellulosic materials such as hardwood, softwood, agricultural waste, and energy crops into ethanol. Unlike corn, this material is not useful for food purposes. The ethanol produced from lignocellulosic material is called cellulosic ethanol.

Lignocellulosic materials are composed of four ingredients: cellulose, hemicellulose, lignin, and extractives. As shown in Figure 9.4, a generalized plant cell wall structure is like a composite material in which rigid (and crystalline) cellulose fibers are embedded in a cross-linked matrix of lignin and hemicellulose that binds the cellulose fibers. Generally, the dry weight of a typical cell wall consists of approximately 30%–50% cellulose, 20%–35% hemicellulose, and 10%–25% lignin [12]. The exact percentages vary with the nature of the feedstock. For example, for woody biomass, cellulose accounts for 40%–50%, and lignin and hemicellulose each account for about 20%–30%. Lignin is aromatic in nature and provides higher heating value than cellulose or hemicellulose. The chemicals in the biomass matrix include extractives such as resins, phenols, and other chemicals and minerals such as calcium, magnesium, and potassium. These extractives are left behind in ash when biomass is combusted. The trace minerals and major elements in lignocellulosic materials display a high degree of variability for most of the elements between different species and between different organs within a given plant, depending on the growing conditions including the soil characteristics [21].

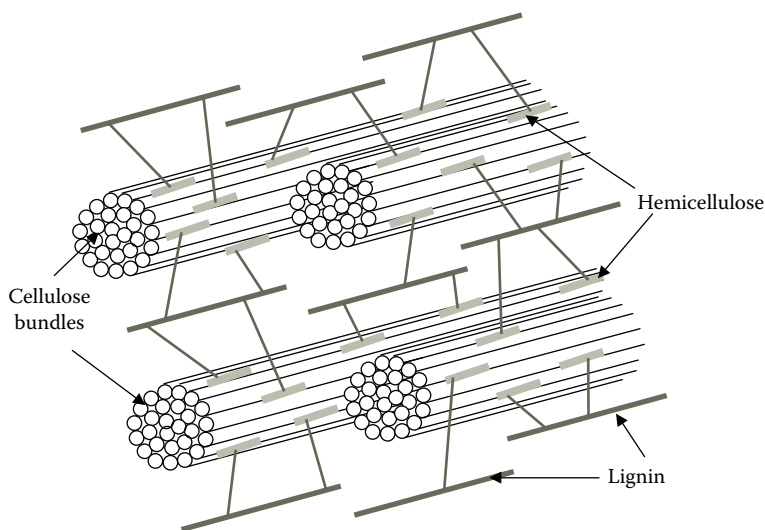


**FIGURE 9.4** A universal description of plant cell wall. (Adapted from Lee, S. and Shah, Y., *Biofuels and Bioenergy—Processes and Technologies*, CRC Press, Boca Raton, FL, 2012.)

Cellulose is a large polymeric molecule composed of many hundreds or thousands of monomeric sugar (glucose) molecules, and in this regard, it can be considered as polysaccharide. The molecular linkages in cellulose form linear chains that are rigid, highly stable, and resistant to chemical attack. It is also crystalline and may be somewhat soluble in a suitable solvent [18]. However, cellulose molecules (which are the predominant source of glucose for ethanol) in their crystalline form are packed so tightly that even small molecules of water cannot easily permeate the structure. It is even more difficult for large enzyme molecules to permeate and diffuse into the cellulose structure. To break the crystalline structure of cellulose and make them more exposed to enzymatic hydrolysis, all processes of cellulosic ethanol require pretreatments. As discussed earlier, this step was not required in the production of grain ethanol.

Starch and sugar can also come from hemicellulose that consists of short and highly branched chains of sugar molecules. It contains both five-carbon sugars (such as D-xylose and L-arabinose) and six-carbon sugars (such as D-galactose, D-glucose, and D-mannose as well as uronic acid. For example, galactan found in hemicellulose is a polymer of sugar galactose. Since hemicellulose is amorphous due to highly branched structures, it is relatively easy to hydrolyze to its constituents—five- and six-carbon sugars [18]. While both five- and six-carbon sugars are in principle fermentable to ethanol, the fermentation chemistry, yeast requirement, and process chemistry for six- and five-carbon sugars (pentose and xylose) are considerably different. In general, five-carbon sugars are more difficult to ferment than six-carbon sugars.

Lignin molecule is a complex and highly cross-linked aromatic polymer that is covalently linked to hemicellulose (Figure 9.4). Lignin contributes to the stabilization of mature cell walls. Due to its high calorific value, it provides more energy than cellulose or hemicellulose, but it cannot be fermented to ethanol. Lignin is a

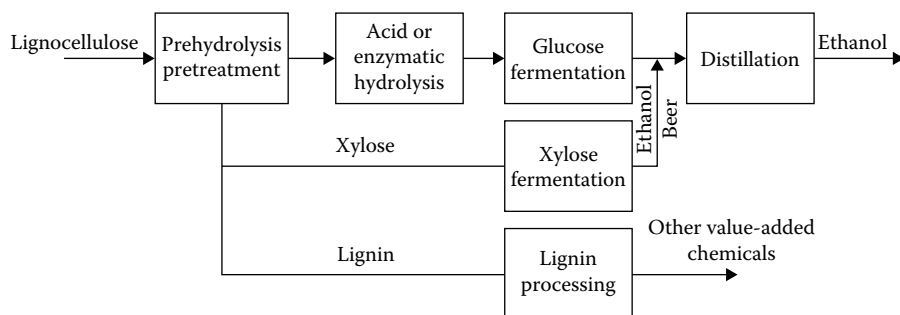


**FIGURE 9.5** Conversion of lignocellulose to ethanol. (Adapted from Lee, S. and Shah, Y., *Biofuels and Bioenergy—Processes and Technologies*, CRC Press, Boca Raton, FL, 2012.)

macromolecule whose typical molecular weight exceeds 10,000. Because of its cross-linked structure, it is difficult to process, extract, and hydrolyze. The major purpose of the pretreatment step of the cellulosic ethanol process is to degrade the cross-linked structure so that both cellulose and hemicellulose are more exposed for subsequent hydrolysis and fermentation steps. An efficient conversion of lignin results in a substantial increase in the overall fuel yield of the cellulosic ethanol process.

A general scheme for the conversion of lignocellulose to ethanol is shown in Figure 9.5. The lignocellulose is pretreated to separate the xylose and sometimes the lignin from the crystalline cellulose. This step is very important because the efficiency of the pretreatment affects the efficiency of the subsequent steps. The xylose can then be fermented to ethanol, whereas the lignin can be further processed to produce other liquid fuels and valuable chemicals. Crystalline cellulose, the largest (about 50%) and most useful fraction, remains behind as solids after pretreatment and is sent to an acid or enzymatic hydrolysis process to break down the cellulose to glucose. Enzymatic hydrolysis (which is more popular now) is very specific and does not break down further sugars. Enzymatic processes are capable of achieving 100% yield. The glucose is then fermented to ethanol and combined with the ethanol from xylose fermentation. This dilute ethanol–water solution is further concentrated by distillation and other dehydration processes.

For an overall efficiency of the conversion process, it is important to convert hemicellulose (which can be up to 25% of lignocellulose) to xylose and xylose to ethanol. Hemicellulose is primarily composed of xylan that can be easily converted to xylose. Xylose constitutes about 17% of woody angiosperms and accounts for a substantially higher percentage of herbaceous angiosperms. Though the fermentation of xylose to ethanol is more difficult than that of glucose, it is very essential for the overall efficiency of the process. Significant new yeast developments for this purpose are currently pursued. Methods have been identified using new strains of or metabolically engineered yeasts [22], bacteria, and processes containing enzymes and yeasts.

Lignin (around 25% of lignocellulose) is a large random phenolic polymer. In lignin processing, the polymer is broken down into fragments containing one or two phenolic rings. Extra oxygen and side chains are stripped from the molecules

by the catalytic methods and the resulting phenol groups are reacted with methanol to produce methyl aryl ethers. These substances are high-value octane enhancers and can be blended with gasoline. We now examine each of the steps outlined in Figure 9.5 in detail.

### 9.4.1 PRETREATMENT

Unlike in the production of grain ethanol, in the production of cellulosic ethanol, pretreatment is essential to achieve the reasonable rates of yields in the enzymatic hydrolysis of biomass [2]. Pretreatment has generally been practiced to reduce the crystallinity of cellulose, to lessen the average degree of polymerization of the cellulose and the lignin–hemicellulose sheath that surrounds the cellulose, and to alleviate the lack of the available surface area for enzymes to attack. The importance of pretreatment can be better understood by examining the hydrolysis process in which the interaction between the enzymes and the substrates must occur. The hydrolysis of cellulose into sugars and other oligomers is a solid-phase reaction in which enzymes must bind to surface to catalyze the reaction. Cellulase enzymes (which are commonly used) are large proteins with molecular weight ranging from 30,000 to 60,000 and are thought to be ellipsoid with major and minor dimensions of 30°A–200°A. The internal surface area of wood is very large; however, only about 20% of the prevolume is accessible to cellulose-sized molecules. By breaking down the tight hemicellulose–lignin matrix, hemicellulose or lignin can be separated and the accessible volume of cellulose can be greatly increased. This removal of materials greatly enhances the enzymatic digestibility.

A typical pretreatment consists of size reduction, pressure sealing, heating, reaction, pressure release, surface area increase, and hydrolyzate/solids separation [23]. Mechanical pretreatments such as intensive ball milling and roll milling to expose more surface area have been found to be very expensive. The hemicellulose–lignin sheath can be disrupted by either acidic or basic catalysts. While basic catalysts simultaneously remove lignin and hemicellulose, its consumption is very large due to its use in neutralization by ash and acidic groups in the hemicellulose. In the recent years, more acidic catalysts such as mineral acids and organic acids generated *in situ* by autohydrolysis of hemicellulose have been tested.

The five important pretreatment processes that are currently being examined and implemented are as follows [2]:

1. Rapid steam hydrolysis (RASH) or autohydrolysis steam explosion
2. Dilute acid prehydrolysis
3. Organosolv pretreatment
4. Combined RASH and organosolv pretreatment
5. Ionic liquid pretreatment

Most pretreatment approaches are not intended to actually hydrolyze cellulose to soluble sugars, but rather to generate the pretreated cellulosic residue that is more hydrolyzable by cellular enzymes than native biomass. Here we examine each pretreatment process in detail.

#### 9.4.1.1 Rapid Steam Hydrolysis

This process was recently described by Lee and Shah [2]. A typical autohydrolysis process uses compressed liquid hot water at a temperature of about 200°C and pressure above the saturation pressure [48]. Thus, the liquid water can hydrolyze hemicellulose in minutes. While hemicellulose recovery is high in this noncatalytic process, wet pyrolysis results in the production of inhibitory compounds. A well-controlled process at high temperature with small particles, however, gives high xylose yields and is desirable. Dekker and Wallis [24] showed that for bagasse, this process gave 90% solubilization of hemicellulose and the product that was highly susceptible to hydrolysis by cellulases from *Trichoderma reesei*. In general, however, the xylose yield in the RASH process is low (30%–50%).

Steam consumption in autohydrolysis strongly depends on the moisture content of the starting material. An important advantage of autohydrolysis is that it breaks down lignin into smaller fragments that can be easily solubilized in either base or organic solvents. This process was first developed in 1925 for hardwood application and more recently for aspen wood (in the 1980s). At a high pressure of 20–50 atm and temperature of 210°C–290°C, the water molecules diffuse into the microporous structure of lignocellulose and the steam condenses at high pressure, thereby wetting the materials [23]. The wetted material is then driven out of the reactor by a small nozzle using a pressure difference. The term “explosion” is used because of the process characteristics of the ejection driven by a sudden large pressure drop of steam.

#### 9.4.1.2 Dilute Acid Prehydrolysis

The pretreatment process can be operated at a lower temperature with reduced sugar degradation by adding a small amount of mineral acid in the pretreatment process. The acid increases the reaction rates at a given temperature, and the ratio of hydrolysis rate to the degradation rate is also increased. The reaction rate can be optimized between the temperature and the reaction time. Higher temperature (200°C) can take 10 s, whereas lower temperature (100°C) may take several hours. Generally, the acid concentration (sulfuric acid) between 0.5 and 4 wt% is used. While sulfuric acid gives the xylose yields of 70%–95%, it produces more condensed lignin. Sulfur dioxide is often used as a catalyst. Numerous reports have indicated good results using this method [2,25]. While acid hydrolysis has been used for more than 100 years, the replacement of dilute acid hydrolysis by more concentrated acid prehydrolysis was found to be more expensive. While sulfuric acid is the most widely used catalyst in this pretreatment, other mineral acids such as hydrochloric, nitric, and trifluoroacetic ( $\text{CF}_3\text{COOH}$ ) acids have also been used.

#### 9.4.1.3 Organosolv Pretreatment

This process is a pulping technique that uses an organic solvent to solubilize lignin and hemicellulose. A process developed by Kraft pulping produces high-quality lignin for added values and easy recovery and recycling of solvents used in the process. The organic solvents such as ethanol, butanol, and methanol are added to the pretreatment reaction to dissolve and remove lignin fraction. The internal lignin and hemicellulose bonds are broken, and both fractions are solubilized while cellulose remains intact as solid. Careful steps are taken such that the process

cleanly separates the feedstock into a solid cellulose residue, a solid lignin that has undergone a few condensation reactions and a liquid stream containing xylon. The process is carried out at high temperature ( $140^{\circ}\text{C}$ – $230^{\circ}\text{C}$ ) and under pressure to achieve the desired bond cleavages. Ethanol is the most desired solvent due to its price, availability, and easy recovery. In general, organosolv processes have higher xylose yields than other processes due to the influence of the organic solvent on hydrolysis kinetics [26].

#### 9.4.1.4 Combined RASH and Organosolv Pretreatment

Attempts have been made to improve the pretreatment process by combining RASH and organosolv treatments [27]. A schematic diagram of this process is shown in Figure 9.6. As shown, for the organosolv pretreatment, in this process the steam generator is disconnected and the condensate valve is closed. The rest of the reactor setup is similar to the typical RASH process. The combination of these two processes, which requires high temperature, leads to an increased solubilization of lignin and hemicellulose. RASH temperature is the major factor in maximizing the percentage of cellulose in the final product. The maximum yield of solubilized lignin was obtained at a temperature of  $240^{\circ}\text{C}$  for RASH and  $160^{\circ}\text{C}$  for the organosolv process.

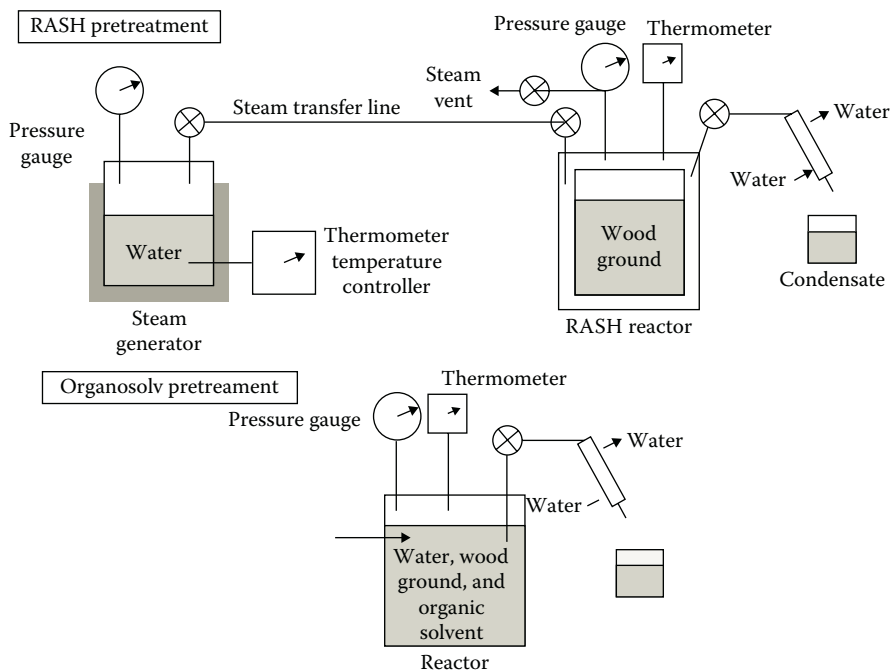


**FIGURE 9.6** A combined RASH and organosolv pretreatment scheme. (Adapted from Lee, S. and Shah, Y., *Biofuels and Bioenergy—Processes and Technologies*, CRC Press, Boca Raton, FL, 2012; Rughani, L. and McGinnis, G.D., *Biotechnology and Bioengineering*, 33, 681–686, 1989.)

#### 9.4.1.5 Ionic Liquid Pretreatment

An ionic liquid is a salt composed of anions and cations that are poorly coordinated and that has a melting point below 100°C. Ionic liquids have been demonstrated as very efficient solvents for hydrogenation, esterification, nanomaterial synthesis, biocatalysis, and selective extraction of aromatics [28,29]. The first demonstration of an ionic liquid as a cellulose solvent under relatively mild operating conditions was reported in 2002 by Swatloski [29]. The treatment used a range of anions and 1-butyl-methylimidazolium cations; some ionic liquids were able to completely dissolve microcrystalline cellulose and cellulose was recovered through the addition of an anti-solvent such as water or ethanol. The most effective cellulose solvents were the ionic liquids that contain chloride anions. An important finding associated with this novel pretreatment method is that enzymes can more efficiently hydrolyze into glucose, an amorphous cellulose produced by ionic liquids, than the microcrystalline cellulose found in lignocellulose naturally [28,30]. More research on this treatment is needed.

### 9.4.2 HYDROLYSIS

There are two types of hydrolysis processes for lignocellulose. The old process that has been practiced for a long time is acid or chemical hydrolysis and the new and novel process is enzymatic hydrolysis. Here we briefly examine both of these processes.

#### 9.4.2.1 Acid or Chemical Hydrolysis

Important parameters in acid or chemical hydrolysis are the surface-to-volume ratio of particles, acid concentration, temperature, and time. The surface-to-volume ratio is especially important because it determines the magnitude of yield of glucose. Smaller particles result in better hydrolysis [31]. An increase in the liquid-to-solid ratio also gives a faster reaction. However, higher ratio requires larger equipment and more capital cost. For chemical hydrolysis, a liquid-to-solid ratio of 10/1 seems to be most suitable [31].

The chemical hydrolysis is carried out by first pulverizing lignocellulose or waste into a fine particle size. The powdered waste is mixed with aqueous solution of weak acid (0.2%–10%) at about 180°C–230°C and moderate pressure. The acid solution converts waste into glucose, but the extent of yield depends on the nature of the waste (i.e., Kraft paper will give 84%–86% yield, whereas ground refuse will give 38%–53% yield). The yield will increase with temperature. Generally, 0.5% H<sub>2</sub>SO<sub>4</sub> concentration is used.

The Tennessee Valley Authority (TVA) developed a two-stage, low-temperature, atmospheric pressure process that utilizes the separate unit operations to convert hemicellulose and cellulose to sugars [32]. An experimental pilot plant was designed and built in 1984. The process showed a very low level of inhibitor concentration. The results of this study are briefly summarized as follows:

1. The size of ground corn stover of 2.5 cm was adequate for the hydrolysis of hemicellulose.
2. The time required for optimum hydrolysis in 10% acid at 100°C was 2 h.

3. For 1 and 3 h reaction times, the overall xylose yields were 86% and 93%, respectively.
4. Recycle leachate, dilute acid, and prehydrolysis acid solutions were stable during the storage for several days.
5. Vacuum drying was adequate in the acid concentration step.
6. Cellulose hydrolysis by cooking stover containing 66%–78% acid for 6 h at 100°C resulted in 75%–99% cellulose conversion to glucose.
7. Fiberglass-reinforced plastics of vinyl ester resin were used for the construction of process vessels and piping.

More detailed description of the process is described by Lee and Shah [2].

#### 9.4.2.2 Enzymatic Hydrolysis

Cellulose differs from other carbohydrates that are generally used as a substrate for fermentation in that cellulose is insoluble and polymerized as beta-1,4 glycosidic linkages. Each cellulose molecule is an unbranched polymer of 15–10,000 D-glucose units. Hydrolysis of crystalline cellulose is the rate-limiting step in the overall conversion of biomass to ethanol because aqueous enzyme solutions have difficulty acting on insoluble, impermeable highly structured cellulose. Cellulose needs to be efficiently solubilized such that an entry can be made into cellular metabolic pathways. Solubilization is brought about by enzymatic hydrolysis catalyzed by the cellulose system of certain bacteria and fungi. Cellulase is a class of enzyme produced primarily by fungi, bacteria, and protozoans that catalyze the hydrolysis of cellulose commonly known as cellulolysis.

The discussion on enzymatic hydrolysis is broken into three parts: enzyme system, enzyme production and inhibition, and mechanism of cellulose hydrolysis that considers cellulase enzyme adsorption on the substrate.

##### 9.4.2.2.1 Enzyme System

There are mechanistically and structurally different types of cellulases. Each cellulolytic microbial group has an enzyme system unique to it. The capabilities of enzyme can vary from hydrolysis of soluble derivatives of cellulose to disrupting the cellulose complex. Cellulase is actually composed of a number of distinctive enzymes based on the specific types of reactions catalyzed. In fact, cellulase can be characterized into five general groups:

1. Endocellulase cleaves the internal bonds to disrupt the crystalline structure of cellulose and expose individual polysaccharide chains.
2. Exocellulase detaches two or four saccharide units from the ends of exposed chains produced by endocellulase, resulting in the production of disaccharides or tetrasaccharides, such as cellobiose. There are two principal types of exocellulases or cellobiohydrolases (CBHs): (1) CBH-I that works processively from the reducing end and (2) CBH-II that works processively from the nonreducing end of cellulose. Here the processivity implies the ability of enzyme to continue repetitively its catalytic

function without dissociating from its substrate. The chance for reaction is significantly increased by an active enzyme adsorbed onto the surface of the substrate.

3. Beta-glucosidase or cellobiase hydrolyzes the disaccharides and tetrasaccharides into individual monosaccharides.
4. Oxidative cellulase depolymerizes cellulose by the free radical reactions as in the case of a cellobiose dehydrogenase (acceptor), an enzyme that catalyzes the dehydrogenation of cellobiose.
5. Cellulose phosphorylase depolymerizes cellulose using phosphates instead of water.

In most cases, the enzyme complex breaks down cellulose to beta-glucose. This type of cellulose enzyme is produced mainly by symbiotic bacteria. Enzymes that break down hemicellulose are called hemicellulase, which are still classified under cellulases. The principal challenge in building an enzyme system is how to make these different enzymes work together for hydrolytic degradation of biomass.

The enzymes described above can also be classified as progressive (or processive) and nonprogressive (or nonprocessive). Progressive cellulase will continue to interact with a single polysaccharide strand, whereas nonprogressive cellulase will interact once, disengage, and then engage another polysaccharide strand. Based on the enzymatic capability, cellulase enzyme is characterized into two groups: C1 enzyme (or factor) and Cx enzyme (or factor). The C1 factor is regarded as an “affinity” or pre-hydrolysis factor that transforms crystalline cellulose (i.e., cotton fiber or Avicel) into linear and hydroglucose chains. The C1 factor has very little effect on the soluble derivatives. The Cx (hydrolytic) factor breaks down the linear chains into soluble carbohydrates, usually cellobiose and glucose. Microbes rich in the C1 factor are more useful in the production of glucose from the cellulose. This is generally a rate-controlling step. *Trichoderma reesei* microbes contain the best amount of C1 factor. This is an industrially important fungus that is capable of screening large amounts of cellulases and hemicellulases [33]. The site of action of cellulolytic enzymes is important in the design of Cx factor. If the enzyme is within cell mass, the material to be reacted must diffuse into the cell mass. Therefore, the enzymatic hydrolysis of cellulose usually takes place extracellularly, where enzyme is diffused from the cell mass into the external medium.

Another important factor in the enzymatic reaction is whether the enzyme is adaptive or constitutive. A constitutive enzyme is present in a cell at all times, whereas an adaptive enzyme is only found in the presence of a given substance and the synthesis of enzyme is triggered by an inducing agent. Most fungal cellulases are adaptive [31,34]. Cellobiose is an inducing agent for microbes *T. reesei*. For high concentration (>0.5%–1%), it can also be an inhibitor. In most practical situations, it acts as an inducing agent.

#### 9.4.2.2.2 Enzyme Production and Inhibition

As mentioned earlier, the most useful enzyme system for hydrolysis of cellulose is cellulase. Cellulase is a multicomponent enzyme system consisting of *endo*-beta-1,4-glycanases, *exo*-beta-1,4-glucan glucohydrolases, and *exo*-beta-1,4-glucan

cellobiohydrolases. Cellobiose is the dominant product of this system, but it is highly inhibitory to the enzymes and is not usable by most organisms. Cellobiase hydrolyzes cellobiose to glucose, which is much less inhibitory and highly fermentable. Many fungi produce this cellobiase and most of the work that is presently conducted is on *T. reesei* (*viride*). The cellulase produced by *T. reesei* is much less inhibited than other cellulases that have the major advantages for industrial purposes [35].

Cellulases can inhibit competitively [36–41], noncompetitively [39,42–44], or uncompetitively [37]. Uncompetitive inhibition takes place when an enzyme inhibitor binds only to the complex formed between the enzyme and the substrate, whereas noncompetitive inhibition takes place when an enzyme inhibitor and the substrate may both be bound to the enzyme at any given time. For purified cellulose, wheat straw and bagasse, *T. reesei* produced enzyme is competitively inhibited by glucose and cellobiose. However, some enzyme is noncompetitively inhibited by cellobiose using other substrates such as rice straw and Avicel (microcrystalline cellulose). *Trichoderma viride* is uncompetitively inhibited by glucose in a cotton waste substrate [37].

Besides *T. reesei*, other mutants such as Rut C-30 [45] and *Clostridium thermocellum* have also been extensively examined. Cellulases isolated from *C. thermocellum* have high specific activities [46], especially against crystalline forms of cellulose that have proven to be resistant to other cellulase preparations. Low-cost but efficient enzymes for the lignocellulosic ethanol technology is continued to be developed to reduce the operational cost and improve the productivity of the process.

#### 9.4.2.3 Mechanism of Cellulose Hydrolysis

The overall cellulose hydrolysis is based on the synergistic action of three distinct cellulase enzymes and depends on the concentration ratio and the adsorption ratio of the component enzymes: *endo*-beta-gluconases, *exo*-beta-gluconases, and beta-glucosidases. The *endo*-beta-gluconases attack the interior of the cellulose polymer in a random fashion [47], exposing new chain ends. This enzyme is strongly but reversibly adsorbed to the microcrystalline cellulose commonly known as Avicel and catalyzes the solid-phase reaction. The strength of the adsorption is greater at the lower temperatures. This enzyme is necessary for the hydrolysis of crystalline substrates of cellulose, resulting in a considerable accumulation of reducing sugars, mainly cellobiose, because the extracellular cellulase complex does not possess the cellobiose activity. Sugars that contain aldehyde groups that are oxidized to carboxylic acids are classified as reducing sugars.

The *exo*-beta-gluconases remove disaccharide cellobiose units from the nonreducing ends of cellulose chains. The *exo*-beta-gluconases adsorb strongly on both crystalline and amorphous substrates, and carry out the solid-phase reaction. The mechanism of the reaction is complex because there are two distinct forms of both *endo*- and *exo*enzymes, each with a different type of synergism with other members of the complex. The concentration of cellobiose in the solution increases as these enzymes continue to split off the cellobiose units. The action of *exo*-beta-gluconases may be severely hampered (or stopped) by the accumulation of cellobiose in the solution.

Beta-glucosidase converts cellobiose to glucose by hydrolysis. In general, glucosidase is any enzyme that catalyzes the hydrolysis of glucoside. Beta-glucosidase catalyzes the hydrolysis of terminal, nonreducing beta-D-glucose residues with the release of beta-D-glucose. Kadam and Demain [48] determined the substrate specificity of the beta-glucosidase and demonstrated that its addition to the cellulase complex enhances the hydrolysis of Avicel, specifically by removing the accumulated cellobiose. They used *C. thermocellum* that is expressed in *Escherichia coli* to determine the surface specificity of the enzyme. The hydrolysis of cellobiose to glucose is a liquid-phase reaction. The action of beta-glucosidase on this reaction can be slowed or halted by the inhibitive action of glucose accumulated in the solution. The accumulation may also induce the entire hydrolysis to a halt as inhibition of the beta-glucosidase results in the buildup of cellobiose, which in turn inhibits the action of exoglucanases. Thus, the hydrolysis of the cellulosic materials depends on the presence of all three enzymes in proper amounts. If any of these enzymes is present in the amount less than the required amount, the other enzymes will be inhibited or lack the necessary substrates upon which to act.

While higher temperature increases the rate of hydrolysis, the high temperature can inactivate or destroy the enzyme. To strike a balance between the increased activity and the simultaneous deactivation rate, enzymatic hydrolysis is generally operated at ~40°C–50°C. While enzymatic reactions are carried out at low temperatures, as mentioned earlier, dilute acid hydrolysis is generally carried out at high temperatures (195°C–215°C).

One of the issues that need to be addressed in enzymatic hydrolysis is the loss of enzyme that is left on the lignocellulose residues, on the cellulose substrate, or in the solution. The enzyme adsorption capacity of the lignocellulose residue decreases as the pretreatment temperature is increased, whereas the capacity of cellulose increases with higher temperature. The reduction of enzyme on the residue is essential for the overall economics of the process.

An enzymatic hydrolysis process involving solid lignocellulosic materials can be designed in many ways. Generally, substrate and enzymes are fed into the process, and sugar solution along with the solid residue leaves the process at various points. The enzyme adsorbed on the residue is lost and this hurts the economics of the process. The recycling and reuse of the enzyme adsorbed on the residue is essential. In essence, the enzymatic process should be designed in such a way that the loss of enzymes is minimal.

### 9.4.3 FERMENTATION

The hydrolysis and fermentation of cellulose can be carried out in sequence often called as separate hydrolysis and fermentation (SHF) process or simultaneously called as simultaneous saccharification and fermentation (SSF) process. Here we briefly examine both of these processes.

#### 9.4.3.1 Separate Hydrolysis and Fermentation

In the SHF process, hydrolysis and fermentation are carried out in two separate vessels. The most expensive items in the overall process costs are the cost of

feedstock, enzyme production, hydrolysis, and utilities. The feedstock and utility costs are high because only about 73% of the cellulose is converted to ethanol in 48 h and the remainder of the cellulose, hemicellulose, and lignin is burned or gasified. Enzyme production is expensive due to a large amount of enzymes that are used in the attempt to overcome the end-product inhibition and the slow reaction rate. The hydrolysis step is also expensive due to the large capital and operating costs. The most important parameters are the hydrolysis section yield, the product quality, and the required enzyme loading, all of which are interrelated. Generally, the process should be operated at the minimum required enzyme loading. Um and Hanley [49] examined the effect of cellulose loading on the performance of the SHF process.

Generally, hydrolysis is carried out at 50°C and fermentation requires a lower temperature (around 30°C). The SHF process accommodates both of these requirements. The fermentation step takes about 48 h.

#### **9.4.3.2 Simultaneous Saccharification and Fermentation**

The operating cost of the SSF process is generally lower than that of SHF process as long as the process integration is synergistically done. Since in the SSF process both hydrolysis and fermentation are carried out in the same vessel, yeast ferments glucose to ethanol as soon as the glucose is produced, thus preventing the sugars from accumulating and causing end-product inhibition. Even in the SSF process, cellobiose inhibition occurs to an appreciable extent. The enzyme loading for SSF is only 7 IU/g of cellulose compared to 33 IU/g in SHF. The cost of energy and feedstock is somewhat reduced because of the improved yield and the increased ethanol concentration, which also considerably reduce the cost of distillation and utilities. The cost of the SSF process is slightly less than the combined cost of hydrolysis and fermentation in the SHF process. The longer reaction time for SSF (about seven days) versus two days for hydrolysis and two days for fermentation for SHF is offset by the reactor volume and high ethanol concentration. In earlier studies, fermentation was the rate-limiting step, but with recent advances in recombinant yeast strains that are capable of effectively fermenting both glucose and xylose, the rate-limiting step may have changed to hydrolysis.

The hydrolysis is carried out at 37°C and an increase in temperature (up to 50°C) increases the reaction rate. However, in the SSF process, the ceiling temperature is usually limited by the yeast cell viability. The concentration of ethanol is also a limiting factor (a periodic removal of ethanol improves the productivity up to 44%). Recycling the residual solids may also increase the process yield. However, enzyme recycling may be limited by the increase in lignin concentration causing handling difficulties.

Two types of enzyme recycling schemes have been examined: in one scheme, enzymes are recovered in the liquid phase and in the other, enzymes are recovered by recycling unreacted solids [47]. The first scheme works well with the SHF process in which hydrolysis is carried out at higher temperatures (50°C). The increase in temperature allows more enzymes to remain in the liquid phase. At lower temperature, more enzymes are adsorbed on the surface, and therefore, for SSF solids recycling becomes a more effective option.

### 9.4.3.3 Comparison between SSF and SHF Processes

Due to low end-product inhibition of the cellulase enzyme complex, the SSF systems offer many advantages over the SHF processes. The SSF process shows higher yields (88% vs. 73%) compared to the SHF process [2] and greatly improves the product glucose concentration (10% vs. 4.4%). The most significant advantage of the SSF process is the enzyme loading that is reduced from 33 to 7 IU/g cellulose, which considerably cuts down the cost of ethanol production. A comparative study of the approximate cost of the two processes reported in the literature [47] showed that based on the ethanol selling price from a production capacity of 25,000,000 gallons per year, the SSF process is found to be more cost effective than the SHF process by a factor of 1.49. These estimates may change with new developments on enzymes and yeasts.

A hybrid hydrolysis fermentation (HHF) process may also gain some acceptance. This process will begin with a separate prehydrolysis step and ends with a simultaneous saccharification and fermentation step. In the first step of hydrolysis, higher temperature enzymatic cellular saccharification takes place, whereas in the second stage of the SSF process, mesophilic (moderate temperature) enzymatic hydrolysis and sugar fermentation take place simultaneously. The optimized process scheme may have to change if a specific enzyme that is proven to be highly efficient and cost effective but also found to be intolerant against certain inhibitors that are associated with any of these processing steps.

### 9.4.3.4 Xylose Fermentation

For certain feedstock such as hardwood and herbaceous biomass, xylose amounts to 30%–60% of fermentable sugars. The efficient fermentation of xylose is therefore very important for the overall economics of ethanol from these feedstock. Co-fermentation of both glucose and xylose is most desirable. Xylose fermentation using pentose yeasts is difficult due to (1) the requirement of O<sub>2</sub> during ethanol production, (2) the acetate toxicity, and (3) the production of xylitol as byproduct. Xylitol is a naturally occurring low-calorie sugar substitute with anticarcinogenic properties. Other approaches to xylose fermentation include conversion of xylose to xylulose using xylose isomerase prior to fermentation by *S. cerevisiae* and the development of genetically engineered strains [50].

A method of integrating xylose fermentation into the overall process is illustrated in Figure 9.7. In this method, dilute acid hydrolysis is adapted as a pretreatment step. The liquid stream is neutralized to remove any mineral or organic acid liberated in the pretreatment process, and is then sent to the xylose fermentation. Water is added before the fermentation, if necessary, so that organisms can make full use of the substrate without having the yield limited by end-product inhibition. The dilute ethanol stream from xylose fermentation is then used to provide the dilution water for the cellulose–lignin mixture entering the SSF process. Thus, the water that enters during the pretreatment process is used in both the xylose fermentation and the SSF process. The conversion of xylose to ethanol using *E. coli* in pH-controlled batch fermentation was investigated [51]. The results showed high concentrations of ethanol (56 g/l) produced from xylose with good efficiencies. Recombinant *E. coli* also gave good conversions of glucose, mannose, arabinose, and galactose to ethanol.

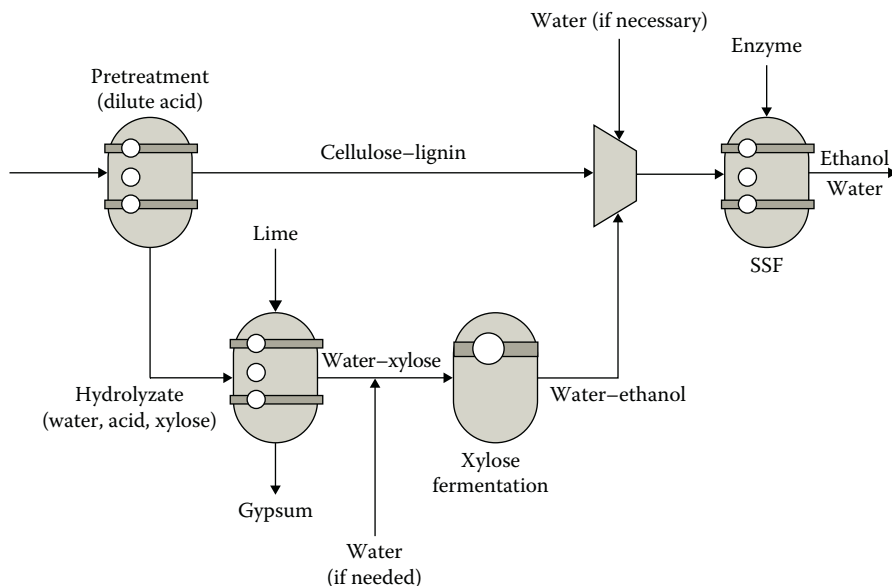


**FIGURE 9.7** Integration of xylose fermentation and SSF. (Adapted from Lee, S. and Shah, Y., *Biofuels and Bioenergy—Processes and Technologies*, CRC Press, Boca Raton, FL, 2012; Wright, J.D., *Chemical Engineering Progress*, 84, 62–74, 1988.)

Slower fermentation was observed for  $\text{pH} < 6$  and addition of metal ions such as calcium, magnesium, and ferrous ions stimulated ethanol production [51].

Xylose fermentation does not require precise temperature control as long as the temperature is between  $25^{\circ}\text{C}$  and  $40^{\circ}\text{C}$ . Higher concentration of xylose slows down the fermentation. Ingram et al. [51–54] showed that *E. coli* of special type can efficiently convert both hexose and pentose sugars to ethanol. Ethanologenic *E. coli* strains require simpler fermentation conditions, produce higher concentration of ethanol, and are more efficient than pentose-fermenting yeasts for ethanol production from xylose and arabinose [55].

Sedlak et al. [56] successfully developed a genetically engineered *Saccharomyces* yeast that can ferment both glucose and xylose simultaneously to ethanol, although xylose was metabolized more slowly than glucose. Ideally, xylose should be consumed simultaneously with glucose at similar efficiency and speed [57]. This new co-fermentation process has a very bright future. They also found that ethanol was the most abundant product from glucose and xylose metabolism, but small amounts of the metabolic byproducts glycerol and xylitol were also obtained [56].

#### 9.4.4 ETHANOL EXTRACTION DURING FERMENTATION

Significant research for concentration of dilute ethanol product to pure ethanol has been carried out to reduce high energy consumption for purification of dilute end products. Conventional distillation suffers from high energy cost and azeotropic phenomenon that allows only about 95% pure ethanol. In the recent years, along

with improved unit operations, liquid–liquid extraction with biocompatible organic solvents, distillation under vacuum, and selective adsorption on the solids have demonstrated the technical feasibility of the extractive fermentation concept. Finally, membrane separation processes that decrease the biocompatibility constraints have been proposed, which include dialysis [58] and reverse osmosis [43].

More recently, the concept of supported liquid membranes has been reported. This method minimizes the amount of organic solvents involved and permits simultaneous realization of the extraction and recovery phases. Enhanced volumetric productivity and high substrate conversion yields have been reported [59] via the use of a porous “Teflon” sheet soaked with isotridecanol as support for the extraction of ethanol during semicontinuous fermentation of *Saccharomyces bayanus*. This selective process results in ethanol purification and combines fermentation, extraction, and re-extraction (stripping). Such a novel process idea can further accomplish maximized alcohol production and energy savings, and reduce the cost in production.

#### 9.4.5 LIGNIN CONVERSION

In the United States, about 250 billion pounds per year of lignin is produced largely as a byproduct of paper and pulp industry. Lignins are complex amorphous phenolic polymers that are not sugar based and fermentable. The phenol in lignins may be either a guaiacyl or a syringyl unit. These units are bonded by alpha- or beta-ether linkages. A variety of C–C linkages may also be present and these are less common [2]. The distribution of linkages in lignin is random and highly resistant to chemical, enzymatic, and microbial hydrolysis due to extensive cross-linking. Lignin protects cellulose and needs to be removed to carry out hydrolysis and fermentation of cellulose. Lignin monomer units are similar to gasoline that has high octane number. The removal of oxygen and the breaking down of lignin molecules make it a suitable transportation fuel. Hydrotreating of lignin will produce a mixture of phenolic and hydrocarbon compounds, which can then be converted to methyl aryl ether by reaction with methanol. The conversion of lignin can be carried out by dual function catalysts. Metals such as molybdenum and molybdenum/nickel catalyze deoxygenation and acidic alumina support promote carbon–carbon bond cleavage. Lignin chemicals have applications in drilling muds, binders for animal feeds, base for artificial vanilla, and surfactants for oil recovery [60]. For the last usage, lignosulfonates are blended with tallow amines and conventional sulfonates. Lignin can react with hydrogen or carbon monoxide to form new class of chemicals called lignin phenols. These phenols are soluble in organic solvents but not in water, and they are good candidates for further conversion to produce chemicals that may be useful in enhanced oil recovery.

#### 9.4.6 COPRODUCTS OF CELLULOSIC ETHANOL TECHNOLOGY

Potential coproducts for cellulosic ethanol technology include hemicellulose hydrolyzate (xylose), cellulose hydrolyzate (glucose of mixed sugars), cell mass, enzymes, soluble and insoluble lignins, lignin-derived chemicals and fuels, solid residues, and so on. Other valuable coproducts include xylitol (which is sugar alcohol sweetener) and is produced by hydrogenation of xylose (an aldehyde) into a primary alcohol.

#### 9.4.7 FUTURE DIRECTIONS FOR CELLULOSIC ETHANOL

While the future for cellulosic ethanol is very bright, the future efforts need to address following issues:

1. While each step, pretreatment, hydrolysis, and fermentation are separate and the needs to further develop their interconnections separately are also very important. For optimization of the cost, an integration of these steps (such as the SSF process described earlier) needs to be further evaluated.
2. More work on the development of enzymes and yeasts that are more tolerant to the product inhibition needs to be carried out. This can be helped by the use of genomics, proteomics, and metabolic engineering techniques for plant systems that are applied to other living systems.
3. From the cost point of view, full use of all parts of plants, namely, cellulose, hemicellulose, and lignin for coproduct development needs to be further considered. The development of the enzyme and yeasts that can simultaneously convert both glucose and xylose needs to be further evaluated. More efficient lignin separation and refining should be further explored.
4. The energy consumption for various unit operations such as distillation and extraction should be further optimized. The transport and storage of biomass feedstock is also an issue that needs to be addressed. Larger-scale operations need to be considered.
5. The work on cellulosic ethanol should be extended to other alcohols, especially butanol, which is discussed in Section 9.5.

#### 9.5 FERMENTATION OF SUGAR TO ISOBUTANOL

Recently, Quereshi et al. [1] presented a review of recent advances in fermentation of isobutanol from various carbohydrates and starch materials. They examined the effectiveness of a number of microbes for the fermentation of various feedstock such as wheat and barley straws, corn stover, switchgrass and dried distillation grains and solubles. Isobutanol is produced in two phases and always found in the mixture of acetone–butanol–ethanol (ABE). Some of their conclusions are outlined as follows:

1. The experiments performed so far gave low productivity due to the toxicity of butanol to the culture.
2. *Clostridium beijerinckii* was found to be the best overall culture followed by *Clostridium actobutylicum* for butanol production.
3. *Escherichia coli* strains and *S. cerevisiae* microbes have also been examined, but they gave low butanol production.
4. Simultaneous removal of butanol while fermentation significantly improved the production rate of butanol (from 1.2 g/l to 461 g/l in batch operation).
5. More butanol-tolerant strains using genetic engineering techniques need to be pursued.

## REFERENCES

1. Quereshi, N., Liu, S., and Ezeji, T.C., "Cellulosic butanol production from agricultural biomass residues: Recent advances in technology," in Lee, J. (ed.), *Advanced Biofuels and Bioproducts*. Springer, New York, 247–265 (2012).
2. Lee, S. and Shah, Y., *Biofuels and Bioenergy—Processes and Technologies*. CRC Press, Boca Raton, FL (2012).
3. Lichts, F.O., "Industry statistics: 2010 World fuel ethanol production," Renewable Fuels Association (2011), <http://www.ethanolrfa.org/pages/statistics# E>.
4. Speight, J.G. and Lee, S., *Handbook of Environmental Technologies*. Taylor & Francis, New York (2000).
5. American Coalition for Ethanol, "All about ethanol" (October 2010), <http://www.ethanol.org/>.
6. Lee, S., Speight, J.G., and Loyalka, S.K., *Handbook of Alternative Fuel Technologies*. CRC Press, Boca Raton, FL (2007).
7. BBI International, *The Ethanol Plant Development Handbook*, 4th ed. BBI International, Salida, CO (2003).
8. Shapouri, H., Duffield, J.A., McAloon, A., and Wang, M. "The 2001 net energy balance of corn ethanol," Technical Report No. AER-814, US Department of Agriculture, Washington, DC (July 2002).
9. Mueller, S. and Copenhaver, K., "News from corn ethanol: Energy use, coproducts, and land use," *Near-Term Opportunities for Biorefineries Symposium*, October 11–12, Champaign, IL (2010).
10. Corn Refiners Association, "The corn refining process," Vol. 2010 (2010).
11. Li, A., Antizar-Ladislao, B., and Khraisheh, M., "Bioconversion of municipal solid waste to glucose for bio-ethanol production," *Bioprocess and Biosystem Engineering*, 30, 189–196 (2007).
12. Saha, B.C., "Lignocellulose biodegradation and applications in biotechnology," in Saha, B.C. and Hayashi, K. (eds.), *Lignocellulose Biodegradation*, ACS Publication, New York, pp. 2–34 (2004).
13. Dickey, L.C., Kurantz, M.J., and Parris, N., "Oil separation from wet-milled corn germ dispersions by aqueous oil extraction and aqueous enzymatic oil extraction," *Industrial Crops and Products*, 27, 303–307 (2008).
14. Prosonix, "AP-40 starch processing for wet milling," (2011), [http://www.prosonix.com/files/AP-40\\_Starch\\_Wet\\_Milling\\_20101210.pdf](http://www.prosonix.com/files/AP-40_Starch_Wet_Milling_20101210.pdf).
15. Singh, V.J. and Eckhoff, S., "Effect of soak time, soak temperature, and lactic acids on germ recovery parameters," *Cereal Chemistry*, 73, 716–720 (1996).
16. ICM, "ICM's dry milling ethanol production."
17. Mueller, S., *Detailed Report: 2008 National Dry Mill Corn Ethanol Survey*. University of Illinois, Chicago, IL (2008), [http://ethanolrfa.3cdn.net/2e04acb7ed88d08d21\\_99m6idfc1.pdf](http://ethanolrfa.3cdn.net/2e04acb7ed88d08d21_99m6idfc1.pdf).
18. Odian, G., *Principles of Polymerization*. Wiley, Hoboken, NJ (2004).
19. Dorland, W.A.N., *Dorland's Illustrated Medical Dictionary*, 30th ed. W.B. Saunders, Philadelphia, PA (2003).
20. Knauf, M. and Krau, K., "Specific yeasts developed for modern ethanol production," *Sugar Industry*, 131, 753–775 (2006).
21. Cohen, D., "Form and distribution of trace elements in biomass for power generation," Technical Report No. 48, QCAT Technology Transfer Center, Pullenvale, QLD (July 2004).
22. Eliasson, A., Christensson, C., Wahlbom, C.F., and Hahn-Hagerdal, B., "Anaerobic xylose fermentation by recombinant *Saccharomyces cerevisiae* carrying XYL1, XYL2, and XKS1 in mineral medium chemostat cultures," *Applied and Environmental Microbiology*, 66, 3381–3386 (2000).

23. Cort, J.B., Pschorn P., and Stromberg, B., "Minimize scale-up risk," *Chemical Engineering Progress*, 106, 3–49 (2010).
24. Dekker, R.F.H. and Wallis, A.F.A., "Enzymic saccharification of sugarcane bagasse pretreated by autohydrolysis-steam explosion," *Biotechnology and Bioengineering*, 25, 3027–3048 (1983).
25. Ojumu, T.V. and Ogunkunle, O.A., "Production of glucose from lignocellulosics under extremely low acid and high temperature in batch process—Autohydrolysis approach," *Journal of Applied Sciences*, 5, 15–17 (2005).
26. Pan, X.J., Xie, D., Yu, R.W., Lam, D., and Saddler, J.N., "Pretreatment of lodgepole pine killed by mountain pine beetle using the ethanol organosolv process: Fractionation and process optimization," *Industrial & Engineering Chemistry Research*, 46, 2609–2617 (2007).
27. Rughani, L. and McGinnis, G.D., "Combined rapid steam hydrolysis and organosolv pretreatment of mixed southern hardwoods," *Biotechnology and Bioengineering*, 33, 681–686 (1989).
28. Simmons, B.A., Singh, S., Holmes B.M., and Blanch, H.W., "Ionic liquid pre-treatment," *Chemical Engineering Progress*, 106, 50–55 (2010).
29. Swatoski, R.P., "Dissolution of cellulose with ionic liquids," *Journal of the American Chemical Society*, 124, 4974–4975 (2002).
30. Dadi, A.P., "Mitigation of cellulose recalcitrance to enzymatic hydrolysis by ionic liquid pretreatment," *Applied Biochemistry and Biotechnology*, 137, 407–421 (2007).
31. Diaz, L.F., Savage, G.M., and Golueke, C.G., "Critical review of energy recovery from solid wastes," *Critical Reviews in Environmental Control*, 14, 285–288 (1984).
32. Farina, G.E., Barrier, J.W., and Forsythe, M.L., "Fuel alcohol production from agricultural lignocellulosic feedstocks," *Energy Sources*, 10, 231–237 (1988).
33. Kumar, R., Singh, S., and Singh, O.V., "Bioconversion of lignocellulosic bio-mass: Biochemical and molecular perspectives," *Journal of Industrial Microbiology and Biotechnology*, 35, 377–391 (2008).
34. Bailey, J.E. and Ollis, O.F., *Biochemical Engineering Fundamentals*, 2nd ed. McGraw-Hill, New York (1986).
35. Holtzaple, M.T., Cognata, M., Shu, Y., and Hendrickson, C., "Inhibition of *Trichoderma reesei* cellulase by sugars and solvents," *Biotechnology and Bioengineering*, 38, 296–303 (1991).
36. Blotkamp, P.J., Takagi, M., Pemberton, M.S., and Emert, G.H., "Biochemical engineering: Renewable sources of energy and chemical feedstocks," in Nystrom, J.M. and Barnett, S.M. (eds.), *Renewable Sources of Energy and Chemical Feedstocks*, AIChE Symposium Series No. 181, New York (1978).
37. Beltrame, P.L., Carniti, P., Focher, B., Marzetti, A., and Sarto, V., "Enzymatic hydrolysis of cellulosic materials: A kinetic study," *Biotechnology and Bioengineering*, 26, 1233–1238 (1984).
38. Ohmine, K., Ooshima, H., and Harano, Y., "Kinetic study on enzymatic hydrolysis of cellulose by cellulase from *Trichoderma viride*," *Biotechnology and Bioengineering*, 25, 2041–2053 (1983).
39. Okazaki, M. and Young, M., "Kinetics of enzymatic hydrolysis of cellulose: Analytic description of mechanistic model," *Biotechnology and Bioengineering*, 20, 637–663 (1978).
40. Ryu, D.Y. and Lee, S.B., "Enzymatic hydrolysis of cellulose: Determination of kinetic parameters," *Chemical Engineering Communications*, 45, 119–134 (1986).
41. Gonzales, G., Caminal, G., de Mas, C., and Santin, J.L., "Kinetic models for pretreated wheat straw saccharification by cellulose," *Journal of Chemical Technology and Biotechnology*, 44 (4), 275–288 (1989).
42. Vallander, L. and Eriksson, K., "Enzymatic hydrolysis of lignocellulosic materials: I. Models for the hydrolysis process—A theoretical study," *Biotechnology and Bioengineering*, 38, 135–138 (1991).

43. Garcia, A., Lannotti, E.L., and Fischer, J.L., "Butanol fermentation liquor production and separation by reverse osmosis," *Biotechnology and Bioengineering*, 28, 785–791 (1986).
44. Vallander, L. and Eriksson, K., "Enzymatic hydrolysis of lignocellulosic materials: II. Experimental investigation of theoretical hydrolysis process models for an increased enzyme recovery," *Biotechnology and Bioengineering*, 38, 139–144 (1991).
45. Szengyel, Z., Zacchi, G., Varga, A., and Reczey, K., "Cellulase production of *Trichoderma reesei* Rut C 30 using steam-pretreated spruce. Hydrolytic potential of cellulases on different substrates," *Applied Biochemistry and Biotechnology*, 84–86, 679–691 (2000).
46. Moses, V., Springham, D.G., and Cape, R.E., *Biotechnology—The Science and the Business*. Harwood Academic, London (1991).
47. Wright, J.D., "Ethanol from biomass by enzymatic hydrolysis," *Chemical Engineering Progress*, 84, 62–74 (1988).
48. Kadam, S. and Demain, A., "Addition of cloned beta-glucosidase enhances the degradation of crystalline cellulose by the *Clostridium thermocellum* cellulase complex," *Biochemical and Biophysical Research Communication*, 161, 706–711 (1989).
49. Um, B.H. and Hanley, T.R. "High-solid enzymatic hydrolysis and fermentation of solka floc into ethanol," *Journal of Microbiology and Biotechnology*, 18, 1257–1265 (2008).
50. Sarthy, A., McConaughy, L., Lobo, Z., Sundstorm, A., Furlong E., and Hall, B., "Expression of the *Escherichia coli* xylose isomerase gene in *Saccharomyces cerevisiae*," *Applied and Environmental Microbiology*, 53, 1996–2000 (1987).
51. Beall, D.S., Ohta, K., and Ingram, L.O., "Parametric studies of ethanol production from xylose and other sugars by recombinant *Escherichia coli*," *Biotechnology and Bioengineering*, 38, 296–303 (1991).
52. Ohta, K., Beall, D.S., Mejia, J.P., Shanmugam, K.T., and Ingram, L.O., "Genetic improvement of *Escherichia coli* for ethanol production: Chromosomal integration of *Zymomonas mobilis* genes encoding pyruvate decarboxylase and alcohol dehydrogenase II," *Applied and Environmental Microbiology*, 57, 893–900 (1991).
53. Ingram, L.O. and Conway, T., "Expression of different levels of ethanologenic enzymes from *Zymomonas mobilis* in recombinant strains of *Escherichia coli*," *Applied and Environmental Microbiology*, 54, 404 (1988).
54. Alterthum, F. and Ingram, L.O., "Efficient ethanol production from glucose, lactose, and xylose by recombinant *Escherichia coli*," *Applied and Environmental Microbiology*, 55, 1943–1948 (1989).
55. Skoog, K. and Hahn-Hagerdal, B., "Xylose fermentation," *Enzyme and Microbial Technology*, 10, 66–80 (1988).
56. Sedlak, M., Edenberg, H.J., and Ho, N.W.Y., "DNA microarray analysis of the expression of the genes encoding the major enzymes in ethanol production during glucose and xylose co-fermentation by metabolically engineered *Saccharomyces* yeast," *Enzyme and Microbial Technology*, 33, 19–28 (2003).
57. US DOE Office of Science and Office of Energy Efficiency and Renewable Energy, "Breaking the biological barriers to cellulosic ethanol: A joint research agenda," A Research Roadmap Resulting from the Biomass to Biofuels Workshop, Technical Report DOE/SC-0095, December 7–9, Rockville, MD (2006).
58. Kyung, K.H. and Gerhardt, P., "Continuous production of ethanol by yeast immobilized in membrane-contained fermenter," *Biotechnology and Bioengineering*, 26, 252 (1984).
59. Christen, P., Minier, M., and Renon, H., "Enhanced extraction by supported liquid membrane during fermentation," *Biotechnology and Bioengineering*, 36, 116–123 (1990).
60. Naege, D.G., *200th National Meeting of the American Chemical Society*, August, 17 (1990).
61. U.S. Grains council, World Corn Production and Trade (October, 2011). <http://www.grains.org/corn>.



Taylor & Francis

Taylor & Francis Group

<http://taylorandfrancis.com>

---

# 10 Fuel Production by Supercritical Water

## 10.1 INTRODUCTION

In recent years, the interest in the use of supercritical water (SCW) for the production of fuels and chemicals as well as for waste treatment has been rapidly expanding. The main reason for this is the unique properties of SCW that allow a variety of organic reactions to occur in SCW, where water not only plays a benign role of solvent but also plays a role as an active reactant or a catalyst. Water under these conditions possesses properties such that important organic reactions can be carried out in a homogeneous medium [1–13] (Aljishi et al., 2010, pers. comm.). SCW can provide five different functions: (1) a medium in which numerous types of organic chemical synthesis occur, (2) a medium for partial or complete oxidation of numerous hazardous or nonhazardous materials, (3) a medium in which complex materials decompose and produce liquids and gases, (4) a medium for thermal or catalytic gasification of simple and complex materials to produce fuels like methane and hydrogen, and (5) a medium to generate hydrogen by catalytic reforming of various carbonaceous materials. This chapter examines the role of SCW in each of these functions, with a special emphasis on the functions that generate synthetic fuels.

SCW technologies offer many advantages [1–13] (Aljishi et al., 2010, pers. comm.):

1. The energy efficiency for SCW gasification of biomass is generally high, particularly for the feedstock containing large water content, because no drying is required.
2. Most organic materials of biomass and other carbonaceous feedstock can be dissolved in SCW due to their high solubility in SCW and high dielectric constant of SCW. These features make the gasification in SCW a homogeneous reaction, with no mass transfer resistance between the two phases.
3. While the SCW requires high pressure of 22.1 MPa and high temperature of 374°C, these conditions are still milder than what is required for conventional gasification and pyrolysis to obtain the same level of conversion efficiency. For example, conventional steam gasification generally requires 1000°C, whereas the complete gasification of glucose can be achieved at 650°C and 35.4 MPa pressure in SCW.
4. SCW gasification produces very little impurities; no  $\text{NO}_x$  and  $\text{SO}_x$  and low CO concentration are generated. The use of catalyst to enhance water–gas shift reaction further reduces the gas-phase impurities.

5. High pressure used in the supercritical gasification helps downstream operations such as storage and transportation of the product gases, carbon capture, and purification of the product gases by reforming or pressure swing adsorption.
6. As shown by Savage and others [1–13] (Aljishi et al., 2010, pers. comm.), SCW provides a homogeneous medium to carry out numerous organic chemical reactions such as decomposition, partial and complete oxidation, hydration/dehydration, hydrogenation/dehydrogenation, hydrolysis, elimination and rearrangement, and C–C bond formation with ease in which water acts as a benign medium, a reactant, or a catalyst.
7. With the use of a suitable catalyst, SCW gasification can be easily accompanied by a reforming reaction.

The major disadvantages deal with the operational issues such as the use of high-pressure water, which may carry some toxic and corrosive substances. The processing of supercritical operations may require the use of special materials that may be expensive and demand substantial maintenance and replacements costs. The capital and operating costs associated with high-pressure operations may be considerably larger than those for low-pressure gasification and pyrolysis operations. In recent years, however, the prices of high-pressure equipment have come down.

## 10.2 PROPERTIES OF SCW

Hydrothermal treatment of carbonaceous materials in supercritical conditions has taken a significant momentum ever since the pioneering work of Modell and coworkers from the Massachusetts Institute of Technology (MIT) in the late 1970s [1–14] (Aljishi et al., 2010, pers. comm.). Figure 10.1 illustrates the thermodynamic region (in terms of pressure–temperature diagram) of SCW treatment of the carbonaceous materials. The three regions shown in the figure take advantage of substantial changes in the properties of water that occur in the vicinity of its critical point at 374°C ( $T_c$ ) and 22 MPa ( $P_c$ ). The behavior of the important properties of water such as density, ion dissociation constant, dielectric constant, and solubility limits of various salts as a function of temperature was described in Chapter 5 and will not be repeated here [1–5]. In that chapter, we examined the role of water as a chemical reactant under subcritical conditions. In this chapter, we focus on the role of SCW for carrying out various organic chemical reactions. In SCW, more chemically and energetically favorable pathways to gaseous and liquid fuels can be achieved by better control of the rate of hydrolysis and phase partitioning and solubility of components.

Water at ambient conditions (25°C and 0.1 MPa) is a good solvent for electrolytes due to its high dielectric constant [1–10] (Aljishi et al., 2010, pers. comm.), whereas most organic matter are sparingly soluble [1–10] (Aljishi et al., 2010, pers. comm.). As water is heated, the H-bonding starts weakening, allowing dissociation of water into acidic hydronium ions ( $H_3O^+$ ) and basic hydroxide ions ( $OH^-$ ). The structure of water changes significantly near the critical point because of the breakage of infinite networks of hydrogen bonds and water exists as separate clusters with a chain structure. In fact, the dielectric constant of water decreases considerably near the critical point,

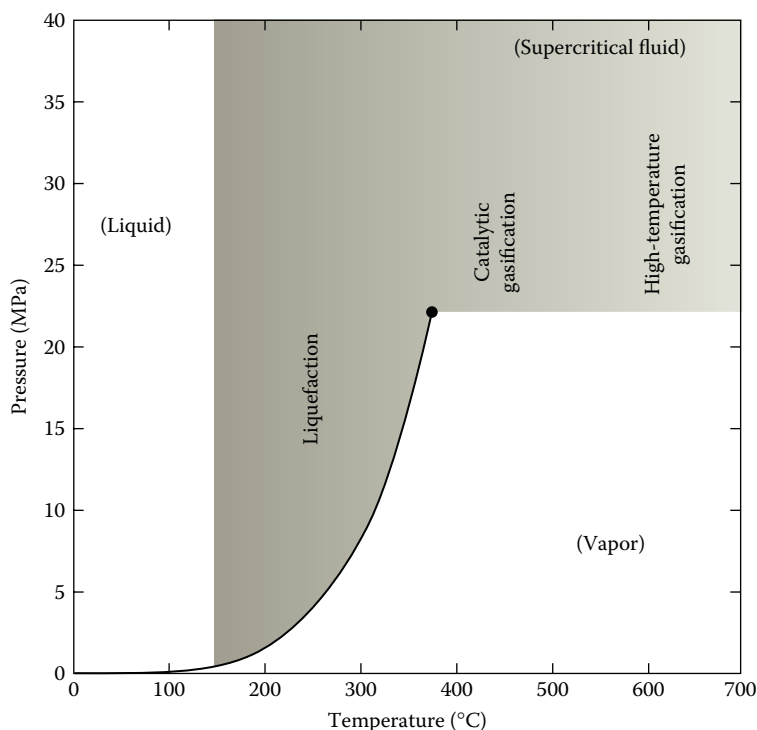


**FIGURE 10.1** Hydrothermal processing regions referenced to the pressure–temperature phase diagram of water. (After Peterson, A., Vogel, F., Lachance, R., Frothing, M., Antal, M., and Tester, J., *Energy & Environmental Science*, 1, 32–65, 2008.)

which causes a change in the dynamic viscosity and an increase in the self-diffusion coefficient of water [1–10] (Aljishi et al., 2010, pers. comm.).

SCW has liquid-like density and gas-like transport properties and behaves very differently than water at room temperature. For example, it is highly nonpolar, permitting complete solubilization of most organic compounds. The resulting single-phase mixture does not have many of the conventional transport limitations that are encountered in multiphase reactors. However, the polar species such as inorganic salts, are no longer soluble and they start precipitating. The physical properties of water, such as viscosity, density, and heat capacity, also change dramatically in the supercritical region. A small change in the temperature or pressure, results in a substantial increase in the rates of chemical reactions.

It is important to mention that the dielectric behavior of 200°C water is similar to that of ambient methanol, 300°C water is similar to ambient acetone, 370°C water is similar to methylene chloride, and 500°C water is similar to ambient hexane [1–10] (Aljishi et al., 2010, pers. comm.). In addition to the unusual dielectric behavior, as shown in Table 10.1 the transport properties of water are significantly different than those of ambient water.

Supercritical water also offers some interesting possibilities for catalytic processes. Supercritical water can dissolve unwarranted hydrocarbons from the

**TABLE 10.1**  
**Comparison of Ambient and SCW**

	Ambient Water	SCW
Dielectric constant	78	<5
Solubility of organic compounds	Very low	Fully miscible
Solubility of oxygen	6 ppm	Fully miscible
Solubility of inorganic compounds	Very high	~0
Diffusivity (cm <sup>2</sup> /s)	10 <sup>-5</sup>	10 <sup>-3</sup>
Viscosity (g cm/s)	10 <sup>-2</sup>	10 <sup>-4</sup>
Density (g/cm)	1	0.2–0.9

Source: Lee, S. and Shah, Y., *Biofuels and Bioenergy—Processes and Technologies*. CRC Press, New York, 2012. With permission.

catalytic surface. Supercritical water has better capacity to handle heat due to high heat capacity. The adsorption/desorption phenomena can be better handled in supercritical water due to higher solubility of absorbing/describing species. The oligomeric coke precursors or sulfur species can be easily dissolved in the supercritical water.

As mentioned earlier, the number and persistence of hydrogen bonds under supercritical conditions are both diminished. The dissociation constant for water at supercritical conditions is about 3 orders of magnitude higher than it is for ambient liquid water. This constant, however, decreases as temperature increases further in supercritical conditions. SCW is an excellent solvent for all organic compounds. It can also have higher H<sup>+</sup> OH<sup>-</sup> ion concentrations than liquid water under certain conditions. Thus, it becomes an effective medium for acid- and base-catalyzed reactions of organic compounds. In fact, the dissociation constant at supercritical conditions generates such high H<sup>+</sup> concentrations that organic compounds can undergo acid-catalyzed reactions without addition of acid. Gases are also miscible in SCW, thus creating a homogeneous medium for any multi-phase reaction. Since there are no interphase mass and heat-transfer resistances, higher concentration of reactants is obtained in a supercritical medium, leading to higher reaction rates.

Recently, Savage [11], Watanabe et al. [12], Matsumura et al. [13], and Ding et al. [15], among others, have shown that SCW provides an excellent medium for chemical synthesis, decomposition, and/or partial or total oxidation of organic materials and compounds. They have shown that a broad range of chemical transformations can be affected in the SCW medium. These transformations include C–C bond formation, dehydration, decarboxylation, hydrodehalogenation, partial oxidation, and hydrolysis. The rates and selectivities of these different reactions can be manipulated by judicious selection of temperature, pH, catalyst, and water density, which controls the functional group transformations in SCW. Catalyst role in SCW can be subtle and may involve participation of water molecules in transition states for elementary reactions.

### 10.3 ROLE OF SCW IN CHEMICAL SYNTHESIS

Due to the unique properties possessed by SCW in which numerous types of organic reactions can be carried out with ease, this medium has been widely exploited for a variety of chemical synthesis [11–13,15–28]. Parsons [16], Katritzky et al. [17], An et al. [18], Leif and Simoneit [19], and Savage [11] provide good reviews of the types of synthetic organic chemistry that can be carried out in SCW. Savage [11] provides a brief account of the types of chemical synthesis that are possible in SCW. These include the following:

1. Hydrogenation/dehydrogenation reactions using transition metal complexes
2. C–C bond formation reaction such as Friedel–Crafts alkylation reactions
3. Rearrangement reactions such as formation of ketones by rearrangement of pinacol and two different bicyclic diols
4. Hydration and dehydration reactions such as conversion of alcohols to olefins (e.g., conversion of *tert*-butyl alcohol to isobutylene)
5. Elimination reaction such as facile decarboxylation of carboxylic acid
6. Hydrolysis such as conversion of esters to carboxylic acids and alcohols
7. Partial oxidation such as conversion of methane to oxygenates or higher hydrocarbons
8. H–D exchange such as substitute of H by D in alpha positions of ketone carboxyl groups

Savage [11] gives numerous examples of these different types of chemical synthesis. He also points out that future research should be more focused on the use of SCW to carry out these and other novel chemical synthesis. While not all chemical synthesis are targeted toward synthetic fuels, many such as hydrogenation/dehydrogenation, C–C bond formation, hydration/dehydration, hydrolysis, and partial oxidation play important role in the generations of synthetic fuels or various important additives to the synthetic fuels. This subject will be under intense future research investigation.

Some details of the specific examples quoted by Savage [11] as they relate to fuels are worth noting. As an example of C–C bond formation, both phenol and *p*-cresol can be successfully alkylated with *tert*-butyl alcohol and 2-propanol at 275°C in the absence of any added acid catalyst to produce sterically hindered phenols [18]. Water in these alkylation reactions serves as both catalyst and reactant. Xu and Antal [21,22] were successful in converting *tert*-butyl alcohol to isobutylene by dehydration reaction. In the absence of an added acid, hydronium ions formed by the dissociation of water are the primary catalytic agents. The dehydration of other alcohols such as cyclohexanol, 2-methylcyclohexanol, and 2-phenylethanol to form alkenes is also reported [23–25]. Esters can undergo an autocatalytic hydrolysis to form carboxylic acids and alcohols [17,18]. Partial oxidation of methane in SCW at 400°C to form methanol has been explored with both homogeneous free radical reactions [26,27] and heterogeneous catalytic reactions [28]. High selectivities for oxygenates, but very low methane conversions, have been obtained. More research to synthesize fuel components or fuel additives in SCW continues to be pursued.

Savage [11] also presented an excellent review of some other organic reactions in SCW. These reactions include decomposition of complex materials, individual hydrocarbons, nitrogen-containing compounds, sulfur-containing compounds, oxygen-containing compounds, compounds with two heteroatoms, and chlorine- and fluorine-containing compounds. He noted that the rates and selectivity of these and other reactions can be manipulated by judicious selection of temperature, pH, catalyst, and water density; one can thus control the functional group transformation in SCW.

## 10.4 OXIDATION IN SCW

Catalytic oxidation that has been used for many wastewater treatment, wet air oxidation, and photolysis is now being used for oxidation of organic compounds in SCW medium [12,14,15,29–72]. As mentioned earlier, water in supercritical conditions behaves like many organic solvents, and it is miscible with these solvents. Thus, SCW provides a homogeneous, benign, and nontoxic environment for many organic reactions in the presence or absence of a catalyst.

Oxidation in SCW (SCWO) is a rapidly developing technology for the destruction of organic wastes [34–39]. Hazardous organic pollutants can be destroyed by SCWO at temperatures around 500°C in less than 1 min [34–47]. The world's first commercial SCWO facility for treating industrial wastewater became operational in 1995 [48,49]. In order to increase process capacity and handle more stubborn refractory compounds and condensation products with an ease, catalytic oxidation in supercritical conditions has become more important. The SCW allows maximum concentration driving forces for the reaction because there are no interfacial mass or heat-transfer resistances to hinder the reaction rate.

In 2000, General Atomics was selected by DOE's hydrogen program to carry out SCW partial oxidation (SWPO) of biomass, municipal solid waste (MSW), and high sulfur coal to generate hydrogen. SWPO carries out oxidative reactions in the SCW environment akin to high-pressure steam in the presence of substoichiometric oxygen or air. SWPO forms more hydrogen and less char and tar than the similar operation in the subcritical conditions. Furthermore, SWPO eliminates the formations of particulates  $\text{NO}_x$ ,  $\text{SO}_x$ , and hazardous air pollutants. High-density aqueous environment is also ideal for reacting and gasifying organics. The high density also allows utilization of compact equipment that minimizes capital cost and the plant footprint requirements.

SCW has density one-tenth of the liquid water and solubility behavior that of high-pressure steam, hydrogen bonding in SCW is totally disrupted, and polarity and many thermal properties are such that they facilitate mass and heat-transfer operations along with many different types of chemical reactions. The effectiveness of SCWO has been demonstrated at the laboratory and pilot scale on hundreds of feedstock, which include sewage sludge; coal slurry; pig manure; various biomass slurries including pulp mill sludge, pulverized wood with ground plastic, rubber, and charcoal; fermentation waste; ground cereal; highly refractory hazardous

wastes such as hexachloro-benzene; and many more [29]. Maximum gaseous hydrogen yield that can be obtained can vary to as high as 26.1 g H<sub>2</sub>/100 g dry feed for ethanol and 42.9 g H<sub>2</sub>/100 g dry feed for polyethylene to as low as 13.7 g H<sub>2</sub>/100 g dry feed for cornstarch. Some of the practical results obtained in SCW conditions are described by Johanson et al. [30] and Hong and Spritzer [29]. One of the earliest patents on processing methods for the oxidation of organics in SCW was published by Modell [14].

In recent years, more efforts have been made to find (1) suitable catalysts to carry out SCWO most efficiently, (2) novel reactor designs to obtain clean syngas through oxidation, and (3) novel approaches to convert methane to methanol in economically viable way under supercritical conditions. Numerous compounds such as alcohols, acetic acid, ammonia, benzene, benzoic acid, phenol, pyridine, quinolone, MEK (methyl ethyl ketone), and dichlorobenzene have been catalytically oxidized in SCW [15]. Special applications have been targeted to various aromatic and aliphatic organic compounds, inorganic compounds, and various wastewaters and sludges. The most notable catalysts used for these purposes are oxides of copper, zinc, vanadium, manganese, as well as noble metal such as platinum. Additional data are reported by Savage et al. [26,53,54], Savage [11], Subramaniam and McHugh [9], Thomason et al. [59], and Tester et al. [48]. Various mechanisms for oxidation reactions are outlined by Ding et al. [15] and Savage [11].

A two-stage approach to SCWO has also been investigated. In the first stage, contaminated waste is exposed to hydrothermal carbonization or liquefaction to extract harmful substances (such as chlorinated and other toxic components) from waste. Biocoal, biocrude, or biochar produced from this first stage then undergo oxidation and reforming in SCW to decompose organic compounds and generate syngas containing hydrogen, carbon dioxide, carbon monoxide, and may be some lower hydrocarbons depending on the temperature of the gasification and the nature of the catalyst. Some practical examples of multistage operations are outlined by Brunner [10].

The most extensive and critical review of oxidation of methanol in SCW was carried out by Vogel et al. [31]. This study is very important for treating aqueous effluents containing methanol by SCWO (an exothermic reaction) and for performing hydrothermal reforming under autothermal (i.e., in the presence of partial oxidation) conditions. They critically evaluated all existing literature data and concluded that there are important differences in the reported kinetics of methanol oxidation. The factors responsible for these differences are (1) the methanol feed concentration, (2) insufficient reaction heat removal from tubular or coiled flow reactors, and (3) inherent difference in apparent kinetics of autocatalytic reactions in continuous stirred-tank reactor (CSTR) and in plug flow reactor (PFR) due to recirculation of radicals (i.e., mixing effect) in a CSTR. The study indicated that the best kinetic data for methanol SCWO cannot be recommended because of lack of information on (1) induction time and (2) influence of wall catalysis on the apparent reaction rate.

Watanabe et al. [41,42] showed that NaOH and ZrO<sub>2</sub> have catalytic effects for partial oxidation of *n*-hexadecane and lignin in SCW. The experiments were carried out

at 400°C. For both compounds,  $\text{ZrO}_2$  catalyst gave hydrogen yield twice higher than those obtained without the catalyst. With NaOH, the yield increase was four times. Both catalysts enhanced the decomposition of aldehyde and ketone intermediates into CO. For lignin, both catalysts enhanced the decomposition of carbonyl compounds, which in turn inhibited the char formation and promoted the formations of CO and  $\text{H}_2$ .

#### 10.4.1 CATALYSTS FOR SCWO

Ding et al. [15] showed that it is possible to develop effective catalysts for SCWO applications. These catalysts can be used either to enhance oxidation rates of organic compounds or to increase destruction of refractory products. The catalyst can be designed to increase the selectivity of certain products. Because of a wide variation in the nature of aqueous wastes, understanding the unique characteristics of SCW and its effect on the catalyst surface, reaction activity, and mechanisms, and the knowledge of preferred crystalline phases of metal oxides is essential for the development and design of an effective SCWO catalytic system. Oxides of Ce, Co, Fe, Mn, Ti, and Zn may be used as catalysts, and their supports can be selected from the oxides of Al, Hf, Zr, and Ti. These supports have been found to be stable in SCWO environments. The additives that can increase the physical strength or stabilize the activity of a catalyst may be an oxide of Bi, Cd, Ga, Ir, K, Mo, Ta, or W. An effective SCWO catalyst must have large surface area and be able to withstand larger surface area changes.

Catalyst activity and stability is affected by the preparation methods. Traditionally, catalysts are produced by coprecipitation, impregnation (coating), fused alloy, fused metal oxide, and crystal growth processes [62–72]. Coprecipitation and impregnation are two of the most popular methods for the preparation of metal and metal oxide catalysts [17,20,62–72]. Many commercial oxidation catalysts are prepared by coating noble metals on metal oxide supports to modify catalyst surface structure and active sites that can result in the increase in catalyst activity and stability. While the physical conditions of these catalysts are adequate for the gas-phase oxidation, they may not be completely suitable for the SCW conditions. Since transition metal oxide catalysts are major components of ceramics, the common methods of ceramic preparation such as sol-gel, coprecipitation, polymeric sponge, and high-temperature aerosol decomposition methods have been adapted for the preparation of metal oxide catalysts. The structure and properties of ceramic catalysts depend on the process parameters such as solvents, pH, temperature, and aging time. Numerous reported studies have evaluated these effects [62–72]. In the final analysis, preparation method must be chosen that gives the desired activity, selectivity, stability, and prepares catalyst that can handle refractory materials and possible poisons in the waste feed.

#### 10.5 DECOMPOSITION AND EXTRACTION OF MATERIALS BY SCW

SCW is a good extracting and decomposition agent for many complex organic materials [73–118] (Kim and Mitchell, 2012, pers. comm.; Swanson et al., 2012, pers. comm.). This application generally produces useful liquids that can be either a fuel or raw materials for various downstream chemicals. Feedstock normally used for

the liquid productions are coal, polymeric materials, rubber tires, cellulose among others, or mixtures of them.

The extraction of coals with SCW is a promising route for the production of liquid fuels and chemical feedstock from coal. Deshpande et al. [73] obtained high conversion for extraction of a German Brown coal and a Bruceton bituminous coal by SCW at 375°C and 23 MPa. They reported conversions of 70%–79% for the brown coal and about 58% for the bituminous coal. Pauliatis et al. [74] reported 35% conversion and only 10% liquid yield for North Dakota lignite at 400°C and 28 MPa pressure. Deshpande et al. [73] also obtained low liquid yield with lignite coal with high sodium content. Other studies report low conversion for bituminous coal, particularly when solvent density is low [75–80,82–84] (Swanson et al., 2012, pers. comm.). Kershaw and Bagnell [78] showed that at 380°C and 22 MPa, the conversions of Australian brown coals were considerably higher for supercritical extraction of water than with toluene. The reverse was, however, true for black coals. In general, they found SCW extraction was more effective for low-rank coals than high-rank bituminous coals. The extraction by water was also more dependent on pressure presumably due to solvent density effect. The hydroxyl concentration of liquid yield by SCW extraction was higher than that obtained in the liquid produced by toluene extraction.

Swanson et al. (2012, pers. comm.) showed that for low-rank coals, the conversion and extract yields increased with increasing temperature and pressure. The conversion also decreased with increasing coal rank and correlated well with the percent volatile matter in the coals. The study also indicated that SCW extracts the volatile hydrogen-rich fraction of the coal. The extract was found to be highly polar in nature, with significant quantities of phenols and long-chain aliphatic fatty acids.

Numerous other studies have also addressed the behavior of coal, shale oil, biomass and mixtures of coal and biomass, polymers, rubber, algal oil, lignin, residual oil, and so on under SCW conditions [77–115] (Kim and Mitchell, 2012, pers. comm.; Swanson et al., 2012, pers. comm.). Three typical studies illustrating the coal decomposition in SCW are reported by Nonaka [89], Nonaka et al. [97], Li and Eglebor [106], Vostrikov et al. [84], and Cheng et al. [83]. These studies showed that as the temperature of SCW increases, more gas and less liquid are produced.

SCW has also been explored as a medium for the degradation of waste synthetic polymers [107–116]. Rubber tires were converted to a 44% oil yield by reaction in SCW at 400°C. When polystyrene-based ion exchange resins were subjected to SCW at 380°C for 1 h [107–116], less than 5% polymer decomposed and the products included styrene and several oxygenated arenes such as acetophenone and benzaldehyde. SCW is also used to extract oil and oil precursors from oil shale [98,100–105]. The process involved C–C bond cleavages, and in the presence of CO, higher hydrocarbon yields were obtained than those obtained in conventional pyrolytic treatment. Holliday et al. [115] showed that water near its critical point is a good medium for the hydrolysis of triglyceride-based vegetable oils into their fatty acid constituents.

A number of studies examined the decomposition of mixed feedstock under SCW conditions [89,95–99]. Veski et al. [98] examined the decomposition of a mixture of kukersite oil shale and pinewood and showed improved liquid and gas yields at 380°C temperature. The mixture indicated a synergistic effect and showed the product to be 1.5–2.0 times better than what would be predicted based on simple additive yields.

The liquid product was richer in heterocompounds including polar ones compared to that predicted from simple additive effects. Kim and Mitchell (2012, pers. com.) examined the decomposition of coal–biomass mixture. The results show that at 647.3 K and 220.9 atm pressure, small polar and nonpolar organic compounds released from the mixture were completely miscible with SCW. The hydrolysis of large organic molecules in SCW resulted in high concentrations of  $H_2$ , CO,  $CO_2$ , and low-molecular-weight hydrocarbons with very little tar, soot, and PAH (polyaromatic hydrocarbons) formation. Sulfur, nitrogen, and many trace elements in coals were oxidized to form insoluble salts in SCW. There were no gaseous emissions, and all products were dissolved in the SCW. The salts can be precipitated from fluid mixture and removed along with ash. Matsumara et al. [90] examined co-liquefaction of coal and cellulose in SCW at 673 K and 25 MPa. The coal used was Ishikari coal. Unlike the results of synergy reported by Veski et al. [98], in this study no synergy between coal and cellulose conversion was found. Simple additive method for each compound product distribution worked well for this system. More discussion on synergistic effects in mixture decomposition has been recently discussed by Lee and Shah [117].

Sunphorka et al. [96] examined co-liquefaction of coal and plastic mixtures containing high-density polyethylene, low-density polyethylene, polystyrene, and polypropylene. The experiments were performed in the temperature range of 450°C–480°C, 40–70 wt% plastic mixtures, and a water/feedstock ratio of 2 to 10. During co-liquefaction, all experimental variables had effects on liquid yield, but temperature did not have a significant effect on the conversion. Long residue in the oil product decreased with increasing temperature while it increased with increasing water/feedstock ratio. For the plastic mixture alone, only temperature had a significant effect on the oil yield. Maximum conversion and liquid yield of 99% and 66%, respectively, were obtained. Onsari et al. [95] examined co-liquefaction of lignite coal and rubber tires in the temperature range of 380°C–440°C and water/feedstock ratio of 4/1 to 10/1 by weight. Variable tire concentration was examined. The maximum conversion and oil yield were obtained at 400°C, 1 min residence time, water/feedstock ratio of 10% and 80% tire concentration. The co-liquefaction of coal and tire yielded a synergistically increased level of oil production. Moreover, the total conversion level with co-liquefaction was almost equal to that obtained in the presence of either  $Fe_2O_3$  or Ni/Mo catalysts under the same conditions. The study concluded that SCW is a good medium for the dissolution of the volatile matter from a coal and used tire matrix.

Mitsubishi Materials Corp. [87] with the project support of Petroleum Energy Center, Japan, developed a thermal process that used SCW to crack vacuum distillation residue (VR) oil into clean lighter oil products. The final volume of solid waste generated was below 5%. The process was carried out in two stages in the same reactor. At the bottom of the reactor, heavy VR components (pitch) are decomposed into lighter components using 5% SCW at temperatures 400°C–450°C and pressures 200–250 atm. In the upper part of the reactor, lighter components are cracked at a slightly higher temperature with SCW and hydrogen to form lighter products. Untreated pitch was withdrawn at the bottom and sent to a reformer where it is partially oxidized at SCW at 1000°C to form hydrogen gas and soot. This hydrogen stream is passed onto the upper section of the cracking reactor. Overall, the process converted 70% of VR into lighter products, which included 15% gas, 7% liquefied petroleum gas (LPG), 11% naphtha,

13% light oil, 24% vacuum gas oil, 21% carbon dioxide and 1% soot, and 8% heavy oil. The process was proven in a test plant of size 1 bbl/day.

The conversion of glycerol in SCW was examined by May et al. [118]. They studied the conversion of glycerol in the temperature range of 510°C–550°C, 350 atm pressure in a bed of inert nonporous  $\text{ZrO}_2$  particles as well as in a bed of 1%  $\text{Ru}/\text{ZrO}_2$  catalyst for the residence time of 2–10 s. The feed solution contained 5 wt% glycerol. The experiments in the absence of a catalyst resulted in the formation of liquid products such as acetaldehyde, acetic acid, hydroxyacetone, allyl alcohol, propionaldehyde, acrolein, and acrylic acid, and gases such as  $\text{H}_2$ ,  $\text{CO}$  and  $\text{CO}_2$ , and methane. The catalyst enhanced the formation of acetic acid and inhibited the formation of acrolein. In the catalytic experiments, the main products formed were hydrogen and carbon dioxide with little methane and ethylene. Complete glycerol conversion occurred at 510°C in 8.5 s and at 550°C in 5 s in the presence of the catalyst. This, however, did not result in complete gasification; some acetic acid and acetaldehyde were still present. At high residence times, methanol and acetaldehyde were formed. The hydrogen yield was only 50% of what is achievable by stoichiometry due to lack of high activity of the catalyst. A simplified reaction pathway for glycerol conversion in supercritical conditions is illustrated in Figure 10.2 [118].

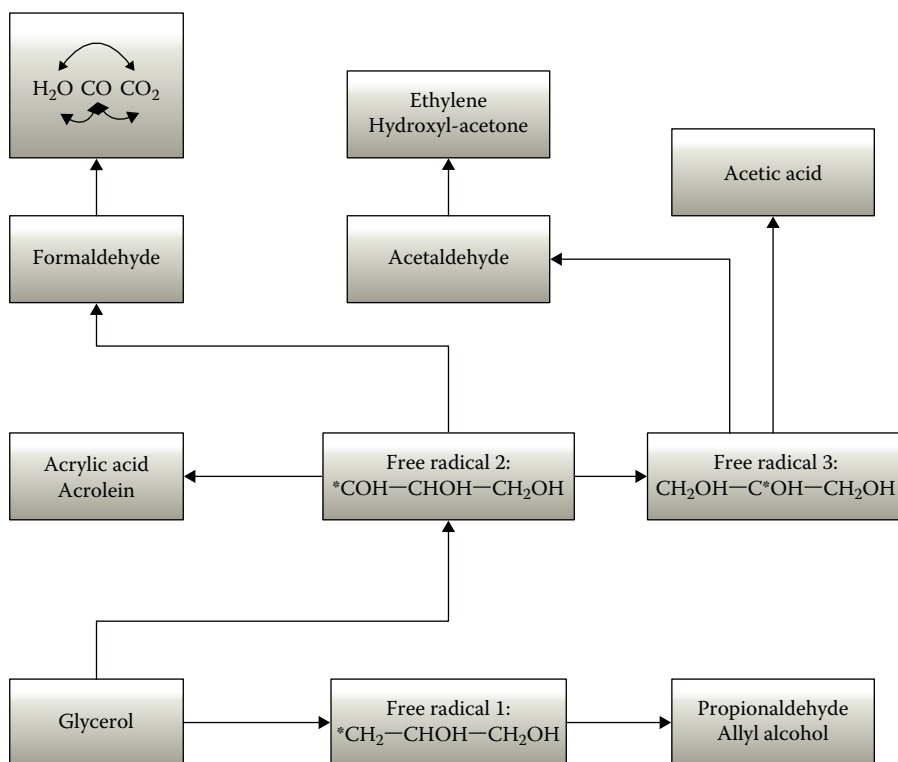


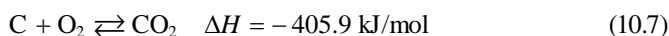
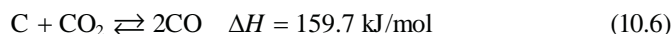
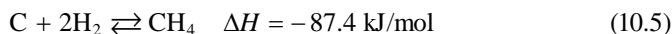
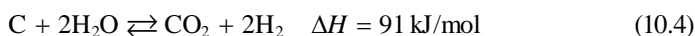
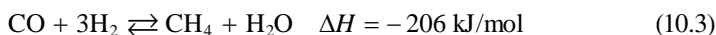
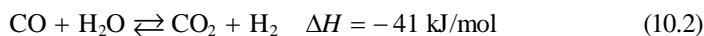
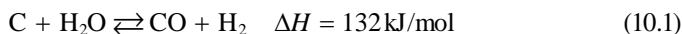
**FIGURE 10.2** Simplified reaction pathways for hydrothermal transformation of glycerol in SCW. (Modified from May, A., Salvado, J., Torras, C., and Montane, D., *Chemical Engineering Journal*, 160, 751–759, 2010.)

All the studies described earlier indicate that near-critical conditions, complex carbonaceous materials tend to decompose into a mixture of liquids and gases. The amount of each phase depends on the nature of feedstock, pressure, and reaction time. The use of a suitable catalyst increases both liquid and gas yields. An increase in temperature generally produces more gas. In a case of a mixture, the synergistic effects between the decompositions of two components depend on the nature of the components.

## 10.6 GASIFICATION IN SCW

While steam gasification occurs at low pressure and high temperature, in recent years gasification of biomass in a pressurized water environment (called hydrothermal gasification) has gained significant support [83,84,119–153] (Antal and Xu, 2012, pers. comm.; Boukis, 2012, pers. comm.; Kruse, 2012, pers. comm.; Veriansyah et al., 2012, pers. comm.). The hydrothermal gasification can be divided into three regions depending on the range of temperature. Osada et al. [119] identified region 1 as the one with a temperature range of 500°C–700°C—a region in which biomass is decomposed in SCW in the presence of either activated carbon to avoid the formation of char or an alkali catalyst to facilitate water–gas shift reaction. In this region, very little solids remained and the main product of the gasification is hydrogen. In region 2 of SCW, where the temperature range is 374°C–500°C, biomass hydrolyzes and metal catalyst facilitates gasification. Here once again, the main product is hydrogen with some carbon dioxide, carbon monoxide, and methane. The third region was described in Chapter 5. Near the critical conditions, methane would be a preferential gas in the absence of a catalyst. However, at high temperature and/or in the presence of a suitable catalyst, hydrogen can be formed by reforming and water–gas shift reactions. The nature of the product will depend on the nature of the feedstock, temperature, pressure, feed concentration, residence time, and the nature of the catalyst (if any). The reported studies for SCW gasification of complex and simple materials are briefly described here.

The main steam gasification reactions under the SCW environment can be listed as follows:



Reactions 10.1 and 10.6 are important for gasification and are endothermic. The overall process is also endothermic. Reaction 10.7 is needed to provide the heat for autothermal conditions.

Li et al. [116] investigated coal gasification in the temperature range of 650°C–800°C and pressure 23–27 MPa,  $K_2CO_3$  and Raney Ni as catalysts, and  $H_2O_2$  as oxidant. Most experiments were performed with inlet slurry containing 16.5 wt% coal and 1.5 wt% CMC (carboxy methyl cellulose). The results showed that high temperature favors the gasification of coal in SCW, whereas pressure has a little effect on the gasification results. An optimum flow rate needs to be found to get the best results. Both gasification and carbon gasification efficiencies were improved by the catalysts;  $K_2CO_3$  performed better than Raney Ni. Less char and tar were formed in the presence of catalysts. An increase in feed concentration decreased the hydrogen and gasification efficiencies. SCW desulfurizes the coal and the solid particles remained had less carbon and hydrogen than original coal. The data of Li et al. [116] indicate that for the entire range they studied, 90% of the gas-phase concentration was for hydrogen (60%) and carbon dioxide (30%).

Vostrikov et al. [84] examined coal gasification in the temperature range of 500°C–750°C, pressure of 30 MPa, and reaction time of 60–720 s with and without  $CO_2$ . Once again, the main gaseous products were  $CH_4$ , CO,  $CO_2$ , and  $H_2$ . Within the range of operating conditions examined, best carbon conversion was obtained at 750°C. The results show a significant temperature dependence on product compositions for temperatures below 650°C. BTX (benzene, toluene, and xylene), methane, and carbon dioxide were the main products below 650°C–700°C. Similar results were obtained by Cheng et al. [83] who studied gasification of lignite coals in the temperature range of 350°C–550°C and reaction time of 0–60 min in  $N_2$  atmosphere. These data along with the data described earlier clearly indicate that product distribution during coal gasification in SCW will depend on the nature of coal along with all the operating parameters.

Battelle Pacific Northwest National Laboratory demonstrated that various alkali carbonate and Ni catalysts can convert wet biomass to methane-rich gas at temperatures between 400°C and 450°C and pressure as high as 34.5 MPa. Yu et al. [120] found that glucose at low concentration (0.1 M) can be completely gasified in 20 s at 600°C and 34.5 MPa, with major products being hydrogen and carbon dioxide. Higher concentration of glucose, however, reduces the product concentration of hydrogen and carbon dioxide and increases the concentration of methane. Xu et al. [129] showed that a wide range of carbons effectively catalyze the gasification of glucose in SCW at 600°C and 34.5 MPa pressure, with nearly 100% carbon gasification efficiency. The available surface area of carbon did not affect the effectiveness of the catalyst. For concentrated organic feeds in water, in the presence of a catalyst, the temperature above 600°C is needed to achieve high gasification efficiencies. Mass transfer resistances at high concentration (if any) can affect the equilibrium of water–gas shift reaction. In the presence of coconut shell, activated carbon, cellobiose, and various whole biomass feeds, as well as depithed bagasse liquid extract and sewage sludge were completely gasified. There was some deactivation of carbon catalyst after 4–6 h of operation.

Demirbas [2,6,131] examined the decomposition of olive husk, cotton cocoon shell, and tea waste by water under both sub- and supercritical conditions. He also observed an increase in hydrogen production with temperature, particularly for temperatures higher than the supercritical temperature. Demirbas [131] observed that as

temperature increased from 600°C to 800°C, hydrogen production increased from 53 to 73 vol% in reaction time of 2–6 s. She indicated that hydrogen productions can be obtained from biomass such as bio-nutshell, olive husk, tea waste, crop straw, black liquor, MSW, crop grain residue, pulp and paper waste, petroleum-based plastic waste, and manure slurry.

An extensive amount of work on SCW gasification of organic wastes has been reported in the literature [129,130,139]. The studies have shown that the gasification generally produces hydrogen and carbon dioxide mixture with simultaneous decontamination of wastes, particularly at higher temperatures. The homogeneous solution of waste and water makes it easy to pump to the high-pressure reactor without pretreatment. Guo et al. [130] presented an excellent review of SCW gasification of biomass and organic wastes. They as well as Lu et al. [133] showed the equilibrium effects of temperature, pressure, and feed concentration of wood sawdust on hydrogen, carbon dioxide, carbon monoxide, and methane concentrations in SCW. The typical effects of temperature on product gas composition are illustrated in Table 10.2. The data showed that equilibrium favors the productions of hydrogen and carbon dioxide at high temperatures. The study also showed that an increase in pressure significantly decreased the product concentration of carbon monoxide and slightly decreased the product concentration of the hydrogen. The pressure change had very little effect on the product concentrations of carbon dioxide and methane. The complex effect of pressure on the product distribution was believed to be due to the complex interplay between hydrolysis and water–gas shift reactions. Besides temperature and pressure, other parameters that affected the gas yield were feedstock concentration, oxidant, reaction time, feedstock composition, inorganic impurities in the feedstock, and biomass particle size. Guo et al. [131] also concluded that alkali such as NaOH, KOH,  $\text{Na}_2\text{CO}_3$ ,  $\text{K}_2\text{CO}_3$ , and  $\text{Ca}(\text{OH})_2$ ; activated carbon; metal oxides and metals such as noble metal catalysts ( $\text{Ru}/\alpha\text{-alumina} > \text{Ru}/\text{carbon} > \text{Rh}/\text{carbon} > \text{Pt}/\alpha\text{-alumina}$ ,  $\text{Pd}/\text{carbon}$ ,  $\text{Pd}/\alpha\text{-alumina}$ ); as well as Ni catalysts and metal oxides such as  $\text{CeO}_2$  particles, nano- $\text{CeO}_2$ , and nano- $(\text{CeZr})_x\text{O}_2$  enhanced

**TABLE 10.2****Equilibrium Gas Yield for 5 wt% Sawdust in SCW at 25 MPa Pressure**

Temperature (°C)	Gas Yield (mol/kg)				
	Hydrogen	Carbon Dioxide	Methane	Carbon Monoxide	Methane/Hydrogen
400	13	24	20	$10^{-3}$	1.54
500	40	31	10	$2.5 \times 10^{-3}$	0.25
600	80	40	~1	$3.1 \times 10^{-3}$	0.0125
700	89	43	0	$1.2 \times 10^{-3}$	0.0
800	89	43	0	$0.5 \times 10^{-3}$	0.0

Source: Guo, L., Cao, C., and Lu, Y., “Supercritical water gasification of biomass and organic wastes,” in Momba, M. and Bux, F. (eds.), *Biomass*, 165–182, 2010. With permission.

Note: These data are the best estimates from the graphical data presented.

the reactivity of biomass gasification in SCW. The last two are important for the reforming under supercritical conditions. These and other studies found that the yields of  $\text{H}_2\text{O}$  and  $\text{CO}$  increased with increasing water density. Yields of  $\text{H}_2$  were 4 times better with  $\text{NaOH}$  and 1.5 times better with  $\text{ZrO}_2$  compared to the reaction without a catalyst. Supercritical fluids gave increased pore accessibility, enhanced catalyst ability to coking, and increased desired product selectivity. While high-temperature SCW gasification produces hydrogen and carbon dioxide, Sinag et al. [152] showed that a combination of two technologies—SCW and hydropyrolysis on glucose in the presence of  $\text{K}_2\text{CO}_3$ —produces phenols, furfurals, organic acids, aldehydes, and gases. Xu and Antal [20,21], Antal and Xu (2012, pers. comm.), and Antal et al. [144] studied gasification of 7.69 wt% digested sewage sludge in SCW and obtained gas that largely contained  $\text{H}_2$ ,  $\text{CO}_2$ , a smaller amount of  $\text{CH}_4$ , and a trace of  $\text{CO}$ . Other waste materials show a similar behavior.

Kong et al. [151] briefly summarized the reported work for the catalytic hydrothermal gasification of various types of biomass in SCW. They showed that in the literature, catalytic hydrothermal gasification in SCW has been examined for glucose, organic wastewater, cellulose, soft and hard wood, grass, lignin, sawdust, rice straw, alkylphenols, corn, potato starch gels, potato waste, glycerol, cellobiose, bagasse, sewage sludge, catchetol, vaniline, glycine, and many others. In all cases, the major products were hydrogen and methane depending on the operating conditions. The catalysts examined included  $\text{Ni}$ ,  $\text{Ru}$ ,  $\text{Rh}$ ,  $\text{Pd}$ ,  $\text{Pt}$  on alumina,  $\text{NaOH}$ ,  $\text{KOH}$ ,  $\text{Na}_2\text{CO}_3$ ,  $\text{K}_2\text{CO}_3$ ,  $\text{ZrO}_2$ , activated carbon, and  $\text{Ni}$  on carbon. The preference was given to the disposable or cheap catalysts or to the reforming catalysts if the objective was to carry out reforming along with gasification. The results show that except at low temperatures, the main product in all cases was hydrogen. Catalytic operations decrease the productions of char and tar and increase the production of hydrogen. Carbon and base catalysts play important roles in the increased gas yields and hydrogen production. Tanksale et al. [7] provided an extensive review of various catalytic and other processes to produce hydrogen from biomass. Supercritical gasification in water was one of these processes. Azadi and Farnood [5] reviewed heterogeneous catalysts for subcritical water and SCW gasification of biomass and wastes. The review provided an extensive information of carbon conversion and hydrogen and methane productions in sub- and supercritical conditions for a variety of biomass by various commercially available and laboratory-made catalysts that included supported and skeletal metal catalysts, activated carbon, metal wires, and other innovative catalysts.

The generation of hydrogen from waste has long-term and strategic implications since hydrogen is the purest form of energy and is very useful for product upgrading, fuel cell, and many other applications. Hydrogen can be produced from waste via numerous high-temperature technologies such as conventional or fast pyrolysis (e.g., olive husk, tea waste, crop straw, etc.), high-temperature or steam gasification (e.g., bio-nutshell, black liquor, wood waste, etc.), supercritical fluid extraction (e.g., swine manure, orange peel waste, crop grain residue, petroleum-based plastic waste, etc.), SCW gasification (e.g., all types of organic waste, agricultural and forestry waste, etc.) as well as low-temperature technologies such as anaerobic digestion and fermentation (e.g., manure slurry, agricultural residue, MSW, tofu wastewater, starch of food waste, etc.). For high-temperature technologies, SCW gasification generates

more hydrogen at a lower temperature than pyrolysis or gasification [2,3,6,83,91] (Kim and Mitchell, 2012, pers. comm.). SCW gasification also does not require drying, sizing, and other methods of feed preparations, thereby costing less for the overall process. The temperature of the pyrolysis and gasification process can be reduced if the gases coming out of these processes are further steam reformed. This, however, adds to the overall cost. The rates for the low-temperature processes such as anaerobic digestion and fermentation can be enhanced with the use of suitable microbes and enzymes. The development of future hydrogen economy will require further research in the improvement of these technologies.

Biomass generally contains three important components: cellulose, hemicellulose, and lignin. Both cellulose and hemicellulose (collectively called homocellulose) are easy to hydrolyze, decompose, dehydrogenate, decarboxylate, and reformed as shown by numerous studies mentioned earlier. Lignin component is generally toughest to convert. Yamaguchi et al. [123,138] studied lignin gasification in SCW. They indicated that lignin gasification involves three steps: (1) lignin decomposition to alkylphenols and formaldehyde in SCW, (2) gasification of alkylphenols and formaldehyde over a catalyst, and (3) formation of char from formaldehyde. They showed that SCW gasification is a promising technique to reduce the lignin gasification temperature. They also studied lignin gasification with three different catalysts at 400°C— $\text{RuCl}_3/\text{C}$ ,  $\text{Ru}(\text{NO})(\text{NO}_3)_3/\text{C}$ , and  $\text{RuCl}_3/\text{C}$ —and found that the order of gasification activity was  $\text{Ru}/\text{C} = \text{Ru}(\text{NO})(\text{NO}_3)_3/\text{C} > \text{RuCl}_3/\text{C}$ . Extended x-ray absorption fine structure (EXAFS) analysis showed that during lignin gasification in SCW, ruthenium particle sizes in  $\text{Ru}(\text{NO})(\text{NO}_3)_3/\text{C}$  and  $\text{Ru}/\text{C}$  catalysts were smaller than that in the  $\text{RuCl}_3/\text{C}$  catalyst. The study concluded that the ruthenium catalysts with smaller particle size of metal particles were more active for the lignin gasification.

Lignin is one of the major fractions of woody biomass that is a polymer of aromatic compounds such as coniferyl alcohol, sinapyl alcohol and, coumaryl alcohol, and it constitutes about 30 wt% and 40% of energy of woody biomass. Yamaguchi et al. [123,138] examined the effects of various noble and transition metal catalysts and titania and activated carbon supports on lignin conversion and hydrogen production rates. The results showed that for the lignin gasification, the activity order followed ruthenium > rhodium > platinum > palladium > nickel, whereas the hydrogen production rate followed the order palladium > ruthenium > platinum > rhodium > nickel. Both titania and activated carbon provided stable support. Hydrogen production rate from lignin increased with temperature and shorter residence time.

Byrd et al. [124] examined a two-stage process to obtain clean fuels from switchgrass. In the first stage, subcritical hydrothermal liquefaction of switchgrass was carried out to obtain biocrude that did not contain some of the inorganic and other undesirable elements. In the second stage, catalytic gasification of biocrude in SCW was carried out to obtain clean syngas dominant in hydrogen. Biocrude contained many oxygenated hydrocarbons of varying molecular structure and weights, including lignin-derived products and sugars and their decomposition products. The supercritical gasification of biocrude was carried out at 600°C and 250 atm pressure. Nickel, cobalt, and ruthenium catalysts were prepared on titania, zirconia, and magnesium aluminum spinel supports. Magnesium aluminum spinel structure did not work. Over time, zirconia-supported catalyst plugged the reactor, although  $\text{Ni}/\text{ZrO}_2$

catalyst gave the best hydrogen production. Titania-supported catalysts gave lower hydrogen conversions but did not plug the reactor over time. All support materials suffered surface area loss due to sintering.

Glycerol ( $\text{HOCH}_2\text{--CHOH--CH}_2\text{OH}$ ) is obtained as a by-product from biodiesel manufacturing by transesterification of vegetable oils. Nine grams of biodiesel generates approximately 1 g of glycerol. With increasing production of biodiesel, glycerol production will rise, and it can be used for food, oral and personal care, tobacco, polymers, pharmaceuticals, and replacements of petroleum feedstock. Kersten et al. [153] have reported gasification results for glycerol and other model compounds in a variety of catalytic and noncatalytic reactors in SCW and found that without addition of a catalyst, only very dilute concentrations of model biomass feeds could be completely gasified. The density of SCW is higher than that of steam, resulting in a higher space time yield. Higher thermal conductivity and specific heat were helpful in carrying out the endothermic reforming reactions. The formation of char and tar was also minimized because of the solubility of hydrocarbons in SCW. Importantly, hydrogen produced from SCW reforming was produced at high pressure, which can be stored directly, thus avoiding large expenses associated with compression.

The above-described studies and many others lead to some general conclusions [83,84,119–153] (Antal and Xu, 2012, pers. comm.; Boukis, 2012, pers. comm.; Kruse, 2012, pers. comm.; Veriansyah et al., 2012, pers. comm.). As the temperature increases above the critical temperature, more gases are generally produced from most carbonaceous materials. At lower temperatures, for higher feedstock concentration, and in the absence of a catalyst, the gas production rate tends to be lower and contain more methane. At high temperature, for lower feedstock concentration, and in the presence of an effective catalyst, hydrogen production rate rapidly increases. Higher temperature and the presence of a catalyst promote reforming of gas and favor reverse water–gas shift reaction, thus producing more hydrogen and carbon dioxide. Pressure also affects the equilibrium of water–gas shift reaction. Higher pressure favors methane formation as opposed to hydrogen production.

## 10.7 REFORMING IN SCW

SCW is an ideal medium to carry out reforming reactions for both single components and complex materials [154–176] (Barendregt 2012, pers. comm.; Cremers et al., 2012, pers. comm.; Veriansyah et al., 2012, pers. comm.). Besides all the positive features of the supercritical medium outlined earlier, SCW provides possibilities of lower temperature, lesser coking issues, and more active and stable catalytic reforming process. In Sections 10.7.1 through 10.7.7, we briefly assess important reported literature on the subject.

### 10.7.1 LIQUID FUELS

Lee et al. [154] showed that reforming of JP-8 fuel and diesel fuel can be carried out in SCW in the absence of a catalyst. High enthalpy level of SCW and high solubilities of fuel in SCW allowed the reforming reactions to occur in the temperature range of 650°C–825°C and 220–330 atm pressure. The study examined the productions

of hydrogen and methane as functions of reactor operating conditions and the possibility of autothermal operation by simultaneously carrying out partial oxidation reaction with reforming reaction. The process handled fuel with sulfur. The results were obtained at temperatures lower than conventional reforming temperature. The autothermal operation was achieved by adding oxygen into the reacting mixture. In a noncatalytic operation, hydrogen production of 14% of theoretical maximum was obtained. Cremers et al. (2012, pers. comm.) studied SCW reforming of logistic diesel fuel at 550°C in the absence of a catalyst and obtained significant hydrogen production.

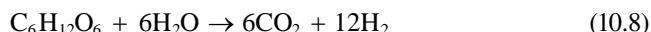
Veriansyah et al. (2012, pers. comm.) examined reforming of gasoline in SCW. They used methanol and isooctane (2,2,4-trimethylpentane) as model compounds for gasoline for experimental and simulation studies. The study presented the following conclusions:

1. SCW reforming of hydrocarbons offers a possible way to convert hydrocarbons to hydrogen at a lower temperature. It does not require a steam reforming catalyst, although nickel in reactor wall can act as a catalyst. It avoids the poisoning and deactivation problems associated with the catalyst.
2. The reactor is much compact compared to conventional steam reforming reactors. It is scalable and the reaction time is in seconds. SCW provides dual functions—excellent reactant and homogeneous medium.
3. As reaction temperature, initial feed concentration, and residence time increase, hydrogen, carbon dioxide, and methane productions increase while carbon monoxide and ethane yields remain stable. At high temperature, methane yield is higher than hydrogen yield because at high temperature methanation reaction is favored. In order to increase the hydrogen yield, methanation reaction needs to be suppressed. High inlet feed temperature decreases yields of hydrogen, carbon monoxide, and carbon dioxide and increases the yields of methane and ethane. High inlet temperature also forms coke in the feed line, which may plug the inlet pipes.

Numerous other studies have also examined catalytic reforming of various hydrocarbons in SCW [122,156,162,163,171,172] (Barendregt 2012, pers. comm.). Shekhawat et al. [171] studied catalytic reforming of liquid hydrocarbon fuels for fuel cell applications. They concluded that supercritical reforming of hydrocarbons occurs at lower temperatures than those required in conventional industrial reforming process. They also showed that hydrogen yield increases by using commercial catalysts even if they are not optimized for these conditions. Acetone and diesel fuel produced black liquor and plugged the reactors. Pinkwart et al. [122] showed that under SCW, *n*-decane can be converted to hydrogen-rich gas. They also showed that reforming of diesel oil by four different commercial reforming catalysts can be carried out at a lower temperature than the conventional steam reforming process. The lower temperature also caused lower production of coke during reforming reaction. Ramasamy and T-Raissi [163] studied hydrogen production during reforming of lube oil in supercritical water. They also examined the role of Ni, carbon, and alkali catalysts on the hydrogen production. Very little catalyst deactivation was observed under supercritical conditions.

### 10.7.2 BIOMASS

A number of investigators have looked at glucose as a model for biomass reforming under SCW. The pertinent reaction in this case is



Generally, hydrogen yield is smaller than predicted from the above equation because varying amounts of methane are produced depending on the reaction conditions. Kruse ([132]; 2012, pers. comm.), Kruse and Gawlik [141], and Kruse and Henningsen [142] gave a simplified reaction mechanism for cellulose reforming. Since glucose (and fructose) is the main product of hydrolysis of cellulose, their reaction mechanism also applies to glucose. The reforming of glucose was accelerated by alkali catalysts such as  $\text{K}_2\text{CO}_3$  and  $\text{KHCO}_3$ . Both of these catalysts increased the hydrogen production and decreased coke formation. For biomass with low salt content and high protein content, these catalysts can increase the hydrogen yield.

Antal and Xu (2012, pers. comm.) and Antal et al. [144] showed the effectiveness of SCW reforming for the production of hydrogen for numerous different types of biomass such as wood sawdust, cornstarch gel, digested sewage sludge, glycerol, glycerol/methanol mixture, poplar wood sawdust, potato starch gels, and potato waste. Once again, higher temperature and catalysts gave better hydrogen productions. The final product distribution did depend on the nature of the feedstock. Similar results were obtained by Boukis et al. (2012, pers. comm.) for biomass slurries and sludges. They also showed an improved heat exchange scheme in “VERENA” German pilot plant for these processes. The VERENA pilot facility successfully demonstrated high carbon and energy efficiency for the SCW reforming of ethanol and corn silage in the temperature range of 540°C–600°C for at least 10 h. On average, the hydrogen concentration in the product for these biomass was about 77 vol%. Zhang et al. [134] examined the SCW reforming of glucose solution (50–200 g/l), a simulated aqueous organic waste (composed of glucose, acetic acid, and guaiacol), and a real aqueous organic waste stream generated from a sludge hydrothermal liquefaction process. The experiments were performed using two different types of catalysts—0.1 RuNi/ $\gamma\text{-Al}_2\text{O}_3$  and 0.1 RuNi/activated carbon catalysts (10 wt% Ni with a Ru-to-Ni molar ratio of 0.1). While the first catalyst was very effective with glucose solutions and simulated aqueous organic waste giving hydrogen yield of 53.9 mol/kg dried feedstock at 750°C, 24 MPa, and weight hourly space velocity (WHSV) of 6 h<sup>-1</sup>, it was not effective in resisting the alkali and nitrogen compounds in the real waste. The second catalyst supported on active carbon exhibited higher stability.

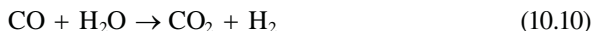
### 10.7.3 GLYCEROL

Reforming of glycerol for hydrogen production can be summarized by the following reactions [118,129,140,148,155,166].

First, the steam reforming of glycerol can be expressed as



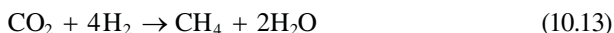
followed by the water–gas shift reaction



The desired overall reaction is then summarized as



Some hydrogen is also lost via the methanation of CO and CO<sub>2</sub>:



As a result, the product stream is a mixture of the above gases. Furthermore, the yield of hydrogen depends on several process variables such as system pressure, temperature, and water-to-glycerol feed ratio.

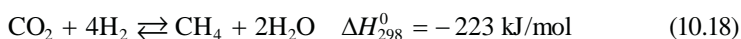
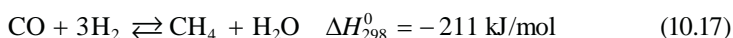
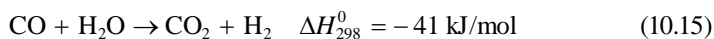
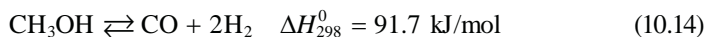
Most recently, Knoef [140] studied the reforming of glycerol over Ru/Al<sub>2</sub>O<sub>3</sub> catalyst in SCW conditions at a temperature range of 700°C–800°C, feed concentration up to 40 wt%, and reaction time less than 5 s. Under these conditions, glycerol was completely gasified to hydrogen, carbon dioxide, and methane along with a small amount of carbon monoxide. Xu and Antal [21,22], Antal and Xu (2012, pers. comm.), Xu et al. [129], and Antal et al. [144] showed that even in the absence of a catalyst glycerol decomposes in SCW to a hydrogen-rich gas, with almost no CO after 44 s at 600°C and 34.5 MPa. Higher temperature, more active reforming catalyst, and longer residence time result in higher gas and hydrogen productions.

#### 10.7.4 ETHYLENE GLYCOL

de Vlieger et al. [164] studied catalytic reforming of ethylene glycol (5 and 15 wt%) in SCW at 450°C and 250 atm pressure. The results were obtained for Pt, Ir, and Ni containing mono- and bimetallic catalysts. The best catalyst was found to be Pt–Ni/Al<sub>2</sub>O<sub>3</sub> having a metal loading of 1.5 wt% (Pt:Ni molar ratio of 1:1). With this catalyst, high hydrogen and carbon dioxide yields (selectivity of around 80%) were obtained by suppressing methanation reaction. The addition of Ni prevented sintering of Pt particles, thereby providing a stable performance by bimetallic catalysts. Ethylene glycol also produced more CH<sub>4</sub> and CO than what was produced in methanol reforming.

#### 10.7.5 METHANOL

Numerous studies have reported methanol reforming in SCW to produce hydrogen [158–160,170]. Compared to water that has a critical pressure of 22.1 MPa, a critical temperature of 374°C, and a critical density of 320 kg/m<sup>3</sup>, methanol has a lower critical temperature of 239°C, a critical pressure of 8.1 MPa, and a critical density of 270 kg/m<sup>3</sup>. Thus, reaction of methanol in SCW also implied that methanol is also under supercritical conditions. Methanol reforming can be described by five chemical reactions:

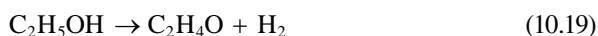


While both methanation reactions and water–gas shift reaction are exothermic, main methanol reforming reaction is endothermic and is favored at higher temperatures. Boukis et al. [158] showed that for reaction time as low as 4 s, at temperature of 600°C, and pressure of 25–45 MPa, high conversion rate of methanol can be obtained. The reaction can occur at temperature as low as 400°C. The heavy metal of the inner surface of Inconel 625 can influence the conversion and the product composition of the reforming reaction. Boukis et al. [158] examined the feed concentration from 5 to 64 wt% methanol. Methanol conversion up to 99.9% can be obtained in the absence of a catalyst. The major product is hydrogen (up to 70%–80%) with small amounts (<20%–30%) of carbon dioxide, carbon monoxide, and methane. An increase in temperature increases methanol conversion, decreases CO concentration, and increases CO<sub>2</sub> concentration in the product. Complete methanol conversion at 600°C is achieved [158].

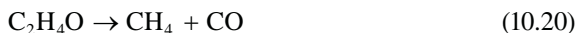
Taylor et al. [159] also examined reforming of methanol under SCW conditions in the temperature range of 550°C–700°C and at 27.6 MPa in an Inconel 625 reactor. They also reported a product rich in hydrogen and low in CH<sub>4</sub> and near the equilibrium ratio of CO and CO<sub>2</sub>. A comparison of the product gas composition with equilibrium predictions indicated that the reaction occurs in two steps. First methanol decomposes to CO and H<sub>2</sub> and subsequently CO is converted to CO<sub>2</sub> by water–gas shift reaction. Higher steam-to-carbon ratios gave lower CO in the product gas. Both methanol decomposition and water–gas shift reactions are kinetically limited at temperatures under 700°C. Also methanation reaction was kinetically limited. As shown by Gadhe and Gupta [160], high pressure favored the formation of methane.

### 10.7.6 ETHANOL

Wenzel [157] studied SCW reforming of ethanol under noncatalytic conditions for the temperature range of 618°C–710°C and pressure of 24.2 MPa [169]. The ethanol feed rate was varied from 0.17 to 2.2 g/min and water flow rate was varied from 6.4 to 19.7 g/min in a 1 l 625 grade 1 alloy tubular reactor. A complete conversion of ethanol was obtained producing hydrogen, carbon dioxide, methane, ethane, and carbon monoxide in the descending order of their concentrations. Hydrogen was produced by two competing reactions: the direct reformation of ethanol into hydrogen and carbon oxides and the pyrolytic dehydrogenation of ethanol:

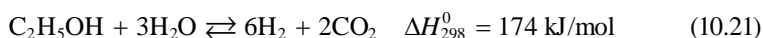


where acetaldehyde goes through further decarbonylation as



This decomposition is fast with Rh–cerium oxide catalyst at temperatures above 650°C. The net result of the above two reactions is to generate hydrogen, methane, and carbon oxides. In this system, forward water–gas shift reaction is active even without the presence of a water–gas shift catalyst. An undesirable competing reaction of dehydration of ethanol to form ethylene occurs, which is subsequently hydrogenated to form ethane. This reaction not only consumes hydrogen but also produces the coking precursor ethylene. Both pyrolytic and direct reforming reactions were first-order reactions.

Byrd et al. [177] studied supercritical reforming of ethanol over Ru/Al<sub>2</sub>O<sub>3</sub> catalyst. Experiments were conducted at various temperature, pressure, residence time, and water-to-carbon ratio to evaluate their effects on the hydrogen yield. The results showed that hydrogen formation was favored at high temperature and high water-to-ethanol ratios. Under the same conditions and for an optimum residence time, methane production was suppressed. Excellent conversions were obtained for the residence time as low as 4 s. Pressure had negligible effect on hydrogen yield above the critical pressure and there was negligible coke formation for ethanol concentration in the feed less than 10 wt%. The overall reforming reaction for ethanol can be expressed as

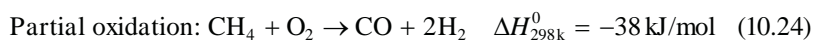
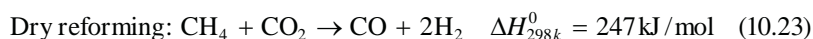
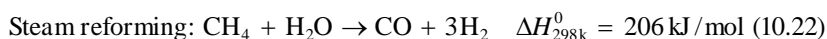


In the presence of Ru/Al<sub>2</sub>O<sub>3</sub> catalyst, high reforming performance may be due to the fact that intermediates formed during ethanol decomposition such as dimethyl ether and acetaldehyde were also gasified in the presence of SCW. In the subcritical steam gasification, formation of significant amount of carbon limits hydrogen production. Reaction products also contain acetaldehyde, diethyl ether, ethane, and ethylene. The gasification under supercritical conditions is accompanied by several complex reactions such as ethanol decomposition, steam reforming, water–gas shift reaction, and methanation reaction. The product distribution depended on the relative rates of these reactions. It was assumed that during reforming, ethanol dehydrogenates on the metal surface to give adsorbed intermediates before the cleavage of C–C and C–O bonds. The water–gas shift reaction reduces CO concentration, and the final products predominantly contain hydrogen and carbon dioxide.

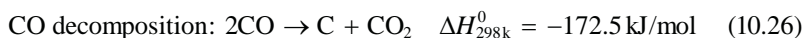
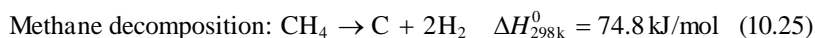
Gadhe and Gupta [160] examined the strategies for the reduction of methane formation and thereby increased the production of hydrogen. Three strategies that were examined were (1) operation at a low residence time by having a smaller reactor length or a high feed flow rate, (2) addition of a small amount of K<sub>2</sub>CO<sub>3</sub> or KOH in the feed, and (3) utilization of the surface catalytic activity of the reactor made of Ni–Cu alloy. All the three strategies worked, resulting in lower methane production and correspondingly higher hydrogen production. The methanation reactions were favored by high pressure, high residence time, and low steam-to-carbon ratio.

## 10.8 TRI-REFORMING IN SCW

Fundamentally, there are three types of high-temperature reforming processes: stream reforming, dry reforming, and partial oxidation [170–176]. The term “tri-reforming” is applied to the process in which all of these reforming processes are combined in a single use. The three reforming processes are expressed by the following set of chemical reactions:

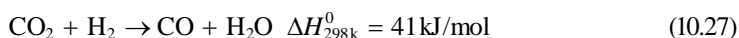


As mentioned above, the three reactions combined are called tri-reforming reactions. It has been established that nickel, cobalt, iron, and the platinum group metals can catalyze steam reforming reaction to the thermodynamic equilibrium. However, the nickel catalyst has emerged as the most practical catalyst because of its fast turnover rates, long-term stability, and cost. The major technical problem for the nickel catalysts is carbon deposition on the catalysts via the following reactions that can lead to rapid deactivation and breakup of the catalyst:



Carbon deposition can be substantially reduced by the use of an excess of water and a temperature of about 800°C. Other drawbacks of stream reforming are as follows:

1. Expensive generation of superheated steam (in excess) at high temperature
2. The production of a significant amount of CO<sub>2</sub> in the product gas via the reverse water–gas shift reaction, that is,  
Reverse water–gas shift reaction:

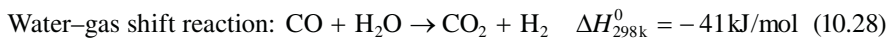


3. The H<sub>2</sub>-to-CO ratio is higher than the optimum required for the down-stream synthesis gas conversion to methanol, acetic acid, or hydrocarbons

Partial oxidation offers some advantages over steam reforming. First, the reaction produces extremely high yields of syngas by an exothermic reaction, and, therefore, the reactor would be more economical to heat. Oxygen is often used in steam reforming to provide heat and high methane conversion. Second, partial oxidation also gives a better ratio of hydrogen to carbon monoxide for subsequent conversion processes. Third, the product gases from the reaction are low in carbon dioxide that must often be removed before the syngas can be used.

Steam reforming and partial oxidation produce syngas. The dry reforming has an added advantage that it simultaneously consumes two greenhouse gases:

hydrocarbons, and  $\text{CO}_2$ . The best reducing agent for  $\text{CO}_2$  is hydrogen. As shown by Rozovskii et al. [170], the synthesis of methanol from  $\text{CO}$  and  $\text{H}_2$  proceeds not by their direct interaction, but by the transformation of  $\text{CO}$  into  $\text{CO}_2$ :



Direct utilization of the last reaction meets opposition because it converts expensive hydrogen into inexpensive water. Thus, a  $\text{CO}_2$  reduction by hydrocarbons is preferred with lower hydrocarbons and alcohols. While dry reforming of hydrocarbons converts carbon dioxide and hydrocarbons into useful syngas, the tri-reforming allows the process to produce the syngas with a variety of  $\text{H}_2/\text{CO}$  ratios.

The  $\text{H}_2/\text{CO}$  ratio in syngas is very important for its further use for a variety of chemical products. Syngas can be converted to acetone, acetic acid, and ethylene by an exothermic reaction, while pure  $\text{CO}$  can be used for the production of acetic acid, formic acid, polyurethane, polycarbonates, methyl acrylates, and so on. A  $\text{H}_2/\text{CO}$  ratio of about 1 is required for the productions of polycarbonates, oxo alcohol, formaldehyde, iron ore reduction reaction, and so on; a  $\text{H}_2/\text{CO}$  ratio of about 2 is required for methanol and Fischer–Tropsch (FT) synthesis, and a  $\text{H}_2/\text{CO}$  ratio of 3 or higher is required for ammonia synthesis and hydrogen production.

Tri-reforming also offers some other advantages. Since dry and steam reforming reactions are highly endothermic, a careful integration of these reactions into any process scheme that internally generates heat (like partial oxidation) is very important in order to make the overall process energy balance more efficient, thus avoiding the need for expensive external heating. Both dry and steam reforming reactions require very high temperatures ( $>600^\circ\text{C}$ ) to reduce the cooking. While steam reduces carbon deposition, an addition of oxygen provides the necessary heat that can jump-start dry and steam reforming reactions and maintain the catalyst in a clean and carbon-free state through oxidation of coke on the catalyst surface. The extent to which oxygenates are added to the reforming reactions is determined strictly by the process conditions and the catalyst employed. While the combination of dry reforming and partial oxidation has been studied by a number of investigators [170–176], these studies have been largely restricted to one or two hydrocarbons. Since dry reforming produces water, the steam reforming always accompanies dry reforming, making these studies relevant for tri-reforming.

The most extensive study of tri-reforming was carried out by Puolakka et al. [172] and Puolakka [173]. The study focused on the tri-reforming of five model compounds—methane, heptanes, *n*-dodecane, toluene, and ethanol—over a number of different catalysts. It was reported that 0.25% Rh on  $\text{ZrO}_2$  catalyst gave the best results, and its performance was comparable to the results for commercial Ni catalyst. The five model compounds were chosen to represent different types of fossil/biofuels. Methane was chosen to represent natural gas, *n*-heptane to represent aliphatic component of gasoline, *n*-dodecane to represent aliphatic component of biodiesel, toluene to represent aromatic part of gasoline, and diesel oil and ethanol to represent oxygenated compounds in biofuel.

The use of SCW as reaction medium for conducting the reforming can be an attractive and novel method. The literature on gasification/reforming under SCW

indicates that in general, SCW reduces coking, lowers the required temperature for the same level of conversion, and modifies the product distribution, particularly in favor of more production of hydrogen. These results imply the need for a study of tri-reforming under SCW (critical point 374°C and 22.1 MPa) conditions. It is expected that the supercritical conditions will bring about significant improvement on product distributions, reaction temperature severity, and catalyst activity, stability, and life. Under SCW gasification, syngas is produced directly at high pressure, which means that a smaller reactor volume and lower energy are needed to pressurize the gas in a storage tank.

While tri-reforming of methane in SCW has been investigated by a number of researchers [171–176], these studies have been carried out with conventional Ni or bimetallic catalysts. The studies have shown that the supercritical conditions lower the required temperature for gasification, and at high temperatures (>600°C), hydrogen and carbon dioxide are the dominating products. The studies [171–176] have also shown that the product composition from tri-reforming under supercritical conditions depends on a number of variables such as temperature, pressure, feedstock and oxygen concentrations, reaction time, biomass properties, presence of inorganic elements, biomass particle size, and the nature of the catalyst. In the SCW environment, the syngas composition will heavily depend on the effectiveness of the dry reforming reaction. More catalytic studies to improve dry reforming reaction are presently being pursued. The use of nanocatalysts is also very heavily examined. In future, more work on tri-reforming in SCW environment with practical feedstock needs to be carried out.

## REFERENCES

1. Gullon, P., Conde, E., Moure, A., Dominguez, H., and Parajo, J., "Selected process alternatives for biomass refining: A review," *The Open Agriculture Journal*, 4, 135–144 (2010).
2. Demirbas, A., "Biorefineries: Current activities and future developments," *Energy Conversion and Management*, 50, 2782–2801 (2009).
3. Demirbas, A., "Sub and supercritical water depolymerization of biomass," *Energy Sources, Part A*, 32, 1100–1110 (2010).
4. Peterson, A., Vogel, F., Lachance, R., Froling, M., Antal, M., and Tester, J., "Thermochemical biofuel production in hydrothermal media: A review of sub- and supercritical technologies," *Energy & Environmental Science*, 1, 32–65 (2008).
5. Azadi, P. and Farnood, R., "Review of heterogeneous catalysts for sub- and supercritical water gasification of biomass and wastes," *International Journal of Hydrogen Energy*, 36, 9529–9541 (2011).
6. Demirbas, A., "Progress and recent trends in biofuels," *Progress in Energy and Combustion Science*, 33, 1–18 (2007).
7. Tanksale, A., Beltramini, J., and Lu, G., "A review of catalytic hydrogen production processes from biomass," *Renewable & Sustainable Energy Reviews*, 14, 166–182 (2010).
8. Huber, G., Iborra, S., and Corma, A., "Synthesis of transportation fuels from biomass: Chemistry, catalysts and engineering," *Chemical Reviews*, 106, 1–51 (2006).
9. Subramaniam, B. and McHugh, M., "Reactions in supercritical fluids: A review," *Industrial & Engineering Chemistry Process Design and Development*, 25, 1–12 (1986).
10. Brunner, G., "Applications of supercritical fluids," *Annual Review of Chemical and Biomolecular Engineering*, 1, 1321–1342 (2010).
11. Savage, P., "Organic chemical reactions in supercritical water," *Chemical Reviews*, 99, 603–621 (1999).

12. Watanabe, M., Sato, T., Inomata, H., Smith, R.L., Jr., Arai, K., Kruse, A., and Dinjus, E., "Chemical reactions of C1 compounds in near-critical and supercritical water," *Chemical Reviews*, 104, 5803–5820 (2004).
13. Matsumura, Y., Sasaki, M., Okuda, K., Takami, S., Ohara, S., Umetsu, M., and Adschiri, T., "Supercritical water treatment of biomass for energy and material recovery," *Combustion Science and Technology*, 178, 509–536 (2006).
14. Modell, M., "Processing methods for the oxidation of organics in supercritical water," Patent No. 4338199 (July 6, 1982).
15. Ding, Z., Frisch, M., Li, L., and Gloyna, E., "Catalytic oxidation in supercritical water," *Industrial & Engineering Chemistry Research*, 35, 3257–3279 (1996).
16. Parsons, E., "Organic reactions in very hot water," *Chemtech*, 26 (6), 30–34 (1996).
17. Katritzky, A., Allin, S., and Siskin, M., *American Chemical Society*, 29 (8), 399–406 (1996).
18. An, J., Bagnell, L., Cablewski, T., Strauss, C., and Trainer, R., *Journal of Organic Chemistry*, 62 (8), 2505–2511 (1997).
19. Leif, R.N. and Simoneit, B., *Origins of Life and Evolution of the Biosphere*, 25, 119–140 (1995).
20. Chandler, K., Deng, F., Dillow, A., Liotta, C., and Eckert, C., *Industrial & Engineering Chemistry Research*, 36 (12), 5175–5179 (1997).
21. Xu, X. and Antal, M., *AIChE Journal*, 40 (9), 1524–1531 (1994).
22. Xu, X. and Antal, M., *Industrial & Engineering Chemistry Research*, 36 (1), 23–41 (1997).
23. Crittendon, R. and Parsons, E., *Organometallics*, 13 (7), 2587–2591 (1994).
24. Duminnie, J., Metts, S., and Parsons, E., *Organometallics*, 14 (8), 4023–4025 (1995).
25. Kuhlmann, B., Arnett, E., and Siskin, M., *Journal of Organic Chemistry*, 59 (11), 3098–3101 (1994).
26. Savage, P., Li, R., and Santini J., *The Journal of Supercritical Fluids*, 7 (2), 135–144 (1994).
27. Lee, J. and Foster, N., *The Journal of Supercritical Fluids*, 9 (2), 99–105 (1996).
28. Aki, S. and Abraham, M., *The Journal of Supercritical Fluids*, 7 (4), 259–263 (1994).
29. Hong, G. and Spritzer, M., "Supercritical water partial oxidation," *Proceedings of the 2002 US DOE Hydrogen Energy Program Review*, General Atomics, San Diego, CA, NREL/CP-610-32405, Golden, CO (2002).
30. Johanson, N., Spritzer, M., Hong, G., and Rickman, W., "Supercritical water partial oxidation," *Proceedings of the 2001 DOE Hydrogen Program Review*, General Atomics, San Diego, CA, NREL/CP-570-30535, Golden, CO (2001).
31. Vogel, F., DiNaro-Blanchard, J., Marrone, P., Rice, S., Webley, P., Peters, W., Smith, K., and Tester, J., "Critical review of kinetic data for the oxidation of methanol in supercritical water," *The Journal of Supercritical Fluids*, 34, 249–286 (2005).
32. Spritzer, M., "Supercritical water partial oxidation," *Hydrogen Fuel Cells and Infrastructure Technologies*, DOE progress report, General Atomics, San Diego, CA (2003).
33. Sato, T., Adschiri, T., Arai, K., Rempel, G., and Ng, F., "Upgrading of asphalt with and without partial oxidation in supercritical water," *Fuel*, 82 (10), 1231–1240 (2003).
34. Youssef, E., Elbeshbishy, E., Hafez, H., Nakhia, G., and Charpentier, P., "Sequential supercritical water gasification and partial oxidation of hog manure," *International Journal of Hydrogen Energy*, 35 (21), 11756–11767 (2010).
35. Gloyna, E. and Li, L., "Supercritical water oxidation: An engineering update," *Waste Management*, 13, 379 (1993).
36. Gloyna, E. and Li, L., "Supercritical water oxidation research and development update," *Environmental Progress*, 14, 182 (1995).
37. Jin, F.M., Ausushi, K., and Heiji, E., "Oxidation of garbage in supercritical water," *High Pressure Research*, 20, 525–531 (2001).
38. Goto, M., Nada, T., Ogata, A., Kodama, A., and Hirose, T., "Supercritical water oxidation for the destruction of municipal excess sludge and alcohol distillery wastewater of molasses," *The Journal of Supercritical Fluids*, 13, 277–282 (1998).

39. Noam, E. and Ronald, M.L., "Review of materials issues in supercritical water oxidation systems and the need for corrosion control," *Transactions of the Indian Institute of Metals*, 56, 1–10 (2003).
40. Takuya, Y. and Yoshito, O., "Partial oxidative and catalytic biomass gasification in supercritical water: A promising flow reactor system," *Industrial & Engineering Chemistry Research*, 43, 4097–4104 (2004).
41. Watanabe, M., Inomata, H., Osada, M., Sato, T., Adschiri, T., and Arai, K., "Catalytic effects of NaOH and ZrO<sub>2</sub> for partial oxidative gasification of *n*-hexadecane and lignin in supercritical water," *Fuel*, 82 (5), 545–552 (2003).
42. Watanabe, M., Inomata, H., Osada, M., Sato, T., Adschiri, T., and Arai, K., "Partial oxidation of *n*-hexadecane and polyethylene in supercritical water," *The Journal of Supercritical Fluids*, 20 (3), 257–266 (2001).
43. Oka, H., Yamago, S., Yoshida, J., and Kajimoto, O., "Evidence for a hydroxide ion catalyzed pathway in ester hydrolysis in supercritical water," *Angewandte Chemie International Edition*, 41, 623–625 (2002).
44. Jin, F.M., Takehiko, M., and Heiji, E., "Oxidation reaction of high molecular weight carboxylic acids in supercritical water," *Environmental Science & Technology*, 37, 3220–3231 (2003).
45. Shamsi, A., "Partial oxidation and dry reforming of methane over Ca/Ni/K (Na) catalysts," *Catalysis Letters*, 109 (3/4), 189–193 (2006).
46. Krietemeyer, S. and Wagner, T., *Supercritical Water Oxidation*. Risk Reduction Engineering Laboratory, Cincinnati, OH (1992).
47. Modell, M., "Supercritical water oxidation," in Freeman, H. (ed.), *Standard Handbook of Hazardous Waste Treatment and Disposal*. McGraw-Hill, New York (1989).
48. Tester, J., Holgate, H., Amellini, F., Webley, P., Killilea, W., Hong, G., and Barner, H., "Supercritical water oxidation technology: Process development and fundamental research," in Tedder, D. and Pohland, F. (eds.), *Emerging Technologies in Hazardous Waste Management III*. American Chemical Society, Washington, DC (1993).
49. McBrayer, R., "Design and operation of first commercial supercritical water oxidation facility," *First International Workshop on Supercritical Water Oxidation*, Jacksonville, FL, February 6–9 (1995).
50. Lourdes, C. and David, V., "Formation of organic acids during the hydrolysis and oxidation of several wastes in sub- and supercritical water," *Industrial & Engineering Chemistry Research*, 41, 6503–6509 (2002).
51. Hodes, M., Marrone, P.A., Hong, G.T., Smith, K.A., and Tester, J.W., "Salt precipitation and scale control in supercritical water oxidation—Part A: Fundamentals and research," *The Journal of Supercritical Fluids*, 29, 265–288 (2004).
52. Svensson, P., "Look no stack, supercritical water destroys organic wastes," *Chemical Technology Europe*, 2, 16 (1995).
53. Savage, P., Gopalan, S., Mizan, T., Martino, C., and Brock, E., "Reactions in supercritical conditions: Application and fundamentals," *AIChE Journal*, 41, 1723 (1995a).
54. Savage, P., Gopalan, S., Mizan, T., Martino, C., and Brock, E., "Oxidation in supercritical water: Pathways, kinetics and mechanisms," *First International Workshop on Supercritical Water Oxidation*, Jacksonville, FL February 6–9 (1995).
55. Watanabe, M., Adschiri, T., and Arai, K., "Polyethylene decomposition via pyrolysis and partial oxidation in supercritical water," *Kobunshi Ronbunshu*, 58 (12), 631 (2001) (Japanese).
56. Lilac, W. and Lee, S., "Kinetics and mechanisms of styrene monomer recovery from waste polystyrene by supercritical water partial oxidation," *Advances in Environmental Research*, 6 (1), 9–16 (2001).

57. Peter, K. and Eckhard, D., "An assessment of supercritical water oxidation (SCWO): Existing problems, possible solutions and new reactor concepts," *Chemical Engineering Journal*, 83, 207–214 (2001).
58. Li, R., Savage, P., and Szmukler, D., "2-Chlorophenol oxidation in supercritical water: Global kinetics and reaction products," *AIChE Journal*, 39 (1), 178–187 (1993).
59. Thomason, T., Hong, G., Swallow, K., and Killilea, W., "The MODAR supercritical water oxidation process," in Freeman, H. (ed.), *Innovative Hazardous Waste Treatments Technology Series*. Technomic Publishing Co., Lancaster, PA (1990).
60. Wantanabe, M., Sato, T., Inomata, H., Smith, R., Arai, K., Kruse, A., and Dinjus, E., "Chemical reactions of C1 compounds in near critical and supercritical water," *Chemical Reviews*, 104, 5803–5821 (2004).
61. Watanabe, M., Hirakoso, H., Sawamoto, S., Adschiri, T., and Arai, K., *The Journal of Supercritical Fluids*, 13, 247–252 (1998).
62. Stiles, A., *Catalyst Manufacture*. Marcel Dekker, New York (1983).
63. Attia, Y., *Sol-Gel Processing and Applications*. Plenum Press, New York (1994).
64. Messing, G., Zhang, S., and Yayanthi, G., "Ceramic powder synthesis by spray pyrolysis," *Journal of the American Ceramic Society*, 76, 2707 (1993).
65. Moser, W., "Hydrocarbon partial oxidation catalysts prepared by the high temperature aerosol decomposition process: Crystal and catalytic chemistry," in Oyama, T. and Hightower, J. (eds.), *Catalytic Selective Oxidation*. American Chemical Society, Washington, DC, 244 (1993).
66. Nanjangud, S., Brezny, R., and Green, D., "Strength and Young's modulus behavior of a partially sintered porous alumina," *Journal of the American Ceramic Society*, 78, 266 (1995).
67. Pugh, R. and Bergstrom, L. (eds.), *Surface and Colloid Chemistry in Advanced Ceramic Processing*. Marcel Dekker, New York (1994).
68. Saggio-Woyansky, J., Scott, C., and Minnear, W., "Processing of porous ceramics," *American Ceramic Society Bulletin*, 72, 1674 (1992).
69. Segal, D., *Chemical Synthesis of Advanced Ceramic Materials*. Cambridge University Press, New York (1983).
70. Vincenzini, P., *Ceramic Powders: Preparation, Consolidation and Sintering*. Elsevier Scientific Publishing Co., New York (1993).
71. Ward, D. and Ko, E., "Preparing catalyst materials by sol-gel method," *Industrial & Engineering Chemistry Research*, 34, 421 (1995).
72. Wold, A. and Dwight, K., *Solid State Chemistry, Synthesis, Structure, and Properties of Selected Oxides and Sulfides*. Chapman & Hill, New York (1993).
73. Deshpande, G., Holder, G., Bishop, A., Gopal, J., and Wender, I., *Fuel*, 63, 956 (1984).
74. Pauliat, M., Penninger, R., Gray, D., and Davidson, P. (eds.), *Chemical Engineering at Supercritical Fluid Conditions*. Ann Arbor Science Publishers, Ann Arbor, MI, 385–407 (1983).
75. Modell, M., Reid, R., and Amin, S., "Gasification process," US Patent No. 4113446 (September 12, 1978).
76. Jezko, J., Gray, D., and Kershaw, J., *Fuel Processing Technology*, 5, 229 (1982).
77. Vasilakos, N., Dobbs, J., and Parasi, A., *American Chemical Society Division of Fuel Chemistry*, preprints, 28 (4), 212 (1983).
78. Kershaw, J. and Bagnell, L., "Extraction of Australian coals with supercritical water," *ACS Reprints*, 101–111 (1988).
79. Minowa, T., Zhen, F., and Ogi, T., "Cellulose decomposition in hot-compressed water with alkali or nickel catalyst," *The Journal of Supercritical Fluids*, 13, 253–259 (1998).
80. Sasaki, M., Kabyemela, B., Malaluan, R., Hirose, S., Takeda, N., Adschiri, T., and Arai, K., "Cellulose hydrolysis in sub-critical and super-critical water," *The Journal of Supercritical Fluids*, 13, 261–268 (1998).

81. Sasaki, M., Fang, Z., Fukushima, Y., Adschiri, T., and Arai, K., "Dissolution and hydrolysis of cellulose in sub-critical and supercritical water," *Industrial & Engineering Chemistry Research*, 39, 2883–2890 (2000).
82. Wahyudiono, Shiraishi, T., Sasaki, M., and Goto, M., "Non catalytic liquefaction of bitumen with hydrothermal/solvothermal process," *The Journal of Supercritical Fluids*, 60, 127–136 (2011).
83. Cheng, L., Zhang, R., and Bi, J., "Pyrolysis of a low rank coal in sub and supercritical water," *Fuel Processing Technology*, 85 (8–10), 921–932 (2004).
84. Vostrikov, A., Psarov, S., Dubov, D., Fedyaeva, O., and Sokol, M., "Kinetics of coal conversion in supercritical water," *Energy & Fuels*, 21, 2840–2845 (2007).
85. Kumar, S. and Gupta, R., "Biocrude production from switchgrass using supercritical water," *Energy & Fuels*, 23, 5151–5159 (2009).
86. Kim, I.C., Park, S.D., and Kim, S., "Effects of sulfates on the decomposition of cellobiose in supercritical water," *Chemical Engineering Process*, 43, 997–1005 (2004).
87. Mitsubishi Material Corp., "Supercritical water cracks residue oil," *Chemical Engineering*, 14 (September 2007).
88. Ayhan, D., "Hydrogen-rich gas from fruit shells via supercritical water extraction," *International Journal of Hydrogen Energy*, 29, 1237–1243 (2004).
89. Nonaka, H., "Development of liquefaction process of coal and biomass in supercritical water," *Fuel and Energy Abstracts*, 39 (1), 18 (1998).
90. Matsumura, Y., Nonaka, H., Yokura, H., Tsutsumi, A., and Yoshida, K., "Co-liquefaction of coal and cellulose in supercritical water," *Fuel*, 78 (9), 1049–1056 (1999).
91. Demirbas, A., "Hydrogen production from biomass via supercritical water extraction," *Energy Sources*, 27, 1409–1417 (2005).
92. Phillip, E., "Organic chemical reactions in supercritical water," *Chemical Reviews*, 99, 603–621 (1999).
93. Duan, P. and Savage, P., "Upgrading of crude algal bio oil in supercritical water," *Bioresource Technology*, 102 (2), 1899–1906 (2011).
94. Duan, P. and Savage, P., "Catalytic hydrotreatment of crude algal bio-oil in supercritical water," *Applied Catalysis B: Environmental*, 104 (1/2), 136–143 (2011).
95. Onsari, K., Prasassarakich, P., and Ngamprasertsith, S., "Co-liquefaction of coal and used tire in supercritical water," *Energy and Power Engineering*, 2, 95–102 (2010).
96. Sunphorka, S., Prasassarakich, P., and Ngamprasertsith, S., "Co-liquefaction of coal and plastic mixture in supercritical water," The 5th Mathematics and Physical Sciences Graduate Congress, Chulalongkorn University, Thailand, December 7–9, 2009 (2011).
97. Nonaka, H., Matsumura, Y., Tsutsumi, A., Yoshida, K., Matsuno, Y., and Inaba, A., "Development of liquefaction process of coal and biomass in supercritical water," *Sekitan Kagaku Kaigi Happyo Ronbunshu*, 33, 73–76 (1996).
98. Veski, R., Palu, V., and Kruusement, K., "Co-liquefaction of kukersite oil shale and pine wood in supercritical water," *Oil Shale*, 23 (3), 236–248 (2006).
99. Yokura, H., Nonaka, H., Matsumura, Y., Tsutsumi, A., and Yoshida, K., "Effect of catalyst addition on co-liquefaction process of coal and biomass in supercritical water," *Sekitan Kagaku Kaigi Happyo Ronbunshu*, 34, 69–72 (1997).
100. Missal, P. and Hedden, K., "Extraction of a Colorado oil shale by water in the sub- and supercritical phases," *Erdoel & Kohle, Erdgas, Petrochemie*, 42 (9), 346–352 (1989).
101. Funazukuri, T., Yokoi, S., and Wasao, N., "Supercritical fluid extraction of Chinese Maoming oil shale with water and toluene," *Fuel*, 67 (1), 10–14 (1988).
102. Hu, H., Zhang, J., Guo, S., and Chen, G., "Extraction of Huadian oil shale with water in sub- and supercritical states," *Fuel*, 78 (6), 645–651 (1999).
103. Canel, M. and Missal, P., "Extraction of solid fuels with sub- and supercritical water," *Fuel*, 73 (11), 1776–1780 (1994).

104. Johnson, D.K., Chum, H.L., Anzick, R., and Baldwin, R.M., "Lignin liquefaction in supercritical water," in Bridgwater, A.V. and Kuester, J.L. (eds.), *Research in Thermochemical Biomass Conversion*. Elsevier, London, 485–496 (1988).
105. Palu, V., Kruusement, K., and Veski, R. "Supercritical water extraction of biomass and oil shale," 29th Estonian Chemistry Days, Tallinn, Estonia, 77 (2005).
106. Li, L. and Eglebor, N., "Oxygen removal from coal during supercritical water and toluene extraction," *Energy & Fuels*, 6 (1), 35–40 (1992).
107. Chen, D., Perman, C., Riechert, M., and Hoven, J., "Depolymerization of tire and natural rubber using supercritical fluids," *Journal of Hazardous Materials*, 44, 53–60 (1995).
108. Park, S. and Gloyna, E., "Statistical study of the liquefaction of used rubber tyre in supercritical water," *Fuel*, 76 (11), 999–1003 (1997).
109. Su, X., Zhao, Y., Zhang, R., and Bi, J., "Investigation on degradation of polyethylene to oils in supercritical water," *Fuel Processing Technology*, 85, 1249–1258 (2004).
110. Moriya, T. and Enomoto, H., "Investigation of the basic hydrothermal cracking conditions of polyethylene in supercritical water," *Shigen to Sozai*, 115, 245 (1999) (Japanese).
111. Matsubara, W. et al., "Development of liquefaction process of plastic waste in supercritical water," *Mitsubishi Juko Giho*, 34, 438 (1997) (Japanese).
112. Broll, D., Kaul, C., Kramer, A., Krammer, P., Richter, T., Jung, M., Vogel, H., and Zehner, P., "Chemistry in supercritical water," *Angewandte Chemie International Edition*, 38, 2998 (1999).
113. Moriya, T. and Enomoto, H., "Characteristics of polyethylene cracking in supercritical water compared to thermal cracking," *Polymer Degradation and Stability*, 65, 373 (1999).
114. Moriya, T. and Enomoto, H., "Role of water in conversion of polyethylene to oils through supercritical water cracking," *Kagaku Kogaku Ronbunshu*, 25 (6), 940 (1999) (Japanese).
115. Holliday, R., King, J., and List, G., "Hydrolysis of vegetable oils in sub- and supercritical water," *Industrial & Engineering Chemistry Research*, 36 (3), 932–935 (1997).
116. Li, Y., Guo, L., and Zhang, X., "Hydrogen production from coal gasification in supercritical water with a continuous flowing system," *International Journal of Hydrogen Energy*, 35, 3036–3045 (2010).
117. Lee, S. and Shah, Y., *Biofuels and Bioenergy—Processes and Technologies*. CRC Press, New York (2012).
118. May, A., Salvado, J., Torras, C., and Montane, D., "Catalytic gasification of glycerol in supercritical water," *Chemical Engineering Journal*, 160 (2), 751–759 (2010).
119. Osada, M., Sato, T., Watanabe, M., Shirai, M., and Arai, K., "Catalytic gasification of wood biomass in subcritical and supercritical water," *Combustion Science and Technology*, 178 (1–3), 537–552 (2006).
120. Yu, D., Aihara, M., and Antal, M., "Hydrogen production by steam reforming glucose in supercritical water," *Energy & Fuels*, 7 (5), 574–577 (1993).
121. D'Jesus, P., Boukis, N., Kraushaar-Czarnetzki, B., and Dinjus, E., "Gasification of corn and clover grass in supercritical water," *Fuel*, 85, 1032–1038 (2006).
122. Pinkwart, K., Bayha, T., Lutter, W., and Krausa, M., "Gasification of diesel oil in supercritical water for fuel cells," *Journal of Power Sources*, 136, 211–214 (2004).
123. Yamaguchi, A., Hiyoshi, N., Sato, O., Osada, M., and Shirai, M., "EXAFS study on structural change of charcoal-supported ruthenium catalysts during lignin gasification in supercritical water," *Catalysis Letters*, 122, 188–195 (2008).
124. Byrd, A., Kumar, S., Kong, L., Ramsurn, H., and Gupta, R., "Hydrogen production from catalytic gasification of switchgrass biocrude in supercritical water," *International Journal of Hydrogen Energy*, 36, 3426–3433 (2011).
125. Sato, T., Osada, M., Watanabe, M., Shirai, M., and Arai, K., "Gasification of alkylphenols with supported noble metal catalysts in supercritical water," *Industrial & Engineering Chemistry Research*, 42, 4277–4282 (2003).

126. Takuya, Y. and Yukihiro, M., "Gasification of cellulose, xylan, and lignin mixtures in supercritical water," *Industrial & Engineering Chemistry Research*, 40, 5469–5474 (2001).
127. Takuya, Y., Yoshito, O., and Yukihiro M., "Gasification of biomass model compounds and real biomass in supercritical water," *Biomass & Bioenergy*, 26, 71–78 (2004).
128. Tang, H.Q. and Kuniyuki, K., "Supercritical water gasification of biomass: Thermodynamic analysis with direct Gibbs free energy minimization," *Chemical Engineering Journal*, 106, 261–267 (2005).
129. Xu, X., Matsumura, Y., Stenberg, J., and Antal, M.J., Jr., "Carbon-catalyzed gasification of organic feedstocks in supercritical water," *Industrial & Engineering Chemistry Research*, 35, 2522–2530 (1996).
130. Guo, L., Cao, C., and Lu, Y., "Supercritical water gasification of biomass and organic wastes," in Momba, M. and Bux, F. (eds.), *Biomass*. 165–182 (2010).
131. Demirbas, A., "Hydrogen production from biomass via supercritical water gasification," *Energy Sources, Part A*, 32, 1342–1354 (2010).
132. Kruse, A., "Supercritical water gasification," *Biofuels, Bioproducts and Biorefining*, 2, 415–437 (2008).
133. Lu, Y., Guo, L., Zhang, X., and Yan, Q., "Thermodynamic modeling and analysis of biomass gasification for hydrogen production in supercritical water," *Chemical Engineering Journal*, 131, 233–244 (2007).
134. Zhang, L., Champagne, P., and Xu, C., "Supercritical water gasification of an aqueous by-product from biomass hydrothermal liquefaction with novel Ru modified Ni catalysts," *Bioresour. Technology*, 102 (17), 8279–8287 (2011).
135. Michael, J.A., Jr., Allen, S.G., Schulman, D., and Xu, X., "Biomass gasification in supercritical water," *Industrial & Engineering Chemistry Research*, 39, 4040–4053 (2000).
136. Paul, T.W. and Jude, O., "Composition of products from the supercritical water gasification of glucose: A model biomass compound," *Industrial & Engineering Chemistry Research*, 44, 8739–8749 (2005).
137. Peter, K., "Corrosion in high-temperature and supercritical water and aqueous solutions: A review," *The Journal of Supercritical Fluids*, 29, 1–29 (2004).
138. Yamaguchi, A., Hiyoshi, N., Sato, O., Bando, K., Osada, M., and Shirai, M., "Hydrogen production from woody biomass over supported metal catalysts in supercritical water," *Catalysis Today*, 146, 192–195 (2009).
139. Guo, Y., Wang, S., Xu, D., Gong, Y., Ma, H., and Tang, X., "Review of catalytic supercritical water gasification for hydrogen production from biomass," *Renewable & Sustainable Energy Reviews*, 14, 334–343 (2010).
140. Knoef, H., *Handbook Biomass Gasification*. Biomass Technology Group Press, Enschede, the Netherlands, 22–23 (2005).
141. Kruse, A. and Gawlik, A., "Biomass conversion in water at 330°C–410°C and 30–50 MPa. identification of key compounds for indicating different chemical reaction pathways," *Industrial & Engineering Chemistry Research*, 42, 267–279 (2003).
142. Kruse, A. and Henningsen, T., "Biomass gasification in supercritical water: Influence of the dry matter content and the formation of phenols," *Industrial & Engineering Chemistry Research*, 42, 3711–3717 (2003).
143. Lee, I.G., Kim, M.S., and Ihm, S.K., "Gasification of glucose in supercritical water," *Industrial & Engineering Chemistry Research*, 41, 1182–1188 (2002).
144. Antal, M., Allen, S., Schulman, D., and Xu, X., "Biomass gasification in supercritical water," *Industrial & Engineering Chemistry Research*, 39, 4040–4053 (2000).
145. Kruse, A., Meier, D., Rimbrecht, P., and Schacht, M., "Gasification of pyrocatechol in supercritical water in the presence of potassium hydroxide," *Industrial & Engineering Chemistry Research*, 39, 4842–4848 (2000).

146. Hao, X.H., Guo, L.J., Mao, X., Zhang, X.M., and Chen, X.J., "Hydrogen production from glucose used as a model compound of biomass gasified in supercritical water," *International Journal of Hydrogen Energy*, 28, 55–64 (2003).
147. Tang, H. and Kitagawa, K., "Supercritical water gasification of biomass: Thermodynamic analysis with direct gibbs free energy minimization," *Chemical Engineering Journal*, 106 (3), 261–267 (2005).
148. Chakinala, A., Brilman, D., van Swaaij, W., and Kersten, S., "Catalytic and non catalytic supercritical water gasification of microalgae and glycerol," *Industrial & Engineering Chemistry Research*, 49 (3), 1113–1122 (2010).
149. Susanti, R., Nugroho, A., Lee, J., Kim, Y., and Kim, J., "Noncatalytic gasification of isooctane in supercritical water: A strategy for high-yield hydrogen production," *International Journal of Hydrogen Energy*, 36 (6), 3895–3906 (2011).
150. Goodwin, A. and Rorrer, G., "Conversion of glucose to hydrogen rich gas by supercritical water in a microchannel reactor," *Industrial & Engineering Chemistry Research*, 47 (12), 4106–4114 (2008).
151. Kong, L., Li, G., Zhang, B., He, W., and Wang, H., "Hydrogen production from biomass wastes by hydrothermal gasification," *Energy Sources, Part A*, 30, 1166–1178 (2008).
152. Sinag, A., Kruse, A., and Rathert, J., "Influence of the heating rate and the type of the catalyst on the formation of key intermediates and on the generation of gases during hydropyrolysis of glucose in supercritical water in a batch reactor," *Industrial & Engineering Chemistry Research*, 43, 502–508 (2004).
153. Kersten, S.R.A., Potic, B., Prins, W., and van Swaaij, W., "Gasification of model compounds and wood in hot compressed water," *Industrial & Engineering Chemistry Research*, 45, 4169–4177 (2006).
154. Lee, S., Lanterman, H., Wenzel, J., and Picou, J., "Noncatalytic reformation of JP-8 fuel in supercritical water for production of hydrogen," *Energy Sources, Part A: Recovery, Utilization, and Environmental*, 31 (19), 1750–1758 (2009).
155. Van Bennekom, J., Venderbosch, R., and Heeres, H., "Supermethanol: Reforming of crude glycerine in supercritical water to produce methanol for re-use in biodiesel plants," Report, University of Groningen, Groningen, the Netherlands (2011).
156. Vos, J., "Reforming of crude glycerine in supercritical water to produce methanol for re-use in biodiesel plants," Report, B.T.G. Biotechnology Group BV, Enschede, the Netherlands (2007).
157. Wenzel, J., "The kinetics of non-catalyzed supercritical water reforming of ethanol," PhD thesis, University of Missouri, Columbia, MO (May 2008).
158. Boukis, N., Diem, V., Habicht, W., and Dinjus, E., "Methanol reforming in supercritical water," *Industrial & Engineering Chemistry Research*, 42, 728–735 (2003).
159. Taylor, J., Herdman, C., Wu, B., Walley, K., and Rice, S., "Hydrogen production in a compact supercritical water reformer," *International Journal of Hydrogen Energy*, 28, 1171–1178 (2003).
160. Gadhe, J. and Gupta, R., "Hydrogen production by methanol reforming in supercritical water: Suppression of methane formation," *Industrial & Engineering Chemistry Research*, 44, 4577–4585 (2005).
161. Guerrero-Perez, M., Rosas, J., Bedia, J., Rodriguez-Mirosol, J., and Cordero, T., "Recent inventions in glycerol transformations and processing," *Recent Patents in Chemical Engineering*, 2, 11–21 (2009).
162. Huidong, W. and Renan, W., "Conversion and reforming of fossil fuel by supercritical water," *Chemical Industry and Engineering Progress*, 3, 1–7 (1999).
163. Ramaswamy, K. and T-Raissi, A., "Hydrogen production from used lube oil via supercritical water reformation," Report, Florida Solar Energy Center, Cocoa, FL (2010).

164. de Vlieger, D., Chakinala, A., Lefferts, L., Kersten, S., Seshan, K., and Brilman, D., "Hydrogen from ethylene glycol by supercritical water reforming using noble and base metal catalysts," *Applied Catalysis B: Environmental*, 111–112, 536–544 (2012).
165. Yamaguchi, A., Hiyoshi, N., Sato, O., Bando, K., Osada, M., and Shirai, M., "Hydrogen production from woody biomass over supported metal catalysts in supercritical water," *Catalysis Today*, 146 (1/2), 192–195 (2009).
166. Byrd, A., Pant, K., and Gupta, R., "Hydrogen production from glycerol by reforming in supercritical water over Ru/Al<sub>2</sub>O<sub>3</sub> catalyst," *Fuel*, 87, 2956–2960 (2008).
167. Penninger, J.M.L., Maassa, G.J.J., and Rep, M., "Compressed hydrogen rich fuel gas (CHFG) from wet biomass by reforming in supercritical water," *International Journal of Hydrogen Energy*, 32 (10/11), 1472–1476 (2007).
168. Penninger, J. and Rep., M., "Reforming of aqueous wood pyrolysis condensate in supercritical water," *International Journal of Hydrogen Energy*, 31 (11), 1597–1606 (2006).
169. Therdthianwong, S., Srisinwat, N., Therdthianwong, A., and Croiset, E., "Reforming of bioethanol over Ni/Al<sub>2</sub>O<sub>3</sub> and Ni/CeZrO catalysts in supercritical water for hydrogen production," *International Journal of Hydrogen Energy*, 36 (4), 2877–2886 (2011).
170. Rozovskii, A.Ya. and Lin, G.I., *Theoretical Basis of Methanol Synthesis*, Khimiya, Moscow, 1990.
171. Shekhawat, D., Berry, D., Gardner, T., and Spivey, J., "Catalytic reforming of liquid hydrocarbon fuels for fuel cell applications," *Catalysis*, 19, 184 (2006).
172. Puolakka, K.J., Juutilainen, S., and Krause, A.O.I., "Combined CO<sub>2</sub> reforming and partial oxidation of n-heptane on noble metal zirconia catalysts," *Catalysis Today*, 115 (1–4), 217–221 (2006).
173. Puolakka, J., "CO<sub>2</sub> reforming," Thesis for the Degree of Licentiate of Science and Technology, University of Technology, Helsinki, Finland (2007).
174. Kang, J.S., Kim, D.H., Lee, S.D., Hong, S.I., and Moon, D.J., "Nickel-based tri-reforming catalyst for the production of synthesis gas," *Applied Catalysis A*, 332 (1), 153–158 (2007).
175. Antal, M.J., Jr., Manarungson, S., and Mok, W.S.-L., "Hydrogen production by steam reforming glucose in supercritical water," in Bridgewater, A.V. (ed.), *Advances in Thermochemical Biomass Conversion*. Blackie Academic & Professional, London, 1367–1377 (1994).
176. Shah, Y. and Gardner, T., "Dry reforming of hydrocarbon feedstocks," *Catalysis Review – Science and Engineering* (in press).
177. Byrd, A., Pant, K., and Gupta, R., "Hydrogen production from ethanol by reforming in supercritical water using Ru/Al<sub>2</sub>O<sub>3</sub> catalyst," *Energy & Fuels*, 21 (6), 3541–3547 (2007).



# Taylor & Francis

Taylor & Francis Group

<http://taylorandfrancis.com>

---

# 11 Water Dissociation Technologies for Hydrogen

## 11.1 INTRODUCTION

The dissociation of water to produce hydrogen reversibly requires a supply of energy as follows:



$$\Delta H_{289\text{K}}^0 = 241.93 \text{ kJ/mol}, \Delta G_{298\text{K}}^0 = 228.71 \text{ kJ/mol}, T\Delta S_{298\text{K}}^0 = 13.22 \text{ kJ/mol}$$

This means that work =  $\Delta G^0$  and heat =  $T\Delta S$  are required to split the water at 25°C and 1 atm. Here  $T$  is the temperature and  $\Delta S$  is the change in entropy.  $\Delta H$  and  $\Delta G$  are changes in heat of formation and free energy of formation. The superscript  $^0$  denotes standard conditions of 1 atm and 25°C. If the reaction does not proceed reversibly, more work is required. The energy needed for this work can be provided in a number of different ways, and these are evaluated in this chapter.

There are three major ways water can be dissociated to produce hydrogen. The first method is electrolysis in which the water is dissociated electrochemically using electrochemical cell. The cell can be operated in a number of different ways (such as high temperature and high pressure), but all of them require significant amount of energy to dissociate water. The second method is the use of photosynthesis and photocatalysis to dissociate water. This method also requires photonic energy with or without a catalyst. The energy can, however, be provided using a solar cell. The third method is thermal or thermochemical dissociation of water in which water is dissociated either thermally or thermochemically. The latter method uses a chemical substance (or substances) to carry out dissociation using a series of chemical reactions. This method not only separates hydrogen and oxygen upon dissociation, but also reduces the temperature required for the thermal dissociation. In the recent years, this method has been heavily explored. Besides these three major methods, some miscellaneous methods such as chemical oxidation, magmalysis, and radiolysis are also explored for water dissociation. All of these are briefly discussed in this chapter.

As discussed in earlier chapter 4, the use of solar energy in steam gasification, reforming, and solar cracking of fuels such as coal, biomass, and natural gas has been gaining more acceptance. Similarly, three major technologies—electrochemical, photochemical/photobiological, and thermochemical—for water dissociation can

also be carried with the use of solar energy. In electrochemical processes, solar electricity made from photovoltaic or concentrating solar thermal systems can be used for electrolytic process. In photochemical/photobiological processes, direct use of solar photon energy carries out photochemical and photobiological processes. Finally, in thermochemical processes, solar heat at high temperature supports endothermic thermochemical water dissociation reactions. While thermochemical route offers some intriguing thermodynamic advantages over other options, in general, irrespective of the type of fuel produced, higher temperature gives higher conversion efficiency but also leads to greater losses by reradiation from the solar cavity receiver. A summary of all the thermochemical processes described earlier to produce solar fuels such as hydrogen is given in Figure 11.1.

The recent report of the International Energy Agency (IEA) shows that a measure of how well solar energy is converted to chemical energy stored in solar fuels is called exergy efficiency (Figure 11.2) [1]. The thermochemical route offers the potential of exergy efficiency to exceed 50%, a number higher than that obtained by all other methods. In solar fuel productions, half of the total investment cost is solar concentrating system. Higher exergy efficiency means lower power required to generate the same level of chemical energy in solar fuels. Thus, high exergy efficiency makes the process economically more attractive.

Numerous excellent reviews on various methods for hydrogen production from water are reported in the literature [2–10]. They examined different methods of hydrogen productions [2,5,8], energy efficiencies of various methods [3,4], economics of various alternatives [2,8], and use of solar energy for hydrogen productions [6,7,9,10].

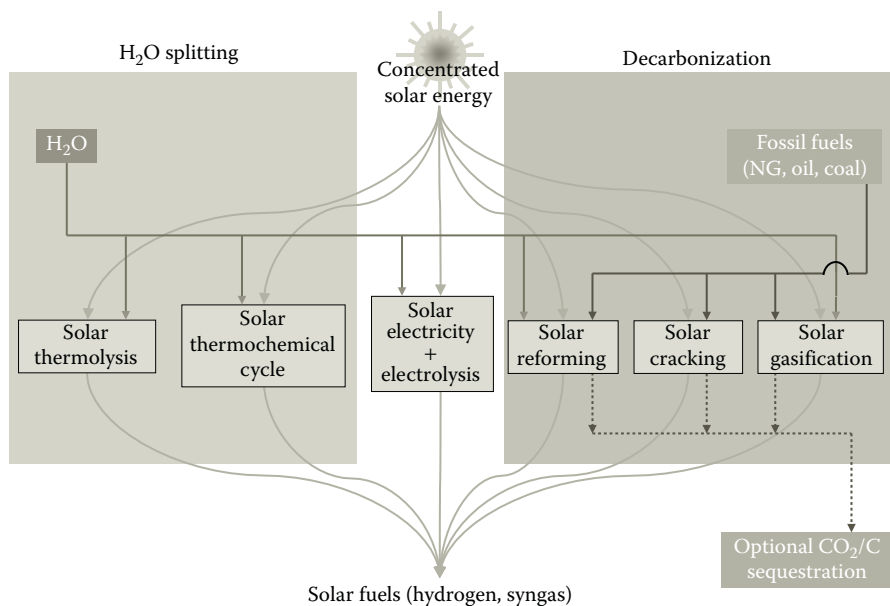


**FIGURE 11.1** (See color insert.) Thermochemical routes for solar hydrogen production. (From Meier, A. and Sattler, C., “Solar fuels from concentrated sunlight,” SolarPACES, Solar Power and Chemical Energy Systems, IEA report, 2009. With permission.)

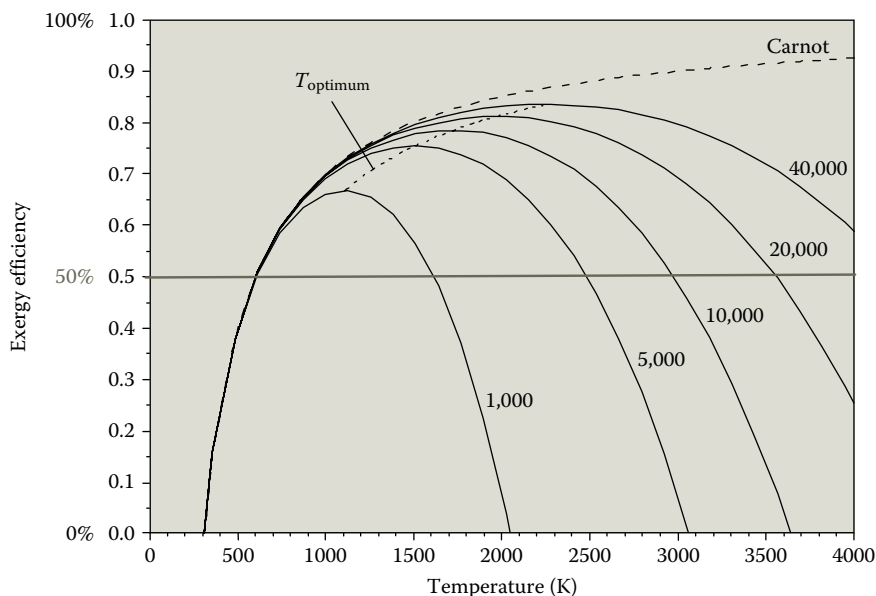


**FIGURE 11.2** (See color insert.) Exergy efficiency—Variation of the exergy efficiency as a function of the process operating temperature for a blackbody cavity receiver converting concentrated solar energy into chemical energy. (From Meier, A. and Sattler, C., “Solar fuels from concentrated sunlight,” SolarPACES, Solar Power and Chemical Energy Systems, IEA report, 2009. With permission; Fletcher, E.A. and Moen, R.L., *Science*, 197, 1050–1056, 1977. With permission.)

## 11.2 ELECTROLYSIS AND ITS DERIVATIVE TECHNOLOGIES

Electrolysis of water is the decomposition of water ( $\text{H}_2\text{O}$ ) into oxygen ( $\text{O}_2$ ) and hydrogen ( $\text{H}_2$ ) by the passage of electric current through it [11–21] (Fateev et al., 2012, pers. comm.; Laguna-Barcero et al., 2012, pers. comm.). This process requires a large amount of electrical energy that can be supplied by numerous sources such as hydropower, wind energy, solar energy, nuclear energy, geothermal energy, and electrical energy generated by fossil fuel and biomass. The electrical power needed can also be supplied by the energy stored in the form of hydrogen that is generated by other sources of renewable energy.

Electrolysis has been known to produce hydrogen since the early nineteenth century. It gives hydrogen at 99.99% purity. Bockris et al. [11] showed that the cost of energy generated by electrolysis can be expressed by the following formula:

$$\text{Cost of 1 GJ (\$)} = 2.29 Ec + 3 \quad (11.2)$$

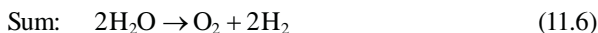
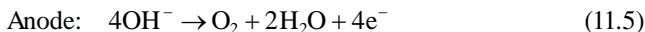
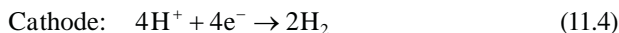
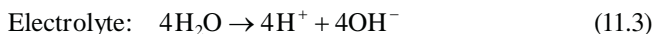
which assumes 100% Faraday efficiency.  $E$  is the potential difference across the electrodes to produce current density in the order  $100\text{--}500 \text{ mA cm}^{-2}$  and  $c$  is the cost of the electricity in cents per kilowatt-hour of electricity. The research carried out between 1970 and 1984 reduced the value of  $E$  from 2.2 V to around 1.6 V at current density of  $500 \text{ mA cm}^{-2}$ . Since 1995, all commercial electrolyzers have

been operating with 1.6 V per cell. There are several indirect methods to improve electrolytic cell performance, and these are described by Bockris et al. [11]. In the recent years, hydrogen is also created by coal slurry electrolysis. Recent advances can also reduce the potential for the electrolysis to as low as 0.5 V.

If the electricity is obtained with a heat engine, Carnot efficiency limitation applies. Thus, if the electricity is obtained from coal, the normal efficiency is about 39% and the remaining 61% is lost as heat. This loss of thermal energy makes the electricity generated by wind or hydroelectric energy more efficient. The processes are often considered in combination with a nuclear or solar heat source. A high-temperature electrolysis (HTE) process may be favorable when high-temperature heat is available as waste heat from other processes. The use of such waste heat makes the overall process cost efficient.

### 11.2.1 ALKALINE ELECTROLYSIS

Alkaline electrolyzers use an aqueous KOH solution (caustic) as an electrolyte that usually circulates through the electrolytic cells [1–11]. Alkaline electrolyzers are suited for stationary applications and are available at operating pressures up to 25 bar. Alkaline electrolysis is a mature technology allowing unmanned remote operation with significant operating experience in industrial applications. The following reactions take place inside the alkaline electrolytic cell:



Commercial electrolyzers usually consist of a number of electrolytic cells arranged in a cell stack. The major research challenges for the future are the design and manufacturing of electrolyzer equipment at lower costs with higher energy efficiency and large turndown ratios.

### 11.2.2 HTE PROCESS

HTE is more efficient economically than traditional room-temperature electrolysis because some of the energy is supplied by heat that is cheaper than electricity and the electrolysis reactions are more efficient at higher temperatures. While at 2500°C, thermal energy alone can dissociate water molecules, generally HTE systems operate between 100°C and 850°C [12,14,16–19] (Laguna-Barcero et al., 2012, pers. comm.). The efficiency of HTE process can be easily estimated by assuming that the heat required comes from heat engines and heat energy required for 1 kg of hydrogen (350 MJ) at 100°C gives the efficiency of 41%. Similar calculation at 850°C gives the efficiency of 64%.

The process requires a careful use of materials for electrodes and electrolyte. For a solid oxide electrolyzer cell (SOEC), numerous materials for electrodes and

electrolytes have been tested. Recent studies have used yttria-stabilized zirconia (YSZ) electrolytes, nickel-cermet steam/hydrogen electrodes, and mixed oxide of lanthanum, strontium, and cobalt oxygen electrodes [18,19] (Laguna-Barcero et al., 2012, pers. comm.). Future advances in the HTE process will require materials that can withstand high temperature, high pressure, and corrosive environment. At the present time, the HTE process appears to be an inefficient way to generate hydrogen. The process will become more efficient if sources such as nuclear, solar, and hydro energy can be the source of thermal energy.

When the energy is supplied in the form of heat, such as by solar or nuclear energy, the production of hydrogen by HTE is very attractive. Unlike in low-temperature electrolysis, in HTE water converts more of initial thermal energy into chemical energy (like hydrogen) by increasing the conversion efficiency. Since energy in the HTE process is supplied in the form of heat, less of the energy must be converted twice (from heat to electricity and then to chemical form), and so less energy is lost and efficiency can be doubled up to 50%.

While the heat required for the HTE process can be obtained by solar energy or nuclear energy, the latter source is more reliable and is often used. The solar form of high-temperature heat is not consistent enough to bring down the capital cost of HTE equipment. More research into HTE and high-temperature nuclear reactors may eventually lead to hydrogen supply that is cost competitive with natural gas steam reforming. This concept of coupling a high-temperature electrolyzer and a high-temperature gas-cooled nuclear reactor (HTGR) has been demonstrated in a laboratory but not at a commercial scale, although Idaho National Laboratory is developing a commercial process based on this concept [17].

### 11.2.3 HPE PROCESS

When electrolysis is conducted at high pressure, the produced hydrogen gas is compressed at around 120–200 bar (1740–2900 psi). By pressurizing the hydrogen in the electrolyzer, the need for an external hydrogen compressor is eliminated. The average energy consumption for internal compression is around 3% [13].

HPE is often carried out using a solid polymer electrolyte (SPE) membrane such as perfluorosulfonic acid (Nafion) rather than classic liquid electrolyte (alkaline electrolyte) under high pressure. Laoun [13], LeRoy et al. [20,21], and Onda et al. [15] carried out a thermodynamic analysis of such a process and showed the importance of temperature and pressure on the entire efficiency of water electrolysis. Using the model and analysis of LeRoy et al. [20,21], Onda et al. [15] showed that a temperature change up to 250°C and pressure changes up to 70 atm can be carried out by polymer electrolytic membranes. They showed that an increase in pressure and a decrease in temperature deliver more power for water electrolysis. The increase is, however, found to be small at pressures above around 200 atm. They also found that hydrogen can be produced with about 5% less power using HPE than that required using atmospheric water electrolysis.

Fateev et al. (2012, pers. comm.) showed that water electrolysis using polymeric electrolyte membrane (PEM) has demonstrated its potential for high cell efficiency (energy consumption of about 4–4.2 kW/Nm<sup>3</sup> H<sub>2</sub>) and gas purity of about 99.99%.

They studied the effects of increasing operating pressure up to several hundred bars for direct storage of hydrogen in a pressurized vessel. Their study showed that while PEM water electrolyzers operating at pressures up to 70 bar can be used to produce hydrogen and oxygen of electrolytic grade with high efficiencies; an increase in cross-permeation at higher pressure, can cause the hydrogen and oxygen mixture concentration to reach the critical level of explosive mixtures. The cross-permeation can be reduced by surface modification of solid electrolytes using low-permeability protective layers of coating. Contaminant concentration in the produced gases can also be reduced by adding catalyst gas recombiners either directly in the electrolytic cells or along the production line. Fateev et al. (2012, pers. comm.) showed that by using gas recombiners inside the electrolysis cell, it was possible to maintain the hydrogen content below 2 vol% at an operating pressure of 30 bar, with Nafion 117 as the solid electrolyte.

#### 11.2.4 PHOTOELECTROLYSIS

In this process, hydrogen and oxygen are separated in a light-driven electrolysis cell. Thus, the reactions that occur at the p-type cathode involve the evolution of hydrogen and those that occur at the n-type anode involve the evolution of oxygen. No external battery is used in the electrolysis process. While ideally the current between electrodes can be used as electricity and hydrogen produced from the process can be used as fuels, the efficiency of the overall process is about 1% [22–26] (Rajeshwar, 2012, pers. comm.). The progress in photoelectrolysis faces three major barriers: (1) There are no valid and significant theoretical analysis on the subject. The works of Scaife et al. [25], Scaife [26], and Ohashi et al. [22] appear to have some deficiencies. (2) The assumption made for years that Fermi level in solution as an important aspect of the conditions under which cells would work is proven not to be true. (3) The corrosion of semiconductor surfaces in contact with solution can be considerable. The corrosion is caused by heat as well as by photoelectrochemical reactions. Photoelectrochemical reaction efficiency is currently the same as that of photosynthesis. In the recent years, the increase in efficiency by photoelectrocatalysis has been achieved. Numerous metals such as  $\text{TiO}_2/\text{pGaP}$ ,  $\text{SrTiO}_2/\text{GaP}$ , tin oxide, and other coatings of  $\text{TiO}_2$  and  $\text{CdS}$  [22–26] (Rajeshwar, 2012, pers. comm.) on electrodes have been tested to improve the efficiency and life of the photoelectrolytic cell. The work of Szklarczyk and Bockris [23,24] showed that photoelectrocatalysis is directly related to electrocatalysis. The rate-determining step in photoelectrocatalysis is dependent on the transfer of charge at the metal–solution interface and not at the semiconductor–solution interface.

#### 11.2.5 PHOTO-AIDED ELECTROLYSIS

One method to improve efficiency is to have light falling upon an electrode. This can be achieved by applying a potential from an outside power source to the concerned electrodes. A 30%–40% efficiency in this case is not very impressive because the overall efficiency includes efficiencies for both light and electricity to hydrogen and not of light alone. The efficiency in this case can be improved by about 3%–4%

[27,28] (Rajeshwar, 2012, pers. comm.). This method is in general not preferred because not only it uses light as a source for hydrogen generation, but the overall process also requires electrical components.

### 11.2.6 PHOTOVOLTAIC ELECTROLYSIS

One way to avoid corrosion problem in photoelectrolysis is to use the concept of photovoltaic cell working in air and electrolyzing a distant electrolyzer [11,28]. Here, semiconductors are not in direct contact with the solution so that corrosion problems cease to exist. This device can effectively be used with solar energy-generated electricity. The device contains two cells.

The best setup for efficiency is, however, recorded by Murphy–Bockris cell [28] using n-on-p gallium arsenide coated with ruthenium oxide and p-on-n gallium arsenide coated with platinum. Such a cell gave about 8% conversion of light to hydrogen production at current density in the range of  $10 \text{ mA cm}^{-2}$ . The cell life was also at least as good as that of the photovoltaics (PV) in air. Two advantages of Murphy–Bockris cell are that (1) cell is in solution so that the concentration of light upon the electrode that gives high temperatures can be used to provide household heat and (2) only one device is needed compared to two that are needed in PV cell in air. There are numerous ways to use PV cell in conjunction with electrolysis. One common method is described in Section 11.2.7.

### 11.2.7 SOLAR ELECTROLYSIS

The process of solar electrolysis involves generation of solar electricity via PV or concentrating solar power (CSP) followed by electrolysis of water [1,2,6,8,9,12]. This process is considered to be a benchmark for other thermochemical solar processes for water splitting that offers potential for energy-efficient large-scale production of  $\text{H}_2$  (Figure 11.1). For solar electricity generated from PV cell and assuming solar thermal efficiencies at 15% or 20% and electrolyzer efficiency at 80%, the overall solar-to-hydrogen conversion efficiency will range from 12% to 16% [1,2,6,8,9,12]. If we assume solar thermal electricity cost of \$0.08/kWh, the projected cost of  $\text{H}_2$  will range from \$0.15 to \$0.20/kWh, that is, from \$6 to \$8/kg  $\text{H}_2$  [1,2,6,8,9,12]. For PV electricity, costs are expected to be twice as high. HTE process can significantly reduce electricity demand if it is operated at around  $800^\circ\text{C}$ – $1000^\circ\text{C}$  via SOEC. The high-temperature heat required for such a process can be supplied by the CSP system [1].

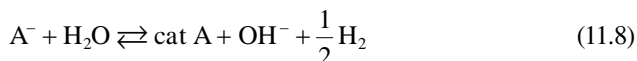
## 11.3 PHOTOCHEMICAL AND ITS DERIVATIVE TECHNOLOGIES

The dissociation of water can be assisted by photocatalysts that are directly suspended in water [29,30]. As shown below, a number of photocatalysts are possible. Early work by Gray et al. [31–34], Whitten et al. [35,36], and Maverick and Gray [37] showed that polynuclear inorganic complexes, excited metal complexes, and surfactant ruthenium complexes can help photochemical decomposition of water to produce hydrogen. Kiwi et al. [38] presented a review of homogeneous and

heterogeneous photoproduction of hydrogen and oxygen from water. The majority of the photoredox systems (heterogeneous photolysis) involve a photosensitizer, an electron acceptor, and an electron donor, with the redox catalyst assisting in the gas evolution step. Excitation of the sensitizer (S) leads to an electron transfer:



which is followed by the catalytic step:



The back conversion of  $S^+$  to S may be achieved by sacrificing a donor D added to the solution



Koriakin et al. [39] used acridine dyes as sensitizers,  $Eu^{3+}$ ,  $V^{2+}$  salicylates as electron acceptors, and “Adams” catalyst ( $PtO_2$ ) as the redox catalysts. Numerous other sensitizers, electron acceptors, and redox catalysts are illustrated by Bockris et al. [11]. An efficiency of up to 30% at an elected wavelength for hydrogen production for a brief duration by photolytic process has been reported by Kalyanasundaram et al. [40].

### 11.3.1 WATER SPLITTING ON SEMICONDUCTOR CATALYSTS (PHOTOCATALYSIS)

Duonghong et al. [41] were the first to investigate the splitting of water by utilizing microsystems [41–65] (Correa, 2009, pers. comm.). In this system, the colloidal particles are made up of suitable conductor materials, for example,  $TiO_2$ . On these colloids are induced two metallic substances, for example, ruthenium oxide and platinum. When the system is irradiated, hydrogen is evolved on the platinum and oxygen on ruthenium oxide. Each colloidal particle is a micro photocell. Using small  $TiO_2$  particles, a large area of  $TiO_2$  can be exposed to light. The system needs to be heated to last more than several hours. There are some doubts whether or not equal production of hydrogen and oxygen is achieved and whether oxygen is engaged in side reactions. It is difficult to measure the efficiency of this system. In addition, hydrogen and oxygen come off from water together and their separations add extra cost. Furthermore, the simultaneous presence of oxygen and hydrogen in water can give rise to chemical catalysis and recombination to water [41–65].

#### 11.3.1.1 Titanium Oxide Photocatalysts

$TiO_2$  was the first semiconductor used in water dissociation reaction [56]. A pure and powdered  $TiO_2$ , however, only absorbs UV fraction of solar light and thus not very effective for total absorption of solar light. The visible light response of  $TiO_2$  was improved by chemical doping of  $TiO_2$  with partially filled d-orbitals such as  $V_5^+$ ,  $Cr_3^+$ ,  $Fe_3^+$ ,  $CO_2^+$ , and  $Ni_2^+$  [44,61]. While these doping improved visible light response, they did not improve water dissociation reaction. Kato, Kudo, and coworkers [57–61] reported that  $TiO_2$  co-doped with a combination of  $Sb_5^+$  and  $Cr_3^+$  became active for  $O_2$  evolution under visible light from an aqueous solution using  $AgNO_3$  as sacrificial

agent. The physical doping of transition metal ions into  $\text{TiO}_2$  by the advanced ion-implantation technique also allowed modified  $\text{TiO}_2$  to work under visible light radiation. The ion implantation technique is, however, very expensive for commercial use. The visible light response can also be obtained by doping of anions such as N, S, or C [62–64] as substitutes for oxygen in the  $\text{TiO}_2$  lattice. When  $\text{TiO}_2$  is fused with metal oxides such as  $\text{SrO}$ ,  $\text{BaO}$ , and  $\text{Ln}_2\text{O}_3$ , metal titanates and intermediate band gaps are obtained [44]. Materials such as  $\text{SrTiO}_3$ ,  $\text{La}_2\text{Ti}_2\text{O}_7$ , and  $\text{Sm}_2\text{Ti}_2\text{O}_7$  have shown some promising results. Promising results have also been shown by using  $\text{Sm}_2\text{Ti}_2\text{S}_2\text{O}_5$ , where sulfur anion is substituted for oxygen [44]. Under visible light radiation, the last material works as a stable photocatalyst for the reduction of  $\text{H}^+$  to  $\text{H}_2$  or the oxidation of  $\text{H}_2\text{O}$  to  $\text{O}_2$  in the presence of sacrificial electron donor  $\text{Na}_2\text{S}$ – $\text{Na}_2\text{SO}_3$  or methanol or acceptor  $\text{Ag}^+$  [44]. A new class of titanium semiconductors, titanium disilicide ( $\text{TiSi}_2$ ) that absorbs a wide range of solar light, has recently been proposed as a prototype photocatalyst for the water dissociation reaction. More description of this catalyst is given in an excellent review by Navarro et al. [44].

#### 11.3.1.2 Tantalates and Niobates

Layered and tunneling structures of oxides are considered as promising materials for water dissociation reaction. Tantalates and niobates oxides with corner-sharing octahedral  $\text{MO}_6$  ( $\text{M} = \text{Ta}$  or  $\text{Nb}$ ) have been examined as photocatalysts for water dissociation [44]. Kato and Kudo [42] observed that  $\text{MTaO}_3$  ( $\text{M} = \text{Li}$ ,  $\text{Na}$ ,  $\text{K}$ ) are effective photocatalysts for water dissociation under UV light. The oxides crystallize in perovskite structure type. Lin et al. [43] showed that  $\text{NaTaO}_3$  produced by sol–gel method gave higher activity for water dissociation than the same material prepared by the high-temperature solid-state synthesis. The most active photocatalysts were those that achieve higher nitrogen substitution, maintaining the original layered structure of  $\text{Sr}_2\text{Nb}_2\text{O}_7$ . More detailed discussion of these types of catalysts is given by Navarro et al. [44].

#### 11.3.1.3 Transition-Metal Oxides, Nitrides, and Oxynitrides

Certain vanadium and tungsten compounds were found to be active in water dissociation reaction.  $\text{BiVO}_4$  with scheelite structure and  $\text{Ag}_3\text{VO}_4$  with perovskite structure showed photocatalytic activity in visible light for oxygen evolution from an aqueous silver nitrate solution [61,65]. The  $\text{WO}_3$  system also oxidizes water at moderately high rates in the presence of  $\text{Ag}^+$  and  $\text{Fe}_3^+$  ions [44]. Under visible light,  $\text{Pt-WO}_3$  alone with  $\text{NaIO}_3$  produces oxygen at high rate but produced no hydrogen [44]. Some other catalysts in this category are also examined by Navarro et al. [44].

Navarro et al. [44] also reported that nitrides and oxynitrides of transition metal cations with  $d10$  electronic configurations ( $\text{Ga}_3^+$  and  $\text{Ga}_4^+$ ) constitute a class of photocatalysts suitable for water dissociation in visible light without sacrificial reagents. Among various cocatalysts examined, the largest improvement in activity was obtained when  $(\text{Ga}_{1-x}\text{Zn}_x)(\text{N}_{1-x}\text{O}_x)$  was loaded with a mixed oxide of  $\text{Rh}$  and  $\text{Cr}$  [44]. This semiconductor evolves hydrogen and oxygen steadily and stoichiometrically under visible light from pure water in the absence of sacrificial agent. The solid solution between  $\text{ZnO}$  and  $\text{ZnGeN}_2$  ( $\text{Zn}_{1+x}\text{Ge}$ ) – ( $\text{N}_2\text{O}_x$ ) has also been found to be active

oxynitride photocatalysts for pure water dissociation in visible light [44]. Finally,  $(\text{Zn}_{1-x}\text{Ge})(\text{N}_2\text{O}_x)$  solid solution loaded with nanoparticulate  $\text{RuO}_2$  cocatalyst is also active under visible light, generating hydrogen and oxygen stoichiometrically from pure water [44].

#### 11.3.1.4 Metal Sulfides

Navarro et al. [44] reported that while small band gaps in metal sulfides make them very attractive photocatalysts for water dissociation, they are unstable for water oxidation reaction under visible light. A common method for the reducing photocorrosion of the sulfides under irradiation is the use of suitable sacrificial agents such as  $\text{Na}_2\text{S}/\text{Na}_2\text{SO}_3$  salt mixture [44]. CdS with wurtzite structure is the best-studied metal sulfide photocatalyst [66–68]. This catalyst property can be improved by improving preparation method that leads to CdS phases with good crystallinity and few crystal defects. Composite systems of CdS with  $\text{TiO}_2$ , ZnO, and CdO [69–71] also improved photoactivity. The incorporation of elements into the structure of CdS to make a solid solution is another strategy for improving the photocatalytic properties of CdS [44]. The substitution of ZnS into CdS structure improved the activity of the composite material [44].

ZnS was also another semiconductor investigated for photocatalytic activity [44]. The chemical doping of ZnS by  $\text{Cu}_2^+$ ,  $\text{Ni}_2^+$ , and  $\text{Pb}_2^+$  [59,60,72,73] allowed ZnS to absorb visible light. These doped ZnS photocatalysts showed high photocatalytic activity under visible light for hydrogen production from aqueous solutions using  $\text{SO}_3^{2-}/\text{S}^2$  as electron donor reagents. Combining ZnS with  $\text{AgInS}_2$  and  $\text{CuInS}_2$  to produce solid solutions  $(\text{CuAgIn})_x\text{Zn}_{2(1-x)}\text{S}_2$  is another strategy for improving optical absorption in the visible light range [44,74–76]. Co catalysts such as Pt loaded on  $(\text{AgIn})_{0.22}\text{Zn}_{1.56}\text{S}_2$  showed the highest activity for hydrogen evolution [44]. The ternary sulfides comprising  $\text{In}^{3+}$  and one type of transition metal cation ( $\text{Cd}_2^+$ ,  $\text{Zn}_2^+$ ,  $\text{Mn}_2^+$ ,  $\text{Cu}^+$ ) found to have low efficiency for water dissociation in visible light. More description of sulfide photocatalysts is given by Navarro et al. [44]. An overview of recently developed photocatalysts for water splitting under visible light illumination is also summarized by Navarro et al. [44].

#### 11.3.2 PHOTOBIOLOGICAL PRODUCTION OF HYDROGEN FROM WATER

The water splitting can also be carried out photobiologically [49]. Biological hydrogen can be produced in an algae bioreactor. In the late 1990s, it was discovered that if the algae are deprived of sulfur, it will switch from the production of oxygen (a normal mode of photosynthesis) to the production of hydrogen. It seems that the production is now economically feasible by the energy efficiency surpassing 7%–10% [49].

Hydrogen can be produced from water by hydrogenase-catalyzed reduction of protons by the electrons generated from photosynthetic oxidation of water using sunlight energy. In the recent years, use of a variety of algae to produce hydrogen from water has been extensively investigated and reviewed [77,78]. These reviews mention the use of sulfur deprivation with *Chlamydomonas reinhardtii* to improve hydrogen production by algae [79,80]. In addition, certain polygenetic and molecular analyses were performed in green algae [81,82]. These methods, however, did

not significantly improve the rate and the yield of algal photobiological hydrogen production. Solar-to-hydrogen energy conversion using algae has efficiency  $<0.1\%$  [83]. The rate and yield of algal photobiological hydrogen production is limited by (1) proton gradient accumulation across the algal thylakoid membrane, (2) competition from carbon dioxide fixation, (3) requirement for bicarbonate binding at photosystem II (PSII) for efficient photosynthetic activity, and (4) competitive drainage of electrons by molecular oxygen. Recently, Lee [84–86] has outlined two inventions for more efficient and robust photobiological production of hydrogen from water: (1) designer proton channel algae and (2) designer switchable PSII algae. These two new inventions eliminate not only the four problems mentioned earlier but also oxygen sensitivity of algal hydrogenase and  $H_2$ – $O_2$  gas separation and safety issue. More work in this area is needed. The details of the two new inventions are described by Lee [49].

### 11.3.3 PLASMA-INDUCED PHOTOLYSIS

It has been suggested that plasma [87] can be used to produce photons of appropriate energy so that water can be dissociated in the gas phase. Thus, in a hypothetical fusion of hydrogen, it would be possible to produce a light in the region of 1800–950 Å by the addition of aluminum to the plasma [11,88]. The main gain from this method is that the thermal energy absorbed would be converted to electricity in a heat engine at about 30% efficiency. A gain in efficiency is obtained because hydrogen will be produced by both photolysis and electrolysis. At the present time, however, the production of high energy protons is only possible by the injections of aluminum into plasmas. The possibility of obtaining very high efficiency (up to 90% which is possible for electrolysis) is unlikely. Furthermore, the recombination of hydrogen and oxygen could be a major drawback of this process [11].

## 11.4 THERMAL AND THERMOCHEMICAL DECOMPOSITION OF WATER

The direct thermal dissociation has been examined since 1960s [1,11,89–140] (Funk, 2011, pers. comm.; Bamberger, 2011, pers. comm.). In direct thermal decomposition, the energy needed to decompose water is supplied by heat only. This requires a minimum temperature of at least 2200°C (even for partial decomposition) and as high as about 4700°C, and this makes the process somewhat unrealistic. At this temperature, about 3% of all water molecules are dissociated as  $H$ ,  $H_2$ ,  $O$ ,  $O_2$ , and  $OH$ . Other reaction products like  $H_2O_2$  or  $HO_2$  remain minor. At about 3200°C, about half of the water molecules are dissociated. It is well known that an initiation of thermal splitting of water even at low pressure requires 2000 K (about 1730°C). As mentioned above, at an atmospheric pressure, 50% dissociation requires about 3500 K. This temperature can be reduced to less than 3000 K (about 2730°C) at 0.01 atm pressure. As will be discussed later, the catalysts can accelerate the dissociation at lower temperature. The lower total pressure favors the higher partial pressure of hydrogen, which makes the reactor to operate at pressures below an atmospheric pressure very difficult [1,11].

While a single-step thermolysis is conceptually simple, its realization is very challenging since it needs a high-temperature heat source above 2200°C for achieving a reasonable degree of dissociation and an effective technique to separate hydrogen and oxygen to avoid explosive mixture. The ideas proposed to separate hydrogen from the products include effusion separation and electrolytic separation. Membranes made of zirconia and other ceramics can withstand such high temperatures, but they fail to absorb severe thermal shocks that often occur when working under high-flux solar radiation. Other techniques that have been evaluated are rapid quench by injecting a cold gas, expansion in a nozzle, or submerging a solar-irradiated target in liquid water. The last technique is workable and simple, but a quench introduces a significant drop in energy efficiency and produces an explosive gas mixture. The efficiency can also be further decreased by reradiation, and the type of temperature (e.g., 2725°C for 64% dissociation at atmospheric pressure) required creates material limitations [1,11].

One of the problems for thermal dissociation of water is the materials that can stand temperatures in the excess of at least 2200°C–2500°C. Several materials such as tantalum boride, tantalum carbide, tungsten, and graphite are possible. However, at these temperatures, only oxides are stable. Graphite is chemically unstable in the presence of hydrogen and oxygen at these high temperatures. Tungsten and tungsten carbide get oxidized at these temperatures. The effect of hydrogen on oxide catalysts at these temperatures is not known. Ceramic materials such as boron nitride can also be useful if its oxidation can be controlled. Recent studies have shown that a low amount of dissociation is possible [11]. The separation of oxygen and hydrogen can be carried out in a semipermeable membrane of palladium or  $\text{ZrO}_2\text{--CeO}_2\text{--Y}_2\text{O}_3$ , which removes oxygen preferentially. Lede et al. [126,127] used a  $\text{ZrO}_2$  nozzle through which steam is forced into a thermal stream and decomposed and unreacted water is quenched suddenly to remove water and oxygen. The resulting gas contained only a small amount (about 1.2 mol%) of hydrogen. Another possible solution is the use of heat-resistant membrane made of Pd or  $\text{ZrO}_2$ , both of which selectively permeate hydrogen. The gas can also be separated using a magnetic field. The source of heat is also an issue. Solar or nuclear sources are possibilities. They are, although at the early stages of development and at the present time, only possible on a smaller scale [11,135–139].

In the recent years, thermal dissociation of water is achieved using nuclear [90,91,93,94] (Funk, 2011, pers. comm.; Bamberger, 2011, pers. comm.) and solar energy [1,92,108–110]. Some prototype generation IV reactors operate at 850°C–1000°C, a temperature considerably higher than the existing commercial nuclear power plants. General Atomics predicts that hydrogen cost using HTGR would cost \$1.53/kg, a cost that compares well with \$1.40/kg costing by steam reforming mechanism. One advantage of nuclear reactor producing both electricity and hydrogen is that it can shift production between the two. For example, plant can produce electricity during the day and hydrogen during night by matching the variations in electricity demand. Thus, hydrogen can act as a storage unit from which electricity can be generated when needed. The peak demand of electricity can be handled by the energy stored in hydrogen.

The high temperature needed to split the water can also be provided by solar energy. In Spain, a 100-kW HYDROSOL II pilot plant is operated at the Plataforma

Solar de Almeria (PSA), which uses sunlight to get 800°C–1200°C to split water [1]. This plant has been in operation since 2008. A megawatt plant based on this concept can be built by having several parallel reactors operated by connecting the plant to heliostat fields (field of sun-tracking mirrors) of a suitable size [1,108,109,113]. H<sub>2</sub> power systems [1,110,113] have proposed a membrane system for solar dissociation of water at temperatures as high as 2200°C. The membrane separates hydrogen as soon as it is produced in the so-called solar water cracker. Such a cracker with 100 m<sup>2</sup> concentrator can produce almost 1 kg of hydrogen per hour during full sunlight conditions.

The required scale of thermal decomposition process such that it is economical remains questionable. Large volume may require exotic refractories. At present, the choice of thermal decomposition takes second place to the thermochemical cycles described later. At a laboratory scale, thermal decomposition has also been analyzed using solar energy as a source of heat. The overall efficiency of solar thermal process for hydrogen generation is considerably higher than that of PV/electrolysis [1,108–113]. As shown below, solar thermal splitting of water is aided by multiple chemical steps, but the following three principles govern the success of solar thermochemical reactions: (1) drive chemical reactions at the highest temperature possible, consistent with other pertinent constraints such as materials of construction and ability to concentrate light; (2) seek simple processes with as few steps as possible, preferably one (e.g., cracking); and (3) for multistep water splitting thermochemical cycles, seek processes involving a highly endothermic step driven using concentrated sunlight, followed by an exothermic step that is autothermal and can run continuously.

### 11.4.1 THERMOCHEMICAL DECOMPOSITION OF WATER

Thermochemical cycles have been intensely investigated over the past more than four decades [1,11,89–139] (Funk, 2011, pers. comm.; Bamberger, 2011, pers. comm.). In this method, two-, three-, or four-step chemical reactions aided by a source of heat such as nuclear or solar can dissociate water and separate hydrogen and oxygen at temperatures around 800°C–900°C. The method has some inherent issues:

1. The original concept [1,11,107] was that since the method avoided the formation of electricity by the conversion of heat to mechanical work, it would avoid Carnot cycle, as this is the fundamental difficulty in reducing the price of hydrogen production by electrolysis method. The thermochemical cycles were thought to produce hydrogen at a cost of about half of that for electrolytic method. This thinking was fallacious because the methods have to have reactions carried out at different temperatures in order that the entropic properties of the partial reactions in each cycle can be used to maximum advantage. Furthermore, when the individual reactions have a positive entropy change, it is desirable to carry out reactions at the highest temperature possible to minimize the overall free-energy change. Conversely, if the entropy changes are negative, the reactions should be carried out at the lowest temperature. However, this requirement of

changing the temperature of the reaction in various cycles gives rise to the requirements to change the pressure too, and so it would be necessary to pump gases from one temperature and one pressure to another and this is similar to the Carnot cycle.

2. With three to four cycles and need to change apparatus for each, plant capital costs for unit hydrogen production are likely to be more than those that occur in the electrolysis. Furthermore, at temperatures such as 800°C–900°C, the corrosion will cause the plant life to be short.
3. Generally, it is assumed [131,132] that the reaction would take place along the free-energy pathway, but in reality it takes place down a reaction rate pathway [133,134] and not necessarily on thermodynamic pathway. Also, because of possible side reactions, the final product may not be what was intended. Due to these reasons, if cyclicity in thermochemical steps fails even by 1%, a considerable amount of unwanted materials will build up and calculated economics based on the cyclical nature of the process is no longer valid.

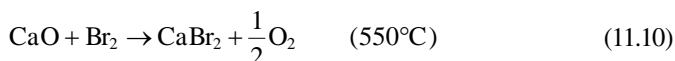
In spite of these arguments, a considerable investigation on thermochemical cycles to produce hydrogen at the temperatures lower than one required for the thermal dissociation has been carried out. The moderate temperatures used in these cycles, in general, also cause less material and separation problems. More than 300 different types of chemical cycles have been proposed and tested. In this section, we evaluate some of the important thermochemical cycles.

Previously, thermochemical cycles were characterized as those that use process heat at temperatures <950°C. These are expected to be available from high-temperature nuclear reactors. These cycles required three or more chemical reaction steps, and they are challenging because of material problems and inherent inefficiency involved with heat transfer and product separation in each step. One example is hybrid sulfuric acid cycle that requires two steps incorporating one electrolysis step. The leading candidates for multistep thermochemical cycles include mainly three-step sulfur–iodine (S–I) cycle based on thermal decomposition of sulfuric acid at 850°C and four-step UT-3 cycle based on hydrolysis of calcium and iron bromide at 750°C and 600°C, respectively [87–131] (Funk, 2011, pers. comm.; Bamberger, 2011, pers. comm.).

Recent advancement in the development of optical systems for large-scale solar concentrations capable of achieving mean solar concentration ratio that exceeds 5000 suns allows high radiation fluxes capable of getting temperature >1200°C. Such high temperatures allowed the development of efficient two-step thermochemical cycles using metal oxide–redox reactions (see Figure 11.3). Some of the important cycles are briefly described in Sections 11.4.1.1 through 11.4.1.10.

#### 11.4.1.1 The UT-3 Cycle

The UT-3 cycle is based on two pairs of chemical reactions [91,93,94] (Funk, 2011, pers. comm.). The first pair is as follows:



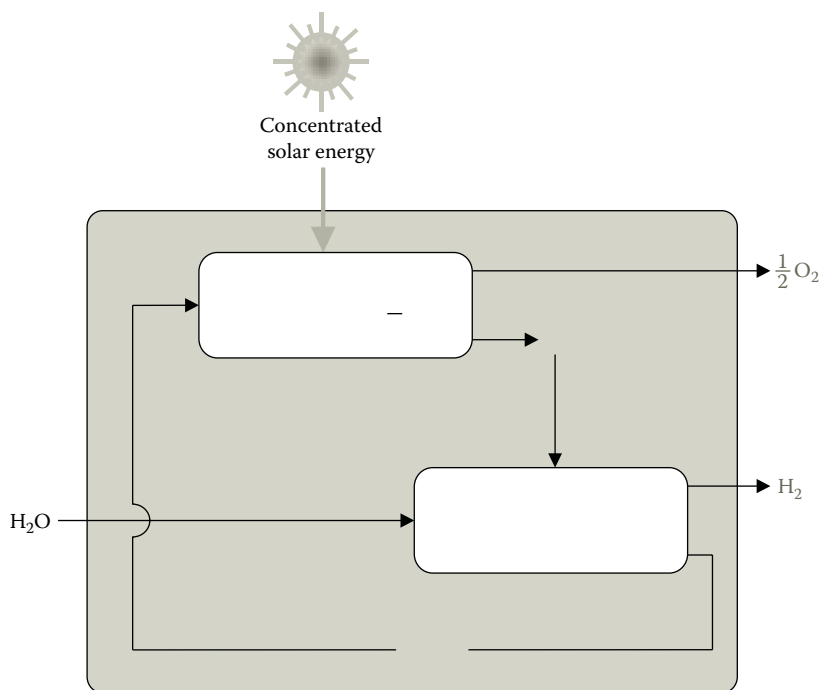
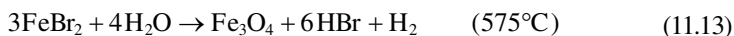
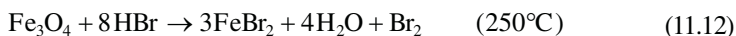


**FIGURE 11.3** (See color insert.) Thermochemical route based on metal oxide–redox reactions. (From Meier, A. and Sattler, C., “Solar fuels from concentrated sunlight,” SolarPACES, Solar Power and Chemical Energy Systems, IEA report, 2009.)



According to these reactions, a production of hydrobromic acid is accompanied by the release of oxygen. The next set of two reactions is as follows:



It indicates the reduction of water by a bromide, accompanied by release of hydrogen. In the original concept, these two reactions operate separately and sequentially in two separate reactors, wherein heterogeneous reactions between gases and solids are carried out. The main difficulty encountered was the cycling behavior of these matrices. For example, in the first reactor during the first cycle, CaO is converted to CaBr<sub>2</sub>; in the second cycle reverse transformation occurs; and so on. The design proved difficult to extrapolate to an industrial scale. Many design issues for commercial applications are still under investigation [91–94] (Funk, 2011, pers. comm.).

### 11.4.1.2 Zn/ZnO Cycle

One of the most researched metal oxide–redox pair is Zn/ZnO [1,91,95,110,111]. Since the product of ZnO decomposition at high temperature (namely, Zn and oxygen) readily recombines, the quenching of the product is necessary (Figure 11.3). Without heat recovery from the quench process, the estimated exergy efficiency [1] of this cycle is around 35%. The electrothermal process to separate Zn and oxygen at high temperatures has been experimentally demonstrated in small-scale reactors. Such high-temperature separation allows recovery of sensible and latent heats of the products to enhance the energy efficiency of the entire process. A high-temperature solar chemical reactor (Figure 11.4) was developed for this process, and solar tests were carried out at the Paul Scherrer Institute (PSI) solar furnace in Switzerland [1,95,107,110,111]. These tests allowed surface temperature to reach 1700°C in 2 s, with very low thermal inertia of the reactor system. In 2010, solar chemical reactor concept for thermal dissociation of ZnO was demonstrated in a 100-kW pilot plant in a larger solar research facility [1,95,107,110,111].

More recent work on this cycle showed that hydrolysis of Zn by the reaction  $\text{Zn} + \text{H}_2\text{O} \rightarrow \text{ZnO} + \text{H}_2$  gave reasonable hydrogen production rate for the temperatures greater than 425°C. This was experimentally verified using nano-Zn particles and water in an aerosol reactor. The required molten Zn and steam for this process can be obtained using heat of reaction. Molten Zn can also be supplied by a quench

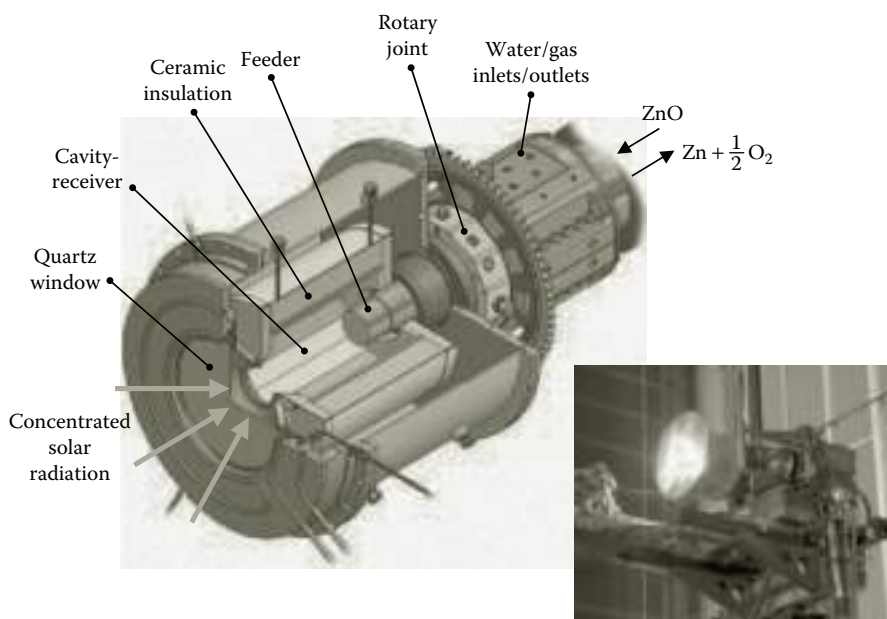


**FIGURE 11.4** (See color insert.) Rotary solar reactor for the thermal dissociation of zinc oxide to zinc and oxygen at above 1700°C. (From Meier, A. and Sattler, C., “Solar fuels from concentrated sunlight,” SolarPACES, Solar Power and Chemical Energy Systems, IEA report, 2009.)

unit of the nearby solar plant. The availability of Zn at the reaction site eliminates the storage and transportation need for the produced hydrogen. Attempts have also been made to store solar energy directly into Zinc–air batteries using Zn energy carrier from the process. The technology of redox batteries for solar energy storage is already commercially available [112,120–122].

### 11.4.1.3 SnO/SnO<sub>2</sub> Cycle

Another successful thermochemical cycle involves SnO/SnO<sub>2</sub> where exergy and energy efficiencies of 30% and 36%, respectively, can be obtained. The work carried out in 1 kW solar reactor at atmospheric and reduced pressure at Odeillo, France, has shown that SnO<sub>2</sub> reduction can be efficiently carried out at 1500°C and SnO hydrolysis can be carried out at 550°C [1,112].

### 11.4.1.4 Mixed Iron Oxide Cycle

Besides those mentioned above, manganese oxide, cobalt oxide, and iron-based mixed oxide–redox pairs have also been tested [90,93,94,106] (Funk, 2011, pers. comm.). The mixed iron oxide cycle was demonstrated at 10 kW level in the European Union's R&D project called “HYDROSOL” (2002–2005). The model for the monolithic solar thermochemical reactor (see Figure 11.5) was the catalyst converter used for automobile exhaust treatment. The multichanneled monoliths reactor with no moving parts absorbed solar radiation. The monolith channels were coated with mixed iron oxides–nanomaterials that can be activated by heating to 1250°C. The reactor dissociated water vapor and trapped oxygen allowing hydrogen to be released in the product stream at 800°C. Thus, a cyclic operation in a single closed receiver–reactor system separated produced oxygen and hydrogen. With the use of two or more reactor chambers in an alternate fashion, quasi-continuous stream of hydrogen was produced. “HYDROSOL II” (2005–2009) process tested 100 kW dual-chamber pilot reactor at PSA, Spain [1,90,93,94,106] (Funk, 2011, pers. comm.).

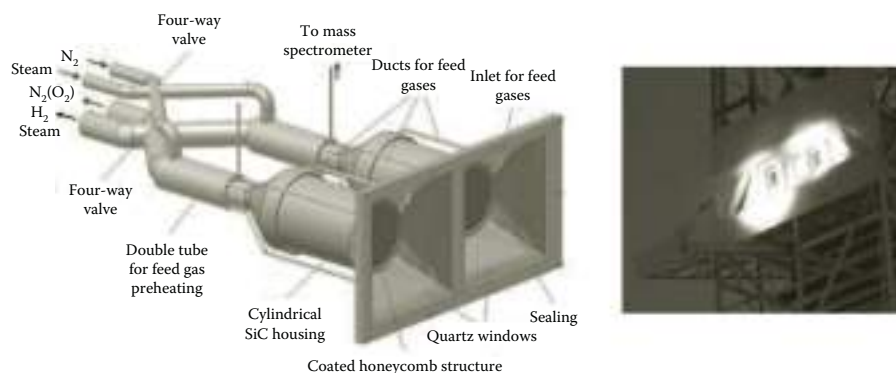


**FIGURE 11.5** (See color insert.) Monolithic dual-chamber solar receiver reactor for continuous hydrogen production. (From Meier, A. and Sattler, C., “Solar fuels from concentrated sunlight,” SolarPACES, Solar Power and Chemical Energy Systems, IEA report, 2009.)

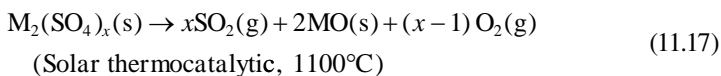
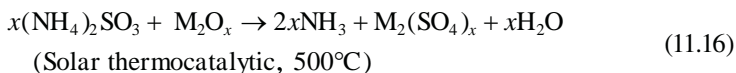
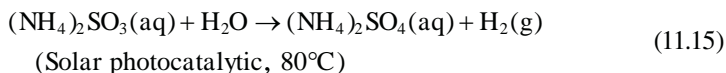
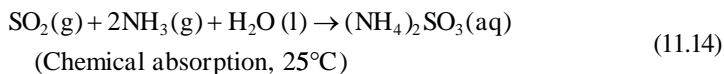
Inoue et al. [89] examined mixed ZnO/MnFe<sub>2</sub>O<sub>4</sub> system for two-step thermochemical cycle for the dissociation of water. This system among many other mixed oxide system is workable for producing hydrogen by thermochemical cycle. At 1000°C, the mixture of ZnO and MnFe<sub>2</sub>O<sub>4</sub> reacted with water to generate hydrogen gas with 60% yield. The oxygen was produced around 1027°C completing a two-step cycle.

#### 11.4.1.5 Carbothermal Reduction of Metal Oxides

In the recent years, under the European Union's R&D project SOLZINC (2001–2005), a 300-kW solar chemical reactor at the solar power research facility of the Weizmann Institute of Science (WIS) in Israel at temperatures ranging from 1000°C to 1200°C yielded up to 50 kg/h of 95% purity Zn and energy conversion efficiency of around 30% [1,90,95,106,121–124]. The process carried out carbothermal reduction of metal oxide (ZnO) using coke, natural gas, and other carbonaceous materials as reducing agents. This brings down the reduction of oxides even to lower temperatures. Carbothermal reductions of metal oxides such as iron oxide, manganese oxide, and zinc oxide with carbon and natural gas to produce the metals and the use of syngas were demonstrated in the solar furnaces. Such a solar chemical reactor concept—PSI's “two-cavity” solar reactor based on the indirect irradiation of ZnO and carbon (C) for producing Zn and carbon monoxide (CO)—was scaled up in the SOLZINC project [1,90,95,121–124].

#### 11.4.1.6 Sulfur Family Thermochemical Water Splitting Cycles

All sulfur family thermochemical water splitting cycles (TCWSCs) depend on concentration and decomposition of sulfuric acid for the oxygen evolution step of the cycle [91,95–105,107,128–131]. The sulfuric acid decomposition step presents serious materials and catalyst deactivation challenges. The most active Pt catalysts deactivate very rapidly. Metal sulfate-based TCWSCs overcome this difficulty, but they use thermal input, thus degrading photonic energy. T-Raissi et al. [107] introduced FSEC's (Florida Energy Systems Consortium) metal sulfate–ammonia (MSO<sub>4</sub>–NH<sub>3</sub>) hybrid photochemical cycle/TCWSC that can be represented as follows:

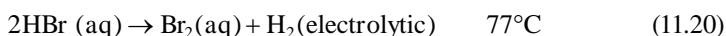
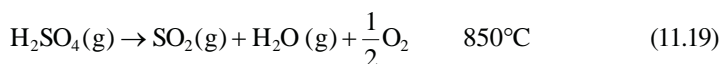
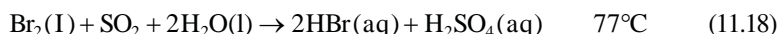


where:

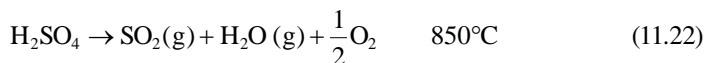
M = Zn, Mg, Ca, Ba, Fe, Co, Ni, Mn, and Cu

Chemical equilibrium calculations for the reaction between ZnO and  $(\text{NH}_4)_2\text{SO}_4$  indicate that both  $\text{ZnSO}_4$  and  $\text{ZnO} \cdot 2\text{ZnSO}_4$  can form stable reaction products. More than 20 sulfuric acid and/or metal sulfate decomposition-based TCWSCs have been reported. Major issue remains to be electrolytic oxidation of sulfur dioxide. The use of a depolarized electrolyzer as well as addition of a third process step such as S–I, S–Br, and S–Fe cycles has also been attempted. Some of these are described below [91,107]:

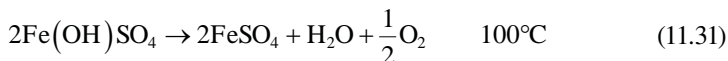
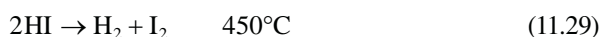
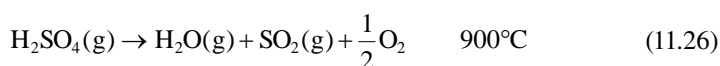
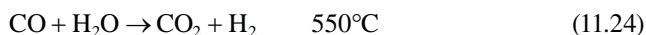
Ispra Mark 13 sulfur/bromine cycle [128]

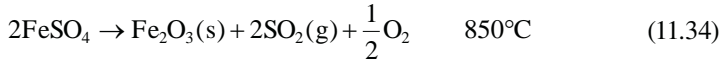
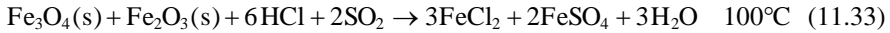


*General Atomics' S–I cycle* is described in Section 11.4.1.7 [129]. *Sulfur–iron cycle* can be described as follows:



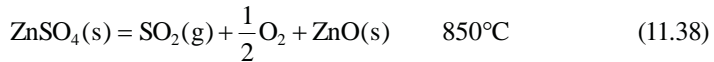
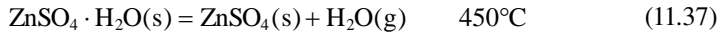
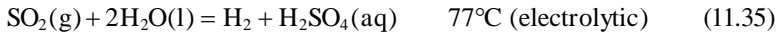
To make the separation of HI and  $\text{H}_2\text{O}$  easier, Sato et al. [130] have proposed a nickel–iodine–sulfur version of S–I cycle. Others include the following:





Although these cycles address the issue of water solubility of  $\text{SO}_2$ , they have other issues of their own. For example, efficient separation of sulfuric acid from reaction products such as HI, HBr, and  $\text{FeSO}_4$  is challenging. The determination and control of solution pH, particularly when other acids such as HI and HBr are formed, is a major issue. Abanades et al. [131] screened 280 TCWSCs and selected 30 as promising. There were nine metal sulfate-based TCWSCs in this selection because  $\text{H}_2\text{SO}_4$  and  $\text{M}_2\text{SO}_4$  present an effective method for the heat-absorbing step of the TCWSCs. Some of these thermochemical cycles are also given by T-Raissi et al. [107].

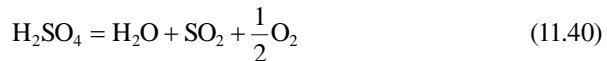
The second approach is to introduce a metal oxide as a catalyst to convert low-concentration sulfuric acid to metal sulfate that is then decomposed to produce oxygen, sulfur dioxide, and metal oxide. Sulfur dioxide and water are sent to acid electrolysis unit for generation of hydrogen and sulfuric acid, thus closing the cycle. Introducing  $\text{ZnO}$  into the Westinghouse TCWSC, a new modified  $\text{ZnSO}_4$  decomposition-based Westinghouse cycle can be written as follows [107]:



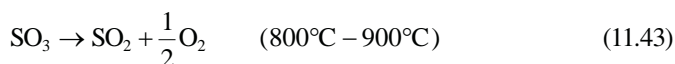
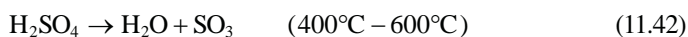
Similarly, metal oxide catalyst can be added to sulfur–bromine, S–I, and sulfur–iron cycles. These will give new modified metal-based TCWSCs. When energy input for these cycles is solar energy, they can utilize only the thermal energy, degrading the photonic portion of solar spectrum to lower grade heat.

#### 11.4.1.7 S–I Cycle

The S–I cycle is one of the promising cycles for thermochemical hydrogen production [107,129,130]. It consists of three pure thermochemical steps that sum to the dissociation of water. These steps are as follows:



The second reaction is a two-step reaction is as follows:



The first exothermic reaction is called Bunsen reaction and is operated at 120°C. The second endothermic reaction needs a temperature of about 850°C (in two steps as shown above). The last endothermic reaction runs at temperatures between 300°C and 450°C. Three reactors that are a part of the cycle are called Gibbs reactor, Bunsen reactor, and equilibrium reactor. The separation of H<sub>2</sub>SO<sub>4</sub>–HI mixture is the most critical part of the S–I cycle [107,129,130].

This cycle has been investigated by several research teams because the cycle involves only liquids and gases. General Atomics has discovered that it is possible to separate two acids in the presence of excess iodine and water. However, an efficient separation of HI from water and excess iodine at the outcome of Bunsen reaction still remains an issue. The high-temperature decomposition of acids is also an issue. The cycle was successfully tested in Japan to produce 45 l of hydrogen. It was also tested in France at the capacity of 50 l/h [107,129,130].

#### 11.4.1.8 The Westinghouse Process

The Westinghouse process is one of the “sulfur family” of thermochemical cycles being considered for the generation of hydrogen [91,107,108]. It is a sulfur cycle using hybrid electrochemical/thermochemical process for decomposing water into hydrogen and oxygen. Sulfurous acid and water are reacted electrolytically to produce hydrogen and sulfuric acid. The resulting sulfuric acid is vaporized to produce steam and sulfur trioxide, which is subsequently reduced at higher temperatures into sulfur dioxide and oxygen. The process may be seen as a variant of the S–I process, in which iodine reactions are substituted for by sulfur dioxide electrolysis as follows:



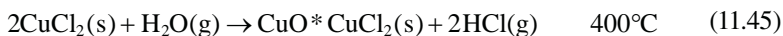
Following the separation of the water and sulfur dioxide for recycle to the electrolyzer, oxygen is available as a by-product. This has the advantage of requiring only one intermediate element. Sulfur was used because it is relatively inexpensive, its properties are well known, and it can assume a variety of valence states, thereby facilitating its use in oxidation–reduction reactions. The process requires electric energy that restricts its efficiency. Electrolysis is carried out in a strong acid medium, leading to corrosion issues. Moreover, this would require several compartments to restrict parasitic sulfur and H<sub>2</sub>S production at the cathode [91,107].

#### 11.4.1.9 Copper–Chlorine Cycle

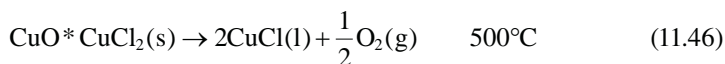
The copper–chlorine (Cu–Cl) cycle is an important cycle due to its requirement for relatively low-temperature heat compared to other thermochemical water decomposition cycles [91,104,107]. It was identified by Atomic Energy of Canada Ltd. as a highly promising cycle for hydrogen production. The advantages of this cycle are (1) reduced

construction materials, (2) inexpensive chemical agents, (3) minimal solids handling, and (4) reactions going to completion with few side reactions. It is well suited for energy supplied by the nuclear reactor. The important five steps in Cu–Cl cycle are as follows [91,104,107]:

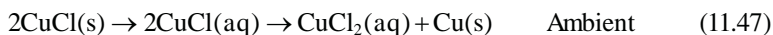
Step 1: HCl production step



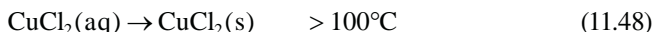
Step 2: Oxygen production step



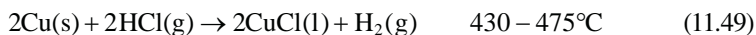
Step 3: Electrochemical process



Step 4: Flash drying



Step 5: Hydrogen production



This cycle is unusual in that it contains five chemical steps, although efforts have been made to reduce the number of chemical steps. Just like S–I cycle, Cu–Cl cycle has a significant potential due to lower temperature requirements. The literature has shown that the cost of hydrogen production by Cu–Cl cycle is better than electrolysis method at higher hydrogen production capacity (>30 tons per day) [91,104,107].

#### 11.4.1.10 Copper–Sulfate Cycle

The copper/sulfate cycle involves two major steps: (1) hydrogen production from the reaction of water,  $\text{SO}_2(\text{g})$ , and  $\text{CuO}(\text{s})$  at room temperature and (2) the thermal decomposition of the products of the first step to form oxygen and to regenerate reagents for the first step [91,97–103]. The first step is performed electrolytically and the second step appears to be possible at a temperature of around  $850^\circ\text{C}$ . More complex versions of the copper/sulfate cycle called H-5 and H-7 involve four and six reactions. Law et al. [97–105] have given a very detailed accounting of this thermochemical cycle.

Brown et al. [90] examined efficiency of more than 100 thermocycles that can use high-temperature heat from advanced nuclear power stations. A basic requirement was the ability to deliver heat to the process interface heat exchanger at temperatures up to  $900^\circ\text{C}$ . They also developed a set of requirements and criteria considering design, safety, operational, economic, and development issues. Helium-cooled nuclear reactor was chosen to interface with the thermochemical cycles. The best two-, three-, and four-step cycles with the greatest commercial potential identified from their analysis are illustrated in Table 11.1 [92,140]. They also concluded that

**TABLE 11.1**  
**Best Two-, Three-, and Four-Step Thermochemical Cycles**

Name/Major Compound	Temperature (°C)	Details of Cycles
<b>Two-Step Cycles</b>		
Tokyo Institute of Technology/ ferrite	1000	$2\text{MnFe}_2\text{O}_4 + 3\text{Na}_2\text{CO}_3 + \text{H}_2\text{O} \rightarrow 2\text{Na}_2\text{MnFe}_2\text{O}_6 + 3\text{CO}_2(\text{g}) + \text{H}_2(\text{g})$
	600	$4\text{Na}_2\text{MnFe}_2\text{O}_6 + 6\text{CO}_2(\text{g}) \rightarrow 4\text{MnFe}_2\text{O}_4 + 6\text{Na}_2\text{CO}_3 + \text{O}_2(\text{g})$
Westinghouse/ sulfur	850	$2\text{H}_2\text{SO}_4(\text{g}) \rightarrow 2\text{SO}_2(\text{g}) + 2\text{H}_2\text{O}(\text{g}) + \text{O}_2(\text{g})$
	77	$\text{SO}_2(\text{g}) + 2\text{H}_2\text{O}(\text{a}) \rightarrow \text{H}_2\text{SO}_4(\text{a}) + \text{H}_2(\text{g})$
Nickel ferrite	800	$\text{NiMnFe}_4\text{O}_6 + 2\text{H}_2\text{O} \rightarrow \text{NiMnFe}_4\text{O}_8 + 2\text{H}_2(\text{g})$
	800	$\text{NiMnFe}_4\text{O}_8 \rightarrow \text{NiMnFe}_4\text{O}_6 + \text{O}_2(\text{g})$
Hallett Air Products/chlorine	800	$2\text{Cl}_2(\text{g}) + 2\text{H}_2\text{O}(\text{g}) \rightarrow 4\text{HCl}(\text{g}) + \text{O}_2(\text{g})$
	25	$2\text{HCl} \rightarrow \text{Cl}_2(\text{g}) + \text{H}_2(\text{g})$
<b>Three-Step Cycles</b>		
Ispra Mark 13/ bromine/sulfur	850	$2\text{H}_2\text{SO}_4(\text{g}) \rightarrow 2\text{SO}_2(\text{g}) + 2\text{H}_2\text{O}(\text{g}) + \text{O}_2(\text{g})$
	77	$2\text{HBr}(\text{a}) \rightarrow \text{Br}_2(\text{a}) + \text{H}_2(\text{g})$
	77	$\text{Br}_2(\text{l}) + \text{SO}_2(\text{g}) + 2\text{H}_2\text{O}(\text{l}) \rightarrow 2\text{HBr}(\text{g}) + \text{H}_2\text{SO}_4(\text{a})$
Ispra Mark 8/ manganese/ chlorine	700	$3\text{MnCl}_2 + 4\text{H}_2\text{O} \rightarrow \text{Mn}_3\text{O}_4 + 6\text{HCl} + \text{H}_2(\text{g})$
	900	$3\text{MnO}_2 \rightarrow \text{Mn}_3\text{O}_4 + \text{O}_2(\text{g})$
	100	$4\text{HCl} + \text{Mn}_3\text{O}_4 \rightarrow 2\text{MnCl}_2(\text{a}) + \text{MnO}_2 + 2\text{H}_2\text{O}$
Ispra/CO/Mn <sub>3</sub> O <sub>4</sub>	977	$6\text{Mn}_2\text{O}_3 \rightarrow 4\text{Mn}_3\text{O}_4 + \text{O}_2(\text{g})$
	700	$\text{C}(\text{s}) + \text{H}_2\text{O}(\text{g}) \rightarrow \text{CO}(\text{g}) + \text{H}_2(\text{g})$
	700	$\text{CO}(\text{g}) + 2\text{Mn}_3\text{O}_4 \rightarrow \text{C} + 3\text{Mn}_2\text{O}_3$
Ispra Mark 3/V/ chlorine	850	$2\text{Cl}_2(\text{g}) + 2\text{H}_2\text{O}(\text{g}) \rightarrow 4\text{HCl}(\text{g}) + \text{O}_2(\text{g})$
	170	$2\text{VOCl}_2 + 2\text{HCl} \rightarrow 2\text{VOCl}_3 + \text{H}_2(\text{g})$
	200	$2\text{VOCl}_3 \rightarrow \text{Cl}_2(\text{g}) + 2\text{VOCl}_2$
Jülich Center EOS/ iron/sulfur	800	$2\text{Fe}_3\text{O}_4 + 6\text{FeSO}_4 \rightarrow 6\text{Fe}_2\text{O}_3 + 6\text{SO}_2 + \text{O}_2(\text{g})$
	700	$3\text{FeO} + \text{H}_2\text{O} \rightarrow \text{Fe}_3\text{O}_4 + \text{H}_2(\text{g})$
	200	$\text{Fe}_2\text{O}_3 + \text{SO}_2 \rightarrow \text{FeO} + \text{FeSO}_4$
Gaz de France/ KOH/K	725	$2\text{K} + 2\text{KOH} \rightarrow 2\text{K}_2\text{O} + \text{H}_2(\text{g})$
	825	$2\text{K}_2\text{O} \rightarrow 2\text{K} + \text{K}_2\text{O}_2$
	125	$2\text{K}_2\text{O}_2 + 2\text{H}_2\text{O} \rightarrow 4\text{KOH} + \text{O}_2(\text{g})$
Aachen University Jülich 1972/Cr/Cl	850	$2\text{Cl}_2(\text{g}) + 2\text{H}_2\text{O}(\text{g}) \rightarrow 4\text{HCl}(\text{g}) + \text{O}_2(\text{g})$
	170	$2\text{CrCl}_2 + 2\text{HCl} \rightarrow 2\text{CrCl}_3 + \text{H}_2(\text{g})$
	800	$2\text{CrCl}_3 \rightarrow 2\text{CrCl}_2 + \text{Cl}_2(\text{g})$
US-Chlorine/Cu/Cl	850	$2\text{Cl}_2(\text{g}) + 2\text{H}_2\text{O}(\text{g}) \rightarrow 4\text{HCl}(\text{g}) + \text{O}_2(\text{g})$
	200	$2\text{CuCl} + 2\text{HCl} \rightarrow 2\text{CuCl}_2 + \text{H}_2(\text{g})$
	500	$2\text{CuCl}_2 \rightarrow 2\text{CuCl} + \text{Cl}_2(\text{g})$
Ispra Mark 9/Fe/Cl	420	$2\text{FeCl}_3 \rightarrow \text{Cl}_2(\text{g}) + 2\text{FeCl}_2$
	150	$3\text{Cl}_2(\text{g}) + 2\text{Fe}_3\text{O}_4 + 12\text{HCl} \rightarrow 6\text{FeCl}_3 + 6\text{H}_2\text{O} + \text{O}_2(\text{g})$
	650	$3\text{FeCl}_2 + 4\text{H}_2\text{O} \rightarrow \text{Fe}_3\text{O}_4 + 6\text{HCl} + \text{H}_2(\text{g})$

(Continued)

**TABLE 11.1****(Continued) Best Two-, Three-, and Four-Step Thermochemical Cycles**

Name/Major Compound	Temperature (°C)	Details of Cycles
LASL-U/uranium	25	$3\text{CO}_2 + \text{U}_3\text{O}_8 + \text{H}_2\text{O} \rightarrow 3\text{UO}_2\text{CO}_3 + \text{H}_2(\text{g})$
	250	$3\text{UO}_2\text{CO}_3 \rightarrow 3\text{CO}_2(\text{g}) + 3\text{UO}_3$
	700	$6\text{UO}_3(\text{s}) \rightarrow 2\text{U}_3\text{O}_8(\text{s}) + \text{O}_2(\text{g})$
Ispira Mark 2	100	$\text{Na}_2\text{O} \cdot \text{MnO}_2 + \text{H}_2\text{O} \rightarrow 2\text{NaOH}(\text{a}) + \text{MnO}_2$
(1972)/Na/Mn	487	$4\text{MnO}_2(\text{s}) \rightarrow 2\text{Mn}_2\text{O}_3(\text{s}) + \text{O}_2(\text{g})$
	800	$\text{Mn}_2\text{O}_3 + 4\text{NaOH} \rightarrow 2\text{Na}_2\text{O} \cdot \text{MnO}_2 + \text{H}_2(\text{g}) + \text{H}_2\text{O}$
Sulfur–Iodine/S/I	850	$2\text{H}_2\text{SO}_4(\text{g}) \rightarrow 2\text{SO}_2(\text{g}) + 2\text{H}_2\text{O}(\text{g}) + \text{O}_2(\text{g})$
	450	$2\text{HI} \rightarrow \text{I}_2(\text{g}) + \text{H}_2(\text{g})$
	120	$\text{I}_2 + \text{SO}_2(\text{a}) + 2\text{H}_2\text{O} \rightarrow 2\text{HI}(\text{a}) + \text{H}_2\text{SO}_4(\text{a})$
<b>Four-Step Cycles</b>		
Vanadium chloride	850	$2\text{Cl}_2(\text{g}) + 2\text{H}_2\text{O}(\text{g}) \rightarrow 4\text{HCl}(\text{g}) + \text{O}_2(\text{g})$
	25	$2\text{HCl} + 2\text{VCl}_2 \rightarrow 2\text{VCl}_3 + \text{H}_2(\text{g})$
	700	$2\text{VCl}_3 \rightarrow \text{VCl}_4 + \text{VCl}_2$
	25	$2\text{VCl}_4 \rightarrow \text{Cl}_2(\text{g}) + 2\text{VCl}_3$
Ispira Mark	850	$2\text{Cl}_2(\text{g}) + 2\text{H}_2\text{O}(\text{g}) \rightarrow 4\text{HCl}(\text{g}) + \text{O}_2(\text{g})$
4/Fe/Cl	100	$2\text{FeCl}_2 + 2\text{HCl} + \text{S} \rightarrow 2\text{FeCl}_3 + \text{H}_2\text{S}$
	420	$2\text{FeCl}_3 \rightarrow \text{Cl}_2(\text{g}) + 2\text{FeCl}_2$
	800	$\text{H}_2\text{S} \rightarrow \text{S} + \text{H}_2(\text{g})$
Ispira Mark	850	$2\text{Cl}_2(\text{g}) + 2\text{H}_2\text{O}(\text{g}) \rightarrow 4\text{HCl}(\text{g}) + \text{O}_2(\text{g})$
6/Cr/Cl	170	$2\text{CrCl}_2 + 2\text{HCl} \rightarrow 2\text{CrCl}_3 + \text{H}_2(\text{g})$
	700	$2\text{CrCl}_3 + 2\text{FeCl}_2 \rightarrow 2\text{CrCl}_2 + 2\text{FeCl}_3$
	420	$2\text{FeCl}_3 \rightarrow \text{Cl}_2(\text{g}) + 2\text{FeCl}_2$
Ispira Mark	100	$2\text{CuBr}_2 + \text{Ca}(\text{OH})_2 \rightarrow 2\text{CuO} + 2\text{CaBr}_2 + \text{H}_2\text{O}$
1C/Cu/Ca/Br	900	$4\text{CuO}(\text{s}) \rightarrow 2\text{Cu}_2\text{O}(\text{s}) + \text{O}_2(\text{g})$
	730	$\text{CaBr}_2 + 2\text{H}_2\text{O} \rightarrow \text{Ca}(\text{OH})_2 + 2\text{HBr}$
	100	$\text{Cu}_2\text{O} + 4\text{HBr} \rightarrow 2\text{CuBr}_2 + \text{H}_2(\text{g}) + \text{H}_2\text{O}$
UT-3 University	600	$2\text{Br}_2(\text{g}) + 2\text{CaO} \rightarrow 2\text{CaBr}_2 + \text{O}_2(\text{g})$
of Tokyo/Fe/	600	$3\text{FeBr}_2 + 4\text{H}_2\text{O} \rightarrow \text{Fe}_3\text{O}_4 + 6\text{HBr} + \text{H}_2(\text{g})$
Ca/Br	750	$\text{CaBr}_2 + \text{H}_2\text{O} \rightarrow \text{CaO} + 2\text{HBr}$
	300	$\text{Fe}_3\text{O}_4 + 8\text{HBr} \rightarrow \text{Br}_2 + 3\text{FeBr}_2 + 4\text{H}_2\text{O}$

Source: Brown, L.C., Besenbrauch, G.E., Schultz, K.R., Showalter, S.K., Marshall, A.C., Pickard, P.S., and Funk, J.F., *Spring National Meeting of AIChE, Nuclear Engineering Session THa01 139-Hydrogen Production and Nuclear Power*, New Orleans, LA, (2002). With permission; Schultz, K., *Presentation to the Stanford Global Climate and Energy Project*, General Atomics, San Diego, CA (2003). With permission.

S–I cycle was overall the best to interlink with the helium-cooled nuclear reactor. The use of solar and nuclear energy for direct thermolysis or thermochemical breakdown of water has also been extensively examined in the literature [135–138,140].

## 11.5 OTHER MISCELLANEOUS TECHNOLOGIES

Bockris et al. [11] described several novel methods for hydrogen production. Some of the methods described closely follow their description in Sections 11.5.2, 11.5.3, 11.5.6, and 11.5.7.

### 11.5.1 CHEMICAL METHODS

A number of materials react with liquid water or water containing acids to release hydrogen [11,139,141–148]. While these methods somewhat resemble steam reforming, they differ in that reactant is liquid water instead of gaseous water and the solids involved are not naturally occurring such as coal and shale oil but those that require a significant energy and efforts recovering such as zinc, aluminum, and iron.

In laboratory, zinc reacts with strong acids in Kipp's apparatus. In the presence of sodium hydroxide, aluminum and its alloys react with water to generate hydrogen [11,107]. This is, however, an expensive process due to the high cost of aluminum, and the process also results in a large amount of waste heat that must be disposed or recovered. In relative terms, aluminum is cheaper and safer than some other materials, and the produced hydrogen can be easily stored and transported than using other hydrogen storage materials such as sodium borohydride.

The reaction between water and aluminum follows the path:



Overall reaction follows:



The first two reactions are similar to the process that occurs inside an aluminum battery. The second reaction precipitates crystalline aluminum hydroxide. This process works well at a smaller scale, and every 1 kg of aluminum can produce up to 0.111 kg of hydrogen that can be very useful in the device such as fuel cell where released hydrogen can generate electricity. Aluminum along with  $\text{NaBH}_4$  can also be used as compact storage devices for hydrogen. The above reaction is mildly exothermic, and hence the reaction is carried out under mild temperatures and pressures providing a stable and compact source of hydrogen. The process can be a backup process for remote or marine applications. The negative effect of passivation of aluminum can be minimized by changing the temperature, alkali concentration, physical form of aluminum, and solution composition.

### 11.5.2 MAGMALYSIS

This process is another form of chemical method in which steam is injected on a magma that is near the surface [11,143]. According to Northrup et al. [143], the following reaction would occur:



Fresh basaltic lava contains on the order of 10 wt% ferrous oxide (FeO) and 1–2 wt% ferric oxide (FeO<sub>1.5</sub>). These components exist as dissolved constituents within the melt and in the mineral suspended in the magma. Northrup et al. [143] calculated hydrogen concentration, which resulted from equilibration of water with a solid assemblage of hematite–magnetite for a total pressure of 100 MPa. The calculation agreed well with the measured data.

As water accumulates in the basaltic lava, most of FeO is converted into FeO<sub>1.5</sub>, resulting in the drop of hydrogen production [144,145]. Northrup et al. [143] also estimated the hydrogen production at 1200°C. The estimates indicate that about  $2.2 \times 10^6$  tons of hydrogen is potentially recoverable by water interacting with 1 km<sup>3</sup> of basalt at high temperatures at 1000 MPa. The exact calculations of hydrogen production rate requires the knowledge of available magma surface area and its cooling rate. Northrup et al. [143] estimated that about 10<sup>5</sup> km<sup>3</sup> of magma bodies in areas of the United States exist where hydrogen production by this method is possible.

### 11.5.3 RADIOLYSIS

Radiolysis involves the injection of radioactive substances such as UO<sub>2</sub>(NO<sub>3</sub>)<sub>2</sub> into water which emits particles that have an energy in the region of 10<sup>6</sup> eV [11,142,149]. This energy will decompose some 10<sup>5</sup> water molecules per particle, and if there were no recombination, significant amounts of hydrogen and oxygen would be generated. When radioactive particles pass by water molecules, they strip a part of electron shells so that protons are produced and the oxygen becomes cationic. The conversion efficiency is, however, low; between 1% and 5% of the radioactive energy is translated in the productions of hydrogen and oxygen [141]. The efficiency can be improved by the use of salts such as B<sup>10</sup> and Li<sup>6</sup> compounds. The process generates hydrogen and oxygen in a mixture, which can be separated using a fuel cell where hydrogen and oxygen are separated by anode and cathode, respectively.

The method can be valuable if the efficiency is improved to greater than 10% and the radioactive material used is waste. Gomberg and Gordus [142] improved the efficiency by using the nuclear fission either in a solid fuel configuration where the radiation energy/heat ratio can be about 1/4 or in a fluid fuel configuration where all the energy is available as radiation.

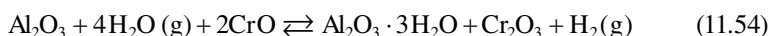
### 11.5.4 SHOCK WAVES AND MECHANICAL PULSES

Attempts to dissociate water using shock waves and mechanical pulses have also been made [11]. The use of shock wave to dissociate diatomic molecules and organic compounds has been successful [149]. It is possible to induce OH bond dissociation

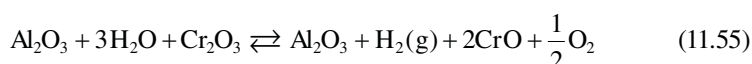
by introducing anharmonic oscillations in the molecule. A novel method could be the excitation of water molecules adsorbed on fiber optics that could be made conductive to allow part of the light wave being transmitted to interact with the adsorbed water.

### 11.5.5 CATALYTIC DECOMPOSITION OF WATER

Another approach to the thermolysis of water is to pass water through a “getter” that will remove oxygen [11]. The getter then needs to be regenerated after obtaining hydrogen. Kasal and Bishop [150,151] used zeolites for this purpose. They [40] also described a simple two-step cycle to decompose water by cycling water over chromium- and indium-substituted aluminosilicates. For a two-step thermochemical process consisting of an endothermic step operating at lower temperature  $T_L$  and the second step operating at higher temperature  $T_H$ , the transition between these two steps will be accompanied by a large entropy change. A large entropy change can also be realized by resorting to a cycle consisting of many reaction steps or a single reaction involving many molecules. England [152] proposed a thermochemical cycle based on the results of Kasal and Bishop as follows:



at low temperatures with an entropy change of  $-128.5$  eu and



at high temperatures with an entropy change of  $139.1$  eu.

### 11.5.6 PLASMOLYSIS

The direct thermal dissociation of water by thermal means at temperatures around  $3000^\circ\text{C}$  suffers from the lack of durable materials for the reactor at these high temperatures [11,139]. One method by which this difficulty may be avoided is to use electrically produced plasmas [139]. Electrical generation of the plasmas involves the transformation of the energy from an electric field (microwave, radio frequency, or d.c.) into kinetic energy of electrons, which is further transformed into molecular excitations and to the kinetic energy of heavy particles. These discharged plasmas are divided into either hot (thermal) or cold (nonthermal) plasmas. Both types of plasmas can result in electron temperature to be several thousand degrees. Although the difference in energy content is a function of temperature, the low-temperature discharge has sufficient energy to dissociate water.

### 11.5.7 MAGNETOLYSIS

The idea of producing high current and low voltage was abandoned for a long time due to the fact that resistance losses are less when electricity is transmitted at high voltages over a power line than when it is transmitted at low voltage and high current [148]. However, in an electrolyzer, what is needed is low voltage and very high currents. This can be achieved by the application of a homopolar generator

conceived by Faraday [147]. Bockris and Gutmann [146] suggested that using this concept electrolysis can be carried out by generating the necessary potential difference by magnetic induction inside the electrolyzer [11,146–148]. Bockris et al. [11] examined the details of this method.

## REFERENCES

1. Meier, A. and Sattler, C., “Solar fuels from concentrated sunlight,” SolarPACES, Solar Power and Chemical Energy Systems, IEA report (August 2009).
2. Smítková, M., Janíček, F., and Riccardi, J., “Analysis of the selected processes for hydrogen production,” *WSEAS Transactions on Environment and Development*, 11 (4), 1026–1035 (2008).
3. Funk, J.E. and Reinstrom, R.M., “Energy requirements in the production of hydrogen from water,” *Industrial & Engineering Chemistry Process Design and Development*, 5 (3), 336–342 (1966).
4. Funk, J.E., “Thermodynamics of multi-step water decomposition processes,” *Proceedings of the Symposium on Non-Fossil Chemical Fuels*, ACS 163rd National Meeting, April, Boston, MA, 79–87 (1972).
5. Abe, I., “Hydrogen productions from water,” *Energy Carriers and Conversion Systems*, 1, 1–3 (2001).
6. Taylan, O. and Berberoglu, H. “Fuel production using concentrated solar energy,” in Rugescu, R. (ed.) *The Applications of Solar Energy*, INTECH, Rijeka, Croatia, 33–67 (2013).
7. Klausner, J., Petrasch, J., Mei, R., Hahn, D., Mehdizadeh, A., and Auyeung, N., “Solar fuel: Pathway to a sustainable energy future,” Florida Energy Summit, University of Florida, Gainesville, FL (August 17, 2012).
8. Ris, T. and Hagen, E., “Hydrogen production-gaps and priorities,” IEA Hydrogen Implementing Agreement (HIA), 1–111 (2005).
9. Suarez, M., Blanco-Marigorta, A., and Peria-Quintana, J., “Review on hydrogen production technologies from solar energy,” International Conference on Renewable Energies and Power Quality, La Palmas de Gran Canaria, April 13–15, Spain (2011).
10. Nowotny, J., Sorrell, C., Sheppard, L., and Bak, T., “Solar-hydrogen: Environmentally safe fuel for the future,” *International Journal of Hydrogen Energy*, 30 (5), 521–544 (2005).
11. Bockris, J., Dandapani, B., Cocks, D., and Ghoroghchian, J., “On the splitting of water,” *International Journal of Hydrogen Energy*, 10 (30), 179–201 (1985).
12. Naterer, G.F., “Economics and synergies of electrolytic and thermochemical methods of environmentally benign hydrogen production,” *Proceedings of the World Hydrogen Energy Conference*, May 16–21, Essen, Germany (2010).
13. Laoun, B., “Thermodynamics aspect of high pressure hydrogen production by water electrolysis,” *Revue des Énergies Renouvelables*, 10 (3), 435–444 (2007).
14. Funk, J.E., “Thermochemical and electrolytic production of hydrogen,” in Vezerglu, T.N. (ed.), *Introduction to Hydrogen Energy*. International Association for Hydrogen Energy, Miami, FL, 19–49 (1975).
15. Onda, K., Kyakuno, T., Hattori, K., and Ito, K., “Prediction of production power for high pressure hydrogen by high pressure water electrolysis,” *Journal of Power Sources*, 132, 64–70 (2004).
16. “High temperature electrolysis,” Wikipedia, the free encyclopedia, 1–3 (2012).
17. McKellar, M., Harvego, E., and Gandrik, A., “System evaluation and economic analysis of a HTGR powered high temperature electrolysis production plant,” *Proceedings of the High Temperature Reactor*, Paper 093, October 18–20, Prague, Czech Republic (2010).

18. Herring, J., O'Brien, J., Stoots, C., Lessing, P., and Anderson, R., "High temperature solid oxide electrolyzer system," Hydrogen, Fuel Cells, and Infrastructure Technologies, DOE Progress Report, May 25, 2004, INEEL, Idaho Falls, ID, 1–5 (2003).
19. Herring, J., O'Brien, J., Stoots, C., Lessing, P., and Hartvigsen, J., "High temperature electrolysis for hydrogen production," Paper presented by Idaho National Laboratory at the Materials Innovations in an Emerging Hydrogen Economy Conference, February 26, Hilton Oceanfront, Cocoa Beach, FL (2008).
20. LeRoy, R.L., Bowen, C.T., and LeRoy, D.J., *Journal of the Electrochemical Society*, 127, 1954 (1980).
21. LeRoy, R.L., Janjua, M.B.I., Renaud, R., and Leuenberger, U., *Journal of the Electrochemical Society*, 126, 1674 (1979).
22. Ohashi, K., McCann, J., and Bockris, J.O.M., *Nature*, 266, 610 (1977).
23. Szklarczyk, M. and Bockris, J.O.M., *Applied Physics Letters*, 42, 1035 (1983).
24. Szklarczyk, M. and Bockris, J.O.M., *Journal of Physical Chemistry*, 88, 1808 (1984).
25. Scaife, D.E., Weller, P.F., and Fisher, W.G., "Crystal preparation and properties of cesium tin(II) trihalides," *Journal of Solid State Chemistry*, 9 (3), 308–314 (1974).
26. Scaife, D., "Oxide semiconductors in photoelectrochemical conversion of solar energy," *Solar Energy*, 25 (1), 41–54 (1980).
27. Shyu, R., Weng, F., and Ho, C., "Manufacturing of a micro probe using supersonic aided electrolysis process," DTIP of MEMS and MOEMS, April 9–11, Nice, France (2008).
28. Bockris, J. and Murphy, O., "One-unit photo-activated electrolyzer," US Patent No. US4790916 A (December 13, 1988).
29. Bockris, J., Gutmann, F., and Craven, W., "The economics of production of hydrogen," in Veziroglu, T., Van Vorst, W., Kelley, J., (eds.), *Hydrogen Energy Progress IV*. International Association of Hydrogen Energy, Miami, FL, 1475 (1982).
30. Okada, G., Guruswamy, V., and Bockris, J., *Journal of the Electrochemical Society*, 128, 2097 (1981).
31. Trogler, W., Geoffrey, G., Erwin, D., and Gray, H., *Journal of the American Chemical Society*, 100, 1160 (1978).
32. Erwin, D., Geoffrey, G., Gray, H., Hammond, G., Solomon, E., Trogler, W., and Zagers, A., *Journal of the American Chemical Society*, 99, 3620 (1977).
33. Tyler, D. and Gray, H., *Journal of the American Chemical Society*, 103, 1683 (1981).
34. Mann, K., Lewis, N., Miskowski, V., Erwin, D., Hammond, G., and Gray, H., *Journal of the American Chemical Society*, 99, 5525 (1977).
35. Sprintschnik, G., Sprintschnik, H., Kirsch, P., and Whitten, D., *Journal of the American Chemical Society*, 98, 2337 (1976).
36. Sprintschnik, G., Sprintschnik, H., Kirsch, P., and Whitten, D., *Journal of the American Chemical Society*, 99, 4947 (1977).
37. Maverick, A. and Gray, H., *Pure and Applied Chemistry*, 52, 2339 (1980).
38. Kiwi, J., Kalyanasundaram, K., and Gratzel, M., *Structure and Bonding*, 49, 37 (1982).
39. Koriakin, B., Dshabiev, T., and Shvlov, A., *Doklady Akademii Nauk SSSR*, 298, 620 (1977).
40. Kalyanasundaram, K., Micic, O., Pramauro, E., and Gratzel, M., *Helvetica Chimica Acta*, 62, 2432 (1979).
41. Duonghong, D., Borgarello, E., and Gratzel, M., *Journal of the American Chemical Society*, 103, 4685 (1981).
42. Kato, H. and Kudo, A., *Chemistry Letters*, 1207 (1999).
43. Lin, W., Cheng, C., Hu, C., and Teng, H., *Applied Physics Letters*, 89, 211904 (2006).
44. Navarro, Y.R., Alvarez-Galvan, M., del Valle, F., Villoria de la Mano, J., and Fierro, J., "Water splitting on semiconductor catalysts under visible light irradiation," *ChemSusChem*, 2 (6), 471–485 (2009).

45. Navarro, R., Yerga, J., and Fierro, G., "Photo catalytic decomposition of water," *ChemSusChem*, 2, 471–485 (2009).
46. Sato, J., Saito, N., Nishiyama, H., and Inoue, Y., "Photocatalytic water decomposition by RuO<sub>2</sub> loaded antimonates, M<sub>2</sub>Sb<sub>2</sub>O<sub>7</sub> (M = Ca, Sr), CaSb<sub>2</sub>O<sub>6</sub> and NaSbO<sub>3</sub> with d10 configuration," *Journal of Photochemistry and Photobiology A: Chemistry*, 148, 85–89 (2002).
47. Zou, Z., Ye, J., Sayama, K., and Arakawa, H., "Photocatalytic hydrogen and oxygen formation under visible light irradiation with M-doped InTaO<sub>4</sub> (M = Mn, Fe, Co, Ni or Cu) photocatalysts," *Journal of Photochemistry and Photobiology A: Chemistry*, 148, 65–69 (2002).
48. "Water splitting," Wikipedia, the free encyclopedia (2012).
49. Lee, J. (ed.), "Designer transgenic, algae for photobiological production of hydrogen from water," in *Advanced Biofuels and Bioproducts*. Springer, New York, 371–404 (2012).
50. Sato, J., Kobayashi, H., Saito, N., Nishiyama, H., and Inoue, Y., "Photocatalytic activities for water decomposition of RuO<sub>2</sub> loaded AInO<sub>2</sub> (A = Li, Na) with d10 configuration," *Journal of Photochemistry and Photobiology A: Chemistry*, 158, 139–144 (2003).
51. Zou, Z. and Arakawa, H., "Direct water splitting into H<sub>2</sub> and O<sub>2</sub> under visible light irradiation with a new series of mixed oxide semiconductor photocatalysts," *Journal of Photochemistry and Photobiology A: Chemistry*, 158, 145–162 (2003).
52. Harda, H., Hosoki, C., and Kudo, A., "Overall water splitting by sonophotocatalytic reaction: The role of powdered photocatalyst and an attempt to decompose water using a visible light sensitive photocatalyst," *Journal of Photochemistry and Photobiology A: Chemistry*, 141, 219–224 (2001).
53. Abe, R., Hara, K., Sayama, K., Domen, K., and Arakawa, H., "Steady hydrogen evolution from water on Eosin Y-fixed TiO<sub>2</sub> photocatalyst using a silane coupling reagent under visible light irradiation," *Journal of Photochemistry and Photobiology A: Chemistry*, 137, 63–69 (2000).
54. Fujishima, A., Rao, T., and Tryk, D., "Titanium dioxide photocatalysis," *Journal of Photochemistry and Photobiology C: Photochemistry Reviews*, 1, 1–21 (2000).
55. Navarro, R., Sanchez-Sanchez, M., Alvarez-Galvan, M., del Valle, F., and Fierro, J., "Hydrogen production from renewable sources: Biomass and photocatalytic opportunities," *Energy & Environmental Science*, 2, 35–54 (2009).
56. Fujishima, A. and Honda, K., *Nature*, 238, 37 (1972).
57. Kato, H. and Kudo, A., *Journal of Physical Chemistry B*, 106, 5029 (2002).
58. Ishii, T., Kato, H., and Kudo, A., *Journal of Photochemistry and Photobiology A*, 163, 181 (2004).
59. Kudo, A. and Sekizawa, M., *Catalysis Letters*, 58, 241 (1999).
60. Kudo, A. and Sekizawa, M., *Chemical Communications*, 1371 (2000).
61. Kato, R., Ishii, T., Kato, H., and Kudo, A., *Journal of Physical Chemistry B*, 108, 8992 (2004).
62. Anpo, M. and Takeuchi, M., *Journal of Catalysis*, 216, 505 (2003).
63. Asahi, R., Morikawa, T., Ohwaki, T., Aoki, K., and Taga, Y., *Science*, 293, 269 (2001).
64. Umebayashi, T., Yamaki, T., Itoh, H., and Asai, K., *Applied Physics Letters*, 81, 454 (2002).
65. Kudo, A., Omori, K., and Kato, H., *Journal of the American Chemical Society*, 121, 11459 (1999).
66. Asokkumar, M., *International Journal of Hydrogen Energy*, 23, 427 (1998).
67. Kalyanasundaram, M., Graetzel, M., and Pelizzetti, E., *Coordination Chemistry Reviews*, 69, 57 (1986).
68. Meissner, D., Memming, R., and Kastening, B., *Journal of Physical Chemistry*, 92, 3476 (1988).
69. Fuji, H. and Guo, L., *Journal of Physical Chemistry B*, 110, 1139 (2006).

70. Spanhel, L., Weller, H., and Hanglein, A., *Journal of the American Chemical Society*, 109, 6632 (1987).
71. Navarro, R., del Valle, F., and Fierro, J., *International Journal of Hydrogen Energy*, 33, 4265 (2008).
72. Tsuji, I. and Kudo, A., *Journal of Photochemistry and Photobiology A*, 156, 249 (2003).
73. Kudo, A., Nishiro, R., Iwase, A., and Kato, H., *Chemical Physics*, 339, 104 (2007).
74. Tsuji, I., Kato, H., and Kudo, A., *Angewandte Chemie International Edition*, 117, 3631 (2005); *Angewandte Chemie International Edition*, 44, 3565 (2005).
75. Kudo, A., Tsuji, I., and Kato, H., *Chemical Communications*, 1958 (2002).
76. Tsuji, I., Kato, H., Kobayashi, H., and Kudo, A., *Journal of Physical Chemistry B*, 109, 7323 (2005).
77. Prince, R. and Khesghi, H., "The photobiological production of hydrogen: Potential efficiency and effectiveness as a renewable fuel," *Critical Reviews in Microbiology*, 31, 19–31 (2005).
78. Ghysels, B. and Franck, F., "Hydrogen photo-evolution upon S deprivation stepwise: An illustration of microalgal photosynthetic and metabolic flexibility and a step stone for future biological methods of renewable H<sub>2</sub> production," *Photosynthesis Research*, 106, 145–154 (2010).
79. Mells, A., Zhang, L., Forestier, M., Ghirardi, M., and Seibert, M., "Sustained photobiological hydrogen gas production upon reversible inactivation of oxygen evolution in the green alga *Chlamydomonas reinhardtii*," *Plant Physiology*, 122, 127–135 (2000).
80. Ghirardi, M., Zhang, L., Lee, J., Flynn, T., Seibert, M., Greenbaum, E., and Melis, A., "Microalgae: A green source of renewable H<sub>2</sub>," *Trends in Biotechnology*, 18, 506–511 (2000).
81. Nguyen, A., Thomas-Hall, S., Malnoe, A., Timmins, M., Mussnug, J., Rupprecht, J., Krause, O., Hankamer, B., and Schenk, P., "Transcriptome for photobiological hydrogen production induced by sulfur deprivation in the green alga *Chlamydomonas reinhardtii*," *Eukaryotic Cell*, 7 (11), 1965–1979 (2008).
82. Timmins, M., Thomas-Hall, S., Darling, A., Zhang, E., Hankamer, B., Marx, U., and Schenk, P., "Phylogenetic and molecular analysis of hydrogen producing green algae," *Journal of Experimental Botany*, 60 (6), 1691–1702 (2009).
83. Berberoglu, H. and Pilon, L., "Maximizing the solar to H<sub>2</sub> energy conversion efficiency of outdoor photobioreactors using mixed cultures," *International Journal of Hydrogen Energy*, 35 (2), 500–510 (2010).
84. Lee, J., "Designer proton channel transgenic algae for photobiological hydrogen production," PCT International Patent Application WO2007/134340 A2 (2007).
85. Lee, J., "Designer proton channel transgenic algae for photobiological hydrogen production," US Patent No. 7932437 B2 (2011).
86. Lee, J., "Switchable photosystem-II designer algae for photobiological hydrogen production," US Patent No. 7642405 B2 (2010).
87. Eastlund, B. and Gough, W., Paper Presented at the 163th National Meeting of American Chemical Society, April 14, Boston, MA (1972).
88. McWhirter, R., "Spectral Intensities," in Huddleston, R. and Leonard, S. (eds.), *Plasma Diagnostic Techniques*. Academic Press, New York, 201 (1965).
89. Inoue M., Uehara, R., Hasegawa, N., Gokon, N., Kaneko, H., and Tamaura, Y., "Solar hydrogen generation with H<sub>2</sub>O/ZnO/MnFe<sub>2</sub>O<sub>4</sub> system," ISES, Solar World Congress, Adelaide, Australia 1723–1729 (2001), [www.aseanenergy.info/Abstract/32008845.pdf](http://www.aseanenergy.info/Abstract/32008845.pdf).
90. Brown, L.C., Besenbrauch, G.E., Schultz, K.R., Showalter, S.K., Marshall, A.C., Pickard, P.S., and Funk, J.F., "High efficiency generation of hydrogen fuels using thermochemical cycles and nuclear power," Spring National Meeting of AIChE, Nuclear Engineering Session THa01 139-Hydrogen Production and Nuclear Power, March 11–15, New Orleans, LA (2002).

91. Rosen, M.A., "Developments in the production of hydrogen by thermochemical water decomposition," *International Journal of Energy and Environmental Engineering*, 2 (2), 1–20 (2011).
92. Steinfeld, A. and Palumbo, R., "Solar thermochemical process technology," in Meyers, R. (ed.), *Encyclopedia of Physical Science and Technology*. Academic Press, New York, Vol. 15, 237–256 (2001).
93. Funk, J.E., Conger, W.L., and Cariy, R.H., "Evaluation of multi-step thermochemical processes for the production of hydrogen from water," *Proceedings of the THEME Conference*, March, Miami, FL, SI-11 (1974).
94. Chao, R.E., "Thermochemical water decomposition processes," *Industrial & Engineering Chemistry Process Design and Development*, 13 (2), 94–101 (1974).
95. Weimer, A., "II.1.2 fundamentals of a solar-thermal hydrogen production process using a metal oxide based thermochemical water splitting cycle," DOE Contract No. DE-FC36-05G015044, Annual Progress Report (2006).
96. Roeb, M. and Sattler, C., "HycycleS—Materials and components of hydrogen production by sulfur based thermochemical cycles," FPS-Energy-212470, German Aerospace Center (DLR), Solar research report (2010).
97. Law, V.J., Prindle, J.C., and Gonzales, R.B., "Analysis of the copper sulfate cycle for the thermochemical splitting of water for hydrogen production," Paper submitted for presentation at the 2007 AIChE National Meeting, November, Salt Lake City, UT (2007).
98. Law, V.J., Prindle, J.C., and Gonzales, R.B., "Level 1 and level 2 analysis of the copper sulfate cycle for the thermochemical splitting of water for hydrogen production," Contract No. 6F-003762, Argonne National Laboratory, Lemont, IL (July 2006).
99. Law, V.J., Prindle, J.C., and Gonzales, R.B., "Level 3 analysis of the copper sulfate cycle for the thermochemical splitting of water for hydrogen production," Contract No. 6F-003762, Argonne National Laboratory, Lemont, IL (August 2006).
100. Law, V.J., Prindle, J.C., Bang, R., Hoerger, K., and Ledbetter, J., "Progress report no. 1 experimental studies of the hydrogen generation reaction for the  $\text{CuSO}_4$  cycle," Contract No. 6F-01144, Argonne National Laboratory, Lemont, IL (October 2006).
101. Law, V.J., Prindle, J.C., Bang, R., Hoerger, K., and Ledbetter, J., "Progress report no. 2, experimental studies of the hydrogen generation reaction for the  $\text{CuSO}_4$  cycle," Contract No. 6F-01144, Argonne National Laboratory, Lemont, IL (January 2007).
102. Law, V.J., Prindle, J.C., Bang, R., Hoerger, K., and Ledbetter, J., "Progress report no. 3, experimental studies of the hydrogen generation reaction for the  $\text{CuSO}_4$  cycle," Contract No. 6F-01144, Argonne National Laboratory, Lemont, IL (March 2007).
103. Law, V.J., Prindle, J.C., Bang, R., Hoerger, K., and Ledbetter, J., "Progress report no. 4, experimental studies of the hydrogen generation reaction for the  $\text{CuSO}_4$  cycle," Contract No. 6F-01144, Argonne National Laboratory, Lemont, IL (May 2007).
104. Law, V.J., Prindle, J.C., and Lupulescu, A.I., "Aspen plus modeling of the three-reaction version of the copper-chloride thermochemical cycle for hydrogen production from water," Contract No. 6F-01144, Argonne National Laboratory, Lemont, IL (August 2007).
105. Law, V., Prindle, J., and Gonzales, R., "Analysis of the copper sulphate cycle for the thermochemical splitting of water for hydrogen production," Chemical Engineering Department, Tulane University, New Orleans, LA (2010).
106. Roeb, M., Sattler, C., Kluser, R., Monnerie, N., Oliveira, L., Konstandopoulos, A., Agrafiotis, C. et al., "Solar hydrogen production by a two step cycle based on mixed iron oxides," *Journal of Solar Energy Engineering*, 128, 125–133 (2006).
107. T-Raissi, A., Huang, C., and Muradov, N., "Hydrogen production via solar thermochemical water splitting," NASA/CR-2009-215441, Report of research for period March 2004–February 2008 (2009).

108. Steinfeld, A. and Palumbo, R., "Solar thermochemical process technology," *Encyclopedia of Physical Science and Technology*, 15 (1), 237–256 (2001).
109. Steinfeld, A. and Meier, A., *Solar Fuels and Materials*. Elsevier, Amsterdam, the Netherlands, 623–637 (2004).
110. Steinfeld, A., "Solar hydrogen production via a two-step water-splitting thermochemical cycle based on Zn/ZnO redox reactions," *International Journal of Hydrogen Energy*, 27 (6), 611–619 (2002).
111. Funke, H.H., Diaz, H., Liang, X., Carney, C.S., Weimer, A.W., and Li, P., "Hydrogen generation by hydrolysis of zinc powder aerosol," *International Journal of Hydrogen Energy*, 33 (4), 1127–1134 (2008).
112. Abanades, S., Charvin, P., Lemont, F., and Flamant, G., "Novel two-step  $\text{SnO}_2/\text{SnO}$  water-splitting cycle for solar thermochemical production of hydrogen," *International Journal of Hydrogen Energy*, 33 (21), 6021–6030 (2008).
113. Meier, A. and Steinfeld, A., "Solar thermochemical production of fuels," *Advances in Science and Technology*, 74 (1), 303–312 (2011).
114. Chueh, W.C. and Haile, S.M., "Ceria as a thermochemical reaction medium for selectively generating syngas or methane from  $\text{H}_2\text{O}$  and  $\text{CO}_2$ ," *ChemSusChem*, 2 (8), 735–739 (2009).
115. Kappauf, T. and Fletcher, E.A., "Hydrogen and sulfur from hydrogen sulfide VI. Solar thermolysis," *Energy*, 14 (8), 443–449 (1989).
116. Zaman, J. and Chakma, A., "Production of hydrogen and sulfur from hydrogen sulfide," *Fuel Processing Technology*, 41 (2), 159–198 (1995).
117. Steinfeld, A., "Solar thermochemical production of hydrogen: A review," *Solar Energy*, 78 (5), 603–615 (2005).
118. Perret, R., "Solar thermochemical hydrogen production research (STCH), thermochemical cycle selection and investment priority," Report No. SAND2011-3622, Sandia National Laboratories, Livermore, CA (2011).
119. Almodaris, M., Khorasani, S., Abraham, J.J., and Ozalp, N. (eds.), "Simulation of solar thermo-chemical hydrogen production techniques," ASME/JSME 8th Thermal Engineering Joint Conference, March 13–17, ASME, Honolulu, HI (2011).
120. Aoki, A., Ohtake, H., Shimizu, T., Kitayama, Y., and Kodama, T., "Reactive metal-oxide redox system for a two-step thermochemical conversion of coal and water to CO and  $\text{H}_2$ ," *Energy*, 25 (3), 201–218 (2000).
121. Osinga, T., Olalde, G., and Steinfeld, A., "Solar carbothermal reduction of ZnO: Shrinking packed-bed reactor modeling and experimental validation," *Industrial & Engineering Chemistry Research*, 43 (25), 7981–7988 (2004).
122. Osinga, T., Frommherz, U., Steinfeld, A., and Wieckert, C., "Experimental investigation of the solar carbothermic reduction of ZnO using a two-cavity solar reactor," *Journal of Solar Energy Engineering*, 126 (1), 633–637 (2004).
123. Epstein, M., Olalde, G., Santén, S., Steinfeld, A., and Wieckert, C., "Towards the industrial solar carbothermal production of zinc," *Journal of Solar Energy Engineering*, 130 (1), 014505 (2008).
124. Wieckert, C., Frommherz, U., Kräupl, S., Guillot, E., Olalde, G., Epstein, M., Santen, S., Osinga, T., and Steinfeld, A., "A 300 kW solar chemical pilot plant for the carbothermic production of zinc," *Journal of Solar Energy Engineering*, 129 (2), 190–196 (2007).
125. Kromer, M., Roth, K., Takata, R., and Chin, P., "Support for cost analyses on solar-driven high temperature thermochemical water-splitting cycles," Report No. DE-DT0000951, TIAx, LLC2011, Lexington, MA (February 22, 2011).
126. Lede, J., Lapique, F., and Villermaux, J., *International Journal of Hydrogen Energy*, 8, 675 (1983).
127. Lapique, F., Lede, J., Villermaux, J., Caler, B., Baumard, J., Anthony, A., Abdul-Aziz, G., Puechbertz, D., and Ledrix, M., *Entropie*, 19, 42 (1983).

128. Beghi, G., "A decade of research on thermochemical water hydrogen at the Joint Research Center, Ispra," *International Journal of Hydrogen Energy*, 11 (12), 761–771 (1986).
129. Besenbruch, G., "General atomic sulfur-iodine thermochemical water splitting process," *American Chemical Society, Division of Petroleum Chemistry*, preprint, 271, 48 (1982).
130. Sato, S., Shimizu, S., Nakajima, N., and Ikezoe, Y., "A nickel-iodine-sulfur process for hydrogen production," *International Journal of Hydrogen Energy*, 8 (1), 15–22 (1983).
131. Abanades, S., Charvin, P., Flamant, G., and Neveu, P., "Screening of water-splitting thermochemical cycles potentially attractive for hydrogen production by concentrated solar energy," *Energy*, 31, 2805–2822 (2006).
132. Marchetti, C., *Chemical Economy & Engineering Review*, 5, 7 (1973).
133. DeBeni, G. and Marchetti, C., "A chemical process to decompose water using nuclear heat," Paper presented at the 163rd National Meeting of the American Chemical Society, April 9, Boston, MA (1972).
134. Appleby, A. and Bockris, J., *International Journal of Hydrogen Energy*, 6, 1 (1981).
135. Pyle, W., Hayes, M., and Spivak, A., "Direct solar-thermal hydrogen production from water using nozzle/skimmer and glow discharge," IECEC96535, Report from H-ION Solar Inc., Richmond, CA (2010).
136. Baykara, S., "Experimental solar water thermolysis," *International Journal of Hydrogen Energy*, 29 (14), 1459–1469 (2004).
137. Harvey, W.S., Davidson, J.H., and Fletcher, E.A., "Thermolysis of hydrogen sulfide in the temperature range 1350–1600 K," *Industrial & Engineering Chemistry Research*, 37 (6), 2323–2332 (1998).
138. Perkins, C. and Weimer, A.W., "Solar-thermal production of renewable hydrogen," *AIChE Journal*, 55 (2), 286–293 (2009).
139. Venugopalan, M. and Jones, R., *Chemistry of Dissociated Water Vapor and Related Systems*. Wiley, New York (1968).
140. Schultz, K., "Thermochemical production of hydrogen from solar and nuclear energy," Presentation to the Stanford Global Climate and Energy Project, April 14, General Atomics, San Diego, CA (2003).
141. Kerr, W. and Majumdar, D., "Aqueous homogeneous reactor for hydrogen production," in Veziroglu, T. (ed.), *Hydrogen Energy, Part A*. Plenum Press, New York, 167 (1975).
142. Gomberg, H. and Gordus, A., *Journal of Fusion Energy*, 2, 319 (1982).
143. Northrup, C., Jr., Gerlach, T., Modreski, P., and Galt, J., *International Journal of Hydrogen Energy*, 3 (1) (1978).
144. Fudali, R., *Geochimica et Cosmochimica Acta*, 29, 529 (1948).
145. Kennedy, G., *American Journal of Science*, 246, 529 (1948).
146. Bockris, J. and Gutmann, F., *Applied Physics Communications*, 1, 121 (1981–1982).
147. Farady, M., *Diary*. Bell, London, Vol. 1, 381 (1932).
148. Appleton, A., "Super conducting DC machines," in Fouer, S. and Schwartz, B. (eds.), *Superconducting Machines and Devices*. Plenum Press, New York, 219 (1973).
149. Boyd, R. and Burns, G., in Lifshitz, A. (ed.), *Shock Waves in Chemistry*. Marcel Dekker, New York, 131 (1981).
150. Kasal, P. and Bishop, R., Jr., US Patent No. 3963830 (1976).
151. Kasal, P. and Bishop, R., Jr., *The Journal of Physical Chemistry*, 81, 1527 (1977).
152. England, C., in Veziroglu, T., Van Vorst, W., and Kelley, H. (eds.), *Hydrogen Energy Progress IV, Proceedings of the World Hydrogen Energy Conference IV*, June 13–17, Pasadena, CA, Vol. 2, p. 462, Pergamon Press, Oxford (1982).
153. Fletcher, E.A. and Moen, R.L., "Hydrogen and oxygen from water," *Science*, 197, 1050–1056 (1977).

---

# 12 Methane from Gas Hydrates

## 12.1 INTRODUCTION: WHAT IS GAS HYDRATE AND HOW IS IT FORMED?

Clathrate hydrates are solid crystalline “inclusion” compounds, which are formed when water is contacted with small hydrophobic molecules such as methane, ethane,  $\text{H}_2\text{S}$ , and  $\text{CO}_2$  [1–7] (Harrison, 2010, pers. comm.) under certain pressure and temperature conditions. When the inclusion compound is a constituent of natural gas, clathrate hydrates are also referred to as gas hydrates [1–15] (Harrison, 2010, pers. comm.). The gas (or methane) hydrate composition is in general 5.75 mol of water for every molecule of methane, although this number does depend on the cage structure of the water ice. Various molecular structures of gas hydrate and clathrate are illustrated in Figure 12.1 [2]. The average density of methane hydrate is about 0.9 g/cc. Under standard conditions, the volume of methane hydrate will be 164 times less than that of methane gas [1–16] (Harrison, 2010, pers. comm.).

Gas hydrates are formed when natural gas and water are brought together under suitable conditions of low temperatures and elevated pressures. The formation depends on (1) the presence of sufficient amount of water, (2) the presence of hydrate former, and (3) the appropriate pressure and temperature conditions. In a gas hydrate reservoir, free gas, ice, water, and other components such as ethane, propane, hydrogen sulfide, and carbon dioxide can be found at different temperatures, pressures, and depth values. Two- and three-phase equilibria curves [5–7,13–16] (Harrison, 2010, pers. comm.) are used for correlation between phases where the amount of components present plays a significant role; very small and large amounts of water are not conducive to the formation of hydrates.

The gas hydrates are unstable compounds in which the water molecules form a sort of cage or lattice around the methane molecules, and the two establish weak chemical bonds with one another. Methane from methane hydrates must be released *in situ* due to the inherent instability of hydrate molecules. The temperature at which methane hydrate is stable depends on the prevailing pressure. For example, at 0°C, it is stable under a pressure of about 30 atm, whereas at 25°C, nearly 500 atm pressure is needed to maintain its integrity. The occlusion of other gases within the ice structure tends to add stability, whereas the presence of salts requires higher stabilizing pressures. Appropriate conditions of temperature/pressure exist on the earth in the upper 2000 m of sediments in two regions: (1) permafrost at high latitudes in polar regions where the surface temperatures are very low and (2) submarine continental slopes and rises where not only is the water cold but the pressures are high (>30 atm). Phase boundary of methane hydrates in permafrost and deep-sea regions

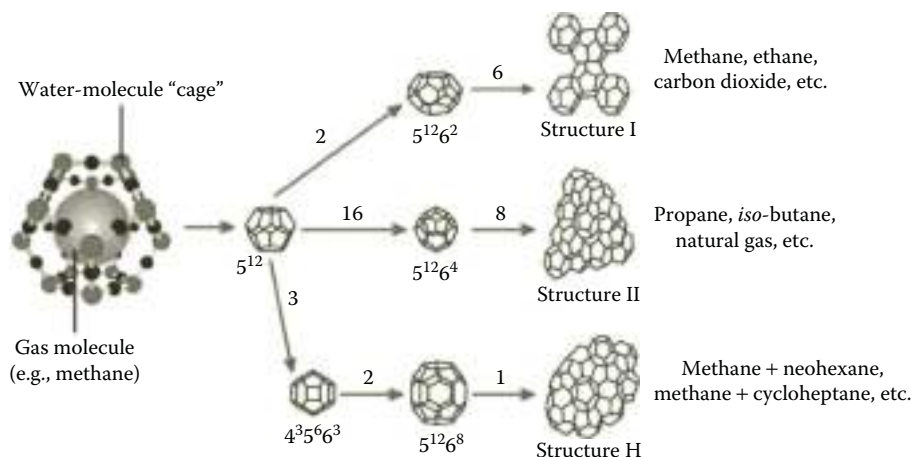


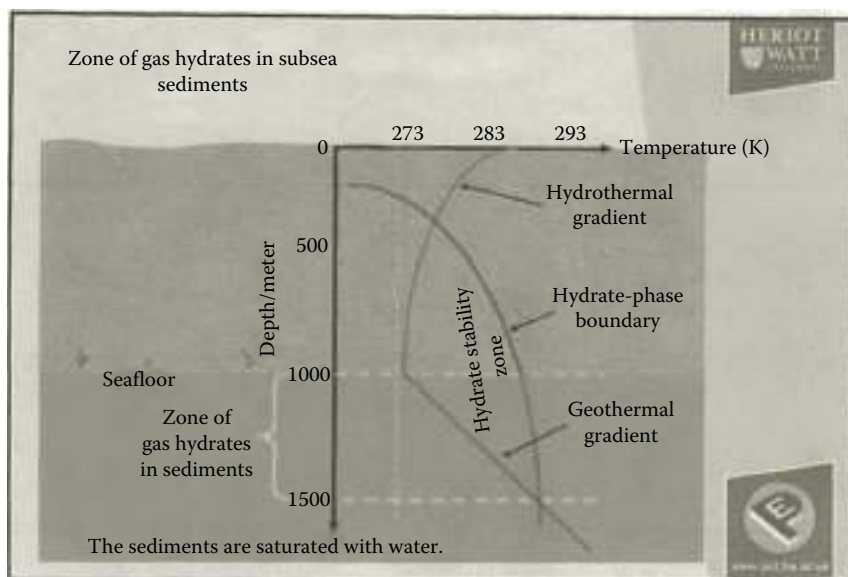
**FIGURE 12.1** (See color insert.) Various molecular structures of gas hydrate and clathrate depending on guest molecules. (From "Methane hydrates," A communication by Center for Gas Hydrate Research, Heriot-Watt University, Edinburgh, The Hydrate forum Org., 2012. With permission.)

are graphically illustrated in Figure 12.2a and b (Tohidi, 2013, pers. comm.). These two figures show the estimations of regions where the stable hydrate formations are most likely to occur. The pressure–temperature phase diagram for methane hydrate is shown in Figure 12.3 [1,2,13–15] (Harrison, 2010, pers. comm.).

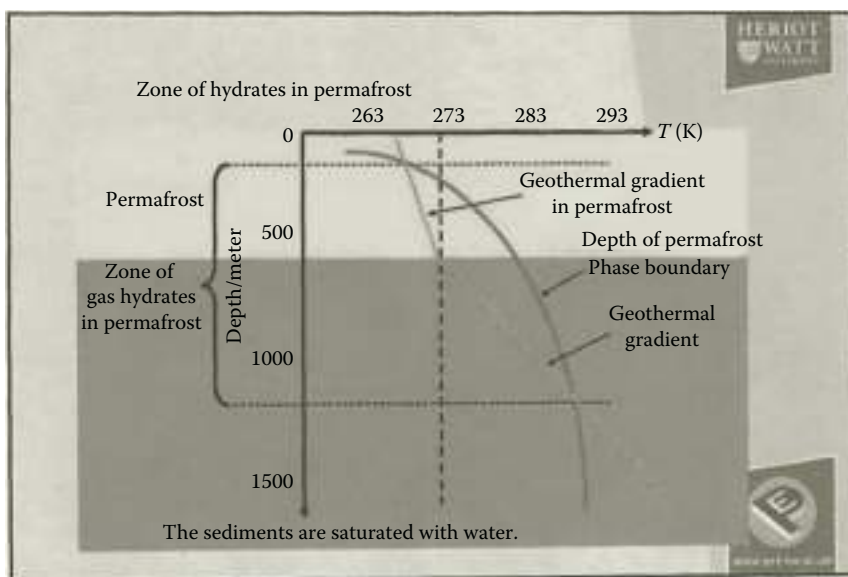
## 12.2 SOURCES, SIZES, AND IMPORTANCE OF GAS HYDRATE DEPOSITS

Gas hydrates were only discovered in the late twentieth century, and along with geopressurized zone gas, they are the best means of prolonging the carbohydrate age of energy [3,9,17–59] (Harrison, 2010, pers. comm.; USGS, 2012, pers. comm.). As mentioned earlier, vast quantities of methane gas hydrates can be discovered in sediments and sedimentary rocks within about 2000 m of the earth surface in polar and deep-water regions. Furthermore, the required conditions are found either in polar continental sedimentary rocks where surface temperature is <0°C or in oceanic sediment at water depths >300 m where the water temperature is around 2°C. Methane hydrates can also be formed in fresh water but not in salt water.

In 1995, the US Geological Survey (USGS) conducted a study to assess the quantity of natural gas hydrate (NGH) resources in the United States and found that the estimated quantity exceeded known conventional domestic gas resources [1]. The USGS estimates that methane hydrates may contain more carbon than world's coal, oil, and conventional natural gas combined. A comparison of estimated carbon in gas hydrates and other carbon sources on this earth is depicted



(a)



(b)

**FIGURE 12.2** (See color insert.) Gas hydrate stability fields for (a) nominal marine settings and (b) permafrost settings. (From Tohidi, 2013, pers. comm. With permission.)

in Table 12.1 [1,60] (Tohidi, 2013, pers. comm., numerous works of Collet and coworkers at USGS). These data clearly show the dominance of gas hydrates as a source of carbon.

Types of methane hydrate deposits found on this earth are graphically illustrated in Figure 12.4 (Methane hydrate..., 2013, pers. comm.). Methane hydrates

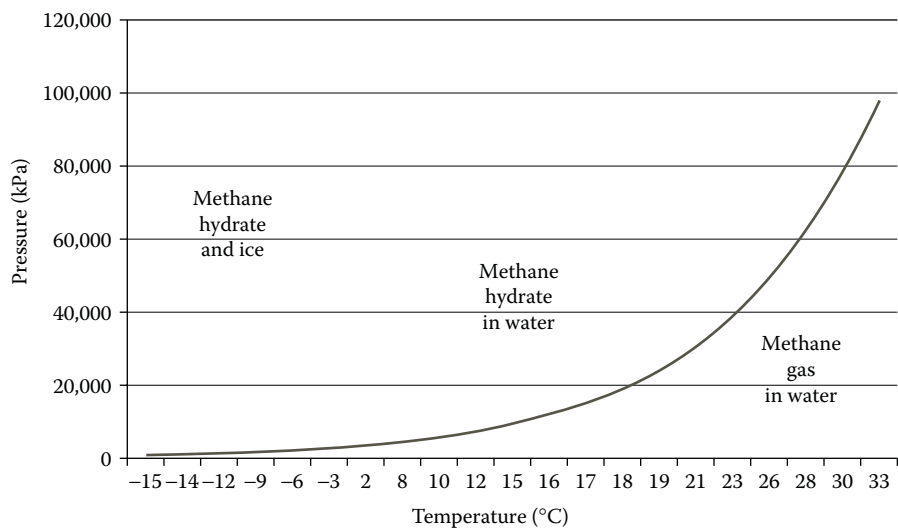


**FIGURE 12.3** Methane hydrate phase diagram. The horizontal axis shows temperature from  $-15^{\circ}\text{C}$  to  $33^{\circ}\text{C}$ , the vertical axis shows pressure from 0 to 120,000 kPa (0–1184 atm). For example, at  $4^{\circ}\text{C}$ , hydrate forms above a pressure of about 50 atm. (Adapted from “Methane hydrate phase diagram,” Wikipedia, the free encyclopedia, 2010.)

**TABLE 12.1**  
**Distribution of Organic Carbon in the Earth**

Source of Carbon	Amount ( $10^5$ g of Carbon) <sup>a</sup>	Total Carbon (%)
Gas hydrates (onshore and offshore)	10,000	53.26
Recoverable and nonrecoverable fossil fuels (coal, oil, natural gas)	5,000	26.63
Soil	1,400	7.46
Dissolved organic matter in water	980	5.22
Land biota	830	4.42
Peat	500	2.68
Detrital organic matter	60	0.33
Atmosphere	3.6	0.0
Marine biota	3	0.0

Source: Englezos, P., *Industrial & Engineering Chemistry Research*, 32, 1251–1274, 1993; Kvenvolden, K.A., *Chemical Geology*, 71, 41–51, 1988. With permission; Tohidi, 2013, pers. comm.; Collet’s work at USGS.

Note: This excludes dispersed organic carbon such as kerogen and bitumen, which equals nearly 1000 times the total amount shown in the table.

<sup>a</sup> These are best estimates.

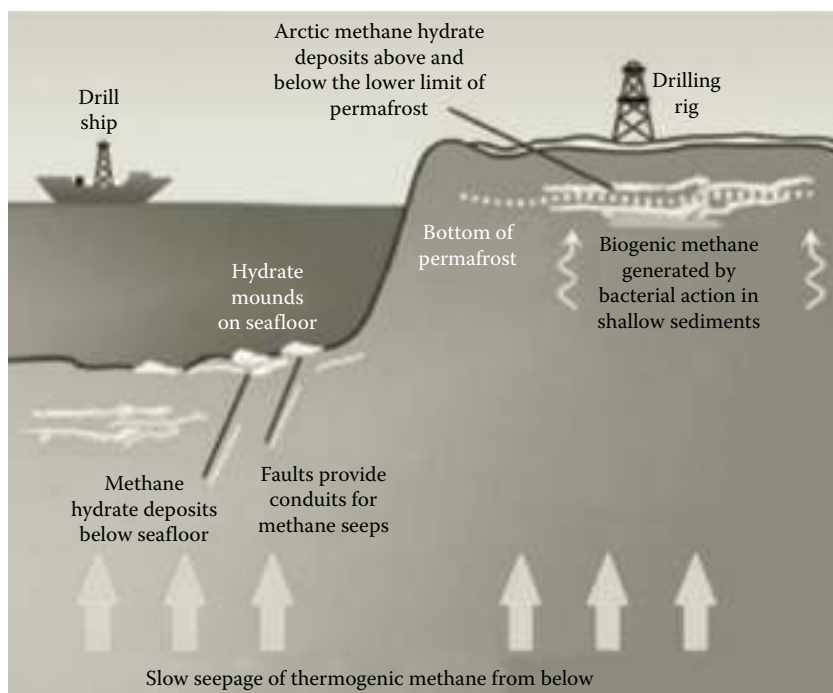


**FIGURE 12.4** Types of methane hydrate deposits. (Adapted from “Methane hydrate—The world largest natural gas resource is trapped beneath permafrost and ocean sediments,” Geology.com, a communication, 2013.)

are believed to be formed by the migration of gas from depth along geological faults, followed by precipitation, or crystallization on contact of the rising gas stream with cold seawater. Methane hydrates are also present in deep arctic sea cores and record a history of atmospheric methane concentrations dating to 800,000 years ago [17–27].

In polar regions, methane hydrates are found where temperatures are cold enough for onshore and offshore permafrost to be present. In offshore sediments, methane hydrates are found at water depths of 300–500 m, according to prevailing water temperatures. Continental deposits have been located in Siberia and Alaska in sandstone and siltstone beds at depth <800 m. Oceanic deposits seem to be widespread in the continental shelf and can occur within the sediments at depth or close to the sediment–water interface. They may cap even larger deposits of gaseous methane. In 2008, Canadian and Japanese researchers extracted a constant stream of natural gas from Mallik gas hydrate field in the Mackenzie River delta [17,36,39,43,48,49,51] (USGS, 2012, pers. comm.). This hydrate field was first discovered by Imperial Oil Co. in 1971–1972.

The occurrence of gas hydrates on the Alaska North Slope was confirmed in 1972 in the northwest part of the PBU (Prudhoe Bay Unit) field [17,46,48,49] (USGS, 2012, pers. comm.), and the North Slope now is known to contain several well-characterized gas hydrate deposits. The methane hydrate stability zone

extends beneath most of the coastal plain province and has thicknesses >1000 m in the Prudhoe Bay, Kuparuk River, and Milne Point oil fields on the North Slope of Alaska. The estimated amount of gas within these gas hydrate accumulations is ~37–44 Tcf, which is equivalent to twice the volume of conventional gas in the Prudhoe Bay field [11]. More details on the locations of gas hydrate reservoirs in Alaska are given in various USGS reports (2012, pers. comm.). As mentioned in Refs. [3,9,17–54] (USGS, 2012, pers. comm.), besides Alaska, hydrate fields have been discovered in other countries of the world, which include Japan, China, India, Korea, Russia, and Canada. In the United States, hydrates have also been discovered in the Gulf of Mexico [3,9,40,47].

The size of the oceanic methane clathrate reservoir is poorly known. The recent estimates constrained by direct sampling suggest the global inventory occupies between 1 and 5 million cubic kilometers. This estimate corresponds to 500–2500 gigatons carbon that is substantially larger than 230 gigatons estimated for other natural gas resources. The reservoir in Arctic permafrost has been estimated at 400 gigatons, but no estimates for Antarctic reservoirs are available. Low concentrations at most sites imply that only small percentage of clathrate deposits may be economically recoverable [3,9,17–54] (USGS, 2012, pers. comm.).

There are two distinct types of oceanic deposits. The most common type is one where methane is contained in I clathrate and generally found in the depth of the sediment. This type is derived from microbial reduction of  $\text{CO}_2$ . These deposits are located within a mid-depth zone around 300–500 m thick in the sediments. The second less common type is found near the sediment surface. This type is formed by the thermal decomposition of organic matter. Examples of this type are found in the Gulf of Mexico and Caspian Sea. Some deposits have characteristics intermediate between the microbial and thermal source types, and they are considered to be formed from a mixture of two.

While the sedimentary methane hydrate reservoir probably contains 2–10 times the currently known reserves of conventional natural gas, the majority of the site's deposits are too dispersed to recover economically. The detection of viable sources is also problematic. The technology for extraction of methane gas from hydrate is also an issue. To date, Messoyakha Gas field in the Russian city of Norilsk is the only sustained commercial operation. Japan is planning to develop a commercial operation by 2016 [20,33,43], and China has invested \$100 million over 10 years to study hydrates [45]. A possible economic reserve in the Gulf of Mexico may contain  $10^{10} \text{ m}^3$  of gas [3,9,40,47].

Gas hydrates are of great importance for a number of reasons graphically illustrated in Figure 12.5 [54]. Naturally occurring methane gas clathrates contain an enormous amount of strategic energy reserve [37,39,46]. In offshore hydrocarbon drilling and production operations, gas hydrates can cause major and potentially hazardous flow assurance problems. The recovery of gas hydrates by carbon dioxide provides an opportunity to dispose carbon dioxide by sequestration [61–83]. Gas hydrates also provide an increasing awareness of the relationship between hydrate and subsea slope stability. Gas hydrates also pose a potential danger to deep-water drilling installations, pipelines, and subsea cables [55–59,84–116] (LaBelle, 2012, pers. comm.; Tohidi, 2012, pers. comm.). Finally, it poses a long-term concern

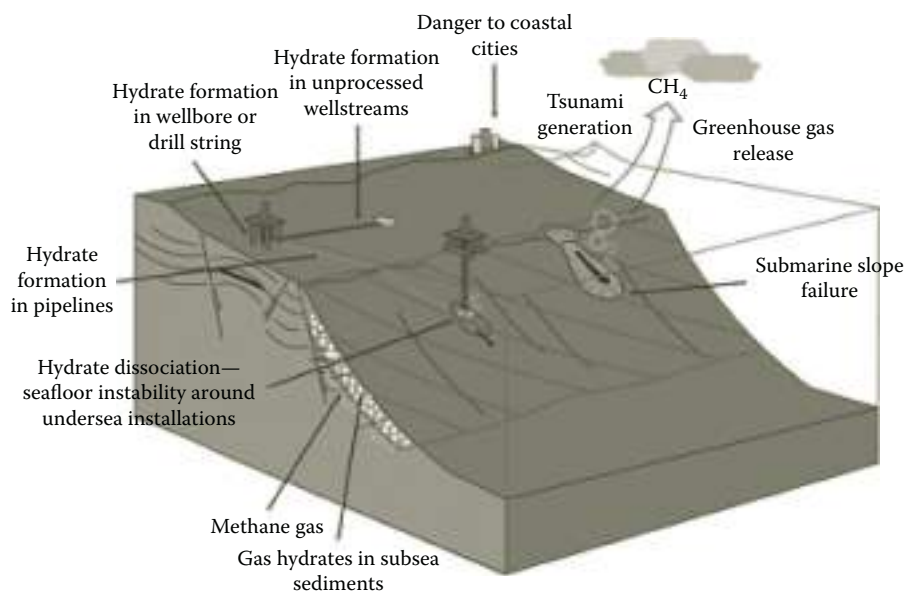


**FIGURE 12.5** Reasons for the importance of methane hydrates. (From “Why are gas hydrates important,” Institute of Petroleum Engineering, Heriot Watt University, Edinburgh, 2011. With permission.)

regarding hydrate stability and methane release and its subsequent effect on global climate change [117–180] (Kennett, 2012, pers. comm.). Some of these topics are briefly discussed in Sections 12.3 through 12.5.

## 12.3 IMPORTANCE OF GAS HYDRATES ON OFFSHORE OIL AND GAS OPERATIONS

The existence of gas hydrates affects both drilling and production of offshore oil and gas operations [55–59,84–116] (LaBelle, 2012, pers. comm.; Tohidi, 2012, pers. comm.). These effects are briefly described in Sections 12.3.1 through 12.3.3 [91–116] (LaBelle, 2012, pers. comm.; Tohidi, 2012, pers. comm.).

### 12.3.1 DRILLING

Methane clathrates (hydrates) are commonly formed during natural gas production operations, when liquid water is condensed in the presence of methane at high pressure. It is known that larger hydrocarbon molecules such as ethane and propane can also form hydrates, although these are not as stable as methane hydrates. Once formed, hydrates can block pipeline and processing equipment. They are generally removed by (1) reduction of the pressure, (2) addition of heat, or (3) dissolving them using chemicals such as methanol and ethylene glycol. Care must be taken to ensure that the removal of the hydrates is carefully controlled, because as the

hydrate undergoes phase transition, the release of water and methane can occur at very high rates. The rapid release of methane gas in a closed system can result in a rapid increase in pressure [104,105], which can be harmful to the drilling operation. In recent years, hydrate formation during drilling operation is controlled with the use of kinetic hydrate inhibitors [96–99,113–116], which dramatically slow the rate of hydrate formation and anti-agglomerates, which prevent hydrates from sticking together to block pipes and other parts of equipment.

When drilling in oil- and gas-bearing formations submerged in deep water [55–59,84,85], the reservoir gas may flow into the well bore and form gas hydrates owing to the low-temperature and high-pressure conditions found during deep-water drilling. The gas hydrates may then flow upward with drilling mud or other discharged fluids. As they rise, the pressure in the annulus decreases and the hydrates dissociate into gas and water. The rapid gas expansion ejects fluid from the well, reducing the pressure further, which leads to more hydrate dissociation and further fluid ejection. The resulting violent expulsion of fluid from the annulus is one potential cause or contributor to what is referred to as a “kick” [104,105], which can cause blowouts. This can cause serious well safety and control problems and create hazardous conditions such as flow blockage, hindrance to drill string movement, loss of circulation, and even abandonment of the well. Since gas hydrates contain 85% water, their formation can withdraw water from drilling fluids, changing the properties of the fluids, thus causing salt precipitation, an increase in fluid weight, or the formation of solid plug.

The condition of the hydrate formation during kick depends on the composition of the kick gas, temperature, and pressure. A combination of salts and chemical inhibitors can provide a required inhibition to avoid hydrate formation, particularly at water depths >1000 m [96–99,115–116].

### 12.3.2 PRODUCTION BY ENHANCED OIL AND GAS RECOVERY METHODS

Enhanced oil and gas recovery methods increase the risk of the gas hydrate formation. Process equipment and multiphase transfer lines from wellhead to the production platform where low-temperature and high-pressure conditions exist are prone to hydrate formation. The following methods are generally adopted to reduce hydrate problems in hydrocarbon transfer lines and process facilities [86–93]:

1. Use high flow rates, which limit the time for hydrate formation in a volume of fluid, thereby reducing the kick potential [104,105]. Make careful measurement of line flow to detect incipient hydrate plugging [104,105], particularly at low gas production rate. Also, monitor the pressure rise in wellcasing after it is “shut in” (isolated). The hydrate formation will decrease the rate of pressure rise [104,105].
2. Additions of energy (e.g., the energy released by setting cement used in well completion) can raise the temperature and convert hydrates to gas, producing a “kick.”
3. For a given pressure, operate at temperatures higher than the hydrate formation temperature. This can be done by insulation or heating of

the equipment. At fixed temperature, operate at pressure below hydrate formation pressure.

4. Reduce water concentration to avoid hydrate formation. Change feed composition.
5. Add compounds such as methanol, salts, or other kinetic inhibitors to prevent hydrate formation. Also prevent hydrate clustering by using hydrate growth modifiers or covering working surfaces with hydrophobic substances [86–93,104,105].

With conventional oil and gas exploration methods extending into progressively deeper waters, the potential hazards gas hydrates can pose to operation are becoming increasingly more important. Two possible events—the release of overpressurized gas (or fluids) trapped below the zone of hydrate stability and destabilization of *in situ* hydrates—can be hazardous. Care must be taken to avoid these incidences [96–102,113–116].

### 12.3.3 NATURAL GAS HYDRATES VERSUS LIQUEFIED NATURAL GAS IN TRANSPORTATION

Since methane clathrates are stable at a higher temperature than liquefied natural gas (LNG) ( $-20^{\circ}\text{C}$  vs.  $-162^{\circ}\text{C}$ ) [108], there is some interest in converting natural gas into clathrates rather than liquefying it when transporting it by seagoing vessels. A significant advantage would be that the production of NGH from natural gas at the terminal would require a smaller refrigeration plant and less energy than LNG would. Offsetting this, for 100 tons of methane transported, 750 tons of methane hydrate would have to be transported. Since this would require a ship of 7.5 times greater displacement, or require more ships, an application of this approach has not been economically attractive.

## 12.4 ENVIRONMENTAL IMPACTS OF GAS HYDRATES

Gas hydrates alter the physical properties of the sediment. In the absence of hydrates, fluids and gas migrate freely at seafloor. The solid hydrates reduce permeability and restrict sediment consolidation, fluid expulsion, and cementation. The hydrate dissociation leads to increased pore fluid pressure and underconsolidated sediments, with a reduced cohesive strength compared to overlying hydrate-bearing sediments, forming a zone of weakness. This zone of weakness could act as a site of failure in the event of increased gravitational loading or seismic activity. The link between seafloor failure and gas hydrate destabilization is a well-established phenomenon [1–15]. The exploration of hydrates from ocean floor by drilling through hydrate zones can create the problem of destabilizing support foundations for platforms and production wells. The disruption of ocean floor can also result in surface slumping or faulting, which can endanger work crews and the environment [1–15].

Since hydrates prevent sediment compaction, their *in situ* dissociation can also cause climate change and falling of sea level. If the hydrate breaks down, it will weaken the

sediment and may cause submarine landslides and simultaneously release methane into the atmosphere. The methane released from the reservoir to the atmosphere can contribute to the climate change. Submarine landslides can cause tsunamis and catastrophic coastal flooding. The thickness of the gas hydrate stability zone (GHSZ) in continental margins depends on water depth (hydrostatic pressure), water temperature, geothermal gradient, and gas composition [1,60] (Tohidi, 2013, pers. comm.).

Methane is a powerful greenhouse gas. Despite its short atmospheric half-life of seven years, methane has a significant global warming potential [1–15] (Harrison, 2010, pers. comm.). Recent research carried out in 2008 in the Siberian Arctic has shown millions of tons of methane being released [153,162,166,168,169,176] (Kennett, 2012, pers. comm.), with concentrations in some regions reaching up to 100 times above normal [1–16] (Harrison, 2010, pers. comm.). Past and future climate changes can be linked to methane released from gas hydrates.

Currently, the link between stability of gas hydrates and global warming is being examined. Since methane warms the environment 15–20 times more than carbon dioxide, the release of methane can create a chain reaction for global warming, leading to more hydrate instability with additional release of methane. Methane release in air eventually (within 10 years) is converted to carbon dioxide, another greenhouse gas [117–180] (Kennett, 2012, pers. comm.).

The analysis of the link between gas hydrate and climate warming can be divided into five parts [117–180] (Kennett, 2012, pers. comm.):

*Region 1: Thick ( $\geq 300$  m) onshore permafrost.* Gas hydrates that occur within or beneath thick terrestrial permafrost will remain largely stable even if climate warming lasts hundreds of years. The warming could, however, cause hydrates at the top of the stability zone, about 625 ft below the earth's surface to dissociate over thousands of years [117–180] (Kennett, 2012, pers. comm.). It contributes <1% of the total hydrates, and its effect on climate change will be minimal.

*Region 2: Subsea permafrost on the circum-Arctic shelves.* The shallow water continental shelves that circle the parts of the Arctic Ocean were formed when sea-level rise during the past 10,000 years inundated permafrost that was at the coastline. The methane hydrates in subsea permafrost that is thawing beneath these continental shelves is being released now. While this methane can rise to ocean surface and then to atmosphere, the amount is only considerably less than about 1% of the world gas hydrates [117–180] (Kennett, 2012, pers. comm.).

*Region 3: Upper edge of stability (or deep-water marine hydrates at the feather edge of GHSZ).* Gas hydrates on upper continental slopes beneath 1000–1600 ft of water lie at the shallowest water depth for which methane hydrates are stable. The upper continental slopes that ring all the continents could host gas hydrates in zones that are roughly 30 ft thick. Within the next 100 years, warm water can completely dissociate these hydrates, but they are more likely to be oxidized in water than released in the atmosphere. These hydrates contribute about 3.5% of the earth's total hydrates [117–180] (Kennett, 2012, pers. comm.).

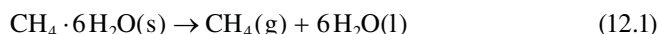
*Region 4: Deep-water gas hydrates.* Ninety-five percent of earth's gas hydrates are at depths >3000 ft. Even with an increase in the ocean temperature, they are likely to stay stable over thousands of years. They also occur deep within the sediments, and the released methane will remain in the sediments, and if they move upward, they will form new hydrates or consumed by oxidation within water [117–180] (Kennett, 2012, pers. comm.).

*Region 5: Seafloor gas hydrate mounds.* At some marine seeps such as the Gulf of Mexico, massive relatively pure gas hydrate occurs in seafloor mounds. While seafloor gas hydrate mounds and shallow subsea floor gas hydrate constitute only a trace amount of the global gas hydrate inventory, they can dissociate rapidly due to the expulsion of warm fluids from the seafloor and release significant amount of methane to the atmosphere.

Based on the analysis of these five regions, a general consensus [117–180] (Kennett, 2012, pers. comm.) is that catastrophic widespread dissociation of methane gas hydrates will not be triggered by continued climate warming at a contemporary rate (0.2°C per decade) over a timescale of few hundred years. In spite of this conclusion, there has been an enormous interest in studying methane release from hydrates to the atmosphere and its effect on environment. The vast literature [117–180] (Kennett, 2012, pers. comm.) is cited here to demonstrate the significant interest on the subject.

## 12.5 PRODUCTION OF METHANE FROM GAS HYDRATE RESERVOIRS

Hydrates are known to occur at temperatures <295 K and pressure >3000 kPa. The dissociation of these hydrates occurs as



with enthalpy = 10–20 kcal/mol of gas dissociated [1–16] (Harrison, 2010, pers. comm.). This reaction requires an external energy source to propagate along the right-hand side [1–16] (Harrison, 2010, pers. comm.).

In conventional gas reservoirs, natural gas migrates to the recovery point via pressure gradients. For these reservoirs, the recovery rate is a function of the formation permeability and pressure gradients established between the reservoir and the extraction well(s). Production of methane from hydrate-bearing deposits requires additional energy to dissociate the crystalline water lattice that forms the gas hydrate structure. A variety of methods have been proposed for producing natural gas from hydrate deposits: (1) thermal stimulation, where the temperature is increased above the hydrate stability region; (2) depressurization, where the pressure is decreased below the hydrate stability region; (3) chemical injection of inhibitors, where the temperature and pressure conditions for hydrate stability are shifted; (4) CO<sub>2</sub> or mixed CO<sub>2</sub> and N<sub>2</sub> exchange, where CO<sub>2</sub> and N<sub>2</sub> replace CH<sub>4</sub> in the hydrate structure; and (5) enhanced gas hydrate recovery (EGHR) methods, where two-phase emulsion (of CO<sub>2</sub> and water) and other solution injection techniques are used to replace methane

from hydrate structure. Each of these methods is briefly reviewed in Sections 12.5.1 through 12.5.6. This section also briefly reviews the numerical simulations that have been carried out for methane recovery from hydrates. Finally, production research that has been carried out for commercial sites is briefly assessed.

### 12.5.1 THERMAL STIMULATION

The recovery of methane gas from gas hydrates via thermal stimulation has been examined both experimentally [181–183] and theoretically [184–187]. Technologies for implementing thermal stimulation include steam injection, cyclic steam injection, fire flooding, hot brine injection and electromagnetic heating. The techniques of steam injection and cyclic steam injection are very similar to those used in the recovery of conventional and unconventional oils. Various possibilities for heating hydrates using steam or cyclic steam injections have been examined in the literature [182,187]. All of these techniques, however, suffer from high heat losses, and by-products of fire flooding can dilute the produced natural gas. The energy efficiency of electromagnetic heating is also low.

A more promising approach is to inject a saline aqueous solution at an elevated temperature into gas hydrate-bearing geological reservoir. In this method, the sensible heat carried by the brine solution is discharged to the gas hydrates by a convective heat-transfer mechanism. The dissolved salt depresses the dissociation temperature of the gas hydrate. The experimental evidences indicate that with the injection of brine, the hydrates become colloidal and migrate convectively with the brine [188–190]. Tang et al. [181,191] showed that the energy efficiency of the hot brine injection process is dependent on the brine temperature, injection rate, and initial hydrate saturation.

The energy efficiency is defined as the ratio of combustion heat of produced gas over the heat input of the brine. The study showed that a better energy efficiency was obtained at higher initial hydrate saturation and lower temperature and injection rates [181–188]. This higher energy efficiency is, however, accompanied by lower production rates. For moderate to high temperature and injection rate, about 50% of the recovered energy from methane is used to heat the brine solution. A modification of this approach was suggested by Chatterji and Griffith [78] who proposed an injection of two aqueous fluids that react and produce the heat required to release methane from the hydrates. This type of acidic and basic solutions reactions will yield a hot salt solution, and this will not require the external heating of brine solution, thereby improving the energy efficiency.

### 12.5.2 DEPRESSURIZATION

Gas hydrate production via depressurization is considered to be the most economically promising technology [190,192–200]. This method has been adopted in Messoyakha field in northern Russia, which contains both free natural gas and hydrates. This reservoir has been constantly producing natural gas because of dissociation of gas hydrates into gas due to depressurization. The production rate in this field is, however, controlled by the heat transfer toward the hydrate dissociation region.

Moridis et al. [197,201,202] and Moridis [203] numerically simulated the effect of depressurization at Mallik site assuming  $0.03^{\circ}\text{C}/\text{m}$  temperature gradient in the hydrate-bearing formation. The simulation showed a vertical drop in temperature in response to depressurization and hydrate dissociation. This temperature drop can be reversed by the injection of warmer water in the well, which provides the needed energy to sustain hydrate dissociation in the depressurized system. The simulation also indicated that, when steam or hot methane gas was injected from a second well, natural gas production was superior in terms of the ratios of produced gas to water and fraction of produced methane from hydrates.

Several other simulation studies showed that hydrate dissociation rates and associated gas productions are controlled by the far-field reservoir pressure and temperature, via energy supplied by natural gas conveyed from the far field to the dissociation front [203–212]. Few studies have reported experimental data of gas recovery by depressurization [194,195]. While depressurization is a viable option because of thermal self-regulation of gas hydrates, the method results in slow production rates. Sustained production requires a heat source, which at the Messoyakha field is supplied by thermal conduction and convection in the dissociation zone. This heat transfer ultimately controls the production rate.

There are three important mechanisms involved in the depressurization of the gas hydrates: (1) kinetics of dissociation, (2) conductive heat transfer, and (3) convective flow of fluids like gas and water. A significant theoretical work that uses a three-dimensional model of a porous media and simulates the exact conditions of a reservoir with regard to all the mechanisms involved has been reported [201–214]. However, to this date, conclusions of such analysis are only based on certain assumptions, whose validity needs to be experimentally verified. Often a two-well system involving a combination of depressurization at the production well and a thermal input (by hot fluid injection) at the injection well appears to be better than a single vertical system [190,192–200].

### 12.5.3 INHIBITOR INJECTION

Sung et al. [214], Kawamura et al. [215], and Li et al. [216,217] showed that the thermodynamic inhibitors lower the hydrate formation temperature, which can result in hydrate dissociation when injected into a gas hydrate-bearing formation. The most important thermodynamic organic inhibitors are methanol, monoethylene glycol (MEG), and diethylene glycol (DEG) commonly referred to as glycol [218–222]. Dissolved salts such as NaCl,  $\text{CaCl}_2$ , KCl, and NaBr can also be inhibitors [191]. While gas hydrate inhibitors are an effective methodology for preventing hydrate formation in engineering applications, their use in the production of NGHs is restrictive due to environmental impact, prohibitive costs, and thermal self-regulation of gas hydrates. Of the inhibitors examined, methanol and glycols are the most successful ones [221]. The principles by which alcohol, glycols, and salts inhibit hydrates are the same. However, salts have corrosion problems, and they cannot be easily vaporized due to their low vapor pressures.

In adding inhibitors, besides temperature and pressure conditions, composition and amount of inhibitors are important. The inhibitor must be at or below its water

dew point (i.e., must be water saturated). In addition, dehydration can be used as an alternative. An addition of an inhibitor can shift pressure–temperature diagram such that the temperature decreases at specific pressures, and this facilitates hydrate dissociation. After temperature depression due to an addition of an inhibitor, free gas will form and hydrate zone will shift to the left to lower the temperature side. Methanol has a high vapor pressure and infinite water solubility and can easily shift to the gas phase.

In most offshore applications, hydrate formation is controlled by injection of a thermodynamic hydrate inhibitor. Inhibitor injection at a given pressure will reduce the temperature at which hydrate is formed. Overall, ethylene glycol seemed to be the most useful inhibitor for the gas hydrates.

#### 12.5.4 GAS EXCHANGE

Exchanging  $\text{CO}_2$  with  $\text{CH}_4$  concept was first advanced by Ohgaki et al. [68]. Their experimental study showed that  $\text{CO}_2$  be preferentially clathrated over  $\text{CH}_4$  in the hydrated phase. They also demonstrated the possibility of producing  $\text{CH}_4$  by injecting  $\text{CO}_2$  gas. Ohgaki et al. [68] noted that during the exchange process, mole fraction of  $\text{CO}_2$  in the hydrate phase was greater than that in the gas phase.

This effect was further studied quantitatively by Seo and Lee [69] and Seo et al. [70]. They showed that  $\text{CO}_2$  concentration in the hydrate phase was  $>90\%$  when gas-phase concentration of  $\text{CO}_2$  in the hydrate formers (i.e.,  $\text{CO}_2$  and  $\text{CH}_4$ ) was above 40%. Pure  $\text{CH}_4$  and  $\text{CO}_2$  form structure I (sI) type hydrates, and their mixtures also form sI type hydrates [61–75]. In forming mixed  $\text{CH}_4$  and  $\text{CO}_2$  hydrates, the  $\text{CH}_4$  molecules occupy both the large and small cages of sI type hydrates, whereas  $\text{CO}_2$  molecules only occupy the large cages. Without hydrate dissociation, there is an upper limit to the substitution of  $\text{CO}_2$  for  $\text{CH}_4$  in hydrates.

Lee et al. [218] showed that  $\sim 64\%$  of  $\text{CH}_4$  can be released by exchange with  $\text{CO}_2$ . In addition to equilibrium considerations, the heat of  $\text{CO}_2$  hydrate formation is higher ( $-57.9$  kJ/mol) than the heat of dissociation of  $\text{CH}_4$  hydrate ( $-54.5$  kJ/mol), making the overall process exothermic that favors the normal exchange of  $\text{CO}_2$  with  $\text{CH}_4$  hydrate.

While the exchange of  $\text{CO}_2$  for  $\text{CH}_4$  is thermodynamically a favorable process, the kinetics of exchange mechanism is slow [61–75,209], with induction time requiring several days. The original studies also did not address the rate of  $\text{CO}_2$  gas penetration further into gas hydrate, beyond the first few hundred manometers at the interface [203]. The exchange of  $\text{CO}_2$  with  $\text{CH}_4$  at high pressure (with liquid  $\text{CO}_2$ ) was also examined in the literature, but once again slow rate of exchange was observed. The use of nitrogen instead of  $\text{CO}_2$  gave a much higher rate. For liquid  $\text{CO}_2$  injection, thermodynamic conditions can either favor  $\text{CO}_2$  or  $\text{CH}_4$  cage occupation [76–83]. This transition occurs when the pure  $\text{CO}_2$  and  $\text{CH}_4$  temperature-versus-pressure equilibrium functions cross at the pressure above the gas–liquid  $\text{CO}_2$  phase boundary.

Thermodynamic properties of hydrates depend on the pore size distribution in the geologic media; hydrate formation will occur in large pores first and then in small pores until equilibrium is achieved [205,212]. Porous media also affect other

thermodynamic properties of hydrates. In geologic media that have distribution of pore sizes, hydrates would form and dissociate over a range of temperatures and pressures according to the distribution of pore radii and the impact of salts in the residual pore water [191]. Goel [67] and Goel et al. [209] indicated that in order to understand gas-exchange technology in porous media, quantitative estimates of formation and dissociation processes in a typical geologic media core samples are needed.

### 12.5.5 EGHR METHOD

As shown above, a strict gas exchange of  $\text{CO}_2$  for  $\text{CH}_4$  in bulk methane hydrate is slow by several orders of magnitude to be considered as an effective method of gas hydrate production. An EGHR process that involves injecting a two-phase emulsion of liquid  $\text{CO}_2$  and water at proper volumetric ratio can considerably enhance (three times or higher) the production rate over injecting cool water ( $15^\circ\text{C}$ ) alone [76–83]. It is important to know the range of reservoir conditions where EGHR technique can be applied. Collett and coworkers [204,222,223] calculated these conditions for Alaska Northern slope (ANS) and concluded that EGHR method can be applied over a large fraction of ANS. They also found that  $\text{CO}_2$  hydrate would be stable under almost any conditions on the ANS short of very near the ground surface. They also suggested that typical ANS reservoir conditions would inject liquid  $\text{CO}_2$  with a density  $\sim 82\%–94\%$  of the water phase. ANS well log temperature data as well as carbon dioxide hydrate and vapor–liquid equilibrium data are described by Collet et al. [204,222,223].

The laboratory studies indicated that there are no signs of coagulation into macrodroplets as the emulsion moves away from the injector—a conclusion that needs to be tested at reservoir scale [73]. Another important restriction is that the temperature of the water– $\text{CO}_2$  emulsion remains above the equilibrium point where  $\text{CO}_2$  hydrate could form in the wellbore or near the wellbore. Interruption of the supply of emulsion fluid during production for an extended period could result in the premature formation of  $\text{CO}_2$  hydrate and plugging [73,77]. Provisions for temporary injection of heat may be needed to allow for flow interruptions, which are important for well maintenance.

The EGHR method has been tested in laboratory for continuous production of a suitable liquid carbon dioxide and water emulsion [73,76–82]. This test is largely one dimensional. A suitable downhole tool that can work in actual field needs to be developed. The injector tool design should be compatible with downhole conditions typical of gas hydrate formations. Wellbore completion requirements such as open hole, uncased, or perforated casing influence the design parameters of the injection tool. Injection of the liquid carbon dioxide and water emulsion in the target formation is the most important requirement. A new design to fit these requirements is depicted in Figure 12.6 [73]. Here, emulsion outlets are located on the side. Surface-warmed liquid carbon dioxide and water can be directed into such an injector from the high-pressure lines. Use of produced water to form emulsion would eliminate issues associated with disposal of these fluids in arctic conditions. Both rate and distance of formation penetration can

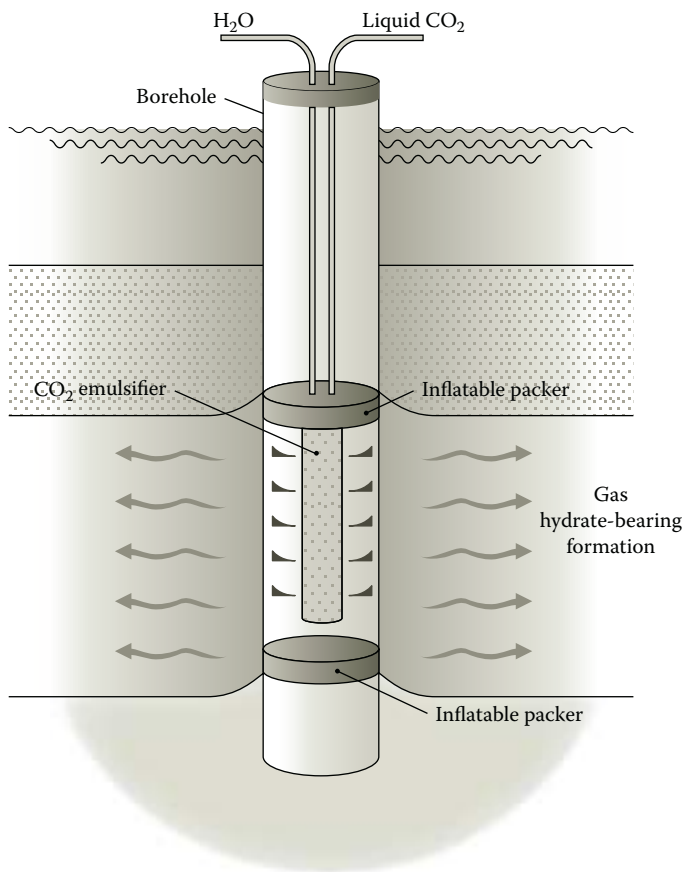


**FIGURE 12.6** A new design of downhole tool for EGHR. (Adapted from McGrail, B., Schaefer, H., White, M., Zhu, T., Kulkarni, A., Hunter, R., Patil, S., Owen, A., and Martin, P., “Using Carbon dioxide to enhance recovery of methane from gas hydrate reservoirs: Final summary report,” US Department of Energy under Contract No. DE-AC06-76RLO 1830, PNNL 17035, Pacific Northwest National Laboratory, 2007.)

be controlled by adjusting the settings on liquid carbon dioxide and water pumps from the surface.

An EGHR technique is still being developed [73,77,81]. A number of questions such as placement of recovery wells including the distance from the injection site and spacing to maximize recovery of  $CH_4$  gas need to be determined. Identification and delivery logistics of an economic supply of carbon dioxide for a given site also need to be ascertained. Both theoretical and experimental works that address these issues need to be pursued [73,77,81].

In sum, the EGHR process has several advantages: (1) Since the heat generated from the formation of  $CO_2$  hydrate is ~20% greater than the heat consumed from the dissociation of methane, the replacement of methane with carbon dioxide

in gas hydrate sediments is thermodynamically favorable. This net exothermic process allows the dissociation of hydrates to be carried out with only minimal requirement of an additional heat source. (2) Once  $\text{CO}_2$ -rich fluid fills pores vacated by methane, the subsequent formation of carbon dioxide hydrate would mechanically stabilize the formation, eliminating subsidence concerns in some production environment, and (3) the overall process is carbon neutral since methane is permanently replaced by carbon dioxide as gas hydrate. Produced water can also be used to form the emulsion, eliminating a problematic disposal issue in arctic settings [73,77,81].

### 12.5.6 COMPUTER SIMULATION

There are some reported computer simulation studies of commercial production methods for gas hydrates, and most of them have examined conventional production concepts of depressurization coupled with some form of thermal stimulation [83,201–214,224–226]. An EGHR process that utilizes a microemulsion of liquid  $\text{CO}_2$  and water to decompose methane hydrate *in situ* and produce free gas described earlier has been successfully demonstrated in laboratory-scale experiments with gas hydrate-bearing sediments. Since these laboratory-based studies were extremely encouraging, a reservoir modeling assessment that compared and contrasted the EGHR process with conventional methods of gas hydrate production was carried under a Department of Energy (DOE) project [73,210,212].

Within the DOE project [73,210], STOMP-HYD simulator was applied to a series of one- and two-dimensional simulations that investigated the production of  $\text{CH}_4$  hydrates in geologic media using  $\text{CO}_2$  injection. Effectively, the project considered two approaches to producing  $\text{CH}_4$  hydrate in geologic media using  $\text{CO}_2$  injection: (1) hydrate dissociation and reformation and (2) direct molecular exchange. In the hydrate dissociation and reformation approach, the injected  $\text{CO}_2$  first dissociates  $\text{CH}_4$  hydrate. This stage is followed by reformation of a mixed gas hydrate, which predominately comprises  $\text{CO}_2$ . In the direct molecular exchange approach, the injected  $\text{CO}_2$  exchanges with the  $\text{CH}_4$  in the hydrate structure, maintaining the hydrate integrity. The dissociation–reformation approach has the advantage of releasing  $\text{CH}_4$  in both the small and large cages. In the direct-exchange approach, only the  $\text{CH}_4$  in the large cages is released. Co-injection of  $\text{CO}_2$  and  $\text{N}_2$  has been shown to allow molecular exchange of  $\text{CH}_4$  in both the small and large cages. Because the STOMP-HYD simulator did not track small- and large-cage occupancies, it is currently limited to  $\text{CO}_2$  exchange with  $\text{CH}_4$  in large cages. The principal conclusion from this series of simulations was that both  $\text{CO}_2$  exchange approaches yielded faster production times, but lower  $\text{CH}_4$  recoveries over pure water injections. Without consideration of the cage occupancies, the direct exchange yielded faster production times over the dissociation–reformation approach, with nearly equivalent  $\text{CH}_4$  recoveries. The  $\text{CO}_2$ -to-water ratio in the injecting fluid primarily affected production rates, with higher ratios yielding faster productions.

STOMP-HYD simulation results also showed the following conclusions [73,213,224]:

1. Preliminary depressurization to a point above the freezing point of the aqueous phase opens pore space for injection of mobile fluids.
2. Kinetics of the direct exchange of hydrate formers (i.e.,  $\text{CO}_2$  with  $\text{CH}_4$ ) are important.
3. Cage occupancies of the sI structure are expected to have significant impacts on the efficiency of direct gas-phase  $\text{CO}_2$ – $\text{CH}_4$  exchange.
4. Controlling secondary hydrate formation is critical to prevent pore plugging.
5. Heat transfer into the production zone is not required under properly controlled production conditions.

One critical finding of the above-described Battelle's simulation modeling work was that the formation of secondary  $\text{CO}_2$  hydrate has the potential to halt the production process by inhibiting fluid migration. A complete exchange of  $\text{CO}_2$  and  $\text{CH}_4$  is possible without forming excessive secondary hydrate and while maintaining elevated hydrate saturations. The pore-water salinity may play a strong role in the inhibition of secondary hydrate formation beyond certain saturation levels, an observation in agreement with the published experimental results [73].

### 12.5.7 COMMERCIAL APPLICATIONS

In the recent years, the above-described production methods and computer simulations have been applied to numerous practical sites [33,222,227–234]. The North Slope of Alaska and numerous sites in that region (such as Mallik field, Milne point) have been tested [33,222,227–229]. Nankai Trough [231] and Ulleung basin of the Korea [233] have also been examined. Several general production strategies have also been investigated [216,234–237]. More work on the applications (both theoretical and experimental) of various production methods to the commercial sites (both on land and in deep water) is needed. The successful commercial operations to recover methane from gas hydrates will significantly increase our energy resource. Once again, water is the cause for this important energy and fuel source.

## REFERENCES

1. Englezos, P., "Clathrate Hydrates," *Industrial & Engineering Chemistry Research*, 32 (7), 1251–1274 (1993).
2. "What are gas hydrates?" a communication by Center for Gas hydrate Research, Heriot-Watt University, Edinburgh, The Hydrate forum Org. (2012).
3. Boswell, R. and Collett, T.S., "Current perspectives on gas hydrate resources," *Energy and Environmental Science*, 4, 1206–1215 (2011).
4. Collett, T.S., Johnson, A.H., Knapp, C.C., and Boswell, R. (eds.), "Natural gas hydrates: A review," in *Natural Gas Hydrates—Energy Resource Potential and Associated Geologic Hazards*, AAPG Memoir 89. AAPG, Tulsa, OK, 146–219 (2009).
5. McIver, R., "Gas hydrates," in Meyer, R. and Olson, J. (eds.), *Long-Term Energy Resources*. Pitman, Boston, MA, 713–726 (1981).
6. Collett, T.S. "Gas hydrates as a future energy resource," *Geotimes*, 49 (11), 24–27 (2004).
7. Sloan, E.D. and Koh, C., *Clathrate Hydrates of Natural Gases*, 3rd ed. Taylor & Francis, Boca Raton, FL (2008).

8. Ruppel, C., "Methane hydrates and the future of natural gas," MITEI Natural Gas Report, Supplement Paper No. 4 (2011).
9. Boswell, R. and Collett, T., "The gas hydrates resource pyramid," *Fire in the Ice*, 6 (3), 5–7 (2006).
10. Ruppel, C., "Ruppel: MITEI Natural Gas Report," Supplementary Paper on Methane Hydrates, 19 (2011).
11. Energy Information Administration (EIA), "Natural gas," in *International Energy Outlook 2010*. US Department of Energy, Washington, DC (2010).
12. Holder, G.D., Kamath, V.A., and Godbole, S.P., "The potential of natural gas hydrates as an energy resource," *Annual Review of Energy*, 9, 427–445 (1984).
13. "Methane hydrate phase diagram," Wikipedia, the free encyclopedia (May 10, 2010).
14. "Clathrate hydrate," Wikipedia, the free encyclopedia, 1–7 (2012).
15. "Methane clathrate," Wikipedia, the free encyclopedia (2012).
16. Makogon, Y.F., Holditch, S.A., and Makogon, T.Y., "Natural gas-hydrates—A potential energy source for the 21st Century," *Journal of Petroleum Science and Engineering*, 56 (1–3), 14–31 (2007).
17. Collett, T.S., "Energy resource potential of natural gas hydrate," *American Association of Petroleum Geologists Bulletin*, 86, 1971–1992 (2002).
18. Ruppel, C., "Ruppel: MITEI Natural Gas Report," Supplementary Paper on Methane Hydrates, 18 (2011).
19. Frye, M., "Preliminary evaluation of in-place gas hydrate resources: Gulf of Mexico Outer Continental Shelf," Minerals Management Service Report 2008-004, US Department of the Interior, Washington, DC (2008).
20. Fujii, T., Saeiki, T., Kobayashi, T., Inamori, T., Hayashi, M., Takano, O., Takayama, T. et al., "Resource assessment of methane hydrate in the Nankai Trough, Japan," Offshore Technology Conference, Paper 19310, Houston, TX (2008).
21. Gornitz, V. and Fung, I., "Potential distribution of methane hydrates in the world's oceans," *Global Biogeochemical Cycles*, 8, 225–347 (1994).
22. Milkov, A., "Global estimates of hydrate-bound gas in marine sediments: How much is really out there?" *Earth-Science Reviews*, 66, 183–197 (2004).
23. Trofimuk, A., Cherskiy, N., and Tsarev, V., "Accumulation of natural gases in zones of hydrate—Formation in the hydrosphere," *Doklady Akademii Nauk SSR*, 212, 931–934 (1973) (Russian).
24. Collett, T.S., "Gas hydrates as a future energy resource," *Geotimes*, 49 (11), 24–27 (2004).
25. Kvenvolden, K.A., Ginsburg, G.D., and Soloviev, V.A., "Worldwide distribution of sub-aquatic gas hydrates," *Geo-Marine Letters*, 13 (1), 32–40 (1993).
26. Kvenvolden, K.A., "Natural-gas hydrate occurrence and issues," *Sea Technology*, 36 (9), 69–74 (1995).
27. Sloan, E.D., Jr., *Clathrate Hydrates of Natural Gases*. Marcel Dekker, New York (1998).
28. Klauda, J.B. and Sandler, S.I., "Global distribution of methane hydrate in ocean sediment," *Energy & Fuels*, 19 (2), 459–470 (2005).
29. Borowski, W.S., "A review of methane and gas hydrates in the dynamic, stratified system of the Blake Ridge region, offshore southeastern North America," *Chemical Geology*, 205, 311 (2004).
30. Cherskiy, N.V., Tsaarev, V.P., and Nikitin, S.P., "Investigation and prediction of conditions of accumulation of gas resources in gas-hydrate pools," *Petroleum Geology*, 21, 65 (1982).
31. Collett, T., "Natural gas hydrates of the Prudhoe Bay and Kuparuk River area, North Slope, Alaska," *American Association of Petroleum Geologists Bulletin*, 77 (5), 793–812 (1993).
32. Collett, T. and Ginsburg, G., "Gas hydrates in the Messoyakha gas field of the West Siberian Basin—A re-examination of the geologic evidence," *International Journal of Offshore and Polar Engineering*, 8 (1), 22–29 (1998).

33. Dallimore, S.R. and Collett, T.S. (eds.), "Scientific results from the Mallik 2002 Gas Hydrate Production Research Well Program, Mackenzie Delta, Northwest Territories, Canada," Geological Survey of Canada Bulletin 585, USGS, Reston, VA (2005).
34. Uchida, T., Lu, H., Tomaru, H., and the MITI Nankai Trough Shipboard Scientists, "Subsurface occurrence of natural gas hydrate in the Nankai Trough area: Implication for gas hydrate concentration," *Resource Geology*, 54, 35–44 (2004).
35. Collett, T., Riedel, M., Boswell, R., Cochran, J., Kumar, P., Sethi, A., and Sathe, A., "International team completes landmark gas hydrate expedition in the offshore of India," *Fire in the Ice*, 6 (3), 1–16 (2006).
36. Park, K.P., "Gas hydrate exploration in Korea," *Proceedings of the 2nd International Symposium on Gas Hydrate Technology*, November 1–2, Daejeon, Korea (2006).
37. Boswell, R., Collett, T., McConnell, D., Frye, M., Shedd, B., Mrozewski, S., Guerin, G. et al., "Joint Industry Project Leg II discovers rich gas hydrate accumulations in sand reservoirs in the Gulf of Mexico," *Fire in the Ice*, 9 (3), 1–5 (2009).
38. Collett, T., Agena, W., Lee, M., Zyrianova, M., Bird, K., Charpentier, T., Houseknecht, D. et al., "Assessment of gas hydrate resources on the North Slope, Alaska, 2008," US Geological Survey Fact Sheet 2008-3073, USGS, Reston, VA, 4 (2002).
39. Collett, T., Riedel, M., Cochran, J.R., Boswell, R., Kumar, P., and Sathe, A.V., "Indian continental margin gas hydrate prospects: Results of the Indian National Gas Hydrate Program (NGHP) expedition 01," *Proceedings of the 6th International Conference on Gas Hydrates*, Vancouver, BC (2008).
40. Dai, J., Snyder, F., Gillespie, D., Koesoemadinata, A., and Dutta, N., "Exploration for gas hydrates in the deepwater northern Gulf of Mexico: Part I. A seismic approach based on geologic model, inversion, and rock physics principles," *Marine and Petroleum Geology*, 25, 830–844 (2008).
41. Dai, J., Banik, N., Gillespie, D., and Dutta, N., "Exploration for gas hydrates in the deepwater northern Gulf of Mexico: Part II. Model validation by drilling," *Marine and Petroleum Geology*, 25, 845–859 (2008).
42. Ryu, B.-J., Riedel, M., Kim, J.-H., Hyndman, R.D., Lee, Y.-J., Chung, B.-H., and Kim, I., "Gas hydrates in the western deep-water Ulleung Basin, East Sea of Korea," *Marine and Petroleum Geology*, 26, 1483–1498 (2009).
43. Tsuji, Y., Ishida, H., Nakamizu, M., Matsumoto, R., and Shimizu, S., "Overview of the MITI Nankai Trough wells: A milestone in the evaluation of methane hydrate resources," *Resource Geology*, 54, 3–10 (2004).
44. Tsuji, Y., Fujii, T., Hayashi, M., Kitamura, R., Nakamizu, M., Ohbi, K., Saeki, T. et al., "Methane-hydrate occurrence and distribution in the Eastern Nankai Trough, Japan: Findings of the Tokai-oki to Kumano-nada methane-hydrate drilling program," in Collett, T., Johnson, A., Knapp, C., and Boswell, R. (eds.), *Natural Gas Hydrates—Energy Resource Potential and Associated Geologic Hazards*, AAPG Memoir 89, AAPG, Tulsa, OK, 228–249 (2009).
45. Wu, N., Yang, S. et al., "Preliminary discussion on gas hydrate reservoir system of Shenhu area, north slope of South China Sea," *Proceedings of the 6th International Conference on Gas Hydrates*, July 6–10, Vancouver, 8 (2008).
46. Zhang, H., Yang, S., Wu, N., Su, X., Holland, M., Schultheiss, P., Rose, K., Butler, H., Humphrey, G., and GMGS-1 Science Team, "Successful and surprising results for China's first gas hydrate drilling expedition," *Fire in the Ice*, 7 (3), 6–9 (2007).
47. Paull, C., Reeburgh, W.S., Dallimore, S.R., Enciso, G., Green, S., Koh, C.A., Kvenvolden, K.A., Mankin, C., and Riedel, M., "Realizing the energy potential of methane hydrate for the United States," National Research Council Report (2010).
48. Cook, A., Goldberg, D., and Kleinberg, R., "Fracture-controlled gas hydrate systems in the Gulf of Mexico," *Marine and Petroleum Geology*, 25 (9), 932–941 (2008).

49. Collett, T.S., Lee, M.W. et al., "Permafrost associated natural gas hydrate occurrences on the Alaskan North Slope," *Marine and Petroleum Geology*, 28, 279–294 (2011).
50. Dallimore, S.R., Uchida, T., and Collett, T.S. (eds.), "Scientific results from the JAPEx/JNOC/GSC Mallik 2L-38 gas hydrate research well," Geological Survey of Canada Bulletin 544, Mackenzie Delta, Northwest Territories (1999).
51. Ruppel, C., "Ruppel: MITEI Natural Gas Report," Supplementary Paper on Methane Hydrates, 21 (2011).
52. Walsh, T., Stokes, P., Panda, M., Morahan, T., Greet, D., MacRae, S., Singh, P., and Patil, S., "Characterization and quantification of the methane hydrate resource potential associated with the barrow gas field," *Proceedings of the 6th International Conference on Gas Hydrates*, Vancouver, BC (2008).
53. Park, K.P., Bahk, J.J. et al., "Korean National Program expedition confirms rich gas hydrate deposits in the Ulleung Basin, East Sea," *Fire in the Ice*, 8 (2), 6–9 (2008).
54. Bahman, T.K., "Why are gas hydrates important," Institute of Petroleum Engineering, Heriot-Watt University, Edinburgh (2011).
55. Collett, T.S. and Ladd, J., "Detection of gas hydrate with downhole logs and assessment of gas hydrate concentrations (saturation) and gas volumes on the Blake Ridge with electrical resistivity log data," in Paull, C.K., Matsumoto, R., Wallace, P.J., and Dillion, W.P. (eds.), *Proceedings of the ODP, Science Results*, Vol. 164, 179–191 (2000).
56. Hato, M., Matsuoka, T., Inamori, T., and Saeki, T., "Detection of methane-hydrate-bearing zones using seismic attributes analysis," *The Leading Edge*, 25, 607–609 (2006).
57. Holbrook, W.S., Gorman, A.R., Hornbach, M., Hackwith, K.L., and Nealon, J., "Direct seismic detection of methane hydrate," *The Leading Edge*, 21, 686–689 (2002).
58. Hovland, M. and Gudmestad, O.V., "Potential influence of gas hydrates on seabed installations," in Paull, C. and Dillon, W. (eds.), *Natural Gas Hydrates—Occurrence, Distribution and Detection*. American Geophysical Union, Washington, DC, 307–315 (2001).
59. Lee, J.Y., Santamarina, J.C., and Ruppel, C., "Parametric study of the physical properties of hydrate-bearing sand, silt, and clay sediments: 1. Electromagnetic properties," *Journal of Geophysical Research*, 115, B11104 (2010).
60. Kvenvolden, K.A., "Methane hydrate-A major reservoir of carbon in the shallow geosphere," *Chemical Geology*, 71, 41–51 (1988).
61. Ersland, G., Husebo, J., Graue, A., Baldwin, B., Howard, J.J., and Stevens, J.C., "Measuring gas hydrate formation and exchange with CO<sub>2</sub> in Bentheim sandstone using MRI tomography," *Chemical Engineering Journal*, 158, 25–31 (2010).
62. Farrell, H., Boswell, R., Howard, J., and Baker, R., "CO<sub>2</sub>-CH<sub>4</sub> exchange in natural gas hydrate reservoirs: Potential and challenges," *Fire in the Ice*, 10 (1), 19–21 (2010).
63. Graue, A., Kvamme, B., Baldwin, B.A., Steven, J., Howard, J., Aspenes, E., Ersland, G., Husebo, J., and Zornes, D., "MRI visualization of spontaneous methane production from hydrates in sandstone core plugs when exposed to CO<sub>2</sub>," *SPE Journal*, 13, 146–152 (2008).
64. Jung, J.W., Espinoza, D.N., and Santamarina, J.C., "Properties and phenomena relevant to CH<sub>4</sub>-CO<sub>2</sub> replacement in hydrate-bearing sediments," *Journal of Geophysical Research*, 115, B10102 (2010).
65. Lee, H., Seo, Y., Seo, Y.-T., Moudrakovski, I., and Ripmeester, J., "Recovering methane from solid methane hydrate with carbon dioxide," *Angewandte Chemie International Edition*, 42 (41), 5048–5051 (2003).
66. Park, Y., Kim, D., Lee, J., Huh, D., Park, K., Lee, J., and Lee, H., "Sequestering carbon dioxide into complex structures of naturally occurring gas hydrates," *Proceedings of the National Academy of Sciences of the United States of America*, 103–34, 12690–12694 (2006).

67. Goel, N. "In situ methane hydrate dissociation with carbon dioxide sequestration: Current knowledge and issues," *Journal of Petroleum Science and Engineering*, 51 (3/4), 169–184 (2006).
68. Ohgaki, K., Takano, K., Sangawa, H., Matsubara, T., and Nakano, S., "Methane exploitation by carbon dioxide from gas hydrates—Phase equilibria for CO<sub>2</sub>–CH<sub>4</sub> mixed hydrate system," *Journal of Chemical Engineering of Japan*, 29 (3), 478–483 (1996).
69. Seo, Y.T. and Lee, H., "Multiple-phase hydrate equilibria of the ternary carbon dioxide, methane, and water mixtures," *Journal of Physical Chemistry B*, 105 (41), 10084–10090 (2001).
70. Seo, Y.T., Lee, H., and Yoon, J., "Hydrate phase equilibria of the carbon dioxide, methane, and water system," *Journal of Chemical & Engineering Data*, 46 (2), 381–384 (2001).
71. Smith, D.H., Seshadri, K., and Wilder, J., "Assessing the thermodynamic feasibility of the conversion of methane hydrate into carbon dioxide hydrate in porous media," *First National Conference on Carbon Sequestration*, National Energy Technology Laboratory (2001).
72. Uchida, T., Takeya, S., Ebinuma, T., and Narita, H., "Replacing methane with CO<sub>2</sub> in clathrate hydrate: Observations using Raman spectroscopy," in Williams, D.J., Durie, R.A., McMullan, P., Paulson, C.A.J., and Smith, A.Y. (eds.), *Proceedings of the 5th International Conference on Greenhouse Gas Control Technologies*. CSIRO Publishing, Collingwood, 523–527 (2001).
73. McGrail, B., Schaef, H., White, M., Zhu, T., Kulkarni, A., Hunter, R., Patil, S., Owen, A., and Martin, P., "Using carbon dioxide to enhance recovery of methane from gas hydrate reservoirs: Final summary report," US Department of Energy under Contract No. DE-AC06-76RLO 1830, PNNL 17035, Pacific Northwest National Laboratory, Richland, WA (September 2007).
74. White, M. and McGrail, P., "Numerical simulation of methane hydrate production from geologic formations via carbon dioxide injection," *Society of Petroleum Engineers, Offshore Technology Conference*, Paper No. OTC-19458 (2008).
75. Yezdimer, E., Cummings, P., and Chalvo, A., "Extraction of methane from its gas clathrate by carbon dioxide sequestration—Determination of the Gibbs Free Energy of gas replacement and molecular simulation," *Journal of Physical Chemistry A*, 106, 7982–7987 (2002).
76. "Comparative assessment of advanced gas hydrate production methods," DOE/NETL methane hydrates projects, DE-FC26-06NT42666 (September 2009).
77. Ota, M., Morohashi, K., Abe, Y., Watanabe, M., Smith, R., and Inomata, H., "Replacement of CH<sub>4</sub> in the hydrate by use of liquid CO<sub>2</sub>," *Energy Conversion and Management*, 46 (11/12), 1680–1691 (2005).
78. Chatterji, J. and Griffith, J., "Methods of decomposing gas hydrates," Patent No. 5713416 (1998).
79. Hirohama, S., Shimoyama, Y., Wakabayashi, A., Tatsuta, S., and Nishida, N., "Conversion of CH<sub>4</sub>-hydrate to CO<sub>2</sub>-hydrate in liquid CO<sub>2</sub>," *Journal of Chemical Engineering of Japan*, 29 (6), 1014–1020 (1996).
80. Cortis, A. and Ghezzehei, T., "On the transport of emulsions in porous media," *Journal of Colloid Interface Science*, 313 (1), 1–4 (2007).
81. Tegze, G., Gránásy, L., and Kvamme, B., "Phase field modeling of CH<sub>4</sub> hydrate conversion into CO<sub>2</sub> hydrate in the presence of liquid CO<sub>2</sub>," *Physical Chemistry Chemical Physics*, 9 (24), 3104–3111 (2007).
82. Yan, L., Thompson, K., and Valsaraj, K., "A numerical study on the coalescence of emulsion droplets in a constricted capillary tube," *Journal of Colloid Interface Science*, 298 (2), 832–844 (2006).

83. Kurihara, M., Funatsu, K., Ouchi, H., Masuda, Y., Yasuda, M., Yamamoto, K., Numasawa, M. et al., "Analysis of the JOGMEC/NRCAN/Aurora Mallik gas hydrate production test through numerical simulation," *Proceedings of the 6th International Conference on Gas Hydrates*, Vancouver, BC (2008).
84. Lee, J.Y., Francisca, F.M., Santamarina, J.C., and Ruppel, C., "Parametric study of the physical properties of hydrate-bearing sand, silt, and clay sediments: 2. Small-strain mechanical properties," *Journal of Geophysical Research*, 115, B11105 (2010).
85. Moridis, G.J., Reagan, M.T., and Zheng, K., "On the performance of Class 2 and Class 3 hydrate deposits during co-production with conventional gas," *Offshore Technology Conference*, OTC 19435-MS (2008).
86. Paull, C.K., Matsumoto, R. et al., "Proceedings of the Ocean Drilling Program," Initial Reports 164, Ocean Drilling Program, College Station, TX (1996).
87. Rutqvist, J. and Moridis, G., "Evaluation of geohazards of in situ gas hydrates related to oil and gas operations," *Fire in the Ice*, 10 (2), 1–4 (2010).
88. Ruppel, C., Collett, T., Boswell, R., Lorensen, T., Buckowski, B., and Waite, W., "A new global gas hydrate drilling map based on reservoir type," *Fire in the Ice*, 11 (1), 15–19 (2011).
89. Satyavani, N., Sain, K., Lall, M., and Kumar, B.J.P., "Seismic attribute study of gas hydrates in the Andaman, offshore India," *Marine Geophysical Research*, 29, 167–175 (2008).
90. Ruppel, C., "Tapping methane hydrates for unconventional natural gas," *Elements*, 3 (3), 193–199 (2007).
91. Ruppel, C., Boswell, R., and Jones, E., "Scientific results from Gulf of Mexico gas hydrates joint industry project Leg 1 drilling: Introduction and overview," *Marine and Petroleum Geology*, 25, 819–829 (2008).
92. Ruppel, C., "Ruppel: MITEI Natural Gas Report," Supplementary Paper on Methane Hydrates, 25 (2011).
93. Birchwood, R.A., Noeth, S., Tjengdrawira, M.A., Kisra, S.M., Elisabeth, F.L., Sayers, C.M., Singh, R. et al., "Modeling the mechanical and phase change stability of wellbores drilled in gas hydrates by the Joint Industry Participation Program (JIP) Gas Hydrates Project Phase II," *SPE Annual Technical Conference*, Anaheim, CA, SPE 110796, November 11–14 (2007).
94. Ameripour, S., "Prediction of gas-hydrate formation conditions in production and surface facilities," MS thesis, A&M University, College Station, TX, 79 (August 2005).
95. Dalmazzone, D., Kharrat, M., Lachet, V., Fouconnier, B., and Clausse, D., "DSC and PVT measurements—Methane and trichlorofluoromethane hydrate dissociation equilibria," *Journal of Thermal Analysis and Calorimetry*, 70, 493–505 (2002).
96. Edmonds, B., Moorwood, R.A.S., and Szczepanski, R., "A practical model for the effect of salinity on gas hydrate formation," *European Production Operations Conference & Exhibition*, SPE 35569, Stavanger, Norway (1996).
97. Grigg, R.B. and Lynes, G.L., "Oil-based drilling mud as a gas-hydrates inhibitor," *SPE Drilling Engineering*, 7, 32–38 (1992).
98. Kotkoskie, T.S., Al-Ubaidi, B., Wildeman, T.R., and Sloan, E.D., Jr., "Inhibition of gas hydrates in water-based drilling muds," *SPE Drilling Engineering*, 7, 130–136 (1992).
99. Lai, D.T. and Dzialowski, A.K., "Investigation of natural gas hydrates in various drilling fluids," *SPE/IADC Drilling Conference*, SPE 18637, February, New Orleans, LA (1989).
100. Tohidi, B., Østergaard, K.K., Danesh, A., Todd, A.C., and Burgass, R.W., "Structure-H gas hydrates in petroleum reservoir fluids," *The Canadian Journal of Chemical Engineering*, 79, 384–391 (2001).
101. Yousif, M.H., Dunayevsky, V.A., and Hale, A.H., "Hydrate plug remediation: Options and applications for deep water drilling operations," *SPE/IADC Drilling Conference*, SPE 37624, March, Amsterdam, the Netherlands (1997).

102. Kim, N., Bonet, E., and Ribeiro, P., "Study of hydrate in drilling operations: A review," *Proceedings of the 4th PDPETRO*, October 21–24, Campinas, SP (2007).
103. Bagirov, E. and Lerche, I., "Hydrate represent gas source, drilling hazard," *Oil & Gas Journal*, 95, 99–104 (1997).
104. Helgeland, L., Kinn, A., Kvalheim, O., and Wenaas, A., "Gas kick due to hydrates in the drilling for offshore natural gas and oil," Report by the Department of Petroleum Engineering and Applied Geophysics, NTNU, Trondheim, Norway (November 2012).
105. Skalle, P., "Pressure control during oil well drilling," in *Special Offshore Safety Issues*, 2nd ed. Ventus Publishing, <http://bookboon.com/en/textbooks/geoscience/pressure-control-during-oil-well-drilling>.
106. Amodu, A.A., "Drilling through gas hydrate formations: Possible problems and suggested solutions," MS thesis, Texas A&M University, Houston, TX (August 2008).
107. Dillon, W.P. and Max, M.D., "Oceanic gas hydrates," in Max, M.D. (ed.), *Natural Gas Hydrates in Oceanic and Permafrost Environments*, Kluwer, London, pp. 61–76 (2003).
108. Skalle, P., "Pressure control during oil well drilling," in *Schlumberger Oilfield Glossary*, "Blowout." <http://www.glossary.oilfield.slb.com/Display.cfm?Term=blowout>.
109. Khabibullin, T., Falcone, G., and Teodoriu, C., "Drilling through gas hydrate sediments: Managing wellbore stability risks," SPE-131332 (June 2006), <http://dx.doi.org/10.2118/131332-MS>.
110. Qadir, M.I., "Gas hydrates: A fuel for future but wrapped in drilling challenges," SPE-156516, *Paper presented at SPE/PAPG Annual Technical Conference*, November 22–23, Islamabad, Pakistan (2011).
111. Williamson, S.C., McConnell, D.R., and Bruce, R.J., "Drilling observations of possible hydrate-related annular flow in the deep water Gulf of Mexico and Implications on Well Planning," *Paper presented at the 2005 Offshore Technology Conference*, OTC 17279, May 2–5, Houston, TX (2005).
112. Hannegan, D., Todd, R.T., Pritchard, D.M., and Jonasson, B., "MPD—Uniquely applicable to methane hydrate drilling," SPE-91560, *Paper presented at the SPE/IADC Underbalanced Technology Conference and Exhibition*, October 11–12, Houston, TX (2004), <http://dx.doi.org/10.2118/91560-MS>.
113. Ebeltoft, H., Yousif, M., and Sægråd, E., "Hydrate control during deepwater drilling: Overview and new drilling-fluids formulations," SPE-68207, March (2001), <http://dx.doi.org/10.2118/68207-PA>.
114. Halliday, W., Clapper, D.K., and Smalling, M., "New gas hydrate inhibitors for deepwater drilling fluids," IADC/SPE-39316, *Paper presented at the 1998 SPE/IADC Drilling Conference*, March 3–6, Dallas, TX (1998).
115. Ravi, K. and Moore, S., "Cement slurry design to prevent destabilization of hydrates in deepwater environment," SPE-113631, *Paper presented at the 2008 Indian Oil and Gas Technical Conference and Exhibition*, March 4–6, Mumbai, India (2008).
116. Catak, E., "Hydrate dissociation during drilling through in-situ hydrate formations," MS thesis, Department of Petroleum Engineering, Louisiana State University, Baton Rouge, LA (May 2006).
117. Ruppel, C., "Methane hydrates and contemporary climate change," *Natural Education Knowledge*, 3 (10), 29 (2011).
118. Buffett, B. and Archer, D., "Global inventory of methane clathrate: Sensitivity to changes in environmental conditions," *Earth and Planetary Science Letters*, 227, 185–199 (2004).
119. Dutta, N.C., Utech, R.W., and Shelandar, D., "Role of 3D seismic for quantitative shallow hazard assessment in deepwater sediments," *The Leading Edge*, 29, 930–942 (2010).
120. Ellis, M., Evans, R.L., Hutchinson, D., Hart, P., Gardner, J., and Hagen, R., "Electromagnetic surveying of seafloor mounds in the northern Gulf of Mexico," *Marine Petroleum Geology*, 25, 969–968 (2008).

121. Hadley, C., Peters, D., Vaughan, A., "Gumusut-Kakap project: Geohazard characterisation and impact on field development plans," *International Petroleum Technology Conference*, 12554-MS, 15pp (2008).
122. Weitemeyer, K., Constable, S., Key K., "Marine EM techniques for gas-hydrate detection and hazard mitigation," *The Leading Edge*, 25 (5), 629–632 (2006).
123. Bunz, S. and Meinert, J., "Overpressure distribution beneath hydrate-bearing sediments at the Storegga Slide on the Mid-Norwegian margin," *Proceedings of the International Conference on Gas Hydrates*, June 13–16, Trondheim, Norway, Vol. 3, Paper 3007, 755–758 (2005).
124. Archer, D. et al., "Ocean methane hydrates as a slow tipping point in the global carbon cycle," *Proceedings of the National Academy of Sciences of the United States of America*, 106, 20596–20601 (2009).
125. Biastoch, A. et al., "Rising arctic ocean temperatures cause gas hydrate destabilization and ocean acidification," *Geophysical Research Letters*, 38, L08602 (2011).
126. Bock, M. et al., "Hydrogen isotopes preclude marine hydrate CH<sub>4</sub> emissions at the onset of Dansgaard-Oeschger events," *Science*, 328, 1686–1689 (2010).
127. Bohannon, J., "Weighing the climate risks of an untapped fossil fuel," *Science*, 319, 1753 (2008).
128. Bowen, R.G. et al., "Geomorphology and gas release from pockmark features in the Mackenzie Delta, Northwest Territories, Canada," in Kane, D.L. and Hinkel, K.M. (eds.), *Proceedings of the 9th International Conference on Permafrost*, Institute of Northern Engineering, Fairbanks, AK, 171–176 (2008).
129. Dickens, G.R. et al., "Dissociation of oceanic methane hydrate as a cause of the carbon isotope excursion at the end of the Paleocene," *Paleoceanography*, 10, 965–971 (1995).
130. Dickens, G.R., "Down the rabbit hole: Toward appropriate discussion of methane release from gas hydrate systems during the Paleocene-Eocene thermal maximum and other past hyperthermal events," *Climate of the Past*, 7, 831–846 (2011).
131. Harvey, L.D.D. and Huang, Z. "Evaluation of potential impact of methane clathrate destabilization on future global warming," *Journal of Geophysical Research*, 100, 2905–2926 (1995).
132. Hesselbo, S.P. et al., "Massive dissociation of gas hydrate during a Jurassic anoxic event," *Nature*, 406, 392–395 (2000).
133. Hinrichs, K.-U. and Boetius, A., "The anaerobic oxidation of methane: New insights in microbial ecology and biochemistry," in Wefer, G. et al. (eds.), *Ocean Margin Systems*. Springer, Berlin, Germany, 457–477 (2002).
134. Hu, L. et al. "Methane fluxes to the atmosphere from deepwater hydrocarbon seeps in the northern Gulf of Mexico," *Journal of Geophysical Research* (2011).
135. Intergovernmental Panel on Climate Change (IPCC). *Climate Change: The Scientific Basis*. Cambridge University Press, New York (2001).
136. Intergovernmental Panel on Climate Change (IPCC). *Climate Change: The Physical Basis*. Cambridge University Press, New York (2007).
137. Jiang, G. et al., "Stable isotope evidence for methane seeps in Neoproterozoic postglacial cap carbonates," *Nature*, 426, 822–826 (2003).
138. Judge, A.S. and Majorowicz, J.A., "Geothermal conditions for gas hydrate stability in the Beaufort-Mackenzie area: The global change aspect," *Palaeogeography, Palaeoclimatology, Palaeoecology*, 98, 251–263 (1992).
139. Kennett, J.P. et al., *Methane Hydrates in Quaternary Climate Change: The Clathrate Gun Hypothesis*. American Geophysical Union, Washington, DC (2003).
140. Kessler, J.D. et al., "A persistent oxygen anomaly reveals the fate of spilled methane in the deep Gulf of Mexico," *Science*, 331, 312–315 (2011).
141. Krey, V. et al., "Gas hydrates: Entrance to a methane age or climate threat?" *Environmental Research Letters*, 4, 034007 (2009).

142. Lachenbruch, A.H., "Permafrost, the active layer, and changing climate," Open File Report 94-694, USGS, Reston, VA (1994).
143. Lachenbruch, A.H. and Marshall, B.V., "Changing climate: Geothermal evidence from permafrost in the Alaskan Arctic," *Science*, 234, 689–696 (1986).
144. Lammers, S. et al., "A large methane plume east of Bear Island (Barents Sea): Implications for the marine methane cycle," *Geologische Rundschau*, 84, 59–66 (1995).
145. Lelieveld, J. et al., "Changing concentration, lifetime and climate forcing of atmospheric methane," *Tellus*, 50B, 128–150 (1998).
146. Liro, C.R. et al., "Modeling the release of CO<sub>2</sub> in the deep ocean," *Energy Conversion and Management*, 33, 667–674 (1992).
147. Macdonald, G., "Role of methane clathrates in past and future climate," *Climatic Change*, 16, 247–281 (1990).
148. Macdonald, I.R. et al., "Thermal and visual time-series at a seafloor gas hydrate deposit on the Gulf of Mexico slope," *Earth and Planetary Science Letters*, 233, 45–59 (2005).
149. Macdonald, I.R. et al., "Gas hydrate that breaches the seafloor on the continental slope of the Gulf of Mexico," *Geology*, 22, 699–702 (1994).
150. Majorowicz, J.A. et al., "Onset and stability of gas hydrates under permafrost in an environment of surface climatic change-past and future," *Proceedings of the 6th International Conference on Gas Hydrates*, Vancouver, BC (2008).
151. Mascarelli, A.L., "A sleeping giant?" *Nature Reports Climate Change*, 3, 46–49 (2009).
152. Maslin, M. et al., "Linking continental-slope failures and climate change: Testing the clathrate gun hypothesis," *Geology*, 32, 53–56 (2004).
153. Maslin, M. et al., "Gas hydrates: Past and future geohazard," *Philosophical Transactions of the Royal Society A: Mathematical, Physical & Engineering Sciences*, 368, 2369–2393 (2010).
154. Mau, S. et al., "Dissolved methane distributions and air-sea flux in the plume of a massive seep field, Coal Oil Point, California," *Geophysical Research Letters*, 34, L22603 (2007).
155. McGinnis, D.F. et al., "Fate of rising methane bubbles in stratified waters: How much methane reaches the atmosphere?" *Journal of Geophysical Research*, 111, C09007 (2006).
156. Niemann, H. et al., "Novel microbial communities of the Haakon Mosby mud volcano and their role as a methane sink," *Nature*, 443, 854–858 (2006).
157. Paull, C. et al., "Tracking the decomposition of submarine permafrost and gas hydrate under the shelf and slope of the Beaufort Sea," *Proceedings of the 7th International Conference on Gas Hydrates*, Edinburgh, Scotland (2011).
158. Petrenko, V. et al., "<sup>14</sup>CH<sub>4</sub> measurements in Greenland ice: Investigating last glacial termination CH<sub>4</sub> sources," *Science*, 324, 506–508 (2009).
159. Rachold, V. et al., "Near-shore arctic subsea permafrost in transition," *Eos, Transactions of the American Geophysical Union*, 88, 149–156 (2007).
160. Reagan, M.T. and Moridis, G.J., "Dynamic response of oceanic hydrate deposits to ocean temperature change," *Journal of Geophysical Research*, 113, C12023 (2008).
161. Reeburgh, W.S., "Oceanic methane biogeochemistry," *Chemical Reviews*, 107, 486–513 (2007).
162. Renssen, H. et al., "Modeling the climate response to a massive methane release from gas hydrates," *Paleoceanography*, 19, PA2010 (2004).
163. Röhl, U. et al., "On the duration of the Paleocene-Eocene thermal maximum," *Geochemistry, Geophysics, Geosystems*, 8, Q12002 (2007).
164. Ruppel, C. et al., "Degradation of subsea permafrost and associated gas hydrates offshore of Alaska in response to climate change," *Sound Waves*, 128, 1–3 (2010).
165. Schmidt, G.A. and Shindell, D.T., "Atmospheric composition, radiative forcing, and climate change as consequence of a massive methane release from gas hydrates," *Paleoceanography*, 18, 1004 (2003).

166. Semiletov, I. et al., "Methane climate forcing and methane observations in the Siberian Arctic Land-Shelf system," *World Resource Review*, 16, 503–543 (2004).
167. Shakhova, N. et al., "Geochemical and geophysical evidence of methane release over the East Siberian Arctic Shelf," *Journal of Geophysical Research*, 115, C08007 (2010).
168. Shakhova, N. et al., "Extensive methane venting to the atmosphere from sediments of the East Siberian Arctic Shelf," *Science*, 327, 1246–1250 (2010).
169. Solomon, E.A. et al., "Considerable methane fluxes to the atmosphere from hydrocarbon seeps in the Gulf of Mexico," *Nature Geoscience*, 2, 561–565 (2009).
170. Sowers, T., "Late quaternary atmospheric  $\text{CH}_4$  isotope record suggests marine clathrates are stable," *Science*, 311, 838 (2006).
171. Suess, E. et al., "Sea floor methane hydrates at Hydrate Ridge, Cascadia Margin," in Dillon, W.P. and Paull, C.K. (eds.), *Natural Gas Hydrates—Occurrence, Distribution and Detection*. American Geophysical Union, Washington, DC, 87–98 (2001).
172. Treude, T. et al., "Anaerobic oxidation of methane at hydrate ridge (OR)," *Geochimica et Cosmochimica Acta*, 67, A491 (2003).
173. Tryon, M.D. et al., "Fluid and chemical flux in and out of sediments posting methane hydrate deposits on Hydrate Ridge, OR. II: Hydrological processes," *Earth and Planetary Science Letters*, 201, 541–557 (2002).
174. Walter, K.M. et al., "Methane bubbling from northern lakes: Present and future contributions to the global methane budget," *Philosophical Transactions of the Royal Society A: Mathematical, Physical & Engineering Sciences*, 365, 1657–1676 (2007).
175. Wang, J.S. et al., "A 3-D model analysis of the slowdown and interannual variability in the methane growth rate from 1988 to 1997," *Global Biogeochemical Cycles*, 18, GB3011 (2004).
176. Westbrook, G.K. et al., "Escape of methane gas from the seabed along the West Spitsbergen continental margin," *Geophysical Research Letters*, 36, L15608 (2009).
177. Yvon-Lewis, S.A. et al., "Methane flux to the atmosphere from the deepwater horizon oil disaster," *Geophysical Research Letters*, 38, L01602 (2011).
178. Zachos, J. et al., "Trends, rhythms, and aberrations in global climate 65 Ma to present," *Science*, 292, 686–693 (2001).
179. Zachos, J. et al., "Rapid acidification of the ocean during the Paleocene-Eocene thermal maximum," *Science*, 308, 1611–1615 (2005).
180. Ruppel, C. and Noserale, D., "Gas hydrates and climate warming," USGS Report, USGS, Reston, VA, 1–9 (January 2012).
181. Tang, L.G., Xiao, R., Huang, C., Feng, Z.P., and Fan, S.S., "Experimental investigation of production behavior of gas hydrate under thermal stimulation in unconsolidated sediment," *Energy & Fuels*, 19 (6), 2402–2407 (2005).
182. Kawamura, T., Ohtake, M., Sakamoto, Y., Yamamoto, Y., Haneda, H., Komai, T., and Higuchi, S., "Experimental study on steam injection method using methane hydrate core samples," *Proceedings of the 7th ISOPE Ocean Mining Symposium*, July 1–6, Lisbon, Portugal, 83–86 (2007).
183. Kamath, V.A., "Study of heat transfer characteristics during dissociation of gas hydrates in porous media," PhD dissertation, University of Pittsburgh, Pittsburgh, PA (1984).
184. Hancock, S., Collett, T.S., Dallimore, S.R., Satoh, T., Huenges, E., and Henningses, J., "Overview of thermal stimulation production test results for the Japex/JNOC/GSC Mallik Gas Hydrate Research Well," in Dallimore, S.R. and Collett, T.S. (eds.), *Scientific Results from Mallik 2002 Gas Hydrate Production Research Well Program*. Geological Survey of Canada Bulletin 585, Mackenzie Delta, NWT (2005).
185. Circone, S., Kirby, S., and Stern, L., "Thermal regulation of methane hydrate dissociation: Implications for gas production models," *Energy & Fuels*, 19 (6), 2357–2363 (2005).

186. Li, G., Li, X., Tang, L.-G., and Li, Q.-P., "Control mechanisms for methane hydrate production by thermal stimulation," *Proceedings of the 6th International Conference on Gas Hydrates*, July 6–10, Vancouver, BC (2008).
187. Computer Modeling Group, Steam, Thermal, and Advanced Processes Reservoir Simulator (STARS), [www.cmggroup.com/software/stars.htm](http://www.cmggroup.com/software/stars.htm).
188. Ruppel, C., Dickens, G., Castellini, D., Gilhooly, W., and Lizzaralde, D., "Heat and salt inhibition of gas hydrate formation in the northern Gulf of Mexico," *Geophysical Research Letters*, 32 (4), L04605 (2005).
189. Bai, Y., Li, Q., Li, X., and Du, Y., "The simulation of nature gas production from ocean gas hydrate reservoir via depressurization," *Science in China Series E: Technological Sciences*, 51, 1272–1282 (2008).
190. Hong, H. and Pooladi-Darvish, M., "Simulation of depressurization for gas production from gas hydrate reservoirs," *Journal of Canadian Petroleum Technology*, 44 (11), 39–46 (2005).
191. Tang, L.G., Li, G., Hao, Y.M., Fan, S.S., and Feng, Z.P., "Effects of salt on the formation of gas hydrate in porous media," *Proceedings of the 5th International Conference on Gas Hydrate*, Trondheim, Norway, 155–160 (2005).
192. Ji, C., Ahmadi, G., and Smith, D., "Natural gas production from hydrate decomposition by depressurization," *Chemical Engineering Science*, 56 (20), 5801–5814 (2001).
193. Kono, H.O., Narasimhan, S., Song, F., and Smith, D.H., "Synthesis of methane gas hydrate in porous sediments and its dissociation by depressurizing," *Powder Technology*, 122 (2–3), 239–246 (2002).
194. Moridis, G.J., Kowalsky, M.B., and Pruess, K., "Depressurization-induced gas production from class 1 hydrate deposits," *SPE Reservoir Evaluation & Engineering*, 10 (5), 458–481 (2007).
195. Tang, L., Li, X., Feng, Z., Li, G., and Fan, S., "Control mechanisms for gas hydrate production by depressurization in different scale hydrate reservoirs," *Energy & Fuels*, 21 (1), 227–233 (2007).
196. Yousif, M.H., Li, P.M., Selim, M.S., and Sloan, E.D., "Depressurization of natural gas hydrates in Berea sandstone cores," *Journal of Inclusion Phenomena and Macrocyclic Chemistry*, 8, 71–88 (1990).
197. Moridis, G.J., Kowalsky, M., and Pruess, K., "Depressurization-induced gas production from class 1 hydrate deposits," *SPE Reservoir Evaluation & Engineering*, 10 (5), 458–481 (2007).
198. Fan, S.S., Zhang, Y.Z., Tian, G.L., Liang, D.Q., and Li, D.L., "Natural gas hydrate dissociation by presence of ethylene glycol," *Energy & Fuels*, 20 (1), 324–326 (2006).
199. Kamath, V.A.M.P.N., Sira, J.H., and Patil, S.L., "Experimental study of Brine injection and depressurization methods for dissociation of gas hydrate," *SPE Formation Evaluation*, 6 (4), 477–484 (1991).
200. Kawamura, T., Yamamoto, Y., Ohtake, M., Sakamoto, Y., Komai, T., and Haneda, H., "Dissociation experiment of hydrate core sample using thermodynamic inhibitors," *Proceedings of the 15th International Offshore and Polar Engineering Conference*, June 19–24, Seoul, South Korea (2005).
201. Moridis, G.J., Collett, T., Dallimore, S., Satoh, T., Hancock, S., and Weatherill, B., "Numerical studies of gas production from several CH<sub>4</sub> hydrate zones at the Mallik Site, Mackenzie Delta, Canada," *Journal of Petroleum Science and Engineering*, 43 (3–4), 219–238 (2004).
202. Moridis, G.J., "Numerical studies of gas production from class 2 and class 3 hydrate accumulations at the Mallik Site, Mackenzie Delta, Canada," *SPE Reservoir Evaluation & Engineering*, 7 (3), 175–83 (2004).

203. Moridis, G.J., Collett, T.S., Boswell, R., Kurihara, M., Reagan, M.T., Koh, C., and Sloan, E.D., "Toward production from gas hydrates: Current status, assessment of resources, and simulation-based evaluation of technology and potential," *SPE Reservoir Evaluation & Engineering*, 12 (5), 745–771 (2009).
204. Moridis, G.J. and Collett, T.S., "Strategies for gas production from hydrate accumulations under various geologic conditions," Report LBNL-52568, Lawrence Berkeley National Laboratory, Berkeley, CA (2004).
205. Moridis, G., Collett, T.S., Boswell, R., Kurihara, M., Reagan, M., Koh, C., and Sloan, E., "Toward production from gas hydrates: Current status, assessment of resources, and simulation-based evaluation of technology and potential," *SPE Unconventional Reservoirs Conference*, SPE 114163 (2008).
206. Moridis, G.J., "Numerical studies of gas production from methane hydrates," *SPE Journal*, 8 (4), 359–370 (2003).
207. Pooladi-Darvish, M., "Gas production from hydrate reservoirs and its modeling," *Journal of Petroleum Technology*, 56 (6), 65–71 (2004).
208. Sun, X., Nanchary, N., and Mohanty, K., "1-D modeling of hydrate depressurization in porous media," *Transport in Porous Media*, 58 (3), 315–338 (2005).
209. Goel, N., Wiggins, M., and Shah, S., "Analytical modeling of gas recovery from in situ hydrates dissociation," *Journal of Petroleum Science and Engineering*, 29 (2), 115–127 (2001).
210. Tsyppkin, G.G., "Mathematical models of gas hydrates dissociation in porous media," *Gas Hydrates: Challenges for the Future*, 912, 428–436 (2000).
211. Moridis, G.J., "Numerical studies of gas production from methane hydrates," *SPE Journal*, 32 (8), 359 (2003).
212. Moridis, G.J., Collett, T., Dallimore, S., Satoh, T., Hancock, S., and Weatherhill, B., "Numerical studies of gas production from several methane hydrate zones at the Mallik Site, Mackenzie Delta, Canada," *Journal of Petroleum Science and Engineering*, 43, 219 (2004).
213. White, M.D. and Oostrom, M., *STOMP: Subsurface Transport over Multiple Phases, Version 4.0, User's Guide*. PNNL-15782, Pacific Northwest National Laboratory, Richland, WA (2006).
214. Sung, W.M., Lee, H., and Lee, C., "Numerical study for production performances of a methane hydrate reservoir stimulated by inhibitor injection," *Energy Sources*, 24 (6), 499–512 (2002).
215. Kawamura, T., Sakamoto, Y., Ohtake, M., Yamamoto, Y., Haneda, H., Yoon, J.H., and Komai, T., "Dissociation behavior of hydrate core sample using thermodynamic inhibitor," *International Journal of Offshore and Polar Engineering*, 16 (1), 5–9 (2006).
216. Li, X.S., Wan, L.H., Li, G., Li, Q.P., Chen, Z.Y., and Yan, K.F., "Experimental investigations into the production behavior of methane hydrate in porous sediment under ethylene glycol injection and hot brine stimulation," *Industrial & Engineering Chemistry Research*, 47 (23), 11 (2008). [www.intechopress.com/download.pdf/11347](http://www.intechopress.com/download.pdf/11347).
217. Li, G., Tang, L., Huang, C., Feng, Z., and Fan, S., "Thermodynamic evaluation of hot brine stimulation for natural gas hydrate dissociation," *Huagong Xuebao/Journal of Chemical Industry and Engineering (China)*, 57 (9), 2033–2038 (2006).
218. Kawamura, T., Yamamoto, Y., Ohtake, M., Sakamoto, Y., Komai, T., and Haneda, H., "Experimental study on dissociation of hydrate core sample accelerated by thermodynamic inhibitors for gas recovery from natural gas hydrate," *The 5th International Conference on Gas Hydrate*, June 12–16, Trondheim, Norway (2005).
219. Li, G., Li, X., Tang, L., and Zhang, Y., "Experimental investigation of production behavior of methane hydrate under ethylene glycol stimulation in unconsolidated sediment," *Energy & Fuels*, 21 (6), 3388–3393 (2007).

220. Li, G., Li, X., Tang, L., Zhang, Y., Feng, Z., and Fan, S., "Experimental investigation of production behavior of methane hydrate under ethylene glycol injection," *Huagong Xuebao/ Journal of Chemical Industry and Engineering* (China), 58 (8), 2067–2074 (2007).
221. Sira, J.H., Patil, S.L., and Kamath, V.A., "Study of hydrate dissociation by methanol and glycol injection," *Proceedings of the SPE Annual Technical Conference and Exhibition*, Society of Petroleum Engineers of AIME, Richardson, TX, 977–984 (1990).
222. Inks, T.L., Lee, M.W., Agena, W.F., Taylor, D.J., Collett, T.S., Zyrianova, M.V., and Hunter, R.B., "Seismic prospecting for gas hydrate and associated free gas prospects in the Milne Point area of northern Alaska," in Collett, T., Johnson, A., Knapp, C., and Boswell, R. (eds.), *Natural Gas Hydrates—Energy Resource Potential and Associated Geologic Hazards*. AAPG Memoir 89, AAPG, Tulsa, OK, 555–583 (2009).
223. Walsh, M.R., Hancock, S.H., Wilson, S.J., Patil, S.L., Moridis, G.J., Boswell, R., Collett, T.S., Koh, C.A., and Sloan, E.D., "Preliminary report on the commercial viability of gas production from natural gas hydrates," *Energy Economics*, 31, 815–823 (2009).
224. Pawar, R.J., Zvyolowski, G., Tenma, N., Sakamoto Y., and Komai, T., "Numerical simulation of gas production from methane hydrate reservoirs," *Proceedings of the 5th International Conference on Gas Hydrates*, Paper 1040, June 13–16, Trondheim, Norway, Vol. 1, 258–267 (2005).
225. Moridis, G.J., Kowalsky, M.B., and Pruess, K., "TOUGH+HYDRATE v1.0 user's manual: A code for the simulation of system behavior in hydrate-bearing porous media," Report LBNL-149E, Lawrence Berkeley National Laboratory, Berkeley, CA (2008).
226. Wilder, J.W., Moridis, G.J., Wilson, S.J., Kurihara, M., White, M., Masuda, Y., Anderson, B.J. et al., "An international effort to compare gas hydrate reservoir simulators," *Proceedings of the 6th International Conference on Gas Hydrates*, Vancouver, BC (2008).
227. Dallimore, S.R., Collett, T.S., Uchida, T., Weber, M., and Takahashi, H.; Mallik Gas Hydrate Research Team, "Overview of the 2002 Mallik Gas Hydrate Production Research Well Program," *Proceedings of the 4th International Conference on Gas Hydrates*, Vol. 1, 36–39 (2002).
228. Hancock, S., Collett, T., Pooladi-Darvish, M., Gerami, S., Moridis, G., Okazawa, T., Osadetz, K., Dallimore, S., and Weatherill, B., "A preliminary investigation on the economics of onshore gas hydrate production based on the Mallik Field discovery," *American Association of Petroleum Geologists Hedberg Conference Proceedings*, Vancouver, CA (2004).
229. Howe, S.J., "Production modeling and economic evaluation of a potential gas hydrate pilot production program on the North Slope of Alaska," MS thesis, University of Alaska Fairbanks, Fairbanks, AK, 138pp (2004).
230. Nakano, S., Yamamoto, K., and Ohgaki, K., "Natural gas exploitation by carbon dioxide from gas hydrate fields—High-pressure phase equilibrium for an ethane hydrate system," *Proceedings of the Institution of Mechanical Engineers*, 212, 159–163 (1998).
231. Ohgaki, K., Takano, K., and Moritoki, M., "Exploitation of CH<sub>4</sub> hydrates under the Nankai Trough in combination with CO<sub>2</sub> storage," *Kagaku Kogaku Ronbunshu*, 20, 121–123 (1994).
232. Takahashi, H., Fercho, E., and Dallimore, S.R., "Drilling and operations overview of the Mallik 2002 Production Research Well Program," in Dallimore, S.R. and Collett, T.S. (eds.), *Scientific Results from Mallik 2002 Gas Hydrate Production Research Well Program, Mackenzie Delta, Northwest Territories, Canada*, Vol. Bulletin 585. Geological Survey of Canada, Vancouver, BC (2005).
233. Moridis, G.J., Reagan, M.T., Kim, S.J., Seol, Y., and Zhang, K., "Evaluation of the gas production potential of marine hydrate deposits in the Ulleung basin of the Korean East Sea," *SPE Journal*, 14 (4), 759–781 (2009).

234. Sung, W.M., Lee, H., Kim, S., and Kang, H., "Experimental investigation of production behaviors of methane hydrate saturated in porous rock," *Energy Sources*, 25 (8), 845–856 (2003).
235. Yousif, M.H., Abass, H.H., Selim, M.,S., and Sloan, E.D., "Experimental and theoretical investigation of methane-gas-hydrate dissociation in porous media," *SPE Reservoir Engineering*, 6 (4), 69–76 (1991).
236. Moridis, G.J. and Reagan, M., "Strategies for production from oceanic Class 3 hydrate accumulations," OTC Paper 18865 (2007).
237. Tohidi, B., Anderson, R., Clennell, M.B., Burgass, R.W., and Biderkab, A.B., "Visual observation of gas-hydrate formation and dissociation in synthetic porous media by means of glass micromodels," *Geology*, 29 (9), 867–870 (2001).



# Taylor & Francis

Taylor & Francis Group

<http://taylorandfrancis.com>

---

# 13 Power and Energy Directly from Water

## 13.1 INTRODUCTION

In Chapters 2 through 12, we examined (1) the benign role water plays for fuel production and energy carrier; (2) water (in the form of steam, water, or supercritical water) as a chemical solvent, reactant, or catalyst to generate fuels; and (3) the direct role it plays to generate hydrogen and methane. In this chapter, we briefly examine the direct role of water for the generation of power and electricity.

Water can directly generate energy and power in three different ways: hydropotential energy (or hydroelectricity), hydrokinetic energy (or a mixture of hydrokinetic energy and hydropotential energy like in tidal wave), and the use of ocean thermal energy conversion (OTEC) technologies. Here, we examine all three methods for generating power with the direct use of water.

The use of water dams to generate hydroelectricity has been practiced for a long time. This is a very clean method for power generation since it has a very little effect on greenhouse gas (GHG) production. Along with hydroelectricity, in recent years, hydrokinetic energy that uses the kinetic energy stored in tidal waves, sea and ocean shore waves, and undercurrents and inland waterways has been harnessed to generate electricity with the numerous different types of devices. The energy can also be harnessed from the temperature difference between the surfaces of the ocean (warm) and deep water (cold) using numerous OTEC devices. All three methods solely use water to generate power. This chapter briefly describes our current state of art on this subject.

## 13.2 HYDROELECTRIC POWER BY WATER DAMS

Water has been used for a long time to directly generate energy and power through hydroelectricity [1–32] (Zainuddin et al., 2012, pers. comm.). In this process, electricity is generated by hydropower, the production of electrical power through the use of the gravitational force of falling or flowing water. It is the most widely used form of renewable energy for power generation and accounts for 16% of global electricity consumption. This method has generated about 3427 TWh of electricity in 2010 [1]. Hydropower is produced in 150 different countries, with the Asia-Pacific region generating 32% of global hydropower in 2010 [1]. The top 10 countries for hydroelectricity generation in 2009 are listed in Table 13.1 [1]. As summarized in Table 13.1, China is the largest producer of hydroelectricity. Major new projects that are under construction worldwide are listed in Table 13.2 [1].

**TABLE 13.1**  
**Ten Largest Hydroelectricity Producers as of 2009**

Country	Annual Hydroelectricity Production (TWh)	Installed Capacity (GW)
China	652.05	196.79
Canada	369.5	88.974
Brazil	363.8	69.080
United States	250.6	79.511
Russia	167.0	45.000
Norway	140.5	27.528
India	115.6	33.600
Venezuela	85.96	14.622
Japan	69.2	27.229
Sweden	65.5	16.209

Source: "Hydroelectricity," Wikipedia, the free encyclopedia, 1–7, 2012.

**TABLE 13.2**  
**Major Global Hydroelectricity Projects ( $\geq 3000$  MW) under Construction**

Country	Name	Maximum Capacity (MW)	Construction (Start/Completion)
China	Xiluodu Dam	12,600	2005/2015
Brazil	Belo Monte Dam	11,181	2011/2015
India	Upper Siang HE project	11,000	2009/2024
Burma	TaSang Dam	7,100	2007/2022
China	Xiangjiaba Dam	6,400	2006/2015
China	Nuozhadu Dam	5,850	2006/2017
China	Jinping-II hydropower station	4,800	2007/2014
Pakistan	Diamer-Bhasha Dam	4,500	2011/2023
China	Jinping-I hydropower station	3,600	2005/2014
Brazil	Santo Antônio Dam	3,150	2008/2013
Brazil	Jirau Dam	3,300	2008/2013
China	Pubugou Dam	3,300	2004/2010
China	Goupitan Dam	3,000	2003/2011
China	Guanyinyan Dam	3,000	2008/2015
China	Lianghekou Dam	3,000	2009/2015
Russia	Boguchany Dam	3,000	1980/2013

Source: "Hydroelectricity," Wikipedia, the free encyclopedia, 1–7, 2012.

The cost of producing hydroelectricity is relatively low, making it competitive with other renewable sources of energy. The average cost of electricity from a hydro-plant larger than 10 MW is about 3–5 cents per kWh [1]. Hydroelectricity is also a very flexible source because plants can be ramped up and down very quickly to adapt the changing energy demands. While hydroelectricity creates very little waste and

GHG emissions, the creation and operation of dams have some environmental effects such as changing ecosystems and displacing people and wildlife, and these issues need to be considered in the development of the new hydroelectricity projects. There are numerous methods for obtaining hydroelectricity. These are briefly described in Sections 13.2.1 through 13.2.3 and in Section 13.2.6 [1–13].

### 13.2.1 CONVENTIONAL DAMS

Most hydroelectric power comes from the potential energy of dammed water driving a water turbine and generator [1–13]. The power extracted from the water depends on the height of the dam and volume of waterfall. The potential energy is proportional to the height of the dam. A large pipe called penstock delivers water to the turbine. A typical cross section of dam, turbine, and generator is graphically illustrated in Figure 13.1.

### 13.2.2 PUMPED STORAGE

In many situations, water at the lower level reservoir is pumped back to the higher level reservoir [1–13]. Thus, when there is a higher demand, water is released back into the lower reservoir through a turbine. The pumped-storage scheme provides the most commercially important means of large-scale grid energy storage and improves the daily capacity factor of the generation system. It also supplies extra energy during emergency needs.

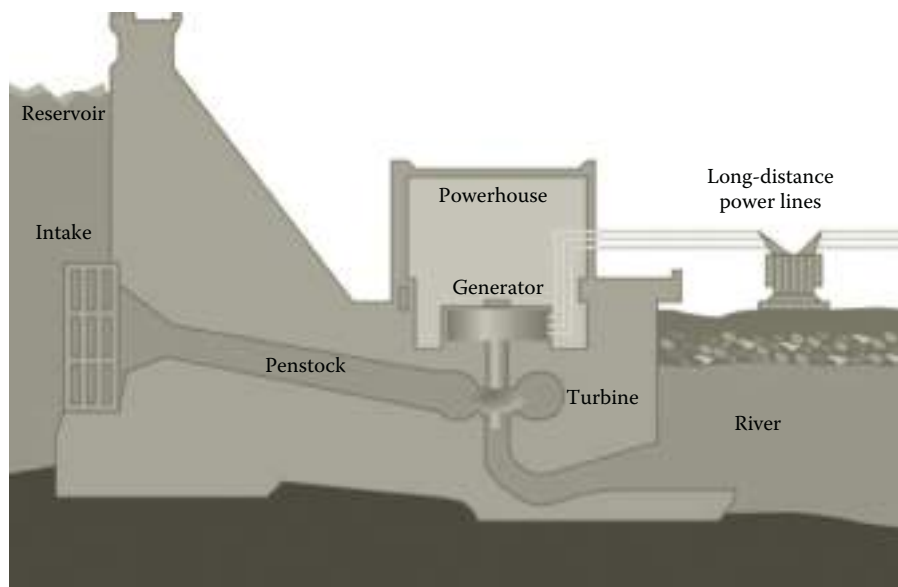


**FIGURE 13.1** (See color insert.) Cross section of a conventional hydroelectric dam. (Adapted from “Hydroelectricity,” Wikipedia, the free encyclopedia, 1–7, 2012.)

### 13.2.3 OTHER METHODS

Numerous other methods are also used to generate hydroelectricity [1–32] (Zainuddin et al., 2012, pers. comm.). Some of these combine the principles of hydrokinetic energy to generate power and electricity. If there is small or no reservoir capacity, the water from the upstream is used for generation according to the need and bypassing the dam. This method is called run-of-the-river hydroelectric station. Hydroelectricity can also be generated using rise and fall of ocean water due to tides. The conditions of tides are predictable, and if reservoirs can be constructed, it can supply hydroelectricity during high demand periods. Sometimes tides are so high (>40 ft [33]) that they provide both potential and kinetic energy for the power generation. This subject is further discussed in Section 13.3.

An underground power station can make use of a large natural difference between two waterways such as waterfall or a mountain lake. An underground tunnel can also be constructed to take the water from high reservoir to the power-generating hall built in an underground cavern near the lowest point of the water tunnel and a horizontal water pipe taking the water away to the lower waterway. The size of the hydroelectricity generated by these methods can be large, small [14–16], micro (<100 kW) [17–25], or pico (<5 kW) [26–32] (Zainuddin et al., 2012, pers. comm.). These different levels of hydropower generations are further discussed in Section 13.2.6.

### 13.2.4 ADVANTAGES AND DISADVANTAGES OF HYDROELECTRIC POWER

Hydroelectric power offers various advantages and disadvantages, some of which are listed in Sections 13.2.4.1 and 13.2.4.2.

#### 13.2.4.1 Advantages

Hydroelectric power offers the following advantages:

1. Hydroelectricity is flexible and relatively inexpensive.
2. The operating costs for dams are usually low because of automation and low manual labor requirement during normal operations.
3. A new plant for specific purposes can be added with relatively low construction cost. The life of dam can be 50–100 years.
4. Hydroelectric plants can also be suitable for specific industrial purposes. For example, dedicated hydroelectric plant provides a substantial amount of electricity needed for aluminum electrolytic plants. There are numerous examples of the use of hydroelectricity in aluminum plants in the United States and New Zealand.
5. Hydroelectricity does not produce carbon dioxide emissions, although some CO<sub>2</sub> emissions can be produced during the manufacture and construction of the project.
6. Hydroelectric dams can also provide water sports, an attraction for tourists, aqua culture, and irrigation support to agriculture industry with constant water supply.
7. Large dams can control floods that can affect people living downstream of the dams.

#### 13.2.4.2 Disadvantages

While hydroelectricity offers many advantages as stated above, it also has some drawbacks. Some of these drawbacks are briefly stated as follows

1. Hydroelectric projects can change the ecosystem and loss of the land. Dams can have a serious effect on salmon and fish populations around the dams.
2. When water flows, it has the ability to transport heavier particles downstream. This has a negative effect on the operation of dams and subsequently their power stations.
3. High siltation can fill a reservoir and reduce its capacity to control floods along with causing additional horizontal pressure on the upstream portion of the dam. This can ultimately result in the failure of the reservoir due to accumulation of large sediments [10,11].
4. When a dam is on the river, the change in river flow can affect the amount of power supply to the neighborhood. This can be important as the temperature of the water and rainfall changes under different climates.
5. In tropical regions, reservoirs of power plants may produce a substantial amount of methane. This is because of the decay of plant materials in an anaerobic environment that results in methane production by microbiological reactions. This type of emission is higher when the reservoir is large compared to its electricity-generating capacity, and the forests surrounding the dams are not cleared [10,11].
6. The new dam projects also displace people. The capital costs for new dam projects are high.
7. For large dams, failure of dam due to poor construction can be the largest man-made disasters in the history. The Banqiao Dam failure in Southern China resulted in the deaths of 26,000 people, with another 145,000 from epidemics, and millions were left without homes [1–13,34].

#### 13.2.5 ENVIRONMENTAL ISSUES

Hydroelectric power is environment friendly. Some evidences toward this fact are as follows

1. Unlike in coal- or gas-driven power plants, hydroelectricity eliminates flue gas emissions, including pollutants such as sulfur dioxide, nitric oxide, carbon monoxide, dust, and mercury. It also eliminates emissions of GHG like methane and carbon dioxide.
2. It eliminates all the health hazards related to coal mining and coal dust emissions.
3. It also eliminates all the negative consequences of “fracking process” to recover unconventional gas for gas-driven power plants.
4. Compared to nuclear power, hydroelectricity generates no nuclear waste and has none of the dangers associated with uranium mining nor nuclear leaks.
5. Unlike coal-, gas-, or uranium-driven power plants, hydroelectricity is a renewable and carbon-free energy source.

Due to all these environmental benefits, the use of hydroelectricity for power generation will grow worldwide over the next several decades.

### **13.2.6 SIZE AND CAPACITIES OF HYDROELECTRIC POWER FACILITIES**

While there are no official breakdowns of the type of hydroelectric power plants, they are generally categorized based on the amount of power generation into four parts:

1. Large power plants (generally >10 GW)—Currently, there are three such plants in the world: Three Gorges dam (22.5 GW), Itaipu dam (14 GW), and Guri dam (10.2 GW) [1–13].
2. Small power plants (generally with capacity up to 10–30 MW) with significant growth in China, Japan, the United States, and India [14–16].
3. Micropower plants (generally with a capacity up to 100 kW) provide power to isolated home or community [17–25].
4. Picopower plants (generally with power capacity under 5 kW) used in remote community requiring small amount of electricity [26–32] (Zainuddin et al., 2012, pers. comm.).

Since we already examined some details on large hydroelectric power generation, in Sections 13.2.6.1 through 13.2.6.3, we briefly assess some of the characteristics of small-, micro-, and picopower plants.

#### **13.2.6.1 Small Hydropower Plants**

Small hydropower plants are generally used in a small community or an industrial plant [14–16]. They may be connected to conventional electrical distribution networks as a source of low-cost renewable energy. They are also often built in remote areas where it would be uneconomical to provide electricity from national electrical distribution network. They have low environmental impact. In a typical installation, water is fed from a reservoir through a channel or pipe into a turbine. The pressure of the flowing water on the turbine blades makes the shaft to rotate. This rotating shaft is connected to the electric generator, which converts the motion of the shaft into electrical energy. Small hydropower plants can be further subdivided into mini-hydro, which has production capacity of less than 1000 kW [1,14–16].

#### **13.2.6.2 Microhydropower Plants**

These type of power plants produce electricity up to 100 kW using flow of water [17–25]. The installation is often just a small dammed pool at the top of a waterfall, with several hundred feet of pipe leading to a small generator housing. They are useful to provide electricity to a small community. This type of power plant is frequently accomplished with a Pelton wheel for high-head, low-flow water supply. Construction details of microhydropower plant are site specific. The production range of such systems is often calculated in terms of “head” and “flow”; the higher each of these are, more power can be generated. The construction of such a power station requires an “intake” structure where water is diverted from natural stream,

river, or waterfall. Such a structure screens out floating debris, fish, and other large objects. Microhydropower plants are very popular in poor countries for local power supply [17–25].

### 13.2.6.3 Picohydropower Plants

This is generally built in a remote community that requires only small amount of electricity (<5 kW) [26–32] (Zainuddin et al., 2012, pers. comm.). These types of setups typically are run-off stream, meaning that dams are not used but pipe diverts some of the flow and drops this down a gradient and through the turbine before being exhausted back to the stream. Two examples of picohydropower stations are in the towns of Kithamba and Thimba in Kenya [26]. Just like microhydropower stations, these are very popular in poor countries. Both micro- and picohydropower stations can be improved by custom-designed power-generation systems [31,32] (Zainuddin et al., 2012, pers. comm.).

## 13.3 HYDROKINETIC ENERGY AND POWER GENERATION

Fundamentally, hydrokinetic energy is the energy generated from moving water [34–71].\*<sup>†</sup> The power of tidal, river, and ocean currents and ocean waves is tremendous, and the basic concept behind hydrokinetic power is not new. For a century, people have harnessed the power of river currents by installing water wheels of various sorts to turn shafts or belts [35,49,50].<sup>‡</sup> Modern tidal/river/ocean current hydrokinetic machines use new technology that is designed to operate in high amplitude waves and fast currents. These emerging technologies have the potential to provide significant amounts of affordable electricity with low environmental impact given proper care in their deployment and operation [53–60] (Bertsch, 2012, pers. comm.).

### 13.3.1 WHY HYDROKINETIC ENERGY?

It is estimated that the amount of hydrokinetic energy that can be feasibly captured can power 67 million homes [50–60] (Bertsch, 2012, pers. comm.). It is expected that by 2025, 13,000 MW of power can be generated using hydrokinetic energy [50–60] (Bertsch, 2012, pers. comm.). This can displace 22 new coal-fired power plants [57,60]. Just like hydroelectricity, hydrokinetic energy has very little effect on air and global climate change. They generate power only from the kinetic energy of moving water (current). This power is a function of the density of water and speed

---

\* Hydrokinetic energy was included as an eligible renewable energy resource by the Energy Policy Act of 2005. Various funding authorizations for research and development were also included in this Act as well as the Energy Independence and Security Act of 2007.

<sup>†</sup> Bertsch, D.J., Juris Doctoral candidate, The University of South Dakota School of Law, 2011; Congress defined hydrokinetic energy as “electrical energy from waves, tides, and currents in oceans, estuaries, and tidal areas; free flowing water in rivers, lakes, and streams, or man-made channels; and differentials in ocean temperature (ocean thermal energy conversion),” The Energy Independence and Security Act of 2007, 42 USC §17211 (2006).

<sup>‡</sup> Hydrokinetic energy was included as an eligible renewable energy resource by the Energy Policy Act of 2005. Various funding authorizations for research and development were also included in this Act as well as the Energy Independence and Security Act of 2007.

of the current cubed. The available hydrokinetic power thus depends on the speed of the river, ocean, or tidal current. The operation of the hydrokinetic device requires a minimum current and water depth. As water flows through a turbine or other device, the kinetic energy of the flowing river, tidal fluctuations, or waves is converted into electricity by the appropriate converting device.

Hydrokinetic energy is different from hydroelectricity in the fact that it does not require a change in elevation. Also, unlike traditional hydropower projects, hydrokinetic energy projects do not require impoundments or diversions of water [34,61–65] (Bertsch, 2012, pers. comm.).<sup>\*</sup> Instead, these projects harness the power of moving water in waves, currents, and tidal channels [34,61–65] (Bertsch, 2012, pers. comm.).<sup>†</sup> Hydrokinetic technologies can thus be distinguished based on these three major sources for harnessing hydrokinetic energy. Waves, currents, and tidal channels can be either from oceans, rivers, or inland waterways. Surface wave energy is generally harnessed near sea or ocean shores while energy from under-currents is harnessed using technologies installed below the water surface [34–47,61–65] (Bertsch, 2012, pers. comm.; Dixon et al., 2008, pers. comm.).<sup>‡,§</sup> Tidal power is harnessed by new tidal power-harnessing technologies, such as tidal barrage, tidal lagoons, and new axial or cross-flow turbine technologies [53,58].

While hydrokinetic energy can be obtained in a number of different ways, capturing the energy contained in near and offshore waves is thought to have the greatest energy production potential among various options. The rise and fall of ocean waves is driven by winds and influenced by oceanic geology. The extraction of only 15% of the energy in coastal waves would generate as much electricity as we currently produce in conventional hydroelectric dams [36–40] (Bertsch, 2012, pers. comm.; Dixon et al., 2008, pers. comm.).<sup>¶</sup> Much of this wave potential is found along our Pacific coast, near big cities and towns. Besides waves, ocean tides hold promise as an energy resource. Each change in the tide creates a current, called tidal stream. Regular tidal streams have the potential to provide a reliable new source of electricity without building dams and barrages. Ocean currents, such as Gulf stream, also offer hydrokinetic energy. These result from winds and equatorial solar heating. Free flowing rivers (without dams) and constructed waterways such as irrigation canals also allow the use of hydrokinetic

<sup>\*</sup> Bertsch, D.J., Juris Doctoral candidate, The University of South Dakota School of Law, 2011; Congress defined hydrokinetic energy as “electrical energy from waves, tides, and currents in oceans, estuaries, and tidal areas; free flowing water in rivers, lakes, and streams, or man-made channels; and differentials in ocean temperature (ocean thermal energy conversion),” The Energy Independence and Security Act of 2007, 42 USC §17211 (2006).

<sup>†</sup> Ibid.

<sup>‡</sup> Hydrokinetic energy was included as an eligible renewable energy resource by the Energy Policy Act of 2005. Various funding authorizations for research and development were also included in this Act as well as the Energy Independence and Security Act of 2007.

<sup>§</sup> Bertsch, D.J., Juris Doctoral candidate, The University of South Dakota School of Law, 2011; Congress defined hydrokinetic energy as “electrical energy from waves, tides, and currents in oceans, estuaries, and tidal areas; free flowing water in rivers, lakes, and streams, or man-made channels; and differentials in ocean temperature (ocean thermal energy conversion),” The Energy Independence and Security Act of 2007, 42 USC §17211 (2006).

<sup>¶</sup> Hydrokinetic energy was included as an eligible renewable energy resource by the Energy Policy Act of 2005. Various funding authorizations for research and development were also included in this Act as well as the Energy Independence and Security Act of 2007.

energy. Stream-based hydrokinetic energy is not as much researched as wave energy, although it is suggested that these resources can provide electricity needs of 23 million homes [34–47,61–65] (Bertsch, 2012, pers. comm.; Dixon et al., 2008, pers. comm.).<sup>\*†</sup> In lower southwest where wind energy has low potential, stream hydrokinetic energy can be a very valuable resource. Waves and ocean currents can provide a continuous power [34,61–65] (Bertsch, 2012, pers. comm.), which is not possible for solar, wind, and tidal stream energy.<sup>‡</sup> Since the kinetic energy from a stream is proportional to the cube of the speed of the current, site location is very important.

The hydrokinetic energy projects are renewable and emission free. The United States can avoid emitting 250 million metric tons of carbon dioxide per year if hydrokinetic energy represented 9% of the US energy consumption [34,61–65] (Bertsch, 2012, pers. comm.).<sup>§</sup> Electric Power Research Institute (EPRI) estimates that hydrokinetic resources can provide about 10% of today's electric consumption in the United States [44] (Dixon et al., 2008, pers. comm.). The sources of hydrokinetic energy are generally predictable and unaffected by weather variability. Wave patterns can be accurately forecast several days in advance [34,61–65] (Bertsch, 2012, pers. comm.) and tides will always reoccur every 12 h 25 min because they are connected to the moon's gravitational pull (Bertsch, 2012, pers. comm.).<sup>¶</sup> Both wave and tidal energy can provide base load power, eliminating the needs for backup sources [34–65] (Bertsch, 2012, pers. comm.).<sup>\*\*††</sup> River currents, however, fluctuate seasonally and are susceptible to wet and dry years, and this makes them difficult to predict from year to year [36].

### 13.3.2 HYDROKINETIC VERSUS HYDROELECTRIC ENERGY: POTENTIALS AND ISSUES

Unlike hydroelectric energy projects, hydrokinetic energy projects have little or no effects on the local aesthetics [36–40] (Bertsch, 2012, pers. comm.; Dixon et al., 2008, pers. comm.).<sup>‡‡</sup> They are generally underwater or a little removed

<sup>\*</sup> Hydrokinetic energy was included as an eligible renewable energy resource by the Energy Policy Act of 2005. Various funding authorizations for research and development were also included in this Act as well as the Energy Independence and Security Act of 2007.

<sup>†</sup> Bertsch, D.J., Juris Doctoral candidate, The University of South Dakota School of Law, 2011; Congress defined hydrokinetic energy as “electrical energy from waves, tides, and currents in oceans, estuaries, and tidal areas; free flowing water in rivers, lakes, and streams, or man-made channels; and differentials in ocean temperature (ocean thermal energy conversion),” The Energy Independence and Security Act of 2007, 42 USC §17211 (2006).

<sup>‡</sup> Ibid.

<sup>§</sup> Ibid.

<sup>¶</sup> Ibid.

<sup>\*\*</sup> Hydrokinetic energy was included as an eligible renewable energy resource by the Energy Policy Act of 2005. Various funding authorizations for research and development were also included in this Act as well as the Energy Independence and Security Act of 2007.

<sup>††</sup> Bertsch, D.J., Juris Doctoral candidate, The University of South Dakota School of Law, 2011; Congress defined hydrokinetic energy as “electrical energy from waves, tides, and currents in oceans, estuaries, and tidal areas; free flowing water in rivers, lakes, and streams, or man-made channels; and differentials in ocean temperature (ocean thermal energy conversion),” The Energy Independence and Security Act of 2007, 42 USC §17211 (2006).

<sup>‡‡</sup> Hydrokinetic energy was included as an eligible renewable energy resource by the Energy Policy Act of 2005. Various funding authorizations for research and development were also included in this Act as well as the Energy Independence and Security Act of 2007.

from shore for visual observations [36–40,61–65] (Bertsch, 2012, pers. comm.; Dixon et al., 2008, pers. comm.).<sup>\*</sup>† They can be installed wherever energy is needed [61–65] (Bertsch, 2012, pers. comm.).<sup>‡</sup> Since many high-demand urban areas are located near water, hydrokinetic energy projects can be easily integrated into existing grid. It can also provide energy to rural and remote areas where other means of power and electricity may not be possible.

In general, hydrokinetic energy differs from traditional hydropower [34–65] in three ways<sup>§¶</sup>:

1. As mentioned earlier, hydrokinetic energy projects do not require impoundments or diversions of water. Hydropower projects drastically alter the surrounding land. They can increase the likelihood of flooding upstream of the dam [1–13]. They also cause an increase in sedimentation in the reservoir [10,11]. It also causes an accelerated erosion of the riverbed caused by sediment-free water released downstream at a high velocity (Bertsch, 2012, pers. comm.).
2. Hydrokinetic projects do not displace a large number of people that hydropower projects do, particularly when the projects are large. For people staying near dam, there is a continuous threat of dam failure due to earthquake or other natural disasters [1–13] (Bertsch, 2012, pers. comm.).
3. Hydrokinetic energy projects can avoid impacts on surrounding wildlife, although it can have an effect on underwater ecosystem if not properly installed. The temperature and sea level fluctuations caused by hydrokinetic power projects can have an effect on the fisheries and other sea life. In general, if properly installed, hydrokinetic energy projects are more environment friendly than hydropower projects.

In this country, waterways in Alaska are well suited for tapping hydrokinetic energy. One of the challenges in hydrokinetic energy is the presence of glacial silt (in Alaska waters). Over time, silt and other sediments in the water flowing through hydrokinetic turbines can erode the machinery. In addition to this, the migration of fish

<sup>\*</sup> Hydrokinetic energy was included as an eligible renewable energy resource by the Energy Policy Act of 2005. Various funding authorizations for research and development were also included in this Act as well as the Energy Independence and Security Act of 2007.

<sup>†</sup> Bertsch, D.J., Juris Doctoral candidate, The University of South Dakota School of Law, 2011; Congress defined hydrokinetic energy as “electrical energy from waves, tides, and currents in oceans, estuaries, and tidal areas; free flowing water in rivers, lakes, and streams, or man-made channels; and differentials in ocean temperature (ocean thermal energy conversion),” The Energy Independence and Security Act of 2007, 42 USC §17211 (2006).

<sup>‡</sup> Ibid.

<sup>§</sup> Hydrokinetic energy was included as an eligible renewable energy resource by the Energy Policy Act of 2005. Various funding authorizations for research and development were also included in this Act as well as the Energy Independence and Security Act of 2007.

<sup>¶</sup> Bertsch, D.J., Juris Doctoral candidate, The University of South Dakota School of Law, 2011; Congress defined hydrokinetic energy as “electrical energy from waves, tides, and currents in oceans, estuaries, and tidal areas; free flowing water in rivers, lakes, and streams, or man-made channels; and differentials in ocean temperature (ocean thermal energy conversion),” The Energy Independence and Security Act of 2007, 42 USC §17211 (2006).

and marine mammals, ice and other debris, as well as river and ocean bed stability can significantly affect the performance of hydrokinetic energy machinery [34–65] (Bertsch, 2012, pers. comm.).<sup>\*,†</sup>

### 13.3.3 HYDROKINETIC POWER DEVICES

While tidal/river/ocean current energy and wave energy converters (WECs) are sometimes categorized separately [51–60], both types of technology can be categorized under the general term “hydrokinetic power devices.” Another marine energy technology, OTEC, is covered later in detail. It is mostly applicable to tropical areas [72–77].

Modern ocean wave energy conversion machines use new technology that is designed to operate in high amplitude waves, and modern tidal/river/ocean current hydrokinetic machines use new technology that is designed to operate in fast currents. Both of these emerging technologies have the potential to provide significant amounts of affordable power with low environmental impact. While each individual device can give a limited amount of power, often, a farm of devices are used to increase the total power generation capacity. All designs require careful thoughts and implementations of their deployment and operation.

The devices that generate energy from waves and currents are called hydrokinetic energy conversion devices. *Hydrokinetic* energy devices typically use vertical- or horizontal-axis turbines similar to those developed for wind generation or old water mills. Since water is approximately 850 times denser than air, the amount of energy generated by a hydrokinetic device is much greater than that produced by a wind turbine of equal diameter. In addition, river and tidal flow do not fluctuate as dramatically from moment to moment as wind does. This predictability benefit is particularly true for tidal energy. It can be predicted years in advance and is not affected by precipitation or evaporation.

Hydrokinetic energy conversion devices are broken into two categories: WECs and rotating devices [50,51]. WECs are generally installed at the surface of the water, while rotating devices are generally installed beneath the water surface. While the industry is still at the growing stage, there are a number of cost-effective and environmentally acceptable devices being developed, constructed, and installed. Some of these devices (and their modifications) have been tested at the pilot- and commercial-scale levels. The industry wants to build “wave parks” and turbine arrays that are capable of delivering clean and renewable electricity from different forms of wave energy.

---

<sup>\*</sup> Hydrokinetic energy was included as an eligible renewable energy resource by the Energy Policy Act of 2005. Various funding authorizations for research and development were also included in this Act as well as the Energy Independence and Security Act of 2007.

<sup>†</sup> Bertsch, D.J., Juris Doctoral candidate, The University of South Dakota School of Law, 2011; Congress defined hydrokinetic energy as “electrical energy from waves, tides, and currents in oceans, estuaries, and tidal areas; free flowing water in rivers, lakes, and streams, or man-made channels; and differentials in ocean temperature (ocean thermal energy conversion),” The Energy Independence and Security Act of 2007, 42 USC §17211 (2006).

### 13.3.3.1 Wave Energy Converters

In its basic design, WEC utilizes the principle of motion of two or more bodies relative to each other [50,51]. One body, called displacer, is acted on by the waves. The second body, called reactor, moves in response to the displacer. While there are a number of designs and configurations of WECs, the four most common ones are graphically depicted in Figure 13.2a through d [50,51].

In the oscillating water column, waves enter and exit in a partially submerged collector from below, causing the water column inside the collector to rise and fall. The changing water level acts as a piston as it drives the trapped air in the device above the water into turbine. The turbine movement generates electricity via a coupled generator. This device is graphically illustrated in Figure 13.2a [50,51].

In overtopping device, shown in Figure 13.2b, a floating reservoir is formed as waves break over the walls of the device. This reservoir creates a head of water higher than that of the surrounding ocean surface. The pressure necessary to turn hydroturbine is provided by this head of water. The water leaves the bottom of the device to return back into the sea [50,51]. The device can be used in tidal currents.

In an attenuator WEC (shown in Figure 13.2c), long, multiple sectioned, floating structures, which are joined and anchored at each end, are aligned parallel to the wave direction and they generate electricity by riding the waves. These heavy-surge devices utilize the passing waves to set each section into the rotational motion relative to the next segment. This relative motion, which is concentrated at the joint between the two consecutive segments, is used to pressurize a hydraulic piston that drives fluids through a motor. The hydraulic piston in turn drives the coupled generator and produces electricity [50,51].

Finally, the point absorber depicted in Figure 13.2d drives a turbine by using waves from all directions at a single point by using the vertical motion of the waves to act as a pump that pressurizes seawater or an internal fluid. While this type of device has many configurations, one of which is the hose pump point absorber that consists of a surface-floating buoy anchored to the seafloor with the turbine as a part of the vertical connection. The wave-induced vertical motion of buoy causes the connection to expand and contract, thereby producing pumping action. The captured energy and the resulting electricity generation by this device can be optimized [50,51] by operating the device and wave in resonance.

### 13.3.3.2 Commercial Applications of WEC

A brief summary of commercial applications of various types of WECs outlined above is given in Table 13.3 [60]. Locations of the devices outlined in Table 13.3 can be shoreline, nearshore, and offshore. Types of power takeoff include hydraulic ram, elastomeric hose pump, pump to shore, hydroelectric turbine, air turbine, and linear electrical generator [60]. Some of these designs incorporate parabolic reflectors to increase the wave energy at the point of capture. These capture systems use the rise and fall of motion of waves to capture energy. Once the energy is captured, power is transmitted to its use or to the electrical grid by transmission power cables [60]. More details on each device outlined in Table 13.3 are given in Ref. [60]. A more detailed

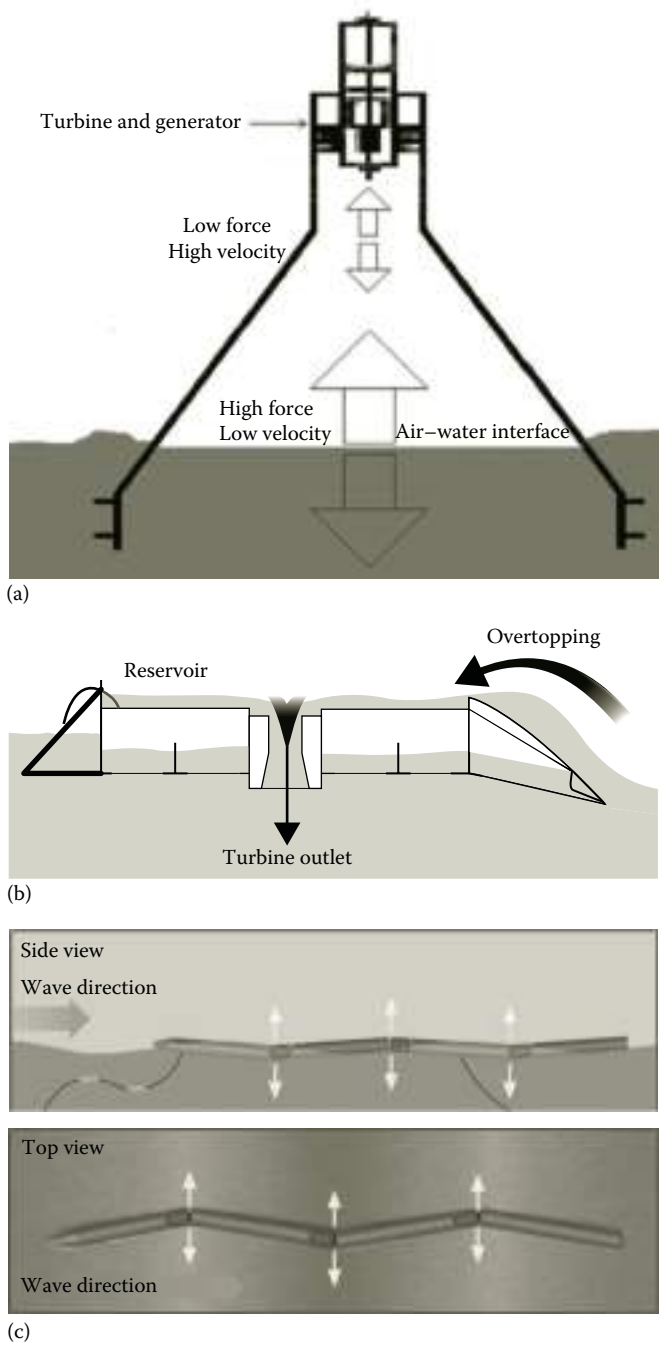


**FIGURE 13.2** Types of WECs: (a) oscillating water column; (b) overtopping WEC; (c) attenuator WEC; (Adapted from “How hydrokinetic energy works?” Union of Concerned Scientists, 1–5, 2012.)



(d)

**FIGURE 13.2** (Continued) Types of WECs: (d) point absorber. (Adapted from “How hydrokinetic energy works?” Union of Concerned Scientists, 1–5, 2012.)

assessment of WECs is also given in an excellent review by Drew et al. [78]. As can be seen from Table 13.3, WECs are used all around the world.

One commercial device, the tethered floating buoy [33,54,79,81], converts the energy in the rise and fall of the passing waves into electricity (often via hydraulics) (Figure 13.8a). This device uses the principle of point absorber depicted in Figure 13.2d. A farm of buoys can be installed in any given location (Section 13.3.4), and these are tied to the bottom of ocean and connected to the electrical grid system.

Other machines have chambers that, when filled and emptied by rising and falling wave water, compress and decompress air to drive an electric generator. One such design—“WaveRoller”—is illustrated in Figure 13.3. It uses the principle of

**TABLE 13.3**  
**Large-Scale Application of Various WECs**

Device/Year	Proponent	Country	Capture Method
<b>Commercial Application of Point Absorber</b>			
AquaBuOY/2003	Finavera Wind Energy SSE Renewable Ltd.	Ireland/Canada/ Scotland	Buoy
CETO wave power/1999	Carnegie	Australia	Buoy
FlanSea/2010	FlanSea	Belgium	Buoy
Lysekil Project/2002	Uppsala University	Sweden	Buoy
Oceanlinx/1997	Oceanlinx	Australia	Buoy
OE buoy/2006	Ocean Energy	Ireland	Buoy
PowerBuoy/1997	Ocean Power Technologies	United States	Buoy
SDE Sea Waves Power Plant/2010	SDE Energy Ltd.	Israel	Buoy
SeaRaser/2008	Alvin Smith (Dartmouth Wave Energy)/Electricity	United Kingdom	Buoy
Unnamed Ocean Wave Powered Generator/2004	SRI International	United States	Buoy
Wavebob/1999	Wavebob	Ireland	Buoy
Wave Star/2000	Wave Star A/S	Denmark	Multipoint Absorber
<b>Commercial Application of Attenuator</b>			
Anaconda Wave Energy Converter/2008	Checkmate Sea Energy	United Kingdom	Surface following attenuator
AWS-III/2010	AWS Ocean Energy	United Kingdom (Scotland)	Surface following attenuator
Pelamis Wave Energy Converter/1998	Pelamis Wave Power	United Kingdom (Scotland)	Surface following attenuator
R38/50 kW, R115/150 kW/2010	40 South Energy	United Kingdom	Underwater attenuator
<b>Commercial Applications of Oscillating Water Column</b>			
Islay LIMPET/1991	Islay LIMPET	Scotland	Oscillating water column
Oyster Wave Energy Converter/2005	Aquamarine Power	United Kingdom, Scotland, Irish	Oscillating wave surge converter
Wave Roller/1994	AW-Energy Oy	Finland	Oscillating wave surge converter
Cycloidal Wave Energy Converter/2006	Atargis Energy Corp.	United States	Fully submerged wave termination device
<b>Commercial Application of Overtopping Device</b>			
Wave Dragon/2003	ErikFrils-Madsen	Denmark	Overtopping device

Source: "Wave power," Wikipedia, the free encyclopedia, 2013.



**FIGURE 13.3** (See color insert.) WaveRoller wave energy farm installation in Peniche, Portugal. (Adapted from “Wave power,” Wikipedia, the free encyclopedia, 2013.)

oscillating water column described in Figure 13.2a. This device has been in operation in Finland since 1994.

Yet another type of machine looks like a giant sea snake (or a farm of snakes) with floating pontoons that heave and sway on the ocean surface, driving hydraulic pumps to power an electric generator [64,81–89]. This Pelamis “snake,” an offshore machine, consist of five tube sections that float on the surface and use the motion of the waves to generate electricity [60,64,81]. They use the principle of attenuator WEC (Figure 13.2c) described above. When the tube sections flex, hydraulic arms move in opposite directions and turn a generator that produces power. The amount of power required will dictate the number of such snakes in a given farm and to some extent the length of each snake (that can be as long as 600 ft). This device is also anchored to the seabed and must withstand marine environments. Waves powerful enough to drive these generators are often found off coasts with large oceans to their west (providing long wind fetch) and strong prevailing winds such as the west coasts of the United States, Chile, Australia, and in the North Sea among many others [46–60]. This technology is graphically illustrated in Reference [35] and extensively described in the Pelamis wave power website [enquiries@pelamiswave.com](mailto:enquiries@pelamiswave.com). The snakes are being commercially used off the shores in Portugal and Scotland [35,64,81–90].

Finally, one device that uses the above-described “overtopping” principle (Figure 13.2b) is “Wave Dragon” (shown in Figure 13.4), which is being used in Denmark since 2003.

### 13.3.3.3 Rotating Hydrokinetic Devices

The kinetic energy of flowing tidal stream, ocean current, or river can also be captured by the rotating device [47–60] shown in Figures 13.5 [50]. Such a device is generally installed underwater to harness maximum energy from the currents.



**FIGURE 13.4** (See color insert.) Wave Dragon seen from reflector. (Adapted from “Wave power,” Wikipedia, the free encyclopedia, 2013.)

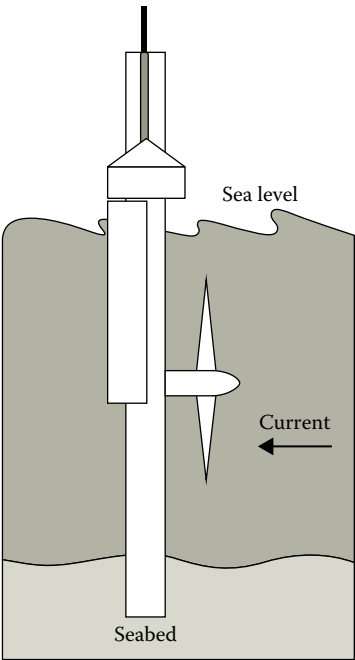


**FIGURE 13.5** (See color insert.) A horizontal-axis hydrokinetic rotating device, tidal turbine. (Adapted from “How hydrokinetic energy works?” Union of Concerned Scientists, 1–5, 2012.)



**FIGURE 13.6** (See color insert.) Cross-flow turbine used in Alaska Rivers: ORPC's TidGen™ power system. [Adapted from "Hydrokinetic energy (in river, tidal, and ocean current)," *Alaska Energy Wiki*, Alaska Center for Energy and Power, 1–4, 2012.]

In this device, the rotational energy created by the rotation of the blades drives turbine and creates electricity by a generator. This device is very similar to the wind turbine used for gathering wind energy for electricity. This similarity has helped a faster movement in its development. Some rotational device designs rotate around horizontal axis just like wind turbines, while others are either oriented around vertical axis or use a design resembling egg beaters. As shown later, this design has been successfully installed at a commercial scale at the bottom of New York City's East River.

The rotating device can also be a cross-flow device depicted in Figure 13.6 [51]. This type of cross-flow turbine is used in Alaska's rivers. The figure shows the Ocean Renewable Power Company (ORPC)'s Beta TidGen™ power system [51]. This design looks similar to old water wheel that was used to drive boats and barges. Such cross-flow turbines typically have a rotor formed by mounting two or more blades substantially parallel to a shaft that is typically vertical or horizontal. Horizontal cross-flow rotors can capture kinetic energy from flows in two directions (e.g., flood and ebb) without an orientation change, while a vertical-axis rotor can be omnidirectional depending on river conditions. The ORPC turbine shown in Figure 13.6 is an example of such a device [51].

Rotating devices also take a variety of forms in commercial applications but in general capture energy from the water flowing through or across a rotor. Some of these devices are shaped like propellers and can swing, or yaw, to face changing tidal currents. Other rotating devices are shaped like a jet engine, having many

vanes turning within a fixed outer ring [35,47–51,53,55–60]. Many other designs for rotating devices are presented in an excellent review by Ortega-Achury et al. [91].

One commercial design—“the open-center turbine”—is designed to be deployed directly on the seabed, and its installation is silent and invisible from the surface. It is located at depth and presents no navigational hazard. Farms of open-center turbines can provide a significant and undetectable supply of clean, predictable, renewable power. More details of this type of turbine are given in “OpenHydro” company website.

Fast currents, like those in the Missouri and Mississippi rivers, in tidal channels such as the Puget Sound, or in ocean currents such as the Gulf Stream off Florida, have enough power to turn large rotating devices. Since the power from a hydrokinetic machine is proportional to the cube of the current velocity, faster currents are better, and sites with current velocities reaching 3 m/s are desirable.

#### 13.3.3.4 Devices to Harness Tidal Power

Harnessing tidal power has traditionally suffered from high cost and limited availability of sites, with sufficiently high tidal ranges or flow velocities. The topic has, however, gained more attention due to new technological developments in design such as dynamic tidal power (DTP) or tidal lagoons and new turbine technology such as new axial flow and cross-flow turbines. Unlike in wave power, in tidal power, both the kinetic energy of the moving water and the potential energy difference between high and low tides can be used.

Tidal stream generator makes use of the kinetic energy of the moving water to power turbines just as wind turbines use wind to power turbines. Some tidal generators can be built in the structures of existing bridges. The world’s first commercial scale and grid-connected *tidal stream generator*—SeaGen—was built in Strangford Lough [92]. This power generator is illustrated in Figure 13.7.

*Tidal barrage* makes use of the potential energy difference in height between high and low tides. Tidal barrage technology takes advantage of predictable ocean tides. A barrage, or dam across an estuary or tidal channel, traps tidal flows and then releases them through turbines as tides fall [47–60]. When using tidal barrages to generate power, the potential energy from a tide is seized through the strategic placement of specialized dams. When the sea level rises and the tide begins to come in, the temporary increase in tidal power is channeled into a large basin behind the dam, holding a large amount of potential energy. With the receding tide, this energy is then converted into mechanical energy as the water is released through large turbines that create electrical power through the use of generators [93]. Barrages are essentially dams across the full width of a tidal channel.

DTP device exploits an interaction between potential and kinetic energies in tidal flows. These are very long dams (about 20–30 miles long) built from coasts straight out into the sea or ocean, without enclosing an area. High and low tidal phase differences are introduced across the dam, leading to a significant water-level differential in shallow coastal seas. These types of tidal currents are often found in the countries like the United Kingdom, China, and Korea. Besides tidal power, tidal lagoons are being rapidly developed and deployed.



**FIGURE 13.7** (See color insert.) The world's first commercial scale and grid-connected tidal stream generator—SeaGen—in Strangford Lough. (Adapted from “Tidal power,” Wikipedia, the free encyclopedia, 2013.)

On a global scale, several countries have long pursued tidal power R&D activities [34,61–63,65,94] (Bertsch, 2012, pers. comm.).\* The 240 MW La Rance barrage dam in France was the world's first tidal power station. This station was opened in 1966 and it has 24 turbines that generate electricity [33]. The Sihwa Lake Power station in Korea that began operating last year is the world's largest tidal power station with a generating capacity of 254 MW [33,90,95,96]. The Annapolis power plant at the Bay of Fundy in Canada which was built in 1984 also generates 20 MW of electricity from the Bay's record 43 ft tides [33].

### 13.3.3.5 Hydrokinetic Power Barges

These are designed for use in river and ocean currents with a horizontal-axis turbine in which a vertically submerged blade has performance characteristics similar to a horizontally mounted cross-flow turbine [52]. The turbine blades are concave such that the leading edge offers reduced resistance while the trailing edge is aerodynamically optimized to reduce the flat dynamic effect. The rotational speed of turbine is low. Since hydrokinetic power is proportional to the cube of velocity,

\* Bertsch, D.J., Juris Doctoral candidate, The University of South Dakota School of Law, 2011; Congress defined hydrokinetic energy as “electrical energy from waves, tides, and currents in oceans, estuaries, and tidal areas; free flowing water in rivers, lakes, and streams, or man-made channels; and differentials in ocean temperature (ocean thermal energy conversion),” The Energy Independence and Security Act of 2007, 42 USC §17211 (2006).

turbine blade can be designed to accommodate flow rate; it could be long and broad for slow-moving deep currents or it could be short and thin for fast-moving shallow currents.

The turbine is horizontally mounted on a barge and partially submerged into the water flowing beneath the barge. The barge on which turbines are mounted is able to cope with fluctuations in water levels, substantial velocity increases, and direct impact from large and fast-moving debris. The power output from the turbine would decrease only when the water flow rate underneath the barge goes down. The barge generates 1 MW and produces 8760 MWh electricity annually at a maximum rating through a synchronous AC induction generator.

The power barge has very low maintenance cost and downtime and life span of about 20 years. These barges can be deployed in rivers such as Mississippi, Amazon, and Nile. Different designs of the barges from different countries (the United Kingdom, Belgium, and Australia) are illustrated by alternative energy website news publication [52].

### 13.3.3.6 Criteria for Choice of a Device and Its Location

Generally, the following criteria and considerations are used to decide on the choice and size of a device and its location [34–65] (Bertsch, 2012, pers. comm.; Dixon et al., 2008, pers. comm.)<sup>\*†</sup>:

1. The use of hydrokinetic energy devices needs to carefully consider local environmental implications, economics, and competing users of the site chosen. The needs of users such as fishermen, shipping vessel operators, recreational boaters, and coastal citizen groups need to be factored in choosing the appropriate site for the recovery of hydrokinetic energy.
2. The device may affect the habitats of benthic animals and plants like oysters, clams, and sea grass; the potential for fish strikes or impingement on device; and the effect of noise on movement and migration of aquatic animals or even alteration of hydrologic and sediment regimes. With careful selection of location, these impacts can, however, be minimized.
3. The cost of electricity produced by these devices depend on the power density of stream ( $\text{kW}/\text{m}^2$ ) or wave crest ( $\text{kW}/\text{m}$  crest height), the distance that electricity must be transmitted to reach consumers, access of the site for maintenance and monitoring and availability of the site for federal subsidy, project financing, or guarantee market for the produced electricity.
4. In general, stronger currents and large wave heights will reduce the cost of the hydrokinetic electricity. The hydrokinetic devices require minimum

<sup>\*</sup> Hydrokinetic energy was included as an eligible renewable energy resource by the Energy Policy Act of 2005. Various funding authorizations for research and development were also included in this Act as well as the Energy Independence and Security Act of 2007.

<sup>†</sup> Bertsch, D.J., Juris Doctoral candidate, The University of South Dakota School of Law, 2011; Congress defined hydrokinetic energy as “electrical energy from waves, tides, and currents in oceans, estuaries, and tidal areas; free flowing water in rivers, lakes, and streams, or man-made channels; and differentials in ocean temperature (ocean thermal energy conversion),” The Energy Independence and Security Act of 2007, 42 USC §17211 (2006).

current and water depth. The minimum current required to operate a hydrokinetic device is typically 2–4 knots, with an optimum requirement being 5–7 knot range. Water depth is an important factor in the total energy that can be extracted from a site since rotor diameter is dependent on adequate water level above the installed device.

5. Hydrokinetic devices are ideally installed in locations with relatively steady flow throughout the year and in locations not prone to serious flooding events, turbulence, or extended period of low water level. In cold weather like Alaska, glacier silt, silt, and other sediments within the water can be harmful to the hydrokinetic devices.

### 13.3.4 RECENT COMMERCIALIZATION EXAMPLES IN THE UNITED STATES

While the technology for the hydrokinetic power devices is still being continuously improved, and the current prices make hydrokinetic energy somewhat less competitive compared to other methods for power generation, there is a significant momentum to commercialize this technology [33,79–89,94–102]. Compared to wind and solar, this renewable technology is more permanent in nature because river currents and ocean tides are more predictable. In recent years, several new commercial installations have taken place within the United States. We site five examples, which are as follows:

1. Wind power buoys (Figure 13.8a) capture the energy in the up and down movement of waves and generate power, which is transmitted by an underwater cable to the electric grid onshore. While several types of buoys are under development, Ocean Power Technologies' Reedsport Wave Park power station commercializes this technology (approved by Federal Energy Regulatory Commission [FERC] in August 2012) and they have 10 large

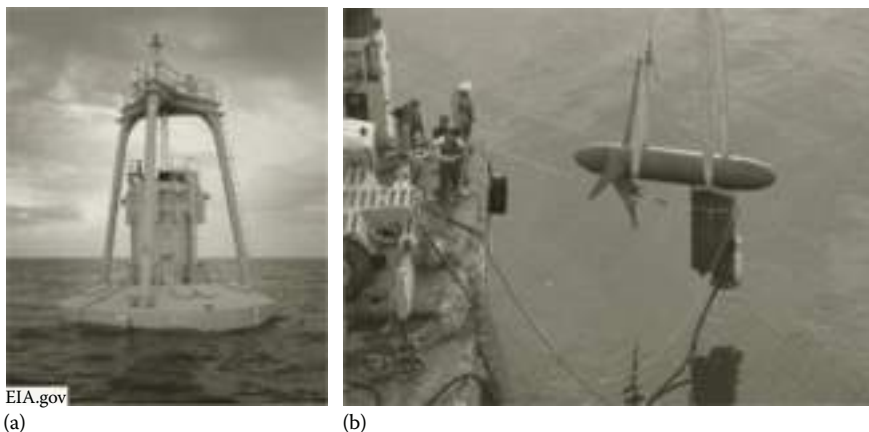


**FIGURE 13.8** First commercial projects for hydrokinetic power generation: (a) ocean wave power buoy off the Oregon coast; (b) underwater turbine in New York City's East River. (Adapted from "Regulators approve first commercial hydrokinetic projects in the United States," *Today in Energy*, US Energy Information Administration, Washington, DC, 2012.)

buoys installed which collectively generate 1.5 MW of electricity. The power wave station is located 2.5 miles off the Oregon coast and is connected to the electric grid by an underwater cable. The construction of this power station is completed [33,79,80,101].

2. Underwater turbines (Figure 13.8b) use water currents to spin underwater blades and generate electricity. These technologies depend on the unconstrained currents found in rivers, tidal areas, or the open ocean. Vedant Powers' Roosevelt Island Tidal Energy project (approved by the FERC in January 2012) installed 30 three-blade hydrokinetic generators on the bottom of New York City's East River to produce about 1.0 MW electricity. With some initial ups and downs, the project is now completed with blades made out of fiberglass and plastic [33,98–100].
3. Tidal power harnesses the water flowing between low and high tides, turning a turbine to generate power. There are only 40 sites known in the world that have the required difference in water levels between the tides needed to produce electricity. Alaska has a significant potential for hydrokinetic development in both rivers and tidal basins. Most inland communities in Alaska are situated along navigable waterways that could host hydrokinetic installations, and Alaska, with 90% of the total US tidal energy resources, is a home of some of the best tidal energy resources in the world.

In 2008, 5-kW, and, in 2009, 100-kW turbines were installed in Yukon River by New Energy Corporation. The New Energy Corp. EnCurrent machine with 5, 10, 25, 125, and 250 kW capabilities were also developed [33,94,100,102]. The water flow in Alaskan rivers is, however, season dependent, dropping off in winter compared to summer. This can create some challenging issues on constant power supply.

4. A company called Hydro Green Energy [102] is developing hydrokinetic power turbine arrays that are composed of truly modular, interchangeable, zero-head, current-based turbines. Hydro Green Energy's dual-duct, axial-flow, interchangeable hydrokinetic array of current-driven turbines operate in river (in-stream, free-flow, open-river, or hydrokinetic run of river), ocean (ocean power), and tidal settings (tidal power). The capacity of the Hydro Green Energy design is 98 kW per unit (at 3.5 m/s) with a rotor diameter of 12 ft.

Due to a surface suspension system, there are inherent operational maintenance and safety advantages of this device. An on-board gantry allows for raising and lowering of individual generating units in the hydrokinetic turbine array. The floating raft provides a platform for operation and maintenance activities. In general, the current-based hydrokinetic energy device provides the following advantages [102]:

- a. High capacity factor (approx. 90%), maximum net energy, and highly predictable base load power for in-stream river and ocean current applications; peak power generation in tidal energy applications.
- b. Large projects consist of robust and simple metal construction. Small projects consist of reinforced plastic construction. It utilizes conventional moving systems and the installation is simple and safe using existing marine vessels.

- c. Scalable to large power-generating stations (100+ MW)-utility scale power production; this turbine has been installed at numerous locations in Alaska.
- 5. In the summer of 2012, a hydrokinetic power-generation project was completed off the coast of Maine. This project was a result of collaboration between the department of energy and local community. The project will provide electricity to the local community. The project used the cross-flow turbine design similar to that shown in Figure 13.6, and it will generate power using the energy generated from underwater currents off the coast of Maine [97]. The electric power will be supplied using underwater power grid to the local town.

Besides the above five examples of commercialization, a number of hydrokinetic generation technologies are moving beyond pilot or demonstration stages [58–63] (Bertsch, 2012, pers. comm.).<sup>\*</sup> In 2011, the United States had less than 1 MW of installed hydrokinetic generation capacity, as compared to more than 77,000 MW of conventional hydroelectric generation capacity [40,42,44] (Dixon et al., 2008, pers. comm.). As of June 2011, the FERC had issued 70 preliminary permits for hydrokinetic projects (27 tidal, 8 wave, and 35 inland) with 9306 MW of generation capacity [37,42,44] (Dixon et al., 2008, pers. comm.). Preliminary permits were pending for an additional 147 projects with 17,353 MW of capacity [37,42,44,90].

The development and implementation of new commercial projects will require strong public/private financial backing, local political support for guaranty use of generated power, an efficient licensing approval system along with all the environmental considerations mentioned above [33,37,49,50,57–63] (Bertsch, 2012, pers. comm.).<sup>†</sup> Areas in the United States with good wave energy potentials include most of the continental US west coast, Hawaii, and Alaska. For tidal energy, good sites exist in the Puget Sound, San Francisco, a variety of east coast tidal channels, and Alaska. For river hydrokinetic energy, large inland rivers such as the Mississippi, Missouri, and Yukon have promising potential power [33,66–71,90].

### 13.4 OCEAN THERMAL ENERGY CONVERSION (OTEC)

This technology uses the temperature difference between warmer surface of the ocean and cooler deep water to run a heat engine to produce electricity. The heat cycle commonly used in the OTEC process is a Rankin cycle using a low-pressure turbine. While the attempt to develop and refine the OTEC technology started in the 1880s [92], one of the first successful plants generating 22 kW electricity was built in Matanzas, Cuba, in 1930 [75].

Japan is the major contributor to the OTEC technology. Tokyo Electric Power Company started building a 100-kW closed-loop cycle OTEC plant on the island of

<sup>\*</sup> Bertsch, D.J., Juris Doctoral candidate, The University of South Dakota School of Law, 2011; Congress defined hydrokinetic energy as “electrical energy from waves, tides, and currents in oceans, estuaries, and tidal areas; free flowing water in rivers, lakes, and streams, or man-made channels; and differentials in ocean temperature (ocean thermal energy conversion),” The Energy Independence and Security Act of 2007, 42 USC §17211 (2006).

<sup>†</sup> Ibid.

Nauru [93] in 1970. While this plant became operational in 1981, it only generated net 30 kW power for a school and other systems [92]. Many earlier efforts made in India and U.S. [75] were not completely successful. Only successful effort was made in 1993 by National Energy Laboratory in Hawaii, which generated 255 kW energy and lasted for six years [75]. Currently only operating OTEC plant is the one built by Saga University with support of a various Japanese industries in March 2013 [75].

Ocean Thermal Energy Corporation has plans to install two 10 MW OTEC plants in the US Virgin Islands and 5–10 MW OTEC facility in the Bahamas [75]. Numerous projects in Hawaii, Hainan, and Japan have been proposed and are being pursued [75,92]. Basic operating principles, operating sites, other usages of OTEC process and barriers to its implementations are well described in Ref. [75]. Sections 13.4.1 through 13.4.4 briefly summarize the descriptions presented in this reference.

### 13.4.1 OPERATING PRINCIPLES

A heat engine gives a higher efficiency when it is run with a higher temperature difference. The tropical area provides the largest temperature difference between ocean surface and deep water around 20°C–25°C. While OTEC can in principle provide 10–100 times more energy than wave power, its thermodynamic efficiency of 1%–3% (with old technology) compared to the theoretical maximum of 6%–7% for 20°C–25°C temperature difference has limited its use. Modern technologies, however, approach to the theoretical maximum efficiency. One approach that has worked is to pump vaporized low boiling fluid into the depths to be condensed, which reduces pumping volumes, technical and environmental problems, and costs.

The heat engine cycle can be operated in three different ways: close, open, and hybrid. Closed-cycle systems use fluid with a low boiling point, such as ammonia (having a boiling point around –33°C at atmospheric pressure), to power a turbine to generate electricity. Ammonia is used because of its superior transport properties, easy availability and low cost. Other fluids (such as CFC, HCFC, etc.) are possible but they have harmful environmental effects. The ammonia is vaporized and condensed by warm and cool water, respectively, with the use of two separate heat exchangers. The power is generated by the expanding vapor.

In an open-cycle OTEC process, warm surface water is converted to steam by passing it into a low-pressure vessel. The expanding steam can drive a low-pressure turbine. The steam is then converted to purified water by exposure to cold temperatures from deep-ocean water. This method thus produces water that is suitable for drinking, irrigation, or aquaculture [72]. The expanding (and rising) steam can also be used in a gas lift technique to lift water to significant heights. Depending on the local circumstances, this technique can generate power with the use of a hydroelectric turbine [73].

A hybrid cycle combines the features of the closed- and open-cycle systems. In a hybrid process, warm seawater enters a vacuum chamber and is flash evaporated. The steam then vaporizes the ammonia, which like in a closed cycle drives a turbine to produce electricity. The steam condenses within the heat exchanger and provides desalinated water. The hybrid cycle thus serves multiple purposes at the same time.

### 13.4.2 OPERATING SITES

While OTEC has the potential to produce a large amount of power and hydrogen (jointly with electrolysis), it is an expensive technology. OTEC plants require a long, large-diameter intake pipe, which is submerged a kilometer or more into the ocean's depths, to bring cold water to the surface. The operating site for OTEC can be land based, shelf based, or floating.

Land-based and near-shore facilities can be installed in sheltered areas so that they are relatively safe from storms and heavy seas. Electricity, desalinated water, and cold, nutrient-rich seawater could be transmitted from near-shore facilities via trestle bridges or causeways. In addition, land-based or near-shore sites allow plants to operate jointly with desalination or aquaculture industries. Land-based or near-shore sites can also support chilled water agriculture. Tanks or lagoons built on shore allow workers to monitor and control miniature marine environments and allow easy transport of the products to the markets.

Favored locations include those with narrow shelves (volcanic islands), steep ( $15^{\circ}$ – $20^{\circ}$ ) offshore slopes, and relatively smooth seafloors. These sites minimize the length of the intake pipe. A land-based plant could be built well inland from the shore, offering more protection from storms, or on the beach, where the pipes would be shorter. In either case, convenient access for construction and operation helps lower costs.

There are few disadvantages to land-based operations. The prolonged turbulent wave action in the surf zone and storms can damage discharge pipes. In addition, the mixed discharge of cold and warm seawater may need to be carried several hundred meters offshore to reach the proper depth before it is released, requiring additional expense in construction and maintenance. This can be avoided by building OTEC system just offshore in waters ranging from 10 to 30 m deep which use shorter intake and discharge pipes. The plant itself, however, would require protection from the marine environment, and the plant output would need to be transmitted to shore [74].

To avoid the turbulent surf zone as well as to move closer to the cold-water resource, the OTEC plants can be mounted to the continental shelf at depths up to 100 m. In general, however, the stress of open-ocean conditions, difficulty in product delivery and higher expenses for its construction and building a power delivery system to reach land make this approach less attractive [74].

Floating OTEC facilities operate offshore. Although potentially optimal for large systems, floating facilities present several difficulties. The difficulty of mooring plants in very deep water complicates power delivery. Cables attached to floating platforms are more susceptible to damage, and for depths  $>1000$  m they are difficult to maintain and repair. The system needs to be connected to the sea floor by riser cables without entanglement [74]. Both warm-water intake and vertically suspended cold-water pipe can be damaged by major storms and heavy seas. This problem can be alleviated with the use of flexible polyethylene materials for pipes, which can be uncoupled from the plant during storm. Surface water can also be drawn directly into the platform. Precautions must be taken to reduce damage and interruptions to intake flow by heavy seas [74]. Connecting a floating

plant to power delivery cables requires the plant to remain relatively stationary. Mooring is an acceptable method, but current mooring technology is limited to depths of about 2000 m (6600 ft). Even at shallower depths, the cost of mooring may be prohibitive.

### 13.4.3 OTHER USAGES OF OTEC

One of the attractions of the OTEC technology is its use for numerous other industries. Both open- and hybrid-cycle plants using surface condensers can desalinate seawater into potable water. A system analysis indicates that a 2-MW plant could produce about 150,000 cu ft of desalinated water each day [75].

The 41°F (5°C) cold seawater made available by an OTEC system creates an opportunity to provide large amounts of cooling to industries and homes near the plant. In 2010, Copenhagen Energy opened a district cooling plant in Copenhagen, Denmark. The plant delivered cold seawater to commercial and industrial buildings and reduced their electricity consumption by 80% [76]. OTEC technology supports chilled-soil agriculture. When cold seawater flows through underground pipes, it chills the surrounding soil. The temperature difference created by this method allows plants that require temperate climates to be grown in the subtropics [75].

Aquaculture is the best-known by-product of OTEC because it reduces the financial and energy costs of pumping large volumes of water from the deep ocean. Nonnative species such as salmon, lobster, abalone, trout, oysters, and clams can be raised in pools supplied by OTEC-pumped water. This extends the variety of fresh seafood products available for nearby markets and provides a low-cost refrigeration that can be used to maintain the quality of harvested fish [75]. In Kona, Hawaii, aquaculture companies working with an OTEC plant (Natural Energy Laboratory of Hawaii Authority [NELHA]) generate about \$40 million annually, a significant portion of Hawaii's gross domestic product (GDP) [77]. Deep-ocean water can also be combined with surface water to deliver water at an optimal temperature.

Hydrogen can be produced via electrolysis using the OTEC electricity. The OTEC process-generated steam with an addition of electrolyte compounds to improve efficiency is a relatively pure medium for hydrogen production [75]. While OTEC can be scaled to generate large quantities of hydrogen, this method is as yet not competitive to other methods of hydrogen production [75].

The OTEC technology can also be used to recover a large number (>50) of trace salt elements, uranium, and other materials from ocean. Japanese investigators are pursuing this approach [75].

A schematic of the OTEC process with its other usages is graphically illustrated in Figure 13.9 [75].

### 13.4.4 BARRIERS TO IMPLEMENTATION

The OTEC technology faces several political, economical, and technical barriers. The stationary surface platforms of the technology may affect the United Nations

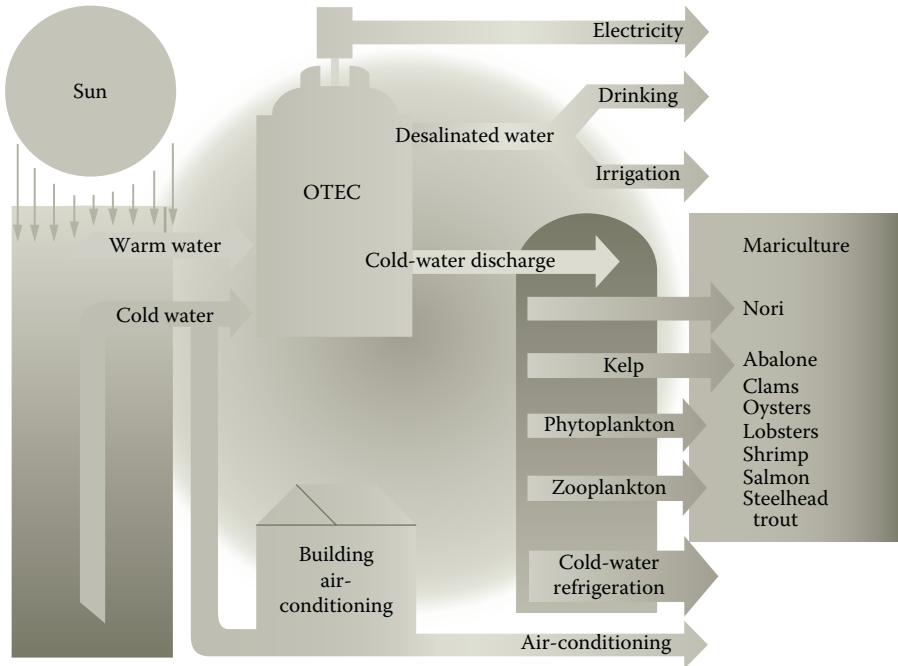


**FIGURE 13.9** (See color insert.) A schematic of OTEC process with applications. (Adapted from “Ocean thermal energy conversion,” Wikipedia, the free encyclopedia, 2013.)

convention on the law of the sea treaty [75]. They can affect fisheries and seabed mining operations. While the technology creates no waste and fuel consumption, its cost estimates are uncertain. It can be as low as 7 cents per kW depending on the cycle efficiency [75]. The technology is mostly applicable within  $20^\circ$  of the equator.

The technology faces several technical difficulties such as dissolved gases, microbial fouling, sealing, and parasitic power consumption by exhaust compressor [75]. The drop in pressure in an intake pipe can evolve gas, which can cause problems to the direct contact condensers. This issue may require installation of a deaeration unit [75]. The deposition of biofouling microbial layer from water in the heat exchanger wall may degrade its performance. Although the layer can be removed by brushing at short times, it may be difficult at longer times. This microbial layer may harden over time requiring more expensive treatment process [75]. The evaporator, turbine, and condenser operate in partial vacuum ranging from 3% to 1% of atmospheric pressure. The system must be carefully sealed to prevent in-leakage of atmospheric air that can degrade or shut down operation. The exhaust compressor parasitic power loss could be significant, and efforts must be made to reduce this loss and improve overall economics [75].

This technology can be in principle extended to cool air/water conversion in Arctic location where this temperature difference can be as high as  $40^\circ\text{C}$  [75].

### 13.5 GROWTH OF HYDROKINETIC ENERGY AND OTEC INDUSTRIES AND COST OF HYDROKINETIC AND OTEC POWER

A 2005 report by the EPRI estimated that some US utility-scale wave power projects could produce electricity for about 10 cents per kWh once the technology has fully matured [37,40,44,90] (Dixon et al., 2008, pers. comm.). They indicated that the present state of technology makes hydrokinetics a long-term investment opportunity, with potentially significant but highly uncertain returns.

A recent report by Pike Research [90] is, however, much more optimistic about the future growth of marine and hydrokinetic energy industry and pricing of hydro-electric power. Based on their own analysis, they made following assertions on the five chosen technologies:

1. *Tidal stream turbines.* These projects comprise over 90% of today's marine kinetic energy projects. However, majority of them depend on first-generation "barrage systems" that still rely on storage dams. The cost of power generation using these technologies is predicted to be 17 cents per kWh for 10 MW industry to as low as 4–9 cents per kWh for 100 MW industry. The target for this industry is 5 cents per kWh [90].
2. *Ocean wave energy technologies.* These "metal snake technologies" can span 600 ft floating on ocean wave horizontally. The generators can also be erected vertically akin to a buoy. Any western coastline in world has this wave energy potential. The cost of power generation for these technologies is 30 cents per kWh for 10 MW industry and 5–32 cents per kWh for 100 MW industry. The target for the industry is 5 cents per kWh [90].
3. *River hydrokinetic technologies.* This relies on the kinetic energy of moving water and it can be enhanced by tidal waves particularly at the intersections of river with sea or ocean. Alaska rivers are well suitable for these technologies. The cost of power generation by these technologies is <65 cents for 10 MW industry and about 18 cents per kWh for 100 MW industry. The target price for these technologies is 7–10 cents per kWh [90].
4. *Ocean current technologies.* This applies to deeper ocean currents near the shoreline. As mentioned in the Section 13.3, they are getting more attention in the recent years. The cost of power production for these technologies is about 20–40 cents for 10 MW industry. The data for the larger power plants using these technologies are not available. The target price for these technologies is 5 cents per kWh [90].
5. *OTEC technologies.* These technologies capture the energy from the difference in temperature between the ocean surface and lower depths. They can deliver power 24 h a day. The cost of power production for these technologies is >40 cents per kWh for 10 MW industry and >20 cents per kWh for 100 MW industry. The target price for these technologies is 15 cents per kWh [90].

Pike Research [90] in their two quarterly reports in 2012 projects very upbeat growth projections for marine and hydrokinetic energy productions. As shown in Figure 13.10,

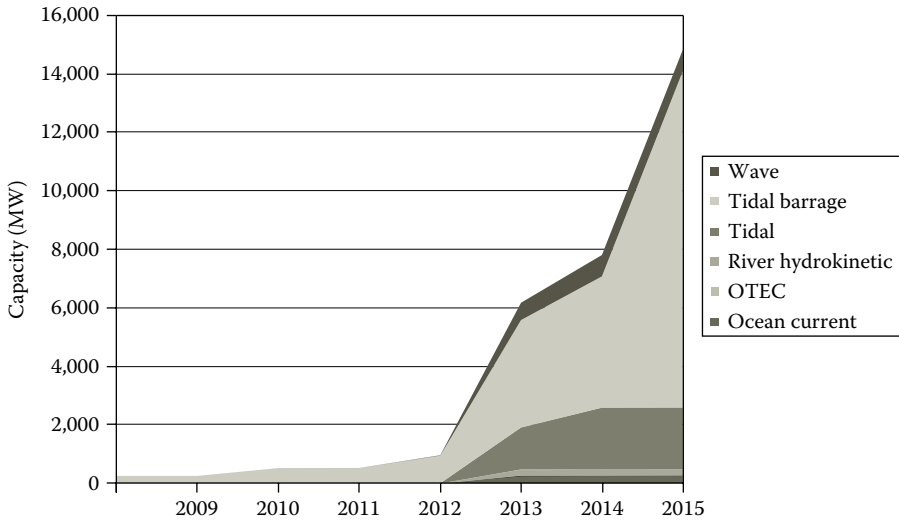


**FIGURE 13.10** (See color insert.) Cumulative marine and hydrokinetic energy installed capacity by technology, world market: 2008–2017. (Adapted from Gauntlett, D. and Asmus, P., “Executive summary: Hydrokinetic and Ocean Energy; Renewable power generation from ocean wave, tidal stream, river hydrokinetic, ocean current, and ocean thermal technologies,” Research report by Pike Research, Cleantech Market Intelligence, Boulder, CO, 2012.)

their growth projections for hydrokinetic energy capacity up to 2015 indicate more than ten-fold increase mainly due to two large projects—a 14 GW tidal barrage in the United Kingdom and a 2.2 GW tidal fence in Philippines—both may or may not be complete by 2015. Their growth projections for wave, river hydrokinetic, and ocean current energies during this period are modest. The figure predicts a negligible growth in energy by the OTEC projects during this period. Pike Research [90] sees Europe as a global leader for hydrokinetic energy producer and sees very significant global growth in wave, tidal stream, and tidal barrage energy by 2025.

## REFERENCES

1. “Hydroelectricity,” Wikipedia, the free encyclopedia, 1–7 (2012).
2. REN21, “Renewables 2011 global status report,” Hydropower, REN21, Paris (July 11, 2011).
3. “History of hydropower,” US Department of Energy (2012).
4. “Hydroelectric power,” *Water Encyclopedia* (2012).
5. “Hydroelectric power—Energy from falling water,” Clara.net (2012).
6. Robbins, P., “Hydropower,” in *Encyclopedia of Environment and Society*, Sage Publications, Thousand Oaks, CA, Vol. 3 (2007).
7. World Watch Institute, “Use and capacity of global hydropower increases” (January 2012).
8. Atkins, W., “Hydroelectric power,” *Water: Science and Issues*, 2, 187–191 (2003).
9. The Economist, “Binge and purge 98–99% of Norway’s electricity comes from hydro-electric plants,” *The Economist* (January 22, 2009).

10. International Rivers, "Sedimentation problems with dams" (July 16, 2010), [Internationalrivers.org](http://Internationalrivers.org).
11. James, P. and Chansen, H., *Teaching Case Studies in Reservoir Siltation and Catchment Erosion*. TEMPUS Publications, Great Britain, 265–275 (1998).
12. Sentürk, F., *Hydraulics of Dams and Reservoirs* (reference ed.). Water Resources Publications, Highlands Ranch, CO, 375 (1994).
13. "DAM," Wikipedia, the free encyclopedia, 1–19 (May 2013).
14. "Small hydro," Wikipedia, the free encyclopedia (2012).
15. Crettenand, N., "The facilitation of mini and small hydropower in Switzerland: Shaping the institutional framework. With a particular focus on storage and pumped-storage schemes," École Polytechnique Fédérale de Lausanne (EPFL), PhD thesis No. 5356 (2012), <http://infoscience.epfl.ch/record/176337?ln=en>.
16. Nachman-Hunt, N., "Small hydropower systems: Energy efficiency and renewable energy clearinghouse," Report DOE/GO-102001-1173, Merrifield, VA, FS217 (July 2001).
17. "Micro hydro," Wikipedia, the free encyclopedia (2012).
18. "How a micro hydro system works," US DOE (November 28, 2010).
19. "Micro hydropower systems," US DOE (November 28, 2010).
20. "Micro hydroelectric systems," Oregon DOE (December 1, 2010).
21. "Determining a potential micro hydropower site's flow," US DOE (November 28, 2010).
22. "Micro hydro," Research Institute for Sustainable Energy (December 9, 2010).
23. "Micro-hydro," The Ashden Awards for Sustainable Energy (November 20, 2010).
24. "Microhydropower," US DOE (November 20, 2010).
25. "Micro hydro power—Pros and cons," Alternative Energy News Network (November 24, 2010).
26. "Pico hydro," Wikipedia, the free encyclopedia (2012).
27. "Pico hydro power," T4cd.org (July 16, 2010).
28. Thomas, B., Jordan, B., and McGhee, R., "Pico-hydropower franchising: A test bed in rural honduras," National Collegiate Inventors and Innovators Alliance (January 24, 2013).
29. "Ashden award for pico hydro power in Kenya," Ashden Awards (September 6, 2010).
30. Khandker, S., Barnes, D., Samad, H., and Huu Minh, N., "Welfare impacts of rural electrification: Evidence from Vietnam," World Bank, Washington, DC (2008).
31. Redfield, S., *Five Gallon Bucket Hydroelectric Generator Build Manual*. Engineering for Change, Appropriate Infrastructure Development Group, Weston, MA (2012).
32. Howey, D., "Axial flux permanent magnet generators for pico-hydropower," Community of Practice: Energy, A conference hosted by Royal Academy of Engineering, February 20, Imperial College London, London (2006).
33. "Regulators approve first commercial hydrokinetic projects in the United States," *Today in Energy*, US Energy Information Administration, Washington, DC (October 2, 2012).
34. Sautter, J.A., "The clean development mechanism in China: Assessing the tension between development and curbing anthropogenic climate change," *Villanova Environmental Law Journal*, 27, 91, 107 (2009).
35. Center for Climate and Energy Solutions, *Hydrokinetic Electric Power Generation*. Center for Climate and Energy Solutions, Arlington, VA, 1–6 (2012).
36. Bedard, R., Previsic, M., Hagerman, G., Polagye, B., Musial, W., Klure, J., Jouanne, A., et al., "North American Ocean energy status—March 2007," *Proceedings of the 7th European Wave and Tidal Energy Conference*, September 11–13, Porto, Portugal (2007).
37. FERC, "Issued hydrokinetics projects preliminary permits," <http://www.ferc.gov/industries/hydropower/indus-act/hydrokinetics/permits-issued.asp>.
38. Minerals Management Service, "Technology whitepaper on ocean current energy potential on the US outer continental shelf," Renewable Energy and Alternate Use Program, US Department of the Interior, Washington, DC, 3 (2006), <http://ocenergy.anl.gov>.

39. Cada, G., Ahlgrimm, J., Bahleda, M., Bigford, T., Stavrakas, S.D., Hall, D., Moursund, R., and Sale, M., "Potential impacts of hydrokinetic and wave energy conversion technologies on aquatic environments," *Fisheries*, 32 (4), 174–181 (2007).
40. Previsic, M., Polagye, B., and Bedard, R., "System level design, performance, cost and economic assessment—San Francisco tidal in-stream power plant, EPRI. EPRI-TP-006-SF CA (2006), <http://oceanenergy.epri.com/streamenergy.html#reports>.
41. Previsic, M., Moreno, A., Bodard, R., Polagye, B., Collar, C., Lockard, D., Toman, W., et al., "Hydrokinetic energy in the United States—Resources, challenges and opportunities," *Proceedings of the 8th European Wave and Tidal Energy Conference*, Uppsala, Sweden, 76–84 (2009).
42. Bedard, R., Previsic, M., Hagerman, G., Polagye, B., Musial, W., Klure, J., et al., "North American ocean energy status," EWTEC, Conference Paper, September 11–14, Porto, Portugal (2007).
43. Previsic, M. et al., "US Ocean energy resources," *Presentation at Hydrovision* (2008).  
Referred by Previsic, M., Moreno, A., Bodard, R., Polagye, B., Collar, C., Lockard, D., Toman, W., et al., "Hydrokinetic energy in the United States—Resources, challenges and opportunities," *Proceedings of the 8th European Wave and Tidal Energy Conference*, Uppsala, Sweden, 76–84 (2009).
44. "EPRI ocean energy reports, <http://oceanenergy.epri.com/>.
45. "Research at the intersection of marine/hydrokinetic energy and the environment," NSF Workshop, October 5–7, St. Anthony Falls Laboratory, University of Minnesota, Minneapolis, MN (2011).
46. Lalander, E., *Modelling Hydrokinetic Energy Resource for In-Stream Energy Converters*. Division of Electricity, Department of Engineering Sciences, Uppsala Universitet, Uppsala, Sweden, (2010).
47. US Department of Energy Wind and Water Power Program, *Marine and Hydrokinetic Technologies*. US Department of Energy, Washington, DC, 1–2, DOE/GO-102010-3038 (2010).
48. Bertsch, D., "Hydrokinetic energy: Trying to navigate the energy and water law framework to develop new renewable energy technology," The University of South Dakota Report, Vermillion, SD, 1–25 (2011).
49. "Hydrokinetic energy (in river, tidal and ocean current)," *Alaska Energy Wiki*, Alaska Center for Energy and Power, 1–6 (2012).
50. "How hydrokinetic energy works?" Union of Concerned Scientists, 1–5 (2012).
51. "Hydrokinetic energy (in river, tidal, and ocean current)," *Alaska Energy Wiki*, Alaska Center for Energy and Power, 1–4 (July 20, 2012).
52. "Hydrokinetic power barges," Future energy, hydro power inventions, alternative energy (August 18, 2009).
53. "Tidal power," Wikipedia, the free encyclopedia (May 9, 2013); also Tidal Power at Cook Inlet; a communication by Ground Truth Trekking (May 9, 2013).
54. Ocean Energy Council, "Tidal energy: Pros for wave and tidal power" (2011).
55. Dorf, R., *The Energy Factbook*. McGraw-Hill, New York (1981).
56. "Tidal energy, ocean energy," Racerocks.com (April 5, 2011).
57. BOEM, "Ocean wave energy," Bureau of Ocean Energy Management, Washington, DC (May 9, 2013).
58. "Hydrokinetic projects," FERC, US Administration, 74, 61–67 (August, 2013).
59. "Low head hydro power," Wikipedia, the free encyclopedia (May 9, 2013).
60. "Wave power," Wikipedia, the free encyclopedia (May 9, 2013).
61. International Energy Agency, *World Energy Outlook Executive Summary* (2009), <http://iea.org/Textbase/npsum/WEO2009SUM.pdf>.
62. Walsh, M.B., "A rising tide in renewable energy: The future of tidal in-stream energy conversion (TISEC)," *Villanova Environmental Law Journal*, 19, 193, 196 (2008).

63. Koch, L., "The promise of wave energy," *Villanova Environmental Law Journal*, 2, 162, 165 (2008).
64. Pelamis Wave Power, *Statement on Portuguese Aguçadoura Project* (2010), [http://www.pelamiswave.com/media/statement\\_on\\_aguadoura\\_project.pdf](http://www.pelamiswave.com/media/statement_on_aguadoura_project.pdf).
65. PEW Center on Global Climate Change, *Hydrokinetic Electric Power Generation* (2009), <http://www.pewclimate.org/docUploads/Hydrokinetic%2009%2012%2004.pdf>.
66. Miller, C., "A brief history of wave and tidal energy experiments in San Francisco and Santa Cruz" (August 2004).  
Referred by Vosough, A. "Wave Energy," *International Journal of Multidisciplinary Sciences and Engineering*, 2 (7), 60 (2011).
67. "Wave energy potential on the US outer continental shelf," US Department of the Interior, Washington, DC (2008).
68. Holthuijsen, L.H., *Waves in Oceanic and Coastal Waters*. Cambridge University Press, Cambridge (2007).
69. Clément, A., McCullen, P., Falcao, A., Fiorentino, A., Gardner, F., Hammarlund, K., Lemonis, G., et al., "Wave energy in Europe: Current status and perspectives," *Renewable & Sustainable Energy Reviews*, 6 (5), 405–431 (2002).
70. "The development of wave power," (December 18, 2009).
71. "Wave energy research and development at JAMSTEC," (December 18, 2009).
72. Vega, L.A., "Open cycle OTEC," *OTEC News*, The GreenOcean Project (1999).
73. Lee, C.K.B., and Ridgway, S., "Vapor/droplet coupling and the mist flow (OTEC) cycle," *Journal of Solar Energy Engineering*, 105, 181–186 (1983).
74. "Design and location," *What is Ocean Thermal Energy Conversion?* National Renewable Energy Laboratory, Washington, DC (January 22, 2012).
75. "Ocean thermal energy conversion," Wikipedia, the free encyclopedia (2013).
76. Green Tech, "Copenhagen's sea water cooling delivers energy and carbon savings," *Forbes*, New York (October 24, 2012).
77. Ponia, B., "Aquaculture updates in the Northern Pacific: Hawaii, Federated States of Micronesia, Palau and Saipan," *SPC Fisheries Newsletter*, July 2006 (2013).
78. Drew, B., Plummer, A., and Sahinkaya, M., "A review of wave energy converter technology," *Proceedings of the IMechE: Journal of Power and Energy*, 223 Part A, 887–902 (2009).
79. "Agreement to develop wave power park in Oregon," (2008), [renewableenergyaccess.com](http://renewableenergyaccess.com).
80. Reedsport OPT Wave Park, "Reedsport OPT Wave Park FERC Project No. 12713 Application for a Major License," Federal Energy Regulatory Commission, Washington, DC (February 15, 2010).
81. "Anaconda WEC," *Science Daily* (July 7, 2008).
82. Siegel, S.G., Jeans, T.L., and McLaughlin, T.E., "Deep ocean wave energy conversion using a cycloidal turbine," *Applied Ocean Research*, 33 (2), 110–119 (2011).
83. Siegel, S.G., Fagley, C., and Nowlin, S., "Experimental wave termination in a 2D wave tunnel using a cycloidal wave energy converter," *Applied Ocean Research*, 38, 92–99 (2012).
84. Kraemer, S., "Wave Roller uses swinging door for underwater wave energy," *Scientific American*, Stevenson Ranch, CA (December 9, 2010).
85. Cruz, J., Gunnar, M., Barstow, S., Mollison, D., and Cruz, J. (eds.), *Green Energy and Technology, Ocean Wave Energy*. Springer, Berlin, Germany, 93 (2008).
86. Jha, A., "Making waves: UK firm harnesses power of the sea ... in Portugal," *The Guardian* (London) (October 9, 2008).
87. "Pelamis sinks Portugal wave power," [cleantech.com](http://cleantech.com) (2009).
88. Lima, J., "Babcock, EDP and Efaced to collaborate on wave energy projects," *Bloomberg Television* (September 24, 2008).
89. Fyall, J., "600ft 'sea snake' to harness power of Scotland," *The Scotsman* (Edinburgh), 10–11 (May 19, 2010).

90. Gauntlett, D. and Asmus, P., "Executive summary—Hydrokinetic and Ocean Energy: Renewable power generation from ocean wave, tidal stream, river hydrokinetic, ocean current, and ocean thermal technologies," Research report by Pike Research, Cleantech Market Intelligence, Boulder, CO (2012).
91. Ortega-Achury, S., McAnally, W., Davis, T., and Martin, J., "Hydrokinetic power review," Prepared for US Army Corps of Engineers Research development Center, Vicksburg, Mississippi, by Bagley College of Engineering, Mississippi State University, Starkville, MS (April 2, 2010).
92. Douglas, C.A., Harrison, G.P., and Chick, J.P., "Life cycle assessment of the SeaGen marine current turbine," *Proceedings of the Institution of Mechanical Engineers, Part M: Journal of Engineering for the Maritime Environment*, 222 (1), 1–12 (2008).
93. Evans, R., *Fueling Our Future: An Introduction to Sustainable Energy*. Cambridge University Press, New York (2007).
94. "China endorses 300 MW ocean energy project," [Renewableenergyworld.com](http://Renewableenergyworld.com) (April 5, 2011).
95. "Korea's first tidal power plant built in Uldolmok, Jindo," [Korea.net](http://Korea.net), Gateway to Korea (2012).
96. "\$3-B tidal power plant proposed near Korean islands," [Korea.net](http://Korea.net), Gateway to Korea (2012).
97. Sharp, D., "1st tidal power delivered to US grid off Maine," *CBS MoneyWatch* (September 14, 2012).
98. "Turbines off NYC East River will create enough energy to power 9,500 homes," US Department of Energy, Washington, DC (February 13, 2012).
99. Johnson, K., "Project aims to harness the power of waves," *New York Times* (September 3, 2012).
100. "Renewable power from the ocean's waves," CETO Wave Power (November 9, 2010).
101. Lockheed Martin, "Woodside, Ocean Power Technologies in wave power project," Portland Victoria Wave Farm (2012).
102. "Hydrokinetic technology," Hydro Green Energy, Westmont, IL (December 7, 2012).

---

# Index

**Note:** Locators “*f*” and “*t*” denote figures and tables in the text

## A

Acetone–butanol–ethanol (ABE) mixture, 256  
Adenosine triphosphate (ATP), 236  
Adsorption-enhanced reforming (AER), 65  
Advanced Steam Reforming of Methane in Heat Exchange (ASTERIX), 92–93  
Advanced thermal recycling (ATR) process, 76  
Alaska Northern slope (ANS), 343  
American Academy of Environmental Medicine (AAEM) species, 61  
Anaerobic digestion  
    biogas yield. *see* Biogas production  
    feedstock effects, 210–218  
        biodiesel production, byproducts, 214–215  
        coir pith, 212  
        dairy effluent, 217  
        distillery spent wash, 212–214  
        food/kitchen organic waste, 216–217  
        fruit waste, 218  
        LCFAs in wastewater, 215–216  
        methane yields, 210*t*, 211*t*  
        palm oil mill effluent, 215  
        swine waste, 214  
        tofu wastewater, 217–218  
        wastewater treatment, 217  
        whey, 212  
    literature studies, 213*t*  
    microbes and operating conditions, effects, 209–210  
        ammonia inhibition, 209  
        nutrients, 209–210  
        pH, 209–210  
        temperature, 209  
    principles, 206–209  
Anaerobic-phased solid (APS) digester, 222  
Aqueous-phase reforming (APR) process, 157–159, 169*f*  
    derivative technologies, 158  
    feedstock, typical, 159*t*  
    Gibbs free energy vs. temperature, 161*f*  
    kinetics and catalysis, effects  
        carbon number, 163  
        feedstock. *see* Feedstock effects, aqueous-phase reforming  
    liquid and solids, promoters/acidity, 165

    novel reactor designs, 170  
    oxygenates, 164*f*  
    pressure, 163  
    supports, 163–165  
    temperature, 163  
    reaction paths, 160*f*  
    steam reforming vs., 159–160  
    thermodynamics, 160–162  
Associated gas, 25  
Avicel, 250

## B

Barrage systems, 389  
Binary system approach, 39  
Bioenergy, 1  
Biofine process, 183  
    features, 183–184, 185*f*  
    intermediate products, upgrading, 191–197  
        biorefinery, family tree, 193*f*  
        char, 197  
        formic acid, 197  
        furfuryl and hydroxymethyl furfuryl, 196  
        gamma-valerolactone, 195–196  
        levulinic acid, transformation, 192–195  
    markets, usage, 191–192  
    large-scale, 200, 200*f*  
    other technologies, comparison, 197–200  
        bioforming process, 199–200  
        DIBANET project, 197–199  
        fermentation process, 199  
    process flow diagram, 189*f*  
Bioforming process, 157  
    two-stage reactor, 178*f*  
    Virent's, 173–178, 177*f*  
Biogas production  
    digester technology, 222  
    harvesting, effects, 219  
    pretreatment, 220  
    purification, 223–224  
    storage, 219  
    utilization, and digestate, 224  
Biological oxygen demand (BOD), 237

## Biomass

- aqueous-phase reforming, 168–170
- cellulose, 168–170
- hydrothermal liquefaction
  - particle size, 130
  - solids concentration, 130–131
- production ways, 157
- steam gasification, 62–67
- steam reforming, 77–78
- supercritical water, reforming in, 279

## Bisphenol A (BPA), 192

Boiling water reactor (BWR), 34–35, 35*f*

## Bubbling fluidized bed system, 65, 67, 83

## Bunsen reaction, 315

## C

## CANada Deuterium Uranium (CANDU), 36–37

## Carbon-emitting fossil energy, 2

## Caustic alkaline solution, 24

## Cellulase, groups, 248–250

## Cellulolysis, 248

## Cellulose, 183–187, 191, 196–197, 199

- aqueous-phase reforming, 168–170
- chemical conversion, 187*f*
- hydrolysis, mechanism, 250–251
- physical structure, 186*f*

## Cellulosic ethanol, 241–256

## coproducts, 255

- fermentation. *see* Fermentation process
- future efforts, 256

hydrolysis. *see* Hydrolysis process

## lignin conversion, 255

## pretreatment, 244–247

## dilute acid prehydrolysis, 245

## ionic liquid, 247

## organosolv, 245–246

## rapid steam hydrolysis, 245

RASH and organosolv, combined, 245–246, 246*f*

## Chemical oxygen demand (COD), 214, 217–218

## Circulating fluidized bed (CFB), 65

Clathrate hydrates. *see* Gas hydrates

## Clean Air Act Amendment (CAAA), 234

Coal bed methane, 21*f*, 25

## Coal mining and preparation, 29

## Coal–water chemistry

- CWF. *see* Coal–water mixture as fuel (CWF)

## liquefaction

- high pressure/temperature, 141–142
- pretreatment, 139–141

## Coal–water mixture as fuel (CWF), 142–148

## combustion, 147–148

## preparation and transportation, 146–147

## production, 144

## CENfuel, 145–146

## hypercoal, 146

## ultra clean coal, 145

## Cocurrent gasifiers, 81–82

## Co-digestion, 218–219

## Combined heat and power (CHP) system, 65, 235

## Compound parabolic concentrator (CPC), 92

## Concentrating solar power (CSP), 301

## Continuous stirred-tank reactor (CSTR), 267

## Corn

kernel, 238*f*

## meal, 235

## refineries, 235

## sugar, 239

uses, 234*f*

## Corn gluten meal (CGM), 239

## Countercurrent gasifiers, 81–82

## D

## Delta-aminolevulinic acid (DALA), 191–192

## Development of Integrated Biomass Approaches

## Network (DIBANET) project, 197–199

## Dextrins, 236

## Dextrose, 239

## D-glucose, 239

## Diesel miscible biofuels (DMBs), 197–198

## objectives, 198–199

process chain, 198*f*

## Digestate fertilizer, 224

## Dimethyl sulfoxide (DMSO), 196

## Diphenolic acid (DPA), 191–192

## Displacer, 372

## Distilled mash, 236

## Dolomite catalysts, 54

## Dried distillers grains (DDGs), 235, 237

## Dry milling corn ethanol technology, 239–241

## Dry reforming, 56–59

## issues, 58–59

## objectives, 59

## Dynamic tidal power (DTP), 379

## E

## Electric Power Research Institute (EPRI), 369, 389

## Electrolysis of water, 297–301

## alkaline, 298

## high pressure, 299–300

## high temperature, 298–299

## photo, 300

## photo-aided, 300–301

## photovoltaic, 301

## solar, 301

## Energy economy, 5

## Energy efficiency, 340

Energy landscape, global, 1–5  
 Enhanced gas hydrate recovery (EGHR)  
   methods, 339, 343–345, 344*f*  
 Enhanced geothermal system (EGS), 41–42  
   projects, commercial, 43*f*  
   recover, steps, 42*f*  
 Enhanced oil recovery (EOR)  
   chemical processes  
     caustic alkaline solution, 24  
     polymer solution, 24  
     surfactant–polymer solution, 23–24  
   thermal processes  
     hot water injection, 25  
     *in situ* combustion, 25  
     steam stimulation, 24–25  
 Enzymatic hydrolysis, 248–250  
   production and inhibition, 249–250  
   system, 248–249  
 Equilibrium reactor, 315  
 Ethanol  
   cellulosic. *see* Cellulosic ethanol  
   from corn, conversion, 237–241  
     dry milling process, 239–241  
     wet milling process, 237–239, 240*f*  
   grain (corn), 235–237  
     byproducts and coproducts, 237  
     environmental implications, 237  
     and product separation, purification, 236–237  
     starch hydrolysis, 236  
     yeast fermentation, 236  
   from lignocellulose, conversion, 243*f*  
   usages, 233  
 Exergy efficiency, 296, 297*f*  
 Explosion, 245  
 ExxonMobil report (EMR), 2–5  
   energy demand projections, 4*t*  
   energy landscape (1800–2040), 3*t*

## F

Fast internally CFB (FICFB) technology, 83  
 Fatty acid methyl esters (FAMES), 194  
 Feedstock effects  
   anaerobic digestion. *see* Anaerobic digestion,  
     feedstock effects  
   aqueous-phase reforming, 166–170  
     alcohols and glycerol, 166–167  
     biomass and cellulose, 168–170  
     ethylene glycol, 166–167  
     sugar and glucose, 167–168  
   primary, 166–168  
   secondary, 168–170  
   steam gasification, 60–70  
     biomass, 62–67  
     black liquor, 69–70  
     coal, 60–62

lignin, 70  
   mixed, 67–68  
   tar, 68–69  
 steam reforming, 70–81  
   biomass, 77–78  
   bio-oil, 80–81  
   carbon and carbon monoxide, 79–80  
   ethanol, 70–72  
   glycerol, 76–77  
   liquid hydrocarbons, 75–76  
   methanol, 72–75  
   mixed, 78–79  
 Fermentation process, 236  
   ethanol extraction, 254–255  
   isobutanol, sugar to, 256  
   methane, stages, 208*f*  
   modeling and control, 222–223  
   separate hydrolysis and fermentation, 251–252  
   SHF and SSF, comparison, 253  
   simultaneous saccharification and fermentation, 252  
   types  
     batch, 221  
     dry, 221  
     two-stage, 221–222  
     wet, 220–221  
   xylose, 253–254  
     integration, 254*f*  
     pentose yeasts, usage difficulties, 253  
   yeast, 236  
 Fischer–Tropsch (FT) process, 56, 120, 284  
 Fixed-bed gasifiers  
   downdraft, 81–82  
   updraft, 81–82  
 Fossil energy, 1  
 Fracking fluid, 19  
 Fracking technique, 19, 43  
   role of water, 25–27  
 Fuel cells (FCs), 47

## G

Gamma-butyrolactone (GBL), 192  
 Gamma-valerolactone (GVL), 185, 191, 195–196  
 Gas-cooled solar tower (GAST) system, 93  
 Gas hydrates, 329  
   carbon, source, 332*t*  
   climate warming, analysis, 338–339  
   deposits, sources/sizes and importance, 330–335  
   environmental impacts, 337–339  
   formation, 329–330  
   methane, production, 339–346  
     commercial applications, 346  
     computer simulation, 345–346  
     depressurization, 340–341

- Gas hydrates (*Continued*)  
 EGHR method, 343–345  
 gas exchange, 342–343  
 inhibitor injection, 341–342  
 phase diagram, 332*f*  
 thermal stimulation, 340  
 molecular structures, 330*f*  
 offshore oil/gas operations, 335–337  
   drilling, 335–336  
   enhanced recovery, production, 336–337  
   transportation vs., liquefied natural gas, 337  
   stability fields, 331*f*  
 Gas hydrate stability zone (GHSZ), 338  
 GASTEC, 88  
 Geopressurized zones, 21–22  
 Geothermal energy, recovery  
   capacity, 38*t*  
   electricity, coproduction, 42–43  
   enhanced geothermal system, 41–42, 42*f*, 43*t*  
   hydrothermal process, 37–43  
   methods, 39*f*–40*f*  
 Geysers, 40  
 Gibbs reactor, 315  
 Glucoamylase, 236  
 Glycol, 341  
 Grain (corn) ethanol  
   byproducts and coproducts, 237  
   environmental implications, 237  
   and product separation, purification, 236–237  
   starch hydrolysis, 236  
   yeast fermentation, 236  
 Grape sugar, 239  
 Graphite-moderated, direct cycle (boiling water)  
   pressure tube reactor (RBMK), 37  
 Greenhouse gas (GHG), 119, 143, 205,  
   216–217, 361
- H**
- H-5 and H-7 cycle, 316  
 Haber process, 79  
 Heating, ventilation, and airconditioning (HVAC)  
   systems, 43  
 Hemicellulase, 249  
 Hexachlorobenzene (HCB), 123  
 High-pressure electrolysis (HPE) process,  
   299–300  
 High-temperature electrolysis (HTE) process,  
   298–299  
 High-temperature gas-cooled nuclear reactor  
   (HTGR), 299  
 High-temperature shift (HTS)  
   catalysts, 79  
   reactor, 66–67  
 Homocellulose, 276  
 Hot dry rock, 41  
 Hot slurry primary and secondary  
   liquefaction, 240  
 Hot water injection, 25  
 Hybrid hydrolysis fermentation (HHF)  
   process, 253  
 Hydraulic retention time (HRT), 209, 215  
 Hydrochar, 117–119, 121–124  
 Hydroelectric power by water dams, 361–367  
   advantages, 364  
   conventional, 363, 363*f*  
   disadvantages, 365  
   environment issues, 365–366  
   other methods, 364  
   plants facilities, size and capacities,  
     366–367  
     micro, 366–367  
     pico, 367  
     small, 366  
   producers, 362*t*  
   projects, 362*t*  
   pumped storage, 363  
 Hydrogen, 2  
   adsorption, inhibition by, 51  
 Hydro Green Energy, 383  
 Hydrokinetic energy and power generation  
   devices, 371–382  
     barges, 380–381  
     choice and location, criteria, 381–382  
     conversion, 371  
     harness tidal, 379–380  
     rotating, 376–379, 377*f*, 378*f*  
     wave energy converters, 372  
   growth and cost, 389–390  
   hydroelectricity vs., 369–371  
   and marine, projections, 389, 390*f*  
   purpose, 367–369  
 Hydrolysis process, 185–191, 247–251  
   cellulose, mechanism, 250–251  
   for lignocellulose, types  
     acid/chemical, 247–248  
     enzymatic, 248–250  
   prehydrolysis, dilute acid, 245  
   rapid steam, 245  
   starch, 236  
 HYDROSOL, 311  
 Hydrothermal carbonization (HTC) process,  
   117–125, 157  
   considerations, 125  
   dry pyrolysis, comparison, 118*f*, 122–123  
   operating conditions, effects, 121–122  
   pressure facilitates, raise, 122  
   product characteristics and usages, 123–125  
   reaction mechanisms, 119–120  
 Hydrothermal convection systems, 38  
 Hydrothermal gasification (HTG), 113, 136–137,  
   157, 272  
   catalysts, 137–139

Hydrothermal liquefaction (HTL), 113,  
125–136, 157  
  feedstock, role of, 132–136  
    algae, 134–136  
    biowastes, 132–133  
    characteristics, 122  
    lignocellulose, 133–134  
  HTU process, 136  
  operating conditions, effects  
    biomass particle size and heating rates,  
      130–131  
    gas and liquid properties, 131  
    pressure, 128–130  
    residence time, 128–130  
    solids concentration, 130–131  
    temperature, 128–130, 129*t*  
  reaction mechanisms, 126–128  
  reducing gas, effect, 127*t*  
  region, 137  
Hydrothermal upgrading (HTU) process,  
  113, 136  
Hydroxymethylfurfural (HMF), 188,  
  190–191, 196

## I

Injection well, 96  
*In situ* combustion, 25  
*In situ* hybridization technique, 209  
*In situ* leaching (ISL), 28  
Integrated algae pond system (IAPS), 217  
Ion transport membranes (ITMs), 52

## K

Kick, 336

## L

Levulinic acid (LA), 183, 190–191, 194–195  
  as platform chemicals, 194*f*  
  transformation, 192–195  
Light water reactor (LWR), 33–34  
  boiling water reactor, 34–35, 35*f*  
  pressurized water reactor, 33,  
    35–36, 36*f*  
Lignin phenols, 255  
Lignocellulose, 133–134  
Liquefied natural gas (LNG), 337  
Long-chain fatty acids (LCFAs), 207  
  in wastewater, 215–216  
Low-temperature shift (LTS) catalysts, 80

## M

Maltodextrin, 236  
Mash, 241

Methane from gas hydrates, production  
  commercial applications, 346  
  computer simulation, 345–346  
  deposits, types, 333*f*  
  depressurization, 340–341  
  EGHR method, 343–345, 344*f*  
  gas exchange, 342–343  
  importance, reasons, 335*f*  
  inhibitor injection, 341–342  
  phase diagram, 332*f*  
  thermal stimulation, 340  
Methyltetrahydrofuran (MTHF), 191,  
  194–195  
Microemulsion flooding process, 23  
Mill starch, 238  
Molten salt steam gasification reactors,  
  84–86, 85*f*  
  iron, Atgas, 86  
  Kellogg–Pullman, 84–86  
Monofunctional groups, 172–173, 175*f*  
Multi-step sequential batch two-phase  
  anaerobic composting (MUSTAC)  
  process, 216  
Municipal solid waste (MSW), 64–67,  
  117, 183, 205–206, 222–223, 266,  
  274–275

## N

National Renewable Energy Laboratory  
  (NREL), 194  
Natural gas hydrate (NGH), 330  
  transportation vs., liquefied natural  
    gas, 337  
Nuclear power  
  commercial operation, 34*t*  
  reactors. *see* Nuclear reactors (water-based)  
  water, role, 33–37  
Nuclear reactors (water-based)  
  boiling water reactor, 34–35  
  graphite-moderated, direct cycle  
    (boiling water) pressure tube  
    reactor (RBMK), 37  
  light water reactor, 33–34  
  pressurized heavy water reactor, 36–37  
  pressurized water reactor, 35–36  
  supercritical water-cooled reactor, 37

## O

Oak Ridge National Laboratory (ORNL), 29  
Obligate hydrogen-producing acetogens  
  (OHPAs), 216  
Ocean current technologies, 389  
Ocean Renewable Power Company (ORPC), 378  
  Beta TidGen™ power system, 378  
  cross-flow turbine, 378*f*

Ocean thermal energy conversion (OTEC)  
technology, 384–388

with applications, 388<sup>f</sup>  
growth and cost, 389–390  
implementation, barriers, 387–388  
operating principles/sites, 385–387  
other usages, 387  
technologies, 389

Ocean wave energy technologies, 389

Oil shale industry, 27

Oligosaccharides, 236

Olivine catalysts, 54

Open-center turbine, 379

Overtopping principle, 376

Oxidation in SCW (SCWO), 266–268  
catalysts, 268

Oxygen exchange, inhibition by, 51

## P

Penstock, 363

Photochemical dissociation technology, water,  
301–305

photobiological production, 304–305

plasma-induced photolysis, 305

semiconductor catalysts (photocatalysis),  
302–304

metal sulfides, 304

tantalates and niobates, 303

titanium oxide, 302–303

transition-metal, nitrides, and oxynitrides,  
303–304

Photovoltaic (PV) systems, 44, 301

Plant cell wall, 242<sup>f</sup>

Plataforma Solar de Almeria (PSA), 306–307

Polychlorinated biphenyl (PCB), 123

Polymer electrolyte membrane (PEM), 158

Polymer solution, 24

Pressure swing adsorption (PSA), 74

Pressurized heavy water reactor, 36–37

Pressurized water reactor (PWR), 33, 35–36, 36<sup>f</sup>

Primary circuit, 34

Primary/secondary oil recovery process, 22–23

Pullulanase, 236

## R

Rapid steam hydrolysis (RASH), 244–245

organosolv pretreatment, 246, 246<sup>f</sup>

Raw fuels, 23

role of water in recovery and production,  
17–29

RBMK reactors, 37

Reactor, 372

River hydrokinetic technologies, 389

Run-of-the-river hydroelectricity, 364

## S

Saccharification, 236

SCW partial oxidation (SWPO), 266

Separate hydrolysis and fermentation (SHF)  
process, 251–252

Shaftless method, 96

Shaft method, 96

Shale, 19

Simultaneous saccharification and fermentation  
(SSF) process, 241, 251–252

Solar energy

heaters, types, 43

water, role of, 43–44

Solar fuels, 5

Solar gasification

reactors and processes, 90–92, 91<sup>f</sup>

technology, 89–90

Solar reforming (SOLREF), 92–95

advantages, 94–95

ASTERIX, 92–93

open-loop solar syngas production, 94

other processes, 94–95

Soltex process, 93–94

Solar thermochemistry, 89–90

Solar water cracker, 307

Solid fuels, mining, preparation, and extraction,  
27–29

coal, 29

oil shale, 27

tar sands and heavy oil, 27–28

uranium, 28–29

Solid oxide electrolyzer cell (SOEC), 298

Solid polymer electrolyte (SPE) membrane, 299

Soltex process, 93–94

Sorbent-enhanced reforming (SER)  
technology, 89

Sour gas catalysts, 80

Steam flood wells, 25

Steam gasification

catalysts, 53–55

metal-based, 54

nickel-based, 55

mechanism, 50–52

novel, 89–99

other processes, 98–99

solar gasification. *see* Solar gasification  
underground coal/reactors, 95–98

product distributions, feedstock effects,  
60–70

biomass, 62–67

black liquor, 69–70

coal, 60–62

lignin, 70

mixed feedstock, 67–68

tar, 68–69

- reactors, 81–86
  - fixed-bed gasifiers, 81–82
  - molten salt, 84–86, 85*f*
  - plasma and free radical gasifiers, 84
  - suspended bed, 82–84
  - underground, 96–98, 97*f*
- Steam–iron process, 98
- Steam reforming
  - catalysts, 55–56
  - considerations, 87
  - disadvantages, 49–50
  - feedstock effects on product distribution, 70–81
    - biomass, 77–78
    - bio-oil, 80–81
    - carbon and carbon monoxide, 79–80
    - ethanol, 70–72
    - glycerol, 76–77
    - liquid hydrocarbons, 75–76
    - methanol, 72–75
    - mixed feedstock, 78–79
  - mechanism, 52–53
  - novel, 89–99
    - microwave-assisted, 95
    - other processes, 98–99
    - solar reforming. *see* Solar reforming (SOLREF)
  - reactors, 87–89
- Steam stimulation, 24–25
- Steam turbines, 44
- Stillage, 236, 241
- Stirrer, 220–221
- STOMP-HYD simulation, 345–346
- Supercritical water (SCW), 261
  - advantages, 261–262
  - and ambient, comparison, 264*t*
  - chemical synthesis, role in, 265–266
  - decomposition/extraction of materials, 268–272
  - functions, 261
  - gasification, 272–277
  - hydrothermal process
    - glycerol pathways, transformation, 271*f*
    - pressure–temperature phase diagram, 263*f*
  - oxidation, 266–268
    - catalysts, 268
    - two-stage approach, 267
  - properties, 262–264
  - reforming, 277–282
    - biomass, 279
    - drawbacks, 283
    - ethanol, 281–282
    - ethylene glycol, 280
    - glycerol, 279–280
    - liquid fuels, 277–278
    - methanol, 280–281
  - sawdust, 274*t*
  - tri-reforming, 283–285
  - Supercritical water-cooled reactors, 37
  - Surfactant–polymer solution, 23–24
  - Suspended bed reactors
    - circulating fluidized bed, 83–84
    - entrained, 84
    - fluidized, 82–83
  - Syngas, 47, 172
    - production, open-loop solar, 94
  - Synthetic fuel/synfuels, 1

**T**

  - Tar sands and heavy oil industry, 27–28
  - Tennessee Valley Authority (TVA), 247
  - Tertiary oil recovery methods, 18
  - Tetrahydrofuran (THF), 191–192, 195
  - Thermochemical water splitting cycles (TCWSCs)
    - copper–chlorine (Cu–Cl), 315–316
      - advantages, 315–316
      - steps, 316
    - copper/sulfate, 316–319
    - hydrogen production, routes
      - metal oxide–redox reactions, 309*f*
      - monolithic dual-chamber, 311*f*
      - solar, 296*f*
    - metal oxides, carbothermal reductions, 312
    - mixed iron oxide, 311–312
    - S–I, 314–315
    - SnO/SnO<sub>2</sub>, 311
    - sulfur family, 312–314
    - two-/three-/four-step, 316, 317*t*–318*t*
    - UT-3, 309–310
    - Westinghouse process, 315
    - Zn/ZnO, 310–311, 310*f*
  - Tidal barrage, 368, 379, 390
  - Tidal stream, 368
    - generator, 379, 380*f*
    - turbines, 389
  - Tight gas, 19
  - Tri-reforming, 56, 59–60
    - reactions, 283
    - in supercritical water, 283–285
  - Turnover frequency (TOF), 52, 73

**U**

  - Ultra clean coal (UCC), 143, 145
  - Unmodified cornstarch, 239
  - Uranium mining and leaching, 28–29
  - US Geological Survey (USGS), 330, 334

**V**

  - Virent Inc., 173–178
  - Volatile fatty acid (VFA), 209–210, 215, 221, 223

**W****Water**

- based refinery, 15–16
- chemistry, coal. *see* Coal–water chemistry
- density, variations, 115*f*
- fatty acid concentration, 116*t*, 117*t*
- hydrogen, dissociation technologies
  - catalytic decomposition, 321
  - chemical methods, 319
  - electrolysis, 297–301
  - magmalysis, 320
  - magnetolysis, 321–322
  - photochemical, 301–305
  - plasmolysis, 321
  - radiolysis, 320
  - shock waves and mechanical pulses, 320–321
  - thermal decomposition, 305–307
  - thermochemical decomposition.
    - see* Thermochemical water splitting cycles (TCWSCs)
- management for future, 15–16
- properties, 114–117
- requirement for
  - coal mining and preparation, 29
  - oil shale mining, 27
  - tar sands and heavy oil mining, 27–28
  - uranium mining and leaching, 28–29
- role in
  - benign thermal energy, 33
  - fracking technique, 25–27

- nuclear power, 33–37
- solar energy, 43–44
- salts, solubility limits, 116*t*
- usage
  - for coal bed methane recovery, 19–21
  - reason for growth, 18–19
  - to recover gas from geopressurized zones, 21–22
- ways, energy and power
  - hydroelectricity, 361–367
  - hydrokinetic, 367–384
- Water–gas shift reaction, 79
- Wave Dragon, 376, 377*f*
- Wave energy converters (WECs), 371–372
  - commercial applications, 372–376, 375*t*
  - types, 373*f*–374*f*
- WaveRoller, 374, 376, 376*f*
- Weizmann Institute of Science (WIS), 93, 312
- Wet milling corn ethanol technology, 237–239, 240*f*
- Wet pyrolysis process. *see* Hydrothermal carbonization (HTC) process

**X**

- Xylose fermentation, 253–254
  - integration, 254*f*
  - pentose yeasts, usage difficulties, 253

**Y**

- Yttria-stabilized zirconia (YSZ) electrolytes, 299